A Novel Control Engineering Approach to Designing and Optimizing Adaptive Sequential Behavioral Interventions

by

Yuwen Dong

A Dissertation Presented in Partial Fulfillment
of the Requirements for the Degree
Doctor of Philosophy

Approved October 2014 by the
Graduate Supervisory Committee:

Daniel E. Rivera, Chair
Lenore Dai
Erica Forzani
Kaushal Rege
Jennie Si

ARIZONA STATE UNIVERSITY

December 2014

ABSTRACT

Control engineering offers a systematic and efficient approach to optimizing the effectiveness of individually tailored treatment and prevention policies, also known as adaptive or "just-in-time behavioral interventions. These types of interventions represent promising strategies for addressing many significant public health concerns. This dissertation explores the development of decision algorithms for adaptive sequential behavioral interventions using dynamical systems modeling, control engineering principles and formal optimization methods. A novel gestational weight gain (GWG) intervention involving multiple intervention components and featuring a pre-defined, clinically relevant set of sequence rules serves as an excellent example of a sequential behavioral intervention; it is examined in detail in this research.

A comprehensive dynamical systems model for the GWG behavioral interventions is developed, which demonstrates how to integrate a mechanistic energy balance model with dynamical formulations of behavioral models, such as the Theory of Planned Behavior and self-regulation. Self-regulation is further improved with different advanced controller formulations. These model-based controller approaches enable the user to have significant flexibility in describing a participant's self-regulatory behavior through the tuning of controller adjustable parameters. The dynamic simulation model demonstrates proof of concept for how self-regulation and adaptive interventions influence GWG, how intra-individual and inter-individual variability play a critical role in determining intervention outcomes, and the evaluation of decision rules.

Furthermore, a novel intervention decision paradigm using Hybrid Model Predictive Control framework is developed to generate sequential decision policies in the closed-loop. Clinical considerations are systematically taken into account through a user-specified dosage sequence table corresponding to the sequence rules, constraints enforcing the ad-

justment of one input at a time, and a switching time strategy accounting for the difference in frequency between intervention decision points and sampling intervals. Simulation studies illustrate the potential usefulness of the intervention framework.

The final part of the dissertation presents a model scheduling strategy relying on gain-scheduling to address nonlinearities in the model, and a cascade filter design for dual-rate control system is introduced to address scenarios with variable sampling rates. These extensions are important for addressing real-life scenarios in the GWG intervention.

This dissertation is dedicated to

my parents and my fiancé

for their consistent encouragement and invaluable support

ACKNOWLEDGEMENTS

I am pleased to acknowledge the many individuals who have played key roles in helping me complete this dissertation. First of all, I would like to express my appreciation to my research advisor, Dr. Daniel E. Rivera. I joined Dr. Rivera's Control Systems Engineering Laboratory in early 2011. Even though I did not have any prior control background, Dr. Rivera was very patient with me, and helped me wisely choose all the important control courses in the first two years so that I was quickly equipped with the skill set that is a prerequisite for doing research. It was Dr. Rivera's endless encouragement and constant guidance that makes my graduate studies one of the most fulfilling phases of my education. In these years, Dr. Rivera always showed his support for my exploration of my research interests, and encouraged me to attend different conferences which enabled me to understand how to make good presentation to different groups and audiences. Dr. Rivera's enthusiasm towards doing research has greatly impressed and motivated me, and he has been willing to sacrifice his weekends for our critical paper deadlines, urgent technical details or important research advice and discussions.

I would also like to thank Drs. Lenore Dai, Erica Forzani, Kaushal Rege and Jennie Si for serving on my graduate committee, offering their time, sharing their comments and knowledge to guide and expand my research.

The nature of this work is highly interdisciplinary. I would like to acknowledge our collaborators at Penn State University. First, I would like to thank Drs. Danielle Downs and Jennifer Savage who serve as PI and co-PI respectively, of an NIH-funded study upon which this work is based. They have provided me with valuable suggestions and professional advice on adaptive interventions; they are conducting the pilot study and designing the clinical trial for this GWG intervention. I also wish to acknowledge Dr. Linda Collins, Director of the Methodology Center at Penn State. Through the collaboration with her and

the Methodology Center, I was amazed at her knowledge, and was offered a platform to learn about some statistical methodologies. I also appreciate the important contributions from Dr. Diana Thomas from Montclair State University for the development of energy balance model, and Dr. Jesús Emeterio Navarro-Barrientos, a former postdoc in our group for the application of fluid analogies to the Theory of Planned Behavior model which inspired me to use production-inventory systems to illustrate our dynamical systems model.

Additionally, I would like to extend my sincere gratitude to Drs. David Nielsen, Veronica Burrows, Konstantinos Tsakalis, Hans Mittlemann, Nital Patel, Daniel Rivera, Armando Rodriguez, Kangping Chen, Erica Forzani, and Jennie Si for providing me with a solid foundation in the graduate courses at ASU.

I am grateful for having excellent colleagues: Sunil Deshpande, Kevin Timms and César Martín who kept the lab a pleasant place to work every day. We attended and presented at conferences together; we took various graduate courses and helped each other with homework and course projects; we discussed and figured out very difficult technical problems in research. Those made my years at ASU the most memorable time in my life. I would also like to wish them all the best in their future endeavors.

An important thanks goes to my parents Rongnian Dong and Yafen Zhang for their unconditional love and tremendous support throughout years. Without their blessings and encouragement, I would not have accomplished my PhD with so much enthusiasm. My most heartfelt thanks goes to my fiancé David Gruza who stands on my side, believes in me all the time, and encourages me to do my best in everything.

This work would not have been completed without the financial support from the following organizations: the Office of Behavioral and Social Sciences Research (OBSSR) of the National Institutes of Health, the National Institute on Drug Abuse (NIDA), and the National Heart, Lung, and Blood Institute (NHLBI) through grants R21 DA024266, K25 DA021173 and R01 HL119245.

TABLE OF CONTENTS

Page

LIST OF TABLES xi

LIST OF FIGURES xiv

CHAPTER

1 INTRODUCTION 1

1.1 Motivation 1

1.2 Adaptive Interventions 2

1.3 Sequential Behavioral Interventions 4

1.4 Excessive Gestational Weight Gain (GWG) 6

1.5 Research Goals 8

1.5.1 Dynamical Modeling 8

1.5.2 Controller Formulations for Self-Regulatory Process 9

1.5.3 Optimization-based Control for Sequential Decision Policies . . . 11

1.5.4 Gain-Scheduling Parameter Varying Control and Multi-Rate Digital Control 13

1.6 Contributions of the Dissertation 15

1.7 Publication Summary 18

1.8 Dissertation Outline 21

2 MODELING OVERVIEW 23

2.1 Overview 23

2.2 Energy Balance Model 25

2.2.1 Model Description 25

2.2.2 Initialization 30

2.2.3 Illustration of Energy Balance using Production-Inventory System 31

2.3 Behavioral Model 32

CHAPTER Page

2.3.1 Theory of Planned Behavior (TPB) 32
2.3.2 Path Analysis Model for TPB 33
2.3.3 Dynamic Fluid Analogy for TPB 35
2.3.4 Model Analysis for TPB Fluid Analogy 37
2.3.5 Illustration of Energy Balance and TPB using Production-Inventory Systems 39
2.4 Self-Regulation Principle 41
2.4.1 Introduction to Self-Regulation 41
2.4.2 Controller Design for Self-Regulation 42
2.4.3 Illustration of Energy Intake, TPB and Self-regulation using Production-Inventory Systems 44
2.5 Intervention Program and Delivery Modeling 45
2.5.1 Intervention Components 45
2.5.2 Intervention Delivery Dynamics 47
2.5.3 Illustration of Energy Intake, TPB, Self-regulation, and Intervention Delivery Module using Production-Inventory Systems 50
2.6 Adaptive Interventions with Decision Rules 51
2.6.1 Adaptive Interventions 52
2.6.2 Decision Rules 52
2.6.3 Illustration of the Overall GWG Dynamical Systems Model using Production-Inventory Systems 53
2.7 Simulation Study 55
2.7.1 Self-Regulation and Intervention Effect 57
2.7.1.1 No Intervention Scenario 59
2.7.1.2 Fixed Intervention Scenario 61
2.7.2 Adaptive Interventions via Decision Rules 64

CHAPTER Page

2.7.2.1 Simulation Study for Overweight Group 65

2.7.2.2 Simulation Study for Obese Group 69

2.8 Fetal Birth Weight Model 72

2.8.1 Fetal Energy Balance Model 72

2.8.2 Simulation Study 75

2.9 Chapter Summary 80

3 ADVANCED CONTROLLER FORMULATIONS FOR SELF-REGULATION 83

3.1 Overview 83

3.2 Internal Model Control (IMC) 84

3.2.1 Introduction 85

3.2.2 Two-Degree-of-Freedom (2 DoF) Internal Model Control 87

3.2.3 2 DoF IMC Design for Self-Regulation 88

3.3 Cascade Control 93

3.3.1 Introduction 93

3.3.2 Cascade Structures and Controller Designs 94

3.3.3 Cascade Control Design for Self-Regulation 95

3.3.3.1 IMC Cascade Control for Energy Intake Self-regulation Loop 95

3.3.3.2 Weighted IMC Cascade Control for Energy Intake and Physical Activity Self-Regulation 101

3.3.3.3 IMC Cascade Control for Physical Activity Self-regulation Loop 103

3.4 Simulation Studies 110

3.4.1 Contrasting Fixed versus Adaptive Interventions 113

3.4.2 Understanding within Participant Variability 118

3.4.3 Understanding Variability between Participants 123

CHAPTER Page

3.5 Chapter Summary 130

4 OPTIMIZED ADAPTIVE BEHAVIORAL INTERVENTIONS WITH SEQUENTIAL DECISION POLICIES USING HYBRID MODEL PREDICTIVE CONTROL 132

4.1 Overview 132

4.2 Hybrid Dynamical Systems 133

4.2.1 Mixed Logical Dynamical (MLD) Systems 136

4.2.2 MPC Prediction 138

4.3 Hybrid Model Predictive Control (HMPC) 144

4.3.1 Objective Functions 145

4.3.2 General Process Constraints 146

4.3.3 Hybrid MPC Controller Move 147

4.3.4 MPC with Three-Degree-of-Freedom (3 DoF) 152

4.3.4.1 Reference Trajectory and Setpoint Tracking 154

4.3.4.2 Measured Disturbance Rejection 155

4.3.4.3 Unmeasured Disturbance Rejection 155

4.4 HMPC Algorithm for Sequential Decision Policies 158

4.4.1 Clinical Considerations and Constraints 158

4.4.2 Discrete Magnitude of Dosages 160

4.4.3 Switching Time Strategy 161

4.4.4 Sequential Decision Policies 163

4.4.4.1 Generation of a Sequence Table 165

4.4.4.2 Manipulating One Input at a Time when Move Size $|\Delta u| \leq 1$ 167

4.4.4.3 Manipulating One Input Signal at a Time for Arbitrary Move Size 169

CHAPTER Page

4.5 Simulation Studies 171

4.5.1 Validation for the Proposed Dosage Sequence Formulation 172

4.5.2 HMPC versus Decision Rules 176

4.5.3 Alternate Sequenced Rules 181

4.6 Chapter Summary 187

5 ENHANCEMENTS TO THE GWG ADAPTIVE INTERVENTION 189

5.1 Overview 189

5.2 Gain-Scheduling Parameter Varying Control for GWG Intervention 190

5.3 Multi-Rate Digital Control 204

5.4 Summary 213

6 SUMMARY AND CONCLUSIONS 215

6.1 Conclusions 215

6.2 Future Research Directions 218

6.2.1 System Identification Modeling 218

6.2.2 Experimental Validation of the Control Scheme 219

6.2.3 Incorporating Infrequent Measurements in Kalman Filter 219

6.2.4 Hybrid Model Predictive Control with Temporal Logic 219

6.2.5 Adaptive Intervention for Infant Birth Weight 221

6.2.6 Metabolic Model for Gestational Diabetes 221

BIBLIOGRAPHY 223

LIST OF TABLES

Table Page

1.1 Summary of Dosage Augmentations and Reductions per the IF-THEN Decision Rules for GWG Adaptive Intervention [1]. 5

2.1 Expressions for Total Body Water as a Function of Gestational Weight per BMI Category, from [2, 3]. 26

2.2 Expressions for Total Body Protein as a Function of Gestational Weight per BMI Category [2–4]. 28

2.3 Expressions for Total Energy Expenditure as a Function of Fat-free Mass (FFM) per BMI Category, from [2, 3]. 29

2.4 Target Gestational Weight Gain (GWG) Recommended by the 2009 Institute of Medicine Guidelines [5] and the Corresponding Trimester-specific Energy Intake that Coincides with this Maternal Weight Gain [4]. 46

2.5 Intervention Components for Hypothetical GWG Intervention. 47

2.6 Intervention Dosages for the Adaptive Intervention Decision Rules [6] 54

2.7 Model Parameters for the Simulation Studies. Time Constants (τ_i) are in Units of Days. 60

2.8 Tabulation for Self-regulatory Controller Gains K_e Applied in the Simulations in Section 2.7.1. 60

2.9 Tabulation for Self-regulatory Controller Gains K_e Applied in the Simulations in Section 2.7.2. 65

2.10 Intervention Dosages for the Decision Rules (BS=Baseline value) 66

2.11 Summary of Dosage Augmentations per the IF-THEN Decision Rules on GWG and Fetal Weight Gain Control. (Notes: Baseline Intervention Includes Self-monitoring, Education and Guidance) 77

Table Page

3.1 Summary of Dosage Augmentations for a Representative GWG Adaptive Intervention Consisting of IF-THEN Decision Rules in Section 3.4 113

3.2 Model Parameters for the Simulation Studies in Section 3.4.1. Time Constants (τ_i), Delays (θ_i), and Self-regulation Adjustable Parameters (λ_r, λ_d) are in Units of Days. 114

3.3 Model Parameter Changes for the Within-individual Variability Simulation Study in Section 3.4.2. 119

3.4 Model Parameter Changes for the Inter-individual Variability Simulation Study in Section 3.4.3 124

4.1 Summary of Dosage Augmentations and Reductions per the IF-THEN Decision Rules for GWG Adaptive Intervention [1] for the Simulations in Section 4.5.1 and Section 4.5.2. 160

4.2 Dosage Sequence Table for the GWG Behavioral Intervention Example in Section 4.5.1 and Section 4.5.2. 166

4.3 Model Parameters for the Simulation Studies in Section 4.5.1. Time Constants (τ_i), Delays (θ_i), and Self-regulation Adjustable Parameters (λ_r, λ_d) are in Units of Days. 175

4.4 Summary of Dosage Augmentations per the IF-THEN Decision Rules for GWG Adaptive Interventions [7] for the Simulation in Section 4.5.3. 182

4.5 Dosage Sequence Table for the GWG Behavioral Intervention Simulation in Section 4.5.3. 184

4.6 Model Parameters for the Simulation Study in Section 4.5.3. Time Constants (τ_i) are in Units of Days. 186

5.1 Model Parameters for the Simulation Studies in Section 5.2. Time Constants (τ_{i_j} where j Refers to the j-th Model), Delays (θ_i), and Self-regulation Adjustable Parameters (λ_r, λ_d) are in Units of Days. 203

Table Page

5.2 Model Parameters for the Simulation Studies in Section 5.3. Time Constants (τ_i), Delays (θ_i), and Self-regulation Adjustable Parameters (λ_r, λ_d) are in Units of Days. 208

LIST OF FIGURES

Figure		Page
1.1	Sequential Decisions in the Intervention Project Active Adult Mentoring Program (AAMP) [8].	4
1.2	General Conceptual Diagram of the Dynamical Systems Model for GWG Change	9
1.3	Illustration of Self-regulation: Behavior and Perception as Elements of a Feedback Loop Guiding Human Action [9]	10
1.4	General Conceptual Diagram of the Dynamical Systems Model for GWG Adaptive Intervention. Blue Dash Line Represents the Information Needed in Self-regulatory Process, and the Pink Dot-dash Line Stands for the Information Exchanged in the Control-oriented Decision Policies.	11
1.5	Performance of Hybrid Model Predictive Control (HMPC) as a Decision Policy to Follow Set Point Change, Measured Disturbance (Energy Intake Increase), and Unmeasured Disturbance (Physical Activity Level Lowers at the Third Trimester). Reference Values are Shown by Red Lines.	13
1.6	Comprehensive Fluid Analogy and Interrelationship between Systems in a Behavioral Intervention for GWG, Shown for the Energy Intake Loop.	16
2.1	Overall Schematic Representation for an Adaptive Gestational Weight Gain (GWG) Intervention [10].	24
2.2	Energy Balance Model Illustration with the Concept of Production-inventory Systems	32
2.3	Path Diagram for the TPB, Obtained from Structural Equation Modeling (SEM) [11].	34
2.4	Fluid Analogy for the Theory of Planned Behavior (TPB).	36

2.5 Dynamical Systems Model for Behavioral Interventions Integrates the Maternal Energy Balance Model and the Dynamic Fluid Analogy for the TPB Illustrated by the Concept of Production-inventory Systems. 40

2.6 Behavior and Perception as Elements of a Feedback Loop Guiding Human Action per the Self-regulation Theory of Carver and Scheier [9]. 42

2.7 Dynamical Systems Model for Behavioral Interventions Integrates the Maternal Energy Balance Model, the Dynamic TPB Model and Self-regulation for the EI Loop Illustrated by the Concept of Production-inventory Systems. . . . 44

2.8 Illustration of the Intervention Delivery Dynamics for PBC Inflow in EI-TPB Model 48

2.9 Dynamical Systems Model for Behavioral Interventions Integrates the Maternal Energy Balance Model, the Dynamic TPB Model, Self-regulation and Intervention Delivery Modeling for the EI Loop Illustrated by the Concept of Production-inventory Systems. 51

2.10 Flow Chart for IF-THEN Decision Rules (Adaptive Intervention) Developed by Downs and Savage [6]. 55

2.11 GWG System Illustration with the Concept of Production-inventory Systems for Energy Intake Loop. 56

2.12 Disturbance Signals for ζ_5 in the EI-TPB (top), PAL with no Intervention and PAL (middle) with Intervention (bottom), respectively. 58

2.13 Simulation Responses for the Energy Intake Behavior (EI-TPB) Model (left) and Physical Activity Behavior (PA-TPB) Models (right). The Black Dashed Lines Represent the Case with no Intervention (Self-regulation only) while the Blue Solid Lines Represent the Case with the Intervention. The Magenta Dashdot Lines in the TPB Model Variables Show the Simulation Responses in these Variables when no Self-regulation is in Effect. 62

2.14 Simulation Responses for Maternal Energy Balance. Red Lines Represent the 2009 IOM Guidelines Applied a Daily Basis; the Black Dashed Lines Represent the Case with no Intervention (Self-regulation only) while the Blue Solid Line Represents the Case with the Intervention and Self-regulation. 63

2.15 Simulation Result for the Behavioral Variables for Energy Intake TPB (EI-TPB) and Physical Activity TPB (PA-TPB) Models, and the Dosage of the Intervention Components for Overweight Participant with the Decision Rules Implemented. 68

2.16 Simulation Responses for the Maternal Body Mass, Energy Intake and Energy Expenditure for Overweight Participants with the Decision Rules Implemented. Red Dashed Lines Represent the 2009 IOM Guidelines Applied on a Daily Basis, Black Dash-dot Lines Show the Simulation Response in these Variables in the Absence of an Intervention. 69

2.17 Simulation Result for the Behavioral Variables for Energy Intake TPB (EI-TPB) and Physical Activity TPB (PA-TPB) Models, and the Dosage of the Intervention Components for Obese Participant with the Decision Rules Implemented. 70

2.18 Simulation Responses for the Maternal Body Mass, Energy Intake and Energy Expenditure for Obese Participants with the Decision Rules Implemented. Red Dashed Lines Represent the 2009 IOM Guidelines Applied on a Daily Basis, Black Dash-dot Lines Show the Simulation Response in these Variables in the Absence of an Intervention. 71

2.19 Schematic Representation for an Adaptive Fetal Birth Weight and Gestational Weight Gain Intervention. 76

2.20 Simulation Responses for the Maternal Body Mass, Energy Intake (EI), Physical Activity Level (PAL) and Fetal Birth Weight. Red Lines Represent the 2009 IOM Guidelines Applied on a Daily Basis; the Blue Solid Lines Represent the Case with Intervention and Self-regulation, while the Black Dashed Lines Represent the Case with no Intervention. 78

3.1 Schematic Representation of the Internal Model Control (IMC) Structure [12]. 85

3.2 Alternate IMC Configuration Expressed as Classical Feedback System [12]. . 87

3.3 Two-Degree-of-Freedom (2 DoF) IMC [12]. 88

3.4 Closed-loop System Implemented with Self-regulation Designed by Two-Degree-of-Freedom (2 DoF) Internal Model Control (IMC). 89

3.5 Example of Different Self-regulation Responses (Scenarios 1 and 2) Resulting from Changes in Tuning Parameters for the Self-regulation Structure of Figure 3.4. Red Dash Lines Represent Setpoints Applied on a Daily Basis; Blue Solid Lines and Black Dash-dot Lines Represent the Two Scenarios with Self-regulation, respectively; Pink Dot Lines Represent the Disturbance. Parameters for Scenario 1 are: $\lambda_{r_1} = 5, \lambda_{r_2} = 10, \lambda_{d_1} = 5, \lambda_{d_2} = 10$; Parameters for Scenario 2 are: $\lambda_{r_1} = 15, \lambda_{r_2} = 20, \lambda_{d_1} = 10, \lambda_{d_2} = 20$. 92

3.6 IMC Cascade Structure [12]. 95

3.7 IMC Cascade Structure 1 for EI Self-regulation. 96

3.8 IMC Cascade Structure 2 for EI Self-regulation. 99

3.9 IMC Cascade Structure for Self-regulation Loops in GWG Model, with Weight Parameter Fraction $w\%$ for the Setpoint. 102

3.10 Example of Self-regulation Response Using the Cascade IMC Structure of Figure 3.9 with Weight Parameter Fraction ($w\% = 0.6$) for Selected Tuning Parameters. Red Dash Lines Represent Setpoints Applied on a Daily Basis; Blue Solid Lines Represent the Participant's Response with Self-regulation; Pink Dot-dash Lines Represent the Disturbance. Parameters for this Simulation are: $\lambda_{r_1} = 10, \lambda_{r_2} = 1, \lambda_{r_3} = 10, \lambda_{d_1} = 15, \lambda_{d_2} = 15, \lambda_{d_3} = 15$. 104

3.11 IMC Cascade Structure for GWG Model, with PA Self-regulation Loop Associated with PA Monitoring Results and IOM Guidelines. 107

3.12 Example of Self-regulation Response Using the Cascade IMC Structure per Figure 3.11 with Selected Tuning Parameters for Fast Tuning of PA. Red Dash Lines Represent Setpoints Applied on a Daily Basis; Blue Solid Lines Represent the Participant's Response with Self-regulation; Pink Dot Lines Represent the Disturbance. Parameters for this Simulation are: $\lambda_{r_1} = 15, \lambda_{r_2} = 20, \lambda_{r_3} = 1, \lambda_{d_1} = 10, \lambda_{d_2} = 10, \lambda_{d_3} = 10$. 108

3.13 Example of Self-regulation Response Using the Cascade IMC Structure per Figure 3.11 with Selected Tuning Parameters for Slow Tuning of PA. Red Dash Lines Represent Setpoints Applied on a Daily Basis; Blue Solid Lines Represent the Participant's Response with Self-regulation; Pink Dot Lines Represent the Disturbance. Parameters for this Simulation are: $\lambda_{r_1} = 15, \lambda_{r_2} = 20, \lambda_{r_3} = 4, \lambda_{d_1} = 10, \lambda_{d_2} = 10, \lambda_{d_3} = 10$. 109

3.14 Adaptive Gestational Weight Gain Intervention Simulation Model, Represented as a Network of Production Inventory Systems. 111

3.15 Simulation Responses Contrasting Adaptive, Fixed, and no Intervention for a Given Participant (Section 7.1). Red Dot Lines Represent the 2009 IOM Guidelines Applied on a Daily Basis; the Blue Solid Lines Represent the Case with Adaptive Interventions via IF-THEN Decision Rules, the Black Dash-dot Lines Represent the Case with Fixed Interventions, and the Dash Pink Lines Represent the Case with no Intervention. 117

3.16 Simulation Response for the Participant's Weight, Energy Intake and Energy Expenditure for the Four Scenarios with Parameters Listed in Table 3.3. The Red Dashed-dotted Lines Represent the 2009 IOM Guidelines Applied on a Daily Basis; the Blue Thick Solid Lines Represent the Scenarios with Adaptive Interventions via IF-THEN Decision Rules, and Black Thin Dashed Lines are the Scenarios with Fixed Interventions. 120

3.17 Simulation Response for the Intervention Components Dosages in Adaptive Interventions for the Four Scenarios with Parameters Listed in Table 3.3. . . . 121

3.18 Simulation Response for the Participant's Weight Change, and Energy Intake Change for the four Participants with Parameters Listed in Table 3.4. The Red Dashed-dotted Lines Represent the 2009 IOM Guidelines Applied on a Daily Basis; the Blue Thick Solid Lines Represent the Scenarios with an Adaptive Intervention via IF-THEN Decision Rules, and the Black Thin Dashed Lines are the Scenarios with a Fixed Intervention. 126

3.19 Simulation Response for the Participant's PBC Inflow Changes to EI-TPB Model and PA-TPB Model for the Four Participants with Parameters Listed in Table 3.4. The Blue Thick Solid Lines Represent the Scenarios with an Adaptive Intervention via IF-THEN Decision Rules, and Black Thin Dashed Lines are the Scenarios with a Fixed Intervention. 127

3.20 Simulation Response for the Participant's Intervention Components Dosages for the Four Participants with Parameters Listed in Table 3.4. The Blue Lines Represent the Scenarios with Adaptive Interventions via IF-THEN Decision Rules, and Black Lines are the Scenarios with Fixed Interventions. 128

4.1 Schematic Representation for an "Adaptive" Optimized Gestational Weight Gain (GWG) Intervention by Hybrid Model Predictive Control (HMPC) [1]. . 134

4.2 Basic Structure of MPC [13]. 145

4.3 Three-Degree-of-Freedom (3 DoF) Controller Block Diagram of MPC. 154

4.4 IF-THEN Decision Rules for Time-varying GWG Intervention Evaluation for Adapting Intervention. 159

4.5 Diagrammatic Illustration of the Switching Time Strategy in Section 4.4.3. . . 162

4.6 Simulation Responses in Section 4.5.1 for Maternal Body Mass, Energy Intake (EI), Energy Expenditure (EE), the Intervention Component Dosages, and the Perceived Behavioral Control (PBC) Inflows to the Theory of Planned Behavior (TPB) Models. Red Dashed Lines Represent the 2009 IOM Guidelines in Table 2.4 Applied on a Daily Basis; the Blue Solid Lines are the Case with Adaptive GWG Intervention Using HMPC Framework Corresponding to the Dosage Sequence Table 4.2; and the Black Dashed-dotted Lines are the Case in the Absence of the Interventions. 174

4.7 Simulation Results in Section 4.5.2 for the Participant's Responses for Maternal Body Mass, Energy Intake (EI), Energy Expenditure (EE), the Intervention Component Dosages, and the Perceived Behavioral Control (PBC) Inflows to the Theory of Planned Behavior (TPB) Models for the HMPC-based Intervention, the Adaptive Intervention Using Decision Rules, and no Intervention Case. The Red Dashed Lines Represent the 2009 IOM Guidelines in Table 2.4 Applied on a Daily Basis; the Blue Solid Lines are the Case with HMPC-based Intervention Corresponding to the Dosage Sequence Table 4.2; the Black Dashed-dotted Lines Represent the Case with Adaptive Intervention Using "IF-THEN" Decision Rules in Sequenced Rules Table 4.1; and the Pink Dotted Lines are the Case in the Absence of the Interventions. 178

4.8 Simulation Responses in Section 4.5.3 for the PBC Inflows to the Two TPB Models, Maternal Body Mass, Energy Intake, PAL Change, Energy Expenditure, and the Dosages of Two Augmented Intervention Components. Red Line Represent the 2009 IOM Guidelines Applied on a Daily Basis; the Blue Solid Lines Represent the Case with Optimized Adaptive Interventions Using HMPC Corresponding to the Dosage Sequence Table in Table 4.5, the Black Dash Lines are Adaptive Interventions via "IF-THEN" Decision Rules in Sequenced Rules Table 4.4, and the Pink Dash-dot Line is the Energy Intake Profile with no Interventions. 185

5.1 Illustration of the Gain Scheduling Strategy for a GWG Intervention Developed in this Chapter 191

5.2 Example of Simulation Responses Using Gain-scheduling Parameter Varying Control in Figure 5.1 and the Single-model Based Control Strategy. Red Dash Lines Represent Setpoint Applied on a Daily Basis; Blue Solid Lines Represent the Participant's Response Using Model Scheduling Strategy; Black Dash-dot Lines Represents the Participant's Response Using Single Model-based Control, and the Pink Dash Lines are the Case with no Intervention. . . 202

5.3 Cascade Structure of the Multi-rate Filter [14], where $\hat{y}_f$ and $\hat{y}_s$ Refer to the Controlled Variables Measured at Faster Sampling and Slower Sampling, respectively; $\bar{y}_f$ and $\bar{y}_s$ Represent the Estimations of Controlled Variables Sampled at Higher and Lower Frequency, respectively. 205

5.4 Example of Simulation Responses Using Cascade Structure of the Multi-rate Filter per Figure 5.3 with $K_s = 0.3$ for Slow Tuning of the Secondary Estimator. Red Dash Lines Represent Setpoint applied on a Daily Basis; Blue Solid Lines Represent the Participant's Response for Maternal Body Mass, Energy Intake (EI), Physical Activity Level (PAL), and the Intervention Component Dosages; Black Dash-dot Lines Represents the Case with no Intervention. 210

5.5 Example of Simulation Responses Using Cascade Structure of the Multi-rate Filter per Figure 5.3 with $K_s = 0.8$ for Fast Tuning of the Secondary Estimator. Red Dash Lines Represent Setpoint applied on a Daily Basis; Blue Solid Lines Represent the Participant's Response for Maternal Body Mass, Energy Intake (EI), Physical Activity Level (PAL), and the Intervention Component Dosages; Black Dash-dot Lines Represents the Case with no Intervention. 211

5.6 Example of Simulation Responses Using Single-rate Control System with $K_s = 0$. Red Dash Lines Represent Setpoint Applied on a Daily Basis; Blue Solid Lines Represent the Participant's Response for Maternal Body Mass, Energy Intake (EI), Physical Activity Level (PAL), and the Intervention Component Dosages; Black Dash-dot Lines Represents the Case with no Intervention. . . 212

Chapter 1

INTRODUCTION

1.1 Motivation

Control engineering focuses on the modeling of a diverse range of dynamic systems and the design of controllers that will make these systems behave in a desired manner. It has a wide range of applications, from flight and propulsion systems in commercial airliners, to the cruise control present in many modern automobiles. Traditional applications of control engineering include those systems that can be mechanical, electrical, fluid, chemical, industrial, aerospace, robotic, power systems and electronics. With the rise of mobile and computerized technologies, and the increased access to the data and information, the application of control engineering concepts to physical systems has increased extensively in the past decade [15]. In recent years, there have been increasing interest on the application of control to non-conventional areas, such as biology and medicine [16, 17], social and behavioral science [1, 10, 15, 18–20], supply chains [21–23] and economics [24].

In this dissertation, we address the application of control engineering to adaptive sequential behavioral intervention problems in the field of behavioral medicine, the potential of which still remains untapped. A behavioral intervention can be defined as a program aimed at improving individual's behavior for the purpose of preventing and treating disease, promoting health, and enhancing well-being [25]. These programs play a prominent role in addressing many important public health concerns, including the abuse of alcohol, tobacco, and other drugs, sexually transmitted infections, cancer screening, mental illness and obesity [26]. Most behavioral interventions are treatment packages made up of multiple components; some components may be pharmacological, while others might be behavioral (e.g., clinician counseling) or community-based (e.g. public alcohol association) [15].

Recently, adaptive interventions have been proposed as a new perspective on research-based prevention and treatment [25]. Adaptive interventions are much like clinical practice [25, 27] which relies on periodic assessment to gauge whether the treatment selected initially is in fact proving helpful. If it is not, adjustments in procedures will be necessary, perhaps several times over the course of the treatment. Because adaptive interventions are tailored to the specific needs of each individual, they have the potential for improved outcomes by enhancing potency, increasing compliance, conserving resources (e.g., cost savings), and reducing any negative effects associated with treatment, in contrast to traditional fixed interventions which provide the same dosages of prevention or treatment components to all program participants without considering any individual dynamics [7,28]. This is the motivating principle for adaptive interventions [25] , which are also referred to as "just-in-time" interventions [27]. The use of adaptive interventions in which the dosage is adapted according to the participant's response over time demonstrates that they constitute a form of engineering control system in behavioral health, which indicates the potential opportunity for employing control-oriented approach to the design of optimized behavioral interventions, and this draws the attentions from the researchers in the field of both control engineering and behavioral science [15, 20, 23, 25, 29–31]. Hence, control engineering can have a crucial influence in developing and improving the efficacy of adaptive, time-varying interventions [25].

1.2 Adaptive Interventions

With recent understanding and advancements in genetics (such as the human genome project), metabolism and pharmacology, there has been increasing interest in the medical community toward developing improved strategies for treating disease by relying on personalized medicine [32]. Adaptive interventions are interventions in which the type and the dosage of the intervention offered to patients is individualized based on patient's charac-

teristics or clinical presentation, and then repeatedly adjusted over time in response to their ongoing performance. This approach is based on the concept that patients differ in their responses to interventions. In order for an intervention to be most effective, it should be individualized and repeatedly adapted over time to individual progress [33]. An adaptive intervention is a multi-stage process that can be operationalized via a sequence of decision rules that recommend when and how much to adapt intervention so that it can link the response of the individual with the specific levels and types of intervention components to maximize long-term primary outcomes. These recommendations are based not only on patients' characteristics but also on intermediate outcomes collected during the intervention, such as the patient's response or adherence [25].

There are many reasons for considering adaptive interventions. First, each individual may vary in his/her response to intervention. Some may respond well to the same intervention type, intensity or duration, while others may not. Second, the effectiveness of an intervention may change over time due to dynamically evolving risk or resiliency (e.g., exogenous disturbances). Therefore, it is important to decide which intervention should follow accordingly if the current one is no longer working. A third reason for considering an adaptive intervention is the presence of comorbidities or its evolution, which require decisions regarding which should be treated first or whether multiple disorders should be treated simultaneously. The fact that relapse may be common is the fourth reason. Fifth, the development of interventions in which the intensity of the treatment is reduced when possible is mainly motivated by the high cost of intensive interventions combined with possible burden and /or side effects. Finally, it is difficult to maintain adherence to interventions, which is another important reason to consider adaptive interventions [33].

Adaptive interventions resemble clinical practice in that different dosages of certain preventions or treatment components are assigned to different individuals, and/or within individuals across time, with dosage varying in response to the intervention needs of in-

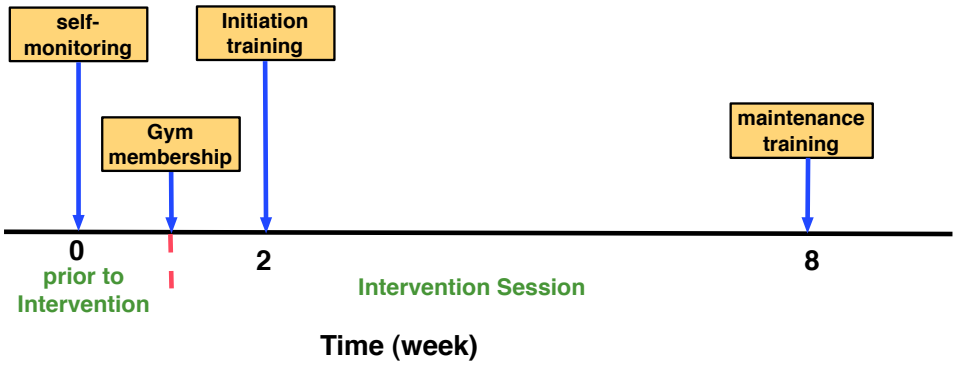

Figure 1.1: Sequential Decisions in the Intervention Project Active Adult Mentoring Program (AAMP) [8].

dividuals. In order to determine intervention need and thus assign dosage, adaptive interventions use pre-specified decision rules based on each participant's values on key characteristics, called tailoring variables (the outcomes of the intervention) [25]. Adaptive interventions describe the use of individualized optimal strategies for prevention, treatment and management of chronic and relapsing disorders.

1.3 Sequential Behavioral Interventions

In behavioral health problem settings, there are some unique clinical considerations and constraints which are different from the ones in traditional problem arenas. Notably, the multiple intervention components featured in adaptive interventions often require behavioral scientists formulating and evaluating decision rules that dictate the proper dosage sequence, that is, the order in which each component should be augmented, reduced or kept unchanged. This basically results from the fact that some intervention components have to be introduced or augmented before the others. For example, Project Active Adult Mentoring Program (AAMP) is an intervention to promote physical activity in older adults [8], and it features four sequenced intervention components depicted in Figure 1.1. Prior to the intervention (week 0), all participants receive self-monitoring component and are encouraged to track their behavior daily. At week 1, the gym membership is given to the

Table 1.1: Summary of Dosage Augmentations and Reductions per the IF-THEN Decision Rules for GWG Adaptive Intervention [1].

Options	**Adaptation**
Step down 3	reduction of other components
Step down 2	reduction of healthy eating active learning
Step down 1	reduction of physical activity active learning
Baseline	base dose for all components
Step up 1	first augmentation of healthy eating active learning
Step up 2	second augmentation of healthy eating active learning
Step up 3	first augmentation of physical activity active learning
Step up 4	second augmentation of physical activity active learning
Step up 5	third augmentation of physical activity active learning

participants so that they can have access to the community exercise facility. From week 2 to 7, the initiation training focused on self-management skills for physical activity initiation is offered, while week 8-12 emphasizes the maintenance training where content focused on relapse prevention and developing a plan to transition to a home- or community-based exercise routines [8]. This example illustrates that these four components are introduced in an established pre-ordained sequence instead of any arbitrary sequence.

Another example of sequential decisions can be found in a gestational weight gain (GWG) behavioral intervention, which is shown in Table 1.1, where an active learning component for physical activity may not be offered until healthy eating active learning component has reached full doses for the adaptation above the baseline program (step up 1 to 5); while the reduction sequence of the components above the baseline requires that healthy eating active learning component will be sustained at its maximum doses until physical activity active learning returns to the base level. Meanwhile, there are also reduction sequence rules below the baseline (step down 1 to 3) as specified in Table 1.1, with the elimination of physical activity active learning first, followed by healthy eating active learning, and other components; and the augmentation sequence from zero dose to

baseline is in the opposite order. Clearly, the sequential decisions in GWG intervention are more complicated than the ones in AAMP intervention, and however, all these unique dosage sequences still have to be systematically addressed when the optimized adaptive interventions are designed.

As mentioned earlier, behavioral interventions address a wide number of public healthy disorders. Among these, GWG intervention is an excellent representative featuring sequential decision policies that address the augmentation and reduction rules. Therefore, this dissertation uses the GWG problem as an example to exemplify and demonstrate how a control-oriented approach can be employed to design and optimize a broad class of adaptive sequential behavioral interventions.

1.4 Excessive Gestational Weight Gain (GWG)

High pre-pregnancy body mass index (BMI) and excessive GWG have become increasingly important public health concerns. Current research shows that excessive weigh gain during pregnancy is associated with maternal obesity post-partum and a number of adverse pregnancy outcomes, such as gestational diabetes mellitus, pregnancy-related hypertension, complications through labor and delivery, and macrosomia [5, 34]. Excessive GWG is also a potential prenatal risk factor for childhood obesity [35]. Thus, preventing high GWG during pregnancy can impact the etiology of obesity development for offspring at a critical time in the life cycle. Meanwhile, most women are concerned about the health of their baby during pregnancy; this also makes pregnancy an opportune moment in the life course to promote healthy lifestyle behaviors for the purpose of weight management.

Among pregnant women, the prevalence of overweight and obesity (BMI $\geq$ 25 kg/m^2 and BMI $\geq$ 30 kg/m^2 respectively) has almost doubled in the last 20 years, from 29.7% in 1983 to 53.7% in 2011, with almost 50% of pregnant women in the United States now entering their pregnancies as either overweight or obese [36]. The American College of Ob-

stetricians and Gynecologists emphasizes the significance to limit excessive weight gain to ensure the health of a woman and her infant [37]. In 2009, the Institute of Medicine (IOM) published the revised recommendations [5] for how much weight a woman should gain during pregnancy based on their pre-gravid BMI. Meanwhile, the World Health Organization (WHO) [38] also advocate for preventive interventions among pregnant women to assist them in meeting the IOM guidelines, and thereby optimizing both maternal and child outcomes. The IOM recommends that overweight and obese pregnant women (OW/OBPW) gain 6.5-10.6 kg (14.33-23.37 lbs) and 4.9-9 kg (10.80-19.84 lbs), respectively. With the prevention efforts, despite of the fact that 20% of underweight women and 37% of normal-weight women exceed the goals [39]; nearly 60% of overweight women and 50% of obese women exceed the GWG guidelines [5]. These data indicates that the traditional interventions appear to reduce the risk of adverse pregnancy outcomes among normal weight women [40, 41], and however, behavioral intervention studies show little to no evidence for effectively intervening and preventing excessive GWG among overweight and obese women. Therefore, there is a critical need to develop scalable, effective and affordable interventions to help OW/OBPW prevent high GWG.

One potential reason for why the traditional interventions have had some success among normal weight but not overweight and obese mothers is that OW/OBPW may have barriers that require a higher dosage of intervention (i.e., more intensive approach) to managing GWG in pregnancy. Although past GWG interventions have yielded some degree of effectiveness, a limitation of these interventions is that the majority have relied on a "one size fits all" approach in which a single set of intervention components and dosage (i.e., fixed, time-invariant intervention) is delivered to all participants. Thus, whether or not an intervention is effective for an individual depends on the components and dosage selected. As pointed out earlier, adaptive interventions have the potential to be more effective, conserve resources (i.e., cost savings), and reduce stigma compared to fixed interventions [25],

because they are tailored to the specific needs and challenges of each woman.

1.5 Research Goals

The conceptual linkages between the problem of adaptive interventions and control engineering can be understood by treating adaptive, time-varying interventions as closed-loop control systems, with the outcome variable (also known as tailoring variable [25]) acting as the controlled variable, the intervention representing the manipulated variables, and the decision policies serving the role of feedback (and feedforward) control laws. The dynamics of the intervention without decision policies can be treated as "open-loop" model to design the controller which is able to assign optimized dosages based on the participant's response. If the measurements of external variables (e.g., disturbance) that influence participant response are available, these can be incorporated in the controller algorithm in a feedforward manner [23]. Therefore, this dissertation aims to providing a systematic and efficient approach to designing and implementing the optimized adaptive sequential behavioral intervention for the prevention of GWG problem, relying on dynamical modeling, control engineering principles, and formal optimization methods.

1.5.1 Dynamical Modeling

One of the primary goals of this research is to improve the understanding of behavioral intervention to prevent excessive GWG by expressing these as dynamical systems. Dynamical system modeling considers how the system output variables (e.g. GWG) respond to the changes of input variables (e.g. intensity and frequency of intervention components, energy intake, physical activity) over time, which can be used to address the questions regarding what variables to measure, how often, and the speed and shape of the outcome responses as a result of decisions regarding the timing, spacing, and dosage levels of intervention components.

Evidence suggests that many factors influence GWG including behavioral (energy in-

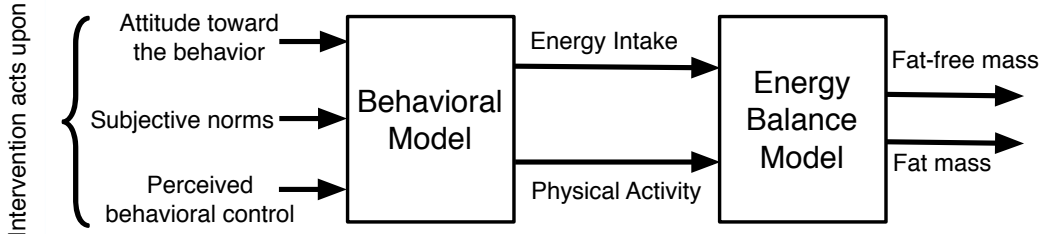

Figure 1.2: General Conceptual Diagram of the Dynamical Systems Model for GWG Change

take and physical activity), psychological (attitudes, subjective norms, perceived behavioral control, intentions), sociodemographic (age, parity), and physical (BMI) factors [5]. Thus, GWG is a dynamical process; interventions are needed that consider how changes in these factors influence changes in GWG.

To achieve this goal, a dynamical systems model for GWG is developed in this dissertation, which relies on integrating a mechanistic energy balance model with dynamical behavior model, illustrated in Figure 1.2 that shows a general diagram of the dynamical systems model for GWG change. The energy balance model predicts the changes in body mass as a result of energy intake and physical activity, while the behavioral model considers how maternal energy intake and physical activity are affected by behavioral variables, such as attitude toward the behavior, subjective norms, and perceived behavioral control. This model can be used to answer questions regarding how much to eat, how much physical activity to undertake, and how the dosages of the intervention components have an impact on GWG.

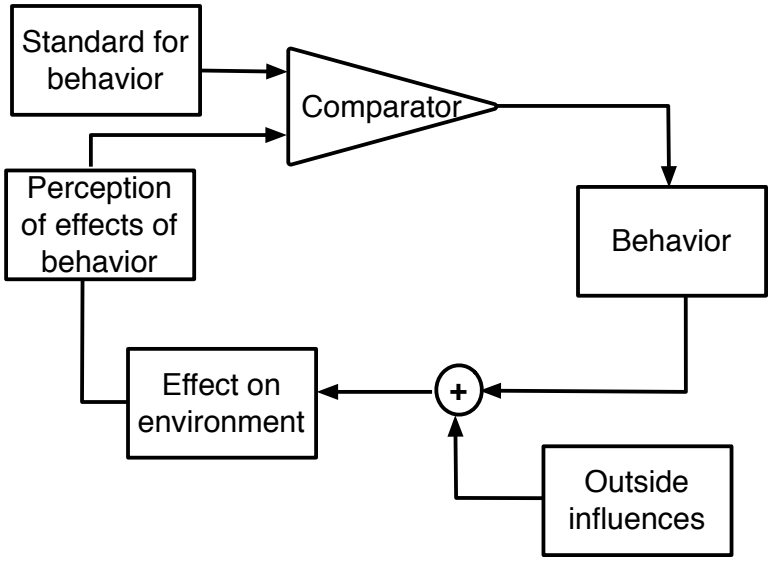

Figure 1.3: Illustration of Self-regulation: Behavior and Perception as Elements of a Feedback Loop Guiding Human Action [9]

1.5.2 Controller Formulations for Self-Regulatory Process

The understanding of behavioral intervention can be extended towards the modeling of self-regulatory process using control-oriented approach. Self-regulation describes how success expectancies during the intervention influence a participant's motivation to achieve a goal. It assumes that human behavior is goal-directed and regulated by feedback control processes, which is illustrated in Figure 1.3, where self-regulation is generally a feedback control loop. In this dissertation, the initial approach to modeling self-regulation is a simple derivative-only controller, which relies on the rate of the improvement. Later in the dissertation, advanced control engineering strategies are applied to the formulation of self-regulatory process that offers significant flexibility in describing a participant's self-regulatory behavior through the tuning parameters.

Figure 1.4 illustrates how self-regulatory process along with behavior model play an important role in depicting an individual's behavior change. Self-regulation not only con-

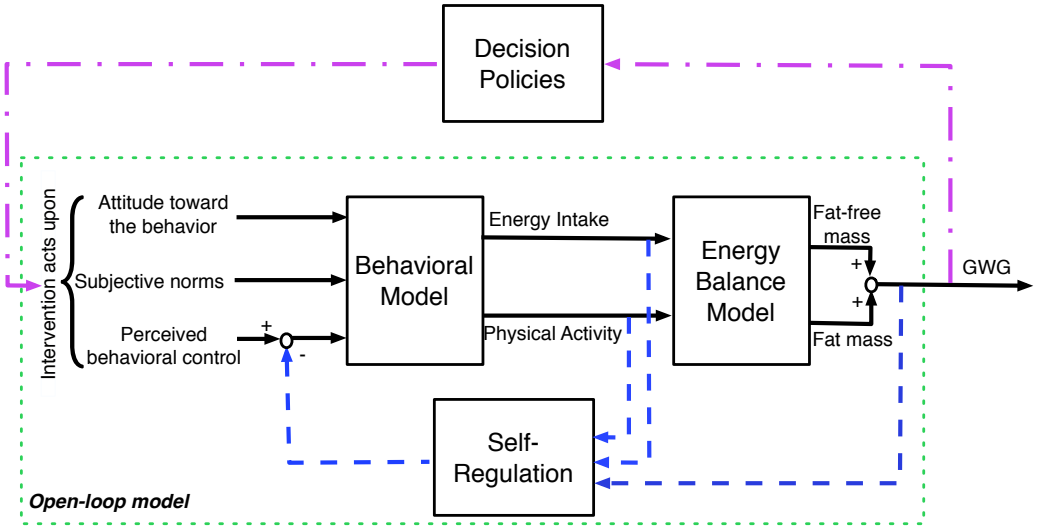

Figure 1.4: General Conceptual Diagram of the Dynamical Systems Model for GWG Adaptive Intervention. Blue Dash Line Represents the Information Needed in Self-regulatory Process, and the Pink Dot-dash Line Stands for the Information Exchanged in the Control-oriented Decision Policies.

stitutes an inner control loop of the dynamical systems model, but also serves as a part of open-loop model to design optimized adaptive intervention. This dynamical systems model for GWG intervention which includes energy balance, the Theory of Planned Behavior, self-regulation, and intervention delivery dynamics where intervention acts upon the three inputs to the behavioral model, can be used by behavioral scientists to evaluate decision rules that would enable adaptive time-varying behavioral interventions, improve the understanding of the optimal choices on the level and duration of intervention components, and how intra-individual and inter-individual variabilities have a great impact on the intervention outcomes, or serve as the basis for applying advanced control engineering strategies (will be discussed in the ensuing subsection), such as Model Predictive Control (MPC) to act as a decision framework for dosage selection in the adaptive interventions.

1.5.3 Optimization-based Control for Sequential Decision Policies

In a control engineering approach to optimizing an adaptive time-varying intervention, the controller assigns dosages of each intervention component to the participant as dictated by model dynamics, problem constraints, and disturbances. We use control algorithms to generate the intervention dosage levels required for the participant based on the open-loop dynamical model. Usually, the simple approach used in adaptive interventions, such as IF-THEN rules, will not yield good performance for a lagged response [15]. Therefore, we try to rely on a well-designed control system to assign systematic dosages based on model dynamics and performance requirements of the intervention.

Optimization-based control refers to the use of online, optimal trajectory generation as feedback loop of a control system. The basic idea is to use a receding horizon control technique (also called Model Predictive Control). This dissertation focuses on the development of an intervention algorithm relying on Model Predictive Control (MPC) framework which systematically personalize the sequence and composition of GWG adaptive sequential behavioral interventions, as depicted in Table 1.1. This control algorithm makes use of feedback and feedforward control action by online optimization of a cost function using a receding horizon and well suited for designing behavioral interventions featuring multiple intervention components. The feedforward control action of MPC is very useful for addressing disturbances which may be known a *priori* or can be measured in the course of the intervention, while the feedback control action can respond to unmeasured disturbance. The discrete nature of the intervention dosage assignment indicates that Hybrid Model Predictive Control (HMPC) schemes [23, 42] should be considered. The novel technical consideration featured in the HMPC controller design for such an adaptive lies in how to systematically address the logical specifications associated with pre-defined dosage sequence.

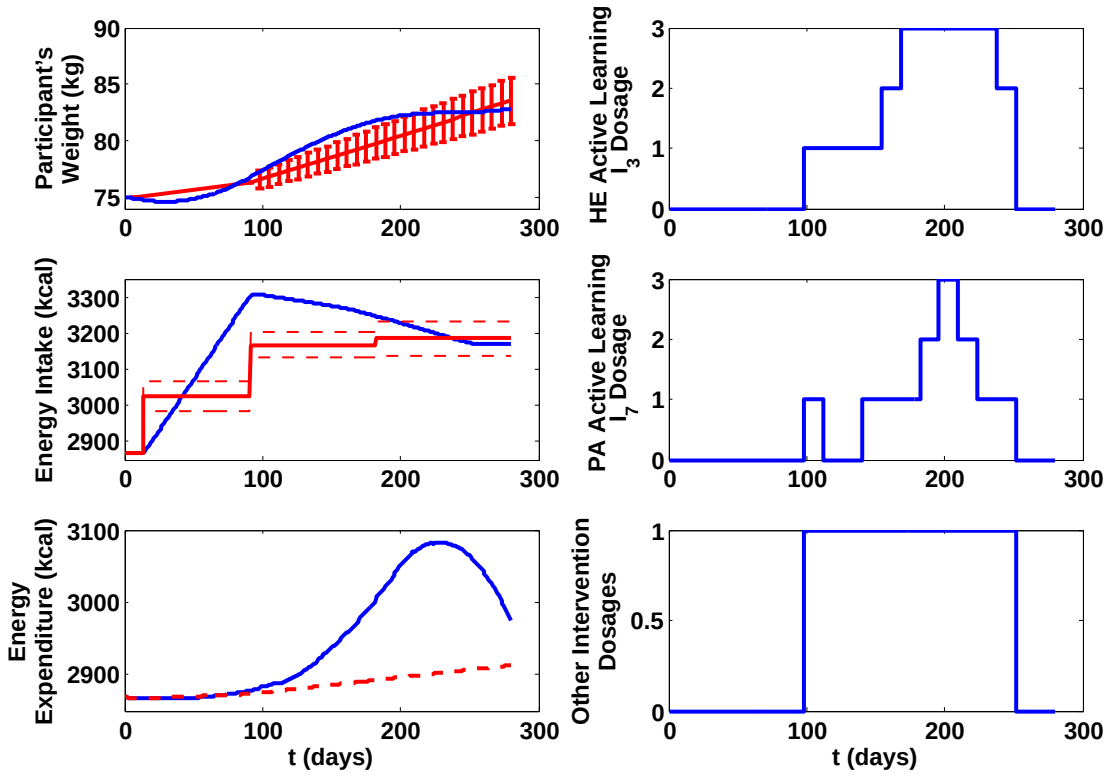

Figure 1.5: Performance of Hybrid Model Predictive Control (HMPC) as a Decision Policy to Follow Set Point Change, Measured Disturbance (Energy Intake Increase), and Unmeasured Disturbance (Physical Activity Level Lowers at the Third Trimester). Reference Values are Shown by Red Lines.

Figure 1.5 is a simulation example for GWG adaptive intervention. Based on the dynamical systems model developed and illustrated in Figure 1.4, we use the HMPC with three-degree-of-freedom (3 DoF) to assign the optimized dosages, with 3 DoF tuning parameters $\alpha_r = 0.9$, $\alpha_d = 0.1$,$f_a = 0.9$. This case study assumes that the participant enters the intervention with the baseline program at week 14. The adaptation of this GWG intervention follows pre-defined augmentation and reduction rules, as depicted in Table 1.1. Therefore, the HMPC algorithm assigns the optimized discrete dosages subject to the process constraints and any other constraints that enforce the generation of pre-defined se-

quential decision policies. Other clinical considerations and constraints that are common in behavioral health problem settings are introduced, and systematically taken into account as well via an HMPC framework. The detailed development of HMPC algorithm for adaptive sequential behavioral intervention will be discussed in Chapter 4.

1.5.4 Gain-Scheduling Parameter Varying Control and Multi-Rate Digital Control

When the changes in process dynamics are nonlinear, it is possible to change the parameters of the controller by monitoring the operating conditions of the process. This idea is called gain scheduling, perhaps one of the most popular nonlinear control design approaches which have been widely and successfully used, and this scheme was originally used to refer to the changes in process gain only. Gain-scheduling is a nonlinear control strategy; it incorporates a set of linear controllers whose parameters are changed as a function of operating conditions in a pre-programmed way.

In this dissertation, the dynamical systems model of GWG intervention is initially developed by the use of linear time-invariant equations. However, there might exist nonlinearity in the model. Such kind of problem can be addressed using the gain-scheduling parameter varying control scheme that we introduced above.

Meanwhile, the real-life pilot study and clinical trial might involve measurements sampled at multiple rates in this GWG intervention. This requires considering multi-rate digital control system. Muti-rate systems occur when signals comprising a system are sampled at different rates. Usually, such case arises when one process outputs are measurable only with large intervals, while the other measurements must be utilized in order to design an effective control system. For example, in the control of product compositions in distillation columns and packed-bed reactors, where sampling delays associated with composition measurements can be quite significant. Temperatures which have some direct or indirect relationships with the product compositions are measured in order to improve the speed of

the response. This also means that the temperatures are typically sampled at a faster rate than the compositions. Multi-rate controllers usually offer better performance than single-rate controllers due to the extra degrees of freedom they allow in manipulating control variables [14]. Therefore, it is conducive to building a multi-rate control system for GWG intervention that is able to make use of the fast sampling measurements to estimate the variables, while the slow sampling measurements can be used to make the extra adjustments of the estimation of these variables.

1.6 Contributions of the Dissertation

This dissertation uses the GWG problem to exemplify and present how a control-oriented approach can be employed to designing optimized adaptive sequential behavioral intervention. It offers a novel and valuable intervention paradigm that systematically individualizes treatment and prevention policies. As discussed in the previous section, we consider the initial problem of modeling the dynamics of such an intervention, with the ultimate goal to develop a real-life implementation of the HMPC-based intervention that is both practical and useful in behavioral settings.

In this dissertation, models corresponding to the behavioral models are developed on the basis of the concept of fluid analogies, as developed in [43]. We focus on the following modules which consist primarily of a network of production-inventory systems that is akin to a supply chain,

- Energy balance model for gestational weight gain;
- The theory of planned behavior (TPB) and its fluid analogy (behavioral model);
- Self-regulation theory (behavioral model);
- Intervention delivery dynamics;
- Hypothetical decision rules or decision policies.

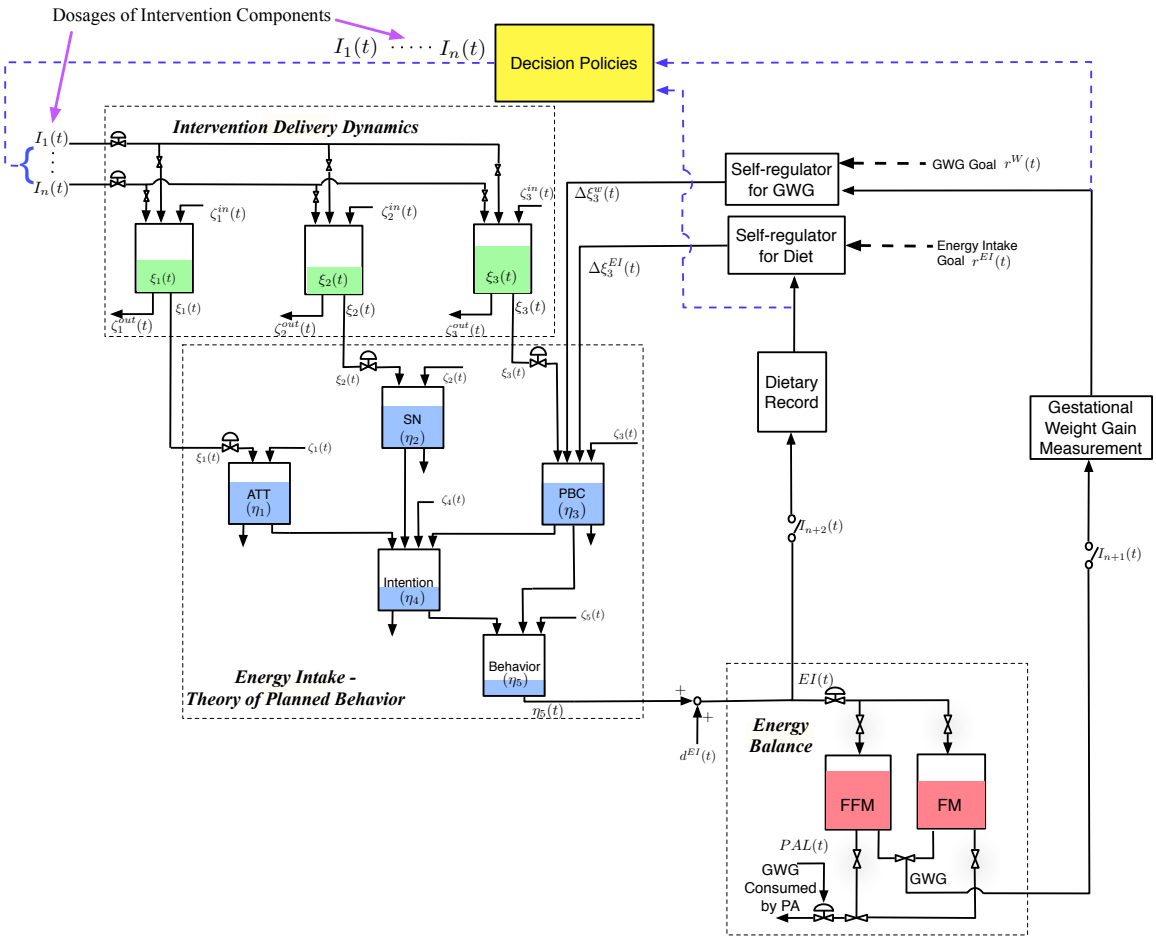

Figure 1.6: Comprehensive Fluid Analogy and Interrelationship between Systems in a Behavioral Intervention for GWG, Shown for the Energy Intake Loop.

Figure 1.6 illustrate the comprehensive fluid analogy and interrelationship between the above systems for the energy intake loop.

As we can see, the dynamical systems model for behavioral intervention to manage GWG requires incorporating both physiological and psychological considerations. For the physiological component, we rely on the concept of energy balance to obtain the model that describe the net effect of maternal energy intake from the food minus maternal energy consumption through physical activity. For the psychological component, we consider a model inspired by the Theory of Planned Behavior (TPB) for the dynamics of diet (energy intake)

and exercise (physical activity) behavior. Besides these two models, an intervention delivery module is required to relate the magnitude and duration of intervention components to the inputs of the TPB models, and the self-regulation module is necessary to model how success expectancies during the intervention influence a participant's motivation to achieve a goal.

The contributions of this dissertation in terms of controller formulations of self-regulatory process can be summarized as follows:

- Development of two self-regulation structures on the basis of a two-degree-of-freedom (2 DoF) Internal Model Control (IMC) strategy, associated with energy intake reference values and weight gain setpoints. The controller tuning rules are illustrated through the simulation.

- Extension of self-regulation formulation by the use of cascade control to make use of all the available measurements in the real-life clinical trial. Multiple cascade control structures are designed and analyzed. Simulation examples are shown to demonstrate the best suitable formulation, which is then compared with the previous 2 DoF IMC strategy.

- Demonstration of the importance that intra-individual and inter-individual variabilities play in the intervention outcomes using the improved self-regulatory process that offers significant flexibility in describing individual's self-regulatory behavior through the tuning parameters.

The contributions of this dissertation in terms of Hybrid Model Predictive Control as sequential decision policies in adaptive intervention can be summarized as follows:

- Development of a novel intervention algorithm relying on Hybrid Model Predictive Control (HMPC) framework that is able to personalize and optimize the treatment of

behavioral interventions.

- Generation of sequential decision policies in adaptive intervention using Mixed Logical Dynamics (MLD)-based HMPC schemes through a user-specified dosage sequence table involving the adapted intervention components, and the corresponding definition of mixed-integer linear inequalities.

- Improvement of the HMPC algorithm by introducing a switching time strategy to address the difference in frequency between intervention decision and sampling intervals.

- Extension of the traditional MLD structure by introducing additional binary variables to restrict the manipulation of only one input at a time. This extension makes our HMPC algorithm for adaptive sequential interventions more generalizable.

The contributions of this dissertation associated with real-life GWG intervention scenario are summarized in the following two points:

- Development of gain-scheduling for Model Predictive Control framework in GWG intervention to address the potential nonlinearity within the model.

- Development of cascade filters for dual-rate GWG system by introducing an additional filter for the slowly-measured energy intake variable.

Although the prevention of excessive GWG is the focus of this dissertation as an illustration and only represents a special case in behavioral interventions, the control engineering techniques are developed in this dissertation without any loss of generality, and hence can be applied to other adaptive sequential behavioral interventions, such as the formulation of the self-regulation, and the HMPC formulation as sequential decision policies involving multiple intervention components to achieve optimized dosage assignments.

1.7 Publication Summary

Most of the work described in this dissertation has been published or submitted for review. The publications are listed as follows,

1. Y. Dong, D. E. Rivera, D. S. Downs, J. S. Savage. A dynamic simulation model for gestational weight gain adaptive interventions; submitted to *Mathematical and Computer Modeling of Dynamical Systems*, 2014.

2. Y. Dong, D. E. Rivera, D. S. Downs, J. S. Savage, J. E. Navarro-Barrientos, and L. M. Collins. A dynamical systems model for adaptive behavioral interventions to manage gestational weight gain; submitted to *Journal of Diabetes Science and Technology*, 2014.

3. J. S. Savage, D. S. Downs, Y. Dong, and D. E. Rivera. Control systems engineering for optimizing a prenatal weight gain intervention to regulate infant birth weight; *American Journal of Public Health*, 104(7): 1247-1254, July 2014.

4. Y. Dong, S. Deshpande, D. E. Rivera, D. S. Downs and J. S. Savage. Hybrid Model Predictive Control for Sequential Decision Policies in Adaptive Behavioral Interventions; In *Proceedings of the 2014 American Control Conference*, pages 4198-4203, Portland, Oregon, USA, June 4 - June 6, 2014.

5. Y. Dong, D. E. Rivera, D. S. Downs, J. S. Savage, D. M. Thomas, and L. M. Collins. Hybrid model predictive control for optimizing gestational weight gain behavioral interventions. In *Proceedings of the 2013 American Control Conference*, pages 1973-1978, Washington, D.C, USA, June 17 - June 19, 2013.

6. Y. Dong, D. E. Rivera, D. M. Thomas, J. E. Navarro-Barrientos, D. S. Downs, J. S. Savage, and L. M. Collins. A dynamical systems model for improving gestational

weight gain behavioral interventions. In *Proceedings of the 2012 American Control Conference*, pages 4059 - 4064, Montréal, Quebec, Canada, June 27 - June 29, 2012.

The presentations at the conference associated with the work in this dissertation are as follows,

1. D. S. Downs, J. S. Savage, D. E. Rivera, Y. Dong, and L. M. Collins. Lessons Learned: Feasibility of Implementing an Individually-Tailored, Adaptive "Just in Time" Intervention to Manage Gestational Weight Gain; In *2014 Conference of Society for Prevention Research*, Washington, D.C, USA, May 27 - May 30, 2014. (presentation only)

2. Y. Dong, D. E. Rivera, D. S. Downs, J. S. Savage, and L. M. Collins. Theory of planned behavior with self-regulation dynamical systems model for an adaptive intervention to manage gestational weight gain; In *2014 Annual Meeting of the Society of Behavioral Medicine*, Philadelphia, PA, USA, April 23 - April 26, 2014. (presentation only)

3. D. S. Downs, J. S. Savage, D. E. Rivera, Y. Dong, and L. M. Collins. Control Systems Engineering for optimizing an individually-tailored, adaptive intervention to manage gestational weight gain; In *2014 Annual Meeting of the Society of Behavioral Medicine*, Philadelphia, PA, USA, April 23 - April 26, 2014. (presentation only)

4. Y. Dong, D. E. Rivera, D. M. Thomas, D. S. Downs, J. S. Savage, and L. M. Collins. A dynamical systems model of an adaptive intervention to prevent excessive gestational weight gain. In *2012 Conference of Society for Prevention Research*, page 77 (116), Washington, D.C, USA, May 29 - June 1, 2012. (presentation only)

Two additional publications are under preparation,

1. Y. Dong, D. E. Rivera, D. S. Downs, J. S. Savage. Hybrid Model Predictive Control design for optimized gestational weight gain interventions; to be submitted to *Control Engineering Practice*

2. Y. Dong, D. E. Rivera, D. S. Downs, J. S. Savage. Optimized adaptive behavioral interventions with sequential decision policies using Hybrid Model Predictive Control; to be submitted to *IEEE Trans. on Control Systems Technology*

1.8 Dissertation Outline

Following this introduction, this dissertation continues Chapter 2 with modeling overview which presents how to develop the dynamical systems model for the GWG problem. The chapter focuses on the introduction and development of each module in the overall schematic representation for an adaptive GWG intervention, and the illustration of how to associate this dynamical model with production-inventory systems. The final section of the chapter extends our work to discuss how our intervention not only manages GWG for the mother, but also alters the obesogenic fetus environment to regulate infant birth weight by including fetal energy balance model into our existing model.

In Chapter 3, advanced controller formulations for self-regulation are developed, including two-degree-of-freedom (2 DoF) internal model control (IMC), three cascade control structures relying on IMC strategy. We analyze the "pros and cons" of each formulation through the design structure and simulation examples. The simulation studies aim at the illustration of how adaptive interventions deliver great degrees of efficacy according to the participant's unique changing needs and responses, leading to overall improved and more effective intervention through the comparison with fixed interventions, and the understanding of the variabilities within a participant and between the participants.

Chapter 4 presents an MLD-based HMPC scheme that offers a potential valuable framework to design optimized adaptive sequential behavioral interventions. The unique clinical

considerations and constraints in behavioral health problem settings are summarized, and are systematically addressed through mixed-integer linear constraints in MLD structure. These are achieved by the use of propositional logic, a user-specified dosage sequence table, the manipulation of one input at a time, and a switching time strategy for assigning dosages at time intervals less frequent than the measurement sampling interval. The simulation studies are shown to verify how HMPC-based intervention assigns the optimized discrete dosages, with its change following pre-defined dosage sequence, highlight why HMPC-based intervention can adjust the dosages of the intervention components in a timely manner through the comparison with adaptive intervention using decision rules, and illustrate how to generate other different pre-defined dosage sequence in behavioral intervention within the HMPC framework.

Chapter 5 improves the simulation work to address real-life scenarios in the GWG intervention by introducing gain-scheduling parameter varying control for addressing the nonlinearity within the model, and a cascade filter design for multi-rate control system. Illustrative numerical examples are shown to highlight the basic workings of these two enhancements.

We conclude the dissertation in Chapter 6 with a summary of the important conclusions and advances achieved in this study. This chapter also includes the direction and comments for future work.

Chapter 2

MODELING OVERVIEW

2.1 Overview

It was established in the last chapter that gestational weight gain (GWG) interventions serve as excellent examples of sequential behavioral interventions. This chapter describes important aspects of the adaptive GWG problem that will be featured throughout the dissertation and will be part of work developed in future chapters.

GWG is a strong predictor of adverse healthy outcomes, particularly obesity and diabetes for both childbearing women and their offspring. In this chapter, dynamical systems modeling will be used to describe how an individually-tailored, behavioral intervention that adapts to the needs of each woman impacts GWG. Thus, the initial approach is to establish a dynamical systems model for a behavioral intervention to manage GWG, which demonstrates how to integrate a mechanistic energy balance model with some dynamical behavioral models that incorporate some well-accepted concepts from psychology: the Theory of Planned Behavior (TPB) and the principles of self-regulation. Some illustrative decision rules are applied to the model to dictate when and how each intervention component should be augmented, reduced or kept unchanged. Lastly, the extension of the GWG dynamical model includes the fetal birth weight model, which demonstrates how the proper design of adaptive intervention can reduce fetus exposure to an "obesogenic" intrauterine environment that can promote healthy GWG and infant birth weight. The overall model can play a useful role in the evaluation of decision policies; the application of the decision framework to the dynamical system and the corresponding simulations can aid the intervention scientists to try out and select the decision rules.

Figure 2.1 [10] shows the overall schematic representation for an adaptive GWG intervention which can be divided into five main segments: (1) a two-compartment energy

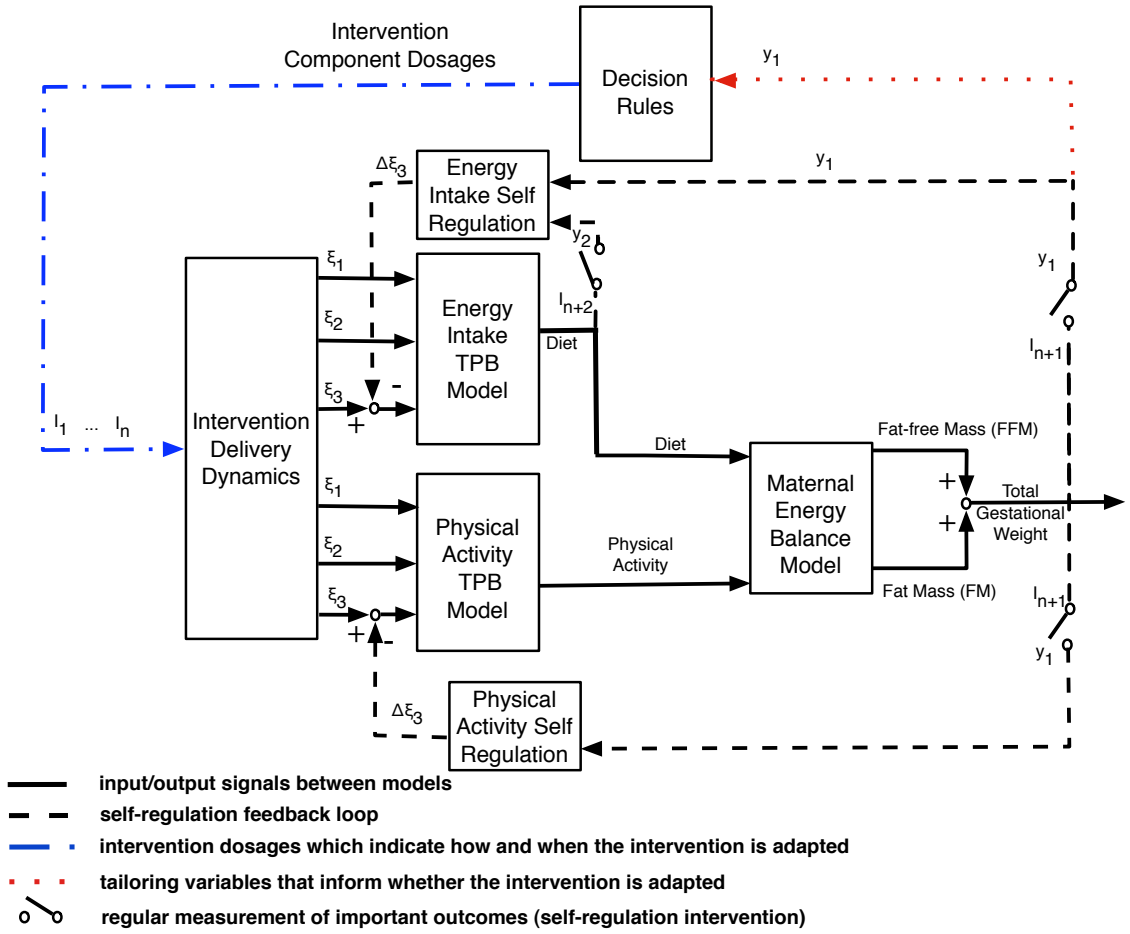

Figure 2.1: Overall Schematic Representation for an Adaptive Gestational Weight Gain (GWG) Intervention [10].

balance model predicting changes in body mass as a result of energy intake (EI) and physical activity (PA), (2) two Theory of Planned Behavior (TPB) models describing how maternal EI and PA, respectively, are affected by behavioral variables, (3) two self-regulation modules illustrating how self-monitoring during the intervention influences a participant's motivation to achieve a goal, (4) an intervention delivery dynamics that relates the magnitude and duration of intervention components to the inputs of the TPB models, and (5) the decision rules informing when and how to adapt intervention dosages for each overweight and obese pregnant woman (OW/OBPW) and enabling tailoring of the intervention to the

specific needs of each woman. Each module is described in more detail in the ensuing section.

2.2 Energy Balance Model

This section presents the maternal weight gain energy balance model derived from the dynamic energy balance models for non-pregnant individuals. There are two main inputs or factors in the problem of assessing GWG: (i) energy intake or diet; and (ii) physical activity or exercise. The basic dynamics governing energy balance for GWG is based on the two-compartment model developed by Thomas *et al.* [4]. Their work was built on the basis of a valid population study.

2.2.1 Model Description

The energy balance model for GWG relies on the conservation of the energy, which can be expressed as,

$$ES(t) = EI(t) - EE(t) \tag{2.1}$$

where *ES(t)* represents the rate of energy stored, *EI(t)* is the rate of energy intake and *EE(t)* is the rate of energy expenditure at time t, measured at daily intervals. The terms of the energy balance equation in (2.1) *ES*, *EI* and *EE* will be developed by separating maternal material, expressed in kg, into two compartments, maternal fat free mass (FFM) and maternal fat mass (FM). The sum of maternal FFM and FM represents total body mass (BM) or pregnancy weight (W):

$$W(t) = BM(t) = FM(t) + FFM(t) \tag{2.2}$$

In order to algebraically relate FFM to FM, Butte study data [2, 3] is applied. This relationship can be formulated via the reported relationships between the changes in FFM

Table 2.1: Expressions for Total Body Water as a Function of Gestational Weight per BMI Category, from [2, 3].

BMI Category	**Total Body Water (TBW)(L)**
Low BMI($\leq 19.8 kg/m^2$)	0.489W+3.875
Normal BMI($19.8 - 26 kg/m^2$)	0.4836W+2.853
High BMI($\geq 26 kg/m^2$)	0.503W+4.885

and pregnancy weight(W).

$$\Delta FFM = \Delta FFM(W) \tag{2.3}$$

In formulating an explicit function of $\Delta FFM(W)$, it requires consideration of how FFM changes during pregnancy in relation to weight. The major change in FFM from the pre-gravid state comes from growth of the uterus, breasts, intestines, blood volume [5] which can be captured by quantifying changes in total body water (TBW) and total body protein (TBP).

Maternal total body water (TBW) has been linearly related to GWG. The Butte study measured TBW through dilution of an orally administered dose of deuterated water at pregnancy and weeks 9, 22, 36 of gestation [2, 3]. Based on Butte's data for the different BMI categories, gestational body weight (W) is measured simultaneously and fit linearly with TBW function. The TBW functions for each BMI category are listed in Table 2.1.

Total body protein (TBP) can be related to gestational weight for each BMI category (Table 2.2), similar to the approach applied for TBW. In each BMI class, TBP was observed to decrease in the first trimester and increase thereafter. Consequently, the approximation of TBP is done as a piecewise linear equation. The advantage of a piecewise linear model is the tractability of solutions [4]. For the underweight BMI category, the derived

piecewise linear model is:

$$TBP = \begin{cases} -0.05W + 9.3 & \text{if W} \leq 52\text{kg} \\ 0.1W + 1.3 & \text{if } 52 < \text{W} \leq 57.7\text{kg} \\ 0.08W + 3.1 & \text{if W}{>}57.7\text{kg} \end{cases} \tag{2.4}$$

The breakpoint of 52 kg is a local minimum of the TBP formula as a function of weight. The breakpoint of 57.7 is a point of inflection as the TBP curve moves from concave up to concave down. The TBP functions for all BMI categories are summarized in Table 2.2.

Now we can formulate FFM as a function of gestational weight by summing pre-gravid FFM and the changes to FFM that occur during pregnancy. We modeled maternal FFM as the sum of pre-gravid FFM ($FFM(0)$), TBW and TBP functions.

$$FFM = FFM(0) + \Delta FFM(W) = FFM(0) + \Delta TBW(W) + \Delta TBP(W) \tag{2.5}$$

The expression of FFM in (2.5) is only a function of pregnancy weight (W) which is also a function of FFM and FM expressed in (2.2), therefore (2.5) shows the relationship between FFM and FM. Because the TBP function is defined as a piecewise function, the resulting function between FFM and FM must also be defined as a piecewise function with identical breakpoint.

By testing for the relation of total energy expenditures to W, FM, and FFM during gestation, EE was found linearly related to FFM [2, 3]. Table 2.3 shows the $EE(t)$ formulas derived from data [2] that are used within the energy balance equation.

The ES term is separated into two compartments of body energy: FFM and FM. Energy density of FM has been well established and documented in the literature as approximately 9500 kcal/kg [44]. Energy density of FFM differs during pregnancy. Based on chemical composition of tissues, 0.93% of FFM consists of glycogen. Analysis of the

Table 2.2: Expressions for Total Body Protein as a Function of Gestational Weight per BMI Category [2–4].

BMI Category	**Total Body Protein (TBP) function (kg)**
Low BMI($\leq 19.8 kg/m^2$)	$TBP = \begin{cases} -0.04762W + 9.28, & \text{if W} \leq 52\text{kg} \\ 0.105263W + 1.33, & \text{if } 52 < \text{W} \leq 57.7\text{kg} \\ 0.075472W + 3.05, & \text{if W}>57.7\text{kg} \end{cases}$
Normal BMI($19.8 - 26 kg/m^2$)	$TBP = \begin{cases} -0.667W + 47.533, & \text{if W} \leq 60.2\text{kg} \\ 0.0204W + 6.17, & \text{if } 60.2 < \text{W} \leq 65.1\text{kg} \\ 0.0724W + 2.783, & \text{if W}>65.1\text{kg} \end{cases}$
High BMI($\geq 26 kg/m^2$)	$TBP = \begin{cases} -0.03226W + 10.43871, & \text{if W} \leq 81.8\text{kg} \\ 0.1W - 0.38, & \text{if } 81.8 < \text{W} \leq 85.8\text{kg} \\ 0.098765W - 0.27407, & \text{if W}>85.8\text{kg} \end{cases}$

Table 2.3: Expressions for Total Energy Expenditure as a Function of Fat-free Mass (FFM) per BMI Category, from [2, 3].

BMI Category	**Energy Expenditure (EE(t)(kcal/d))**
Low BMI($\leq 19.8 kg/m^2$)	12.3FFM+1822
Normal BMI($19.8 - 26 kg/m^2$)	33.0FFM+1008.7
High BMI($\geq 26 kg/m^2$)	10.5FFM+2403.8

Butte study data revealed that on average 16.7% of FFM during pregnancy consists of protein. We calculated the energy density of FFM by using the energy density of 4380 kcal/kg for protein and 4200 kcal/kg for glycogen to arrive at the energy density of a kg of FFM during pregnancy:

$$4380 \times 0.167 + 0.0093 \times 4200 = 771 kcal/kg \tag{2.6}$$

The ES term is expanded into the instantaneous change of the sum of the two compartments (FFM an FM), multiplying by their respective energy densities as follows,

$$ES(t) = 771 \frac{dFFM(t)}{dt} + 9500 \frac{dFM(t)}{dt} \tag{2.7}$$

If we use ΔEI representing the average trimester dependent increase in energy intake during gestation, we can have,

$$771 \frac{dFFM}{dt} + 9500 \frac{dFM}{dt} = (1-g)(EI_0 + \Delta EI(t)) - EE \tag{2.8}$$

where g is nutrient partitioning constant and EI_0 is the initial energy intake.

The change ΔPA on the dimensionless physical activity level (PAL) from baseline is used to express changes in physical activity; its effect on the energy balance model is

obtained by multiplying $EE(t)$ by $(1+\Delta PA)$. Our final energy balance model is as follows,

$$771\frac{dFFM}{dt}+9500\frac{dFM}{dt}=(1-g)(EI_0+\Delta EI(t))-(1+\Delta PA(t))EE(t) \tag{2.9}$$

2.2.2 *Initialization*

For the initialization of the model, one of the assumptions is that initially the maternal energy is balanced, i.e. ES=0 in (2.1). Thus, we can estimate the initial energy intake EI_0 using regression formulas for baseline energy expenditure EE_0 data using doubly labeled water (DLW) method from the Institute of Medicine (IOM)/ National academy of Sciences (NAS) database [45].

$$EI_0=EI(0)=EE_0=EE(0)=0.278W(0)^2+9.2893W(0)+1528.90 \tag{2.10}$$

For the energy expenditure, the physical activity is modeled using the coefficient $PAL(t)$ which times the resting metabolic rate ($RMR(t)$) to describe the total energy expenditure as follows,

$$EE(t)=PAL(t)RMR(t) \tag{2.11}$$

There are different estimations and representations for $RMR(0)$ available, and for the dynamics of the simulation, a regression formula that fits the data obtained by Butt *et al.* [3] is used,

$$RMR(0)=248W(0)^{0.4356}-5.09Age \tag{2.12}$$

where the body mass $W(0)$ is the pre-gravid weight, expressed in kg, and Age is expressed in years. With the initial EE and RMR, we can calculate the dynamic physical activity level $PAL(0)$ through (2.11).

Data from the National Health and Nutrition Examination Survey (NHANES) was used to obtain the following body composition formula, the baseline maternal fat mass is obtained by solving the equation (2.13) below for $FM(0)$, where age is expressed in years and height is expressed in cm.

$$\begin{aligned} W(0) = & - 72.055453 + 2.4837412FM(0) - 0.038273age + 0.6555023height \\ & + FM(0) - 0.002296ageFM(0) - 0.013308heightFM(0) \\ & - 0.0390627FM(0)^2 + 0.332 \times 10^{-4} ageFM(0)^2 \\ & + 0.2721 \times 10^{-3} heightFM(0)^2 + 0.2291 \times 10^{-3} FM(0)^3 \\ & - 0.187 \times 10^{-5} heightFM(0)^3 + 3.5 \times 10^{-7} FM(0)^4 \end{aligned} \tag{2.13}$$

Baseline fat-free mass ($FFM(0)$) is calculated by equation (2.14)

$$FFM(0) = W(0) - FM(0) \tag{2.14}$$

2.2.3 Illustration of Energy Balance using Production-Inventory System

The production-inventory system in supply chain management is a classical problem in enterprise systems that has application in many problem arenas, and it is established by introducing fluid flow systems which are very common in process control. These types of systems usually involve components such as: 1) process: liquid-holding tanks and pipes, 2) actuators: valves, 3) measured values (sensors): level and flow.

Figure 2.2 shows a level control diagram of production-inventory systems for the energy balance model. There are two inputs *EI* and *PAL* in the model. At the steady state (no changes in *EI* and *PAL*), there exists no weight changes. When a woman increases her EI as a consequence of pregnancy, the increased *EI* will be stored inside the body as FFM and FM, the sum of which gives GWG. The two inputs *EI* and *PAL* can be manip-

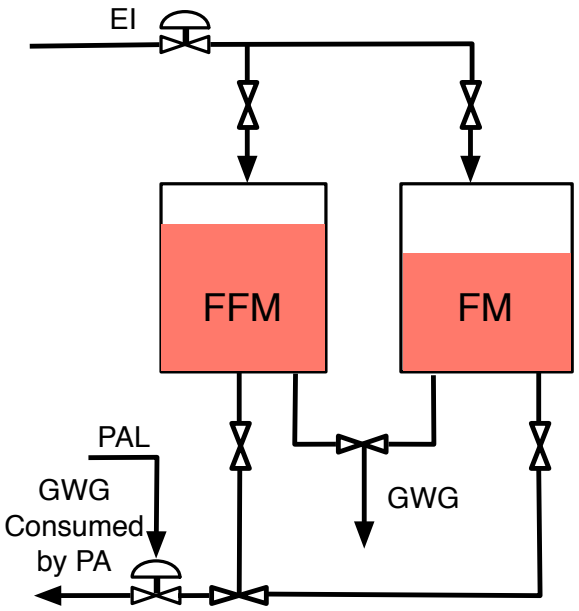

Figure 2.2: Energy Balance Model Illustration with the Concept of Production-inventory Systems

ulated via adaptive interventions to manage GWG, such as lowering *EI* to reduce GWG, and increasing *PAL* to consume GWG.

More detailed descriptions about production-inventory systems will be described in the next few sections in this chapter.

2.3 Behavioral Model

In this section, we present a dynamic formulation of the Theory of Planned Behavior (TPB) [46] to describe the behavioral component of human weight change interventions. The model is based on the concept of fluid analogies, as developed in [43]. The Theory of Planned Behavior (TPB) is a broadly used paradigm for describing the relationship between behaviors and intentions.

2.3.1 Theory of Planned Behavior (TPB)

Icek Ajzen's theory of planned behavior [46–48] stems from his earlier work with Martin Fishbein: the theory of reasoned action (TRA) [49]. Ajzen's theory has been verified

through many experimental results, and therefore it is well established in the psychology literature.

In the framework of the TPB, intention is an indication of the readiness of a person to perform a given behavior, and behavior is an observable response in a given situation with respect to a given target. According to TPB, intention is influenced by the following components:

- *Attitude toward the behavior*: This is the degree to which performing the behavior is positively or negatively valued. It is determined by the *strength of beliefs about the outcome* and the *evaluation of the outcome*.

- *Subjective norm*: This is the perceived social pressure to engage or not engage in a behavior. It is determined by the strength of the beliefs what people want the person to do, also called *normative beliefs*, and the desire to please people, also called *motivation to comply*.

- *Perceived behavioral control (PBC)*: This reflects the perception of the ability to perform a given behavior, i.e. the beliefs about the presence of factors that may facilitate or impede performance of the behavior. It is determined by the *strength of each control belief* and the *perceived power of the control factor*.

In comparison to TRA [50], TPB states that intention is influenced by perceived behavioral control (PBC), while TRA does not.

A standard mathematical representation for TPB relies on Structural Equation Modeling (SEM) [11], the detail of which will be described in the subsection below.

2.3.2 Path Analysis Model for TPB

The field of Structural Equation Modeling (SEM) is substantial, but in this research, we limit ourselves to a special case of SEM called path analysis, which is an approach

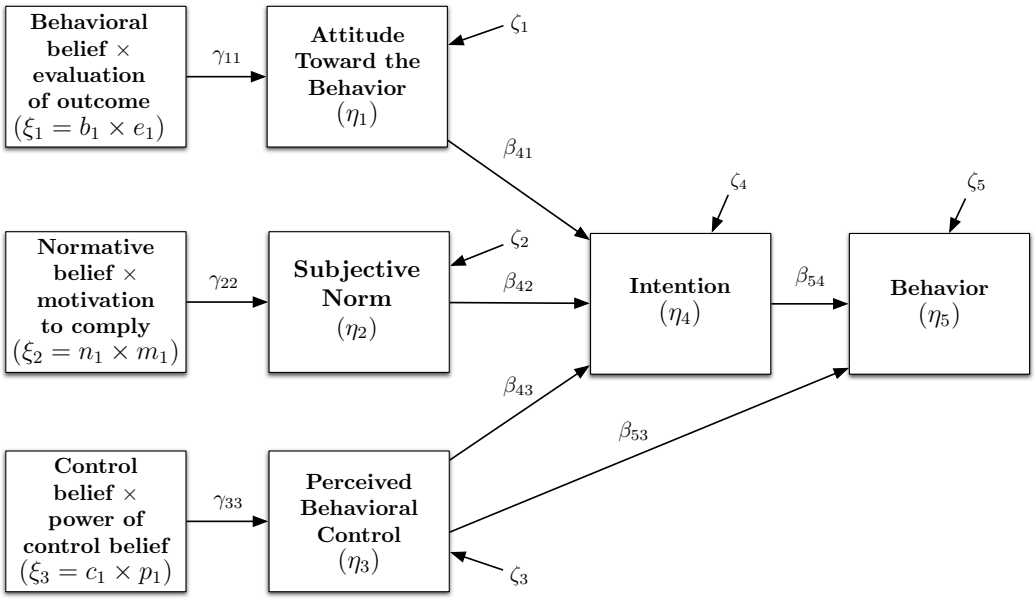

Figure 2.3: Path Diagram for the TPB, Obtained from Structural Equation Modeling (SEM) [11].

to modeling explanatory relationships between observed variables that are measured on a sample of subjects, and are also called manifest variables.

Figure 2.3 shows the path diagram for TPB which comes from SEM [11] and depicts the steady-state relationships between variables where η_i represents endogenous variables, ξ_i exogenous variables, β_{ij} and γ_{ij} are regression weights and ζ_i are disturbance variables.

The TPB represented as a path analysis model with a vector η of endogenous variables and a vector ξ of exogenous variables is expressed as follows:

$$\eta = \mathbf{B}\eta + \Gamma\xi + \zeta \tag{2.15}$$

$$\begin{bmatrix} \eta_1 \\ \eta_2 \\ \eta_3 \\ \eta_4 \\ \eta_5 \end{bmatrix} = \begin{bmatrix} 0 & 0 & 0 & 0 & 0 \\ 0 & 0 & 0 & 0 & 0 \\ 0 & 0 & 0 & 0 & 0 \\ \beta_{41} & \beta_{42} & \beta_{43} & 0 & 0 \\ 0 & 0 & \beta_{53} & \beta_{54} & 0 \end{bmatrix} \begin{bmatrix} \eta_1 \\ \eta_2 \\ \eta_3 \\ \eta_4 \\ \eta_5 \end{bmatrix} + \begin{bmatrix} \gamma_{11} & 0 & 0 \\ 0 & \gamma_{22} & 0 \\ 0 & 0 & \gamma_{33} \\ 0 & 0 & 0 \\ 0 & 0 & 0 \end{bmatrix} \begin{bmatrix} \xi_1 \\ \xi_2 \\ \xi_3 \end{bmatrix} + \begin{bmatrix} \zeta_1 \\ \zeta_2 \\ \zeta_3 \\ \zeta_4 \\ \zeta_5 \end{bmatrix} \tag{2.16}$$

where **B** and Γ are matrices of β_{ij} and γ_{ij} regression weights, respectively, and ζ is a vector of disturbance variables.

The exogenous variables ξ are expressed as follows,

$$\xi_1 = b_1 \times e_1 \tag{2.17}$$

$$\xi_2 = n_1 \times m_1 \tag{2.18}$$

$$\xi_3 = c_1 \times p_1 \tag{2.19}$$

where b_1 represents the strength of beliefs about the outcome, e_1 the evaluation of the outcome, n_1 the strength of normative beliefs, m_1 the strength of the motivation to comply to the different normative beliefs, c_1 the strength of the control belief and p_1 the perceived power of the control factor.

2.3.3 Dynamic Fluid Analogy for TPB

The classical TPB model in path diagram expressed in the SEM equation (2.15) only shows the static (i.e., steady state) relationship between variables that do not capture any changing behavior over time. In order to expand TPB model to include its dynamic effects, Navarro-Barrientos and Rivera in [43] presented how the path diagram associated with TPB can be postulated as a fluid analogy which parallels the problem of the production-inventory systems in supply chain management [21]. Figure 2.4 shows a dynamic TPB

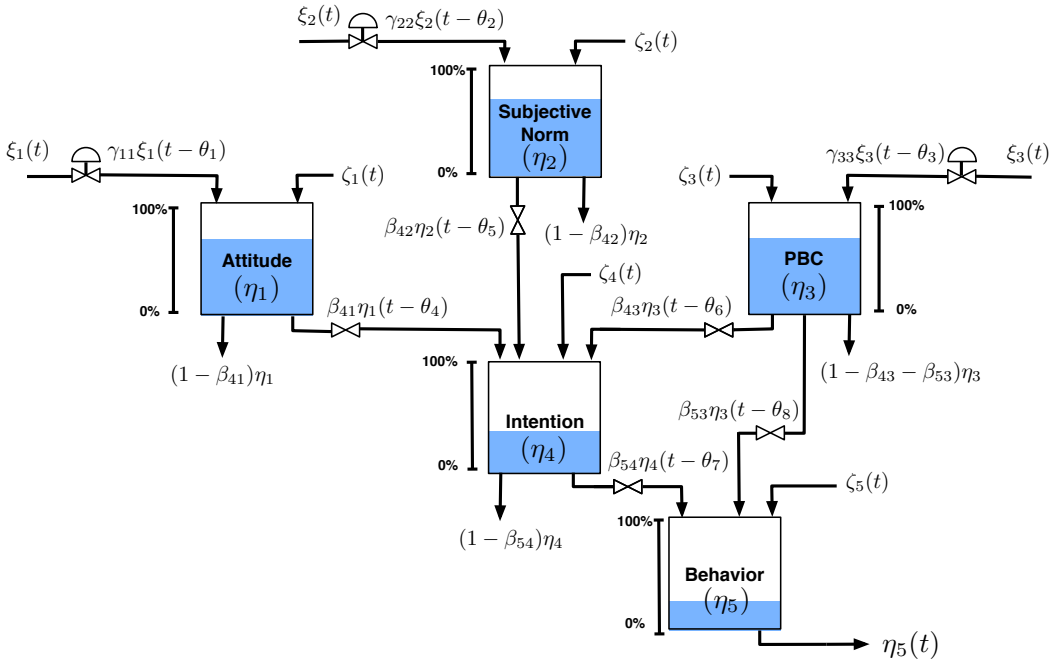

Figure 2.4: Fluid Analogy for the Theory of Planned Behavior (TPB).

model consisting of five inventories: attitude η_1, subjective norm η_2, perceived behavioral control η_3, intention η_4 and behavior η_5. The inflows of the inventories correspond to the exogenous variables ξ_1, ξ_2, and ξ_3. Each inventory is replenished by inflow streams and depleted by outflow streams. The path diagram model coefficients $\gamma_{11}, \ldots, \gamma_{33}$ are the inflow resistances and $\beta_{41}, \ldots, \beta_{54}$ are the outflow resistances, which can be physically interpreted as those fractions of the inventories of the system that serve as inflows to the subsequent layer in the path analysis model.

To generate the dynamical system description, the principle of conservation of mass is applied to each inventory, where accumulation (represented by a derivative term) equals mass inflows minus mass outflows:

$$Accumulation = Inflow - Outflow \tag{2.20}$$

Then a system of differential equations based on (2.20) can be obtained:

$$\tau_1 \frac{d\eta_1}{dt} = \gamma_{11}\xi_1(t-\theta_1) - \eta_1(t) + \zeta_1(t) \quad (2.21)$$

$$\tau_2 \frac{d\eta_2}{dt} = \gamma_{22}\xi_2(t-\theta_2) - \eta_2(t) + \zeta_2(t) \quad (2.22)$$

$$\tau_3 \frac{d\eta_3}{dt} = \gamma_{33}\xi_3(t-\theta_3) - \eta_3(t) + \zeta_3(t) \quad (2.23)$$

$$\tau_4 \frac{d\eta_4}{dt} = \beta_{41}\eta_1(t-\theta_4) + \beta_{42}\eta_2(t-\theta_5) + \beta_{43}\eta_3(t-\theta_6) - \eta_4(t) + \zeta_4(t) \quad (2.24)$$

$$\tau_5 \frac{d\eta_5}{dt} = \beta_{54}\eta_4(t-\theta_7) + \beta_{53}\eta_3(t-\theta_8) - \eta_5(t) + \zeta_5(t) \quad (2.25)$$

where τ_i are time constants, θ_i are time delays, and ζ_i are disturbances. In this dynamical TPB representation, the regression weights β_{ij} and γ_{ij} from SEM correspond to gains of the system. These parameters can be used to determine how fast (or slow) an individual can transition between values for η_1,...,η_5 as a result of changes in the variables ξ_i. At steady-state (i.e., when $\frac{d\eta_i}{dt} = 0$), the dynamical model in equation (2.21) through (2.25) corresponds exactly to the TPB SEM in (2.16) without approximation.

Higher-order derivatives with corresponding parameters can be used to enhance the model in (2.21) - (2.25) to capture underdamped responses, inverse response, and the like. For reasons of simplicity, these will not be considered in this dissertation, but are presented in work describing weight change interventions with non-pregnant individuals [43].

2.3.4 Model Analysis for TPB Fluid Analogy

This subsection focuses on the model analysis in Laplace domain, which is necessary when we apply the techniques of model-based control, such as internal model control (IMC) and model predictive control (MPC) to design the controller in this research. In the previous subsection, we present the dynamic TPB model based on the fluid analogy that can be described by the first-order differential equations (2.21) through (2.25).

With the attitude inventory equation (2.21), we can take the Laplace transform of (2.21) and have the following equations,

$$\begin{aligned} \tau_1 \frac{d\eta_1}{dt} &= \gamma_{11}\xi_1(t-\theta_1) - \eta_1(t) + \zeta_1(t) \\ (\tau_1 s+1)\eta_1(s) &= \gamma_{11}e^{-\theta_1 s}\xi_1(s) + \zeta_1(s) \qquad (2.26) \\ \eta_1(s) &= \frac{\gamma_{11}}{\tau_1 s+1}e^{-\theta_1 s}\xi_1(s) + \frac{1}{\tau_1 s+1}\zeta_1(s) \qquad (2.27) \end{aligned}$$

Similarly, for the subjective norm inventory equation (2.22) and the PBC inventory equation (2.23), Laplace transform can be applied and the following equations can be obtained,

$$\eta_2(s) = \frac{\gamma_{22}}{\tau_2 s+1}e^{-\theta_2 s}\xi_2(s) + \frac{1}{\tau_2 s+1}\zeta_2(s) \qquad (2.28)$$

$$\eta_3(s) = \frac{\gamma_{33}}{\tau_3 s+1}e^{-\theta_3 s}\xi_3(s) + \frac{1}{\tau_3 s+1}\zeta_3(s) \qquad (2.29)$$

As discussed in section 2.3.3, intention is determined by attitude toward the belief, subjective norm and PBC, its expression in Laplace domain can be obtained as follows,

$$\eta_4(s) = \frac{\beta_{41}e^{-\theta_4 s}}{\tau_4 s+1}\eta_1(s) + \frac{\beta_{42}e^{-\theta_5 s}}{\tau_4 s+1}\eta_2(s) + \frac{\beta_{43}e^{-\theta_6 s}}{\tau_4 s+1}\eta_3(s) + \frac{1}{\tau_4 s+1}\zeta_4(s) \qquad (2.30)$$

The behavior inventory is influenced by PBC and intention inventories, and its expression in Laplace domain can be simplified by substituting $\eta_1(s)$, $\eta_2(s)$, $\eta_3(s)$, and $\eta_4(s)$ above,

$$
\begin{aligned}
\eta_5(s) &= \frac{\beta_{54}e^{-\theta_7 s}}{\tau_5 s+1}\eta_4(s)+\frac{\beta_{53}e^{-\theta_8 s}}{\tau_5 s+1}\eta_3(s)+\frac{1}{\tau_5 s+1}\zeta_5(s) \\
&= \frac{\beta_{54}e^{-\theta_7 s}}{\tau_5 s+1}[\frac{\beta_{41}e^{-\theta_4 s}}{\tau_4 s+1}\eta_1(s)+\frac{\beta_{42}e^{-\theta_5 s}}{\tau_4 s+1}\eta_2(s)+\frac{\beta_{43}e^{-\theta_6 s}}{\tau_4 s+1}\eta_3(s) \\
&\quad +\frac{1}{\tau_4 s+1}\zeta_4(s)]+\frac{\beta_{53}e^{-\theta_8 s}}{\tau_5 s+1}\eta_3(s)+\frac{1}{\tau_5 s+1}\zeta_5(s) \\
&= \frac{\beta_{54}\beta_{41}\gamma_{11}e^{-(\theta_1+\theta_4+\theta_7)s}}{(\tau_5 s+1)(\tau_4 s+1)(\tau_1 s+1)}\xi_1(s)+\frac{\beta_{54}\beta_{42}\gamma_{22}e^{-(\theta_2+\theta_5+\theta_7)s}}{(\tau_5 s+1)(\tau_4 s+1)(\tau_2 s+1)}\xi_2(s)+ \\
&\quad [\frac{\beta_{54}\beta_{43}\gamma_{33}e^{-(\theta_3+\theta_6+\theta_7)s}}{(\tau_5 s+1)(\tau_4 s+1)(\tau_3 s+1)}+\frac{\beta_{53}\gamma_{33}e^{-(\theta_3+\theta_8)s}}{(\tau_5 s+1)(\tau_3 s+1)}]\xi_3(s)+ \\
&\quad \frac{\beta_{54}\beta_{41}e^{-(\theta_4+\theta_7)s}}{(\tau_5 s+1)(\tau_4 s+1)(\tau_1 s+1)}\zeta_1(s)+\frac{\beta_{54}\beta_{42}e^{-(\theta_5+\theta_7)s}}{(\tau_5 s+1)(\tau_4 s+1)(\tau_2 s+1)}\zeta_2(s)+ \\
&\quad [\frac{\beta_{54}\beta_{43}e^{-(\theta_6+\theta_7)s}}{(\tau_5 s+1)(\tau_4 s+1)(\tau_3 s+1)}+\frac{\beta_{53}e^{-\theta_8 s}}{(\tau_5 s+1)(\tau_3 s+1)}]\zeta_3(s)+ \\
&\quad \frac{\beta_{54}e^{-\theta_7 s}}{(\tau_5 s+1)(\tau_4 s+1)}\zeta_4(s)+\frac{1}{\tau_5 s+1}\zeta_5(s) \qquad (2.31)
\end{aligned}
$$

The transfer function of this dynamic TPB model has eight inputs (three inflows and five disturbances), and one output (behavior). It is a 1×8 transfer function vector.

2.3.5 Illustration of Energy Balance and TPB using Production-Inventory Systems

The dynamic TPB model is built based on the the concept of fluid analogies. These modules consist primarily of networks of production-inventory systems that are akin to supply chains. Figure 2.5 shows a detail diagram of the dynamical system which incorporates both physiological and psychological factors illustrated by the use of the concept of production-inventory systems.

The inputs for the behavioral model are the effects of intervention levels applied to the three components of the TPB. The outputs of the behavioral model, the changes on behavioral eating habits and exercise, are translated into changes on diet and physical activity, respectively, which serve as the inputs to the energy balance model.

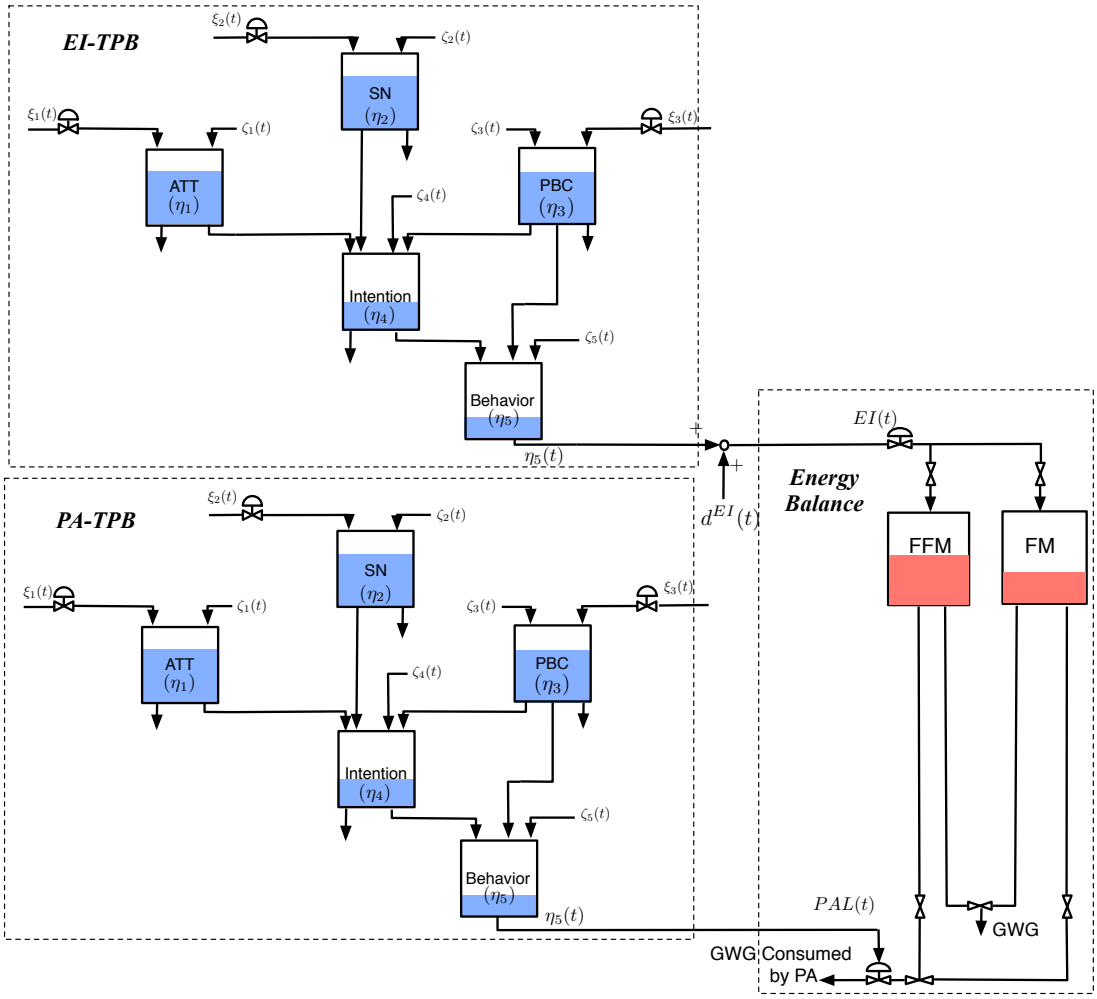

Figure 2.5: Dynamical Systems Model for Behavioral Interventions Integrates the Maternal Energy Balance Model and the Dynamic Fluid Analogy for the TPB Illustrated by the Concept of Production-inventory Systems.

2.4 Self-Regulation Principle

In social cognitive theory, human behavior is greatly motivated and managed by the ongoing exercise of self-influence. The major self-regulative mechanism operates through self-monitoring of one's behavior, and its effects; judgment of one's behavior related to personal standards and environmental circumstances; and affective self-reaction [51] . This section focuses on the introduction to self-regulation theory and how self-regulatory effect is designed, modeled and integrated to the dynamical model.

2.4.1 Introduction to Self-Regulation

Compared to other living creatures, humans are known for having an extensive ability to exert control over their inner states, processes, and responses [52]. People are able to resist their own impulses, adapt their behavior to a range of standards, and change their current behaviors in order to attain the goals [53]. The term self-regulation is often used to refer widely to efforts by humans to have alterations of their thoughts, feelings, desires, and actions in the perspective of such higher goals [9, 54]. Hence, self-regulation refers to the person as an active agent and decision-maker, and is key for human to adapt to the changing life [55].

Self-regulatory systems lie at the center of causal processes. They not only mediate the effects of most external influences, but also provide the very basis for purposeful action. Most human behavior is regulated by forethought. People form beliefs about what they can do, they anticipate the likely consequences of prospective actions, they set goals for themselves, and they otherwise plan courses of action that are likely to produce desired outcomes. Through exercise of forethought, people motivate themselves and guide their actions in an anticipatory proactive way [51].

Successful self-regulation requires the strategic mobilization of thought, feeling, and action [56, 57], in particular when individual is facing obstacles and conflicts between

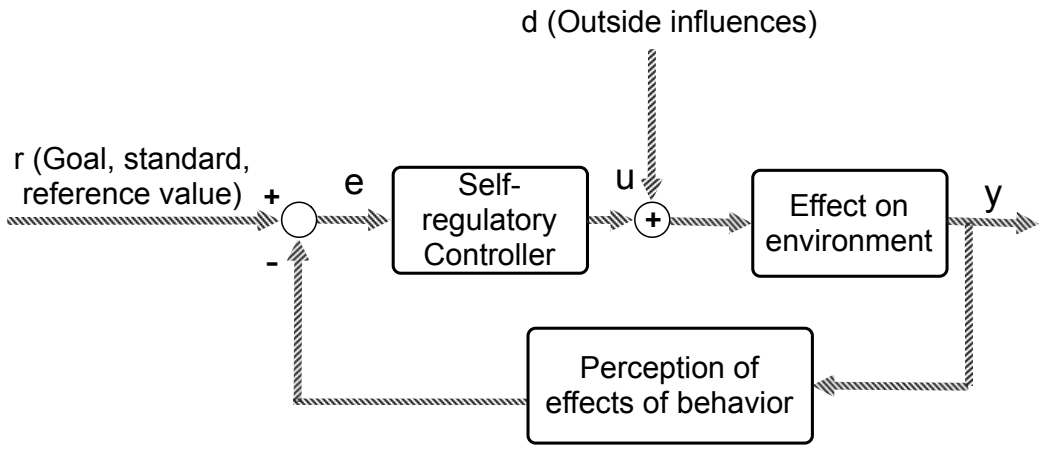

Figure 2.6: Behavior and Perception as Elements of a Feedback Loop Guiding Human Action per the Self-regulation Theory of Carver and Scheier [9].

goals, and self-regulation generally is inferred as a systematic process that involves conscious effort to influence thoughts, feelings, and behaviors in the service of achieving a goal in case of a changing environment [58]. Self-regulation involves individual to manage their own change processes [59], including the conscious consideration of the relative importance of potentially competing goals, and goal prioritization in particular [60].

2.4.2 Controller Design for Self-Regulation

Self-regulation theory in psychology has been largely influenced by the work of Carver and Scheier [9] who proposed that human behavior is goal-directed and regulated by feedback control processes (Figure 2.6). Self-regulation reflects the capacity of individuals to alter their own behavior, enabling people to adjust their actions to a broad range of social and situational demands. Individuals tend to engage in activities they believe they can succeed in; this confidence in performance success will influence the inflow of PBC, which reflects the individual's perception of her ability to perform a given behavior. As a result, self-monitoring and goal setting are core strategies of behavior modification. Self-regulation is enhanced by repeated measurement and assessment of important outcomes in

an intervention.

In this work, self-regulation comes from repeated GWG measurement and EI monitoring. There are three self-regulation loops in Figure 2.1 which are parametrized as derivative-only controllers. Two of these controllers adjust the inflows to PBC in the TPB models based on the discrepancies between the reference values and measured GWG. The reason for this choice is that when a participant improves on her GWG, even though it may lie outside the target boundaries, the presence of improvement will nonetheless strengthen her confidence in aiming to maintain her GWG within target goal, which in turn, promotes PBC, and hence behavior in both the EI and PA TPB models. However, if the participant tries her best to only find that she cannot control her GWG as she desires, her control belief will diminish, with PBC, as well as intention and behavior correspondingly reduced. The expressions for the self-regulation control system used in this chapter are as follows:

$$e(t) = GWG(t) - IOM(t) \tag{2.32}$$

$$\Delta\xi_3(t) = K_e \Delta e(t) \tag{2.33}$$

$$\Delta e(t) = \frac{e(t) - e(t-T)}{T} \tag{2.34}$$

$$\xi_3(t) = \xi_{3b}(t) - \Delta\xi_3(t) \tag{2.35}$$

where *e(t)* represents the discrepancy between the reference values (IOM guidelines) and the measured GWG; T is the sampling time at which the participant regularly checks her weight; $\Delta e(t)$ expresses the rate of improvement; K_e is the controller gain which varies at different periods in time and will depend on personal characteristics and baseline parameters; $\xi_{3b}(t)$ is the PBC inflow independent of self-regulatory control action. The self-

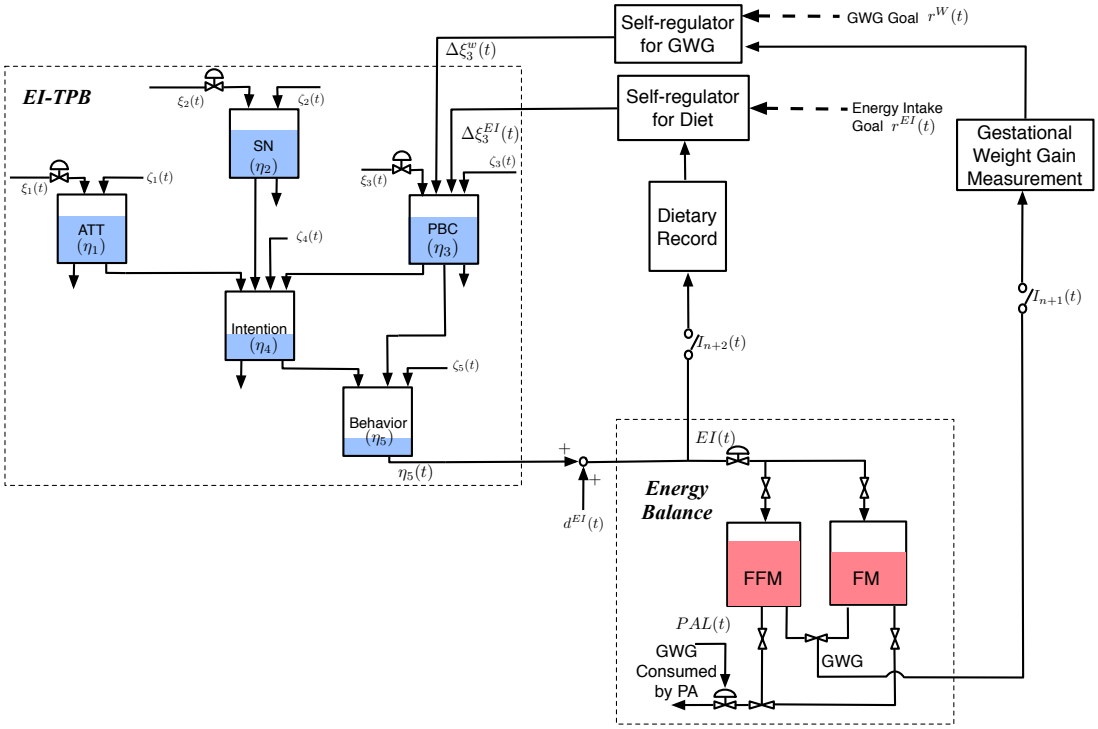

Figure 2.7: Dynamical Systems Model for Behavioral Interventions Integrates the Maternal Energy Balance Model, the Dynamic TPB Model and Self-regulation for the EI Loop Illustrated by the Concept of Production-inventory Systems.

regulation can also be working based on the discrepancies between the energy intake reference value and the dietary record, and this constitutes the third derivative-only controller in the self-regulation loop in Figure 2.1. Its expression can be obtained similarly, with the expression of $e(t)$ in equation (2.32) replaced by the expression of $e(t)$ below,

$$e(t) = EI(t) - EI_{IOM}(t) \tag{2.36}$$

2.4.3 Illustration of Energy Intake, TPB and Self-regulation using Production-Inventory Systems

As described in the previous subsection, self-regulation works as a controller in the dynamical systems model for behavioral intervention to help promote individual's PBC, which in turn improves the outcome of the behavior: healthy eating and physical activ-

ity. Figure 2.7 is a detail diagram of the dynamical system which incorporates the energy balance model, the dynamic TPB model and self-regulation for the EI loop by the use of the concept of production-inventory systems. There are two self-regulation loops associated with EI and GWG, respectively, influencing PBC. Self-regulator for diet will be working based on the differences between the reference values of EI and the individual's dietary record; while self-regulator for GWG works based on the discrepancies between the IOM guidelines and the individual's measured GWG. Both of these two self-regulatory loops help better adjust the individual's PBC inflows to the TPB model, with the help of self-monitoring.

2.5 Intervention Program and Delivery Modeling

A number of diverse behavioral interventions for GWG have been developed with healthy eating (HE) and/or physical activity (PA) behavioral components [40, 41, 61–66]; however, the recommendation is that both elements should be included to improve effectiveness [61]. In our research, we consider hypothetical interventions whose goals are to provide OW/OBPW with advice and feedback about weight control, and promote both HE and PA in order to manage GWG within the IOM guidelines (Table 2.4).

2.5.1 Intervention Components

The proposed intervention components in this research are informed by past research and experience [66, 67], and include GWG, HE and PA education, goal-setting, self-monitoring, active learning and behavioral modification. Evidence shows that these components can effectively manage weight, and when people are taught how to use these strategies, they are more likely to achieve their goals and positively impact outcomes [68–70]. Participants who are engaged in PA active learning have higher PA attitude, PBC, intention and subjective norms, lower depression, and better body image compared to those who are not actively engaged in these behaviors [69, 70].

Table 2.4: Target Gestational Weight Gain (GWG) Recommended by the 2009 Institute of Medicine Guidelines [5] and the Corresponding Trimester-specific Energy Intake that Coincides with this Maternal Weight Gain [4].

Classification	**Pre-gravid BMI (kg/m^2)**	**Target GWG (kg) Trimester**		**Model Predicted ΔEI (kcal/d) Trimester**		
		1	**2 - 3**	**1**	**2**	**3**
Underweight	$<$20	0.5 - 2.0	11.4 - 15.8	94 - 184	400 - 511	442 - 574
Normal	20 - 25	0.5 - 2.0	9.1 - 13.0	94 - 200	381 - 492	444 - 635
Overweight	25 - 30	0.5 - 2.0	6.0 - 8.6	117 - 200	263 - 333	269 - 364
Obese	$>$30	0.5 - 2.0	4.4 - 7.0	116 - 200	223 - 295	227 - 326

Table 2.5: Intervention Components for Hypothetical GWG Intervention.

	Description	**Influence**	**Frequency**
$I_1(u_1)$	Healthy Eating Education	EI-TPB	weekly
$I_2(u_2)$	Healthy Eating Weekly Plan	EI-TPB	weekly
$I_3(u_3)$	Healthy Eating Active Learning	EI-TPB	weekly
$I_4(u_4)$	Goal Setting	EI-TPB & PA-TPB	weekly
$I_5(u_5)$	Physical Activity Education	PA-TPB	weekly
$I_6(u_6)$	Physical Activity Weekly Plan	PA-TPB	weekly
$I_7(u_7)$	Physical Activity Session	PA-TPB & Energy Balance	bi-weekly
$I_8(y_1)$	Daily Weight Scale	PA & EI self regulation	daily
$I_9(y_2)$	Dietary Record	EI self regulation	daily
$I_{10}(y_3)$	PA monitor output	PA self-regulation	daily

The list of intervention components for this hypothetical intervention is summarized in Table 2.5. Intervention components can be classified according to two types. The first consists of manipulated variables whose magnitude or "dosage" can be changed over time; examples include healthy eating and physical activity education (I_1 and I_5), healthy eating and physical activity weekly plans (I_2 and I_6), healthy eating active learning (I_3), goal setting (I_4) and physical activity sessions (I_7). The second type of intervention component consists of signals that are used by either the closed-loop decision rules or influence the participant's self-regulation. These intervention components include daily weighting (I_8), dietary records (I_9), and physical activity monitoring (I_{10}). The role these components play as either inputs to the TPB and energy balance models, or as outputs from the TPB and energy balance models but inputs to the self-regulation modules and decision rules are depicted in Figure 2.1.

2.5.2 Intervention Delivery Dynamics

How the intervention components act on the inflows to the TPB model is illustrated in Figure 2.8. The modeling of the intervention delivery dynamics is treated like a pro-

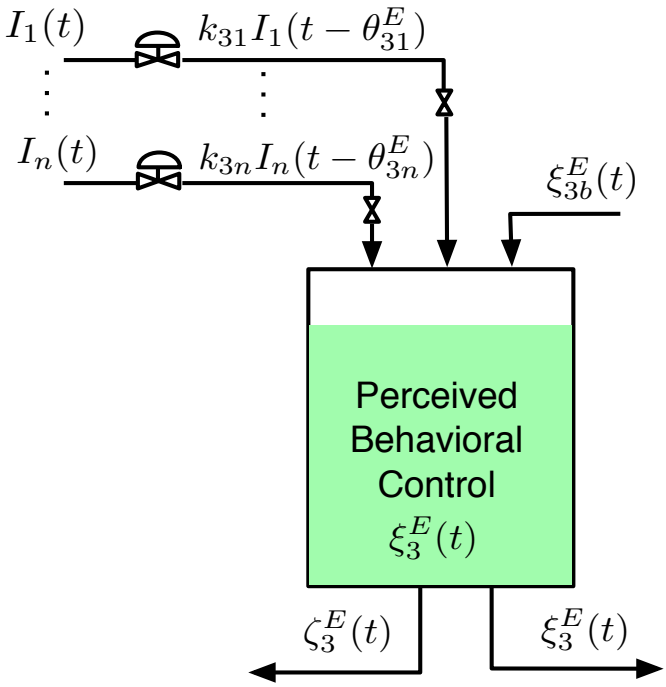

Figure 2.8: Illustration of the Intervention Delivery Dynamics for PBC Inflow in EI-TPB Model

duction inventory system, the concept of which is already explained in Section 2.2. We treat each input ($I_1 \ldots I_7$) as contributing to the inflows $\xi_1 \ldots \xi_3$ for each of the two TPB models. We would expect that the effect of the intervention on the beliefs, evaluations, and other variables that comprise the inflows $\xi_1 \ldots \xi_3$ accumulate and hence integration is required. At the intervention delivery level we include the possibility of delayed effects and disturbances that could potentially undermine the intervention delivery. We illustrate these concepts with the inflow to the PBC inventory for the energy intake TPB (EI-TPB) model. The signal ξ_3^E includes the sum of a baseline PBC (ξ_{3b}^E) as well as the change contributed by intervention components such as healthy eating education, healthy eating weekly plans, healthy eating active learning, and goal setting. Equation (2.37) shows the new inflow to the PBC inventory for the energy intake TPB (EI-TPB) model under the influence of the intervention,

$$\begin{aligned}\xi_3^E(t) &= \xi_{3b}^E + \int_{t_0}^{tf}\left[\sum_{i=1}^{n} k_{3i}I_i(t-\theta_{3i}^E)\right]\mathrm{d}t + \zeta_3^E(t) \\ &= \xi_{3b}^E + \int_{t_0}^{tf}[k_{31}I_1(t-\theta_{31}^E) + k_{32}I_2(t-\theta_{32}^E) \\ &\quad + k_{33}I_3(t-\theta_{33}^E) + k_{34}I_4(t-\theta_{34}^E)]\,\mathrm{d}t + \zeta_3^E(t) \end{aligned} \tag{2.37}$$

where n is the number of intervention components that fall into the category of manipulated variables; I_i is the dosage of the corresponding intervention components; k_{3i} correspond to intervention gains that will be a function of personal characteristics or baseline conditions such as age, social economic status, and social support; θ_{3i}^E and ζ_3^E are the corresponding time delay and disturbances. Since these intervention components are used to improve the PBC in EI-TPB, all the gains are positive-valued.

Following from (2.37), we can obtain similar expressions for the other inputs in the EI-TPB and PA-TPB models. We use the Laplace transforms and vector-matrix notation to obtain

$$\xi(\mathbf{s}) = \frac{1}{s}\mathbf{K^I}(\mathbf{s})\mathbf{I}(\mathbf{s}) + \xi_{\mathbf{b}} + \zeta^{\mathbf{I}}(\mathbf{s}) \tag{2.38}$$

where $\xi(s)$, $\xi_b(s)$, and $\zeta^I(s)$ are all 6×1 vectors, representing the new inflows, the baseline inflows and disturbances respectively; **I(s)** is a 7×1 vector, representing the manipulated intervention inputs, $\mathbf{K}^I$**(s)** is a 6×7 matrix for intervention gains. All are defined below,

$$\xi(\mathbf{s}) = \begin{bmatrix}\xi_1^E(s) & \xi_2^E(s) & \xi_3^E(s) & \xi_1^P(s) & \xi_2^P(s) & \xi_3^P(s)\end{bmatrix}^T \tag{2.39}$$

$$\mathbf{K^I(s)} = \begin{bmatrix} k^I_{11} & k^I_{12} & k^I_{13} & k^I_{14} & 0 & 0 & 0 \\ k^I_{21} & k^I_{22} & k^I_{23} & k^I_{24} & 0 & 0 & 0 \\ k^I_{31} & k^I_{32} & k^I_{33} & k^I_{34} & 0 & 0 & 0 \\ 0 & 0 & 0 & k^I_{44} & k^I_{45} & k^I_{46} & k^I_{47} \\ 0 & 0 & 0 & k^I_{54} & k^I_{55} & k^I_{56} & k^I_{57} \\ 0 & 0 & 0 & k^I_{64} & k^I_{65} & k^I_{66} & k^I_{67} \end{bmatrix} \tag{2.40}$$

$$k^I_{ij} = k_{ij} e^{-\theta^x_{ij} s}, x = E \text{ (for EI) or } x = P \text{ (for PA)} \tag{2.41}$$

$$\mathbf{I(s)} = \begin{bmatrix} I_1(s) & I_2(s) & \cdots & I_6(s) & I_7(s) \end{bmatrix}^T \tag{2.42}$$

$$\xi_{\mathbf{b}} = \begin{bmatrix} \xi^E_{1b} & \xi^E_{2b} & \xi^E_{3b} & \xi^P_{1b} & \xi^P_{2b} & \xi^P_{3b} \end{bmatrix}^T \tag{2.43}$$

$$\zeta^{\mathbf{I}}(s) = \begin{bmatrix} \zeta^E_1(s) & \zeta^E_2(s) & \zeta^E_3(s) & \zeta^P_1(s) & \zeta^P_2(s) & \zeta^P_3(s) \end{bmatrix}^T \tag{2.44}$$

2.5.3 Illustration of Energy Intake, TPB, Self-regulation, and Intervention Delivery Module using Production-Inventory Systems

The intervention delivery dynamics build the bridge between the magnitude / frequency of intervention components and the behavioral variables in the TPB models, which makes it easy to implement the intervention, track its status, and quantify its outcome in psychological view. As described in 2.5.2, the intervention delivery modeling is developed based on the concept of the production-inventory systems, and can be integrated into Figure 2.7.

Figure 2.9 is the diagram of the dynamical systems model including energy balance model, the behavioral TPB model, self-regulation and intervention delivery dynamics for

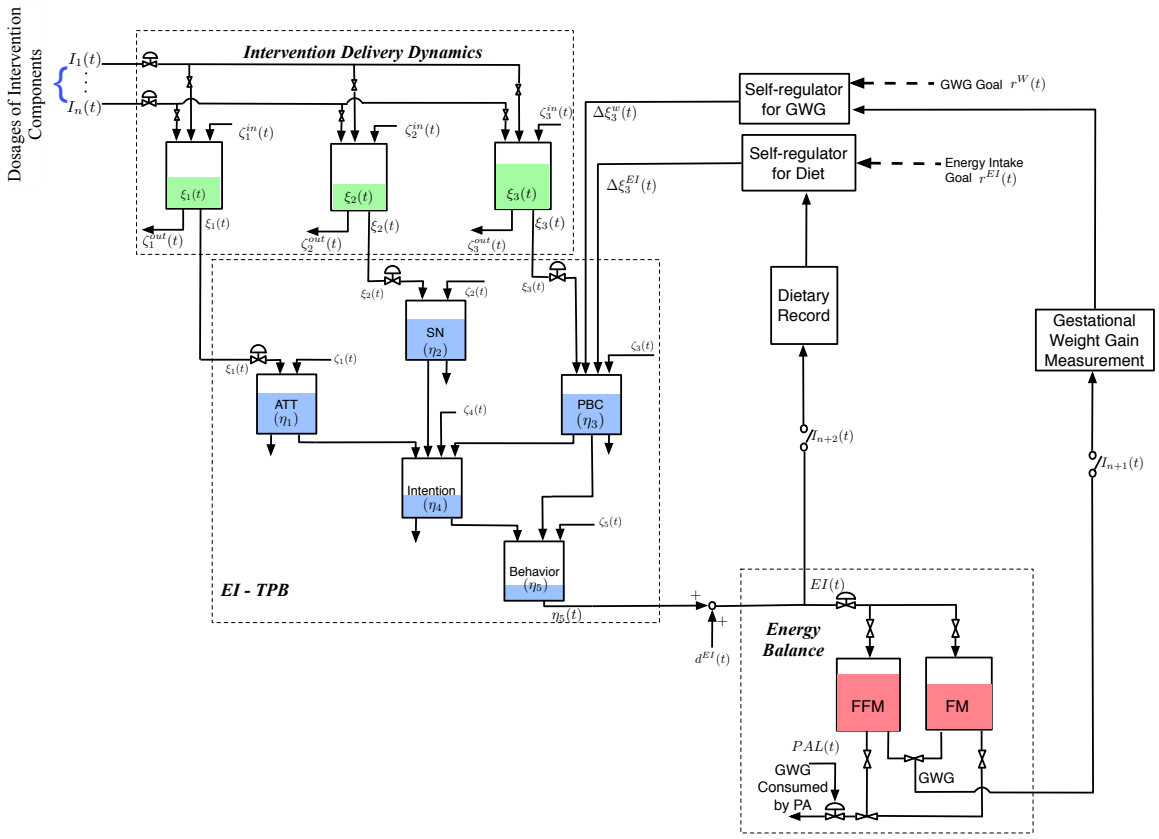

Figure 2.9: Dynamical Systems Model for Behavioral Interventions Integrates the Maternal Energy Balance Model, the Dynamic TPB Model, Self-regulation and Intervention Delivery Modeling for the EI Loop Illustrated by the Concept of Production-inventory Systems.

the EI loop by the use of the concept of production-inventory systems. The outflows of the inventories in intervention delivery dynamics work as the inflows to the TPB models.

2.6 Adaptive Interventions with Decision Rules

Adaptive interventions have been emerging as a new perspective on research-based prevention and treatment. In adaptive interventions, different dosages of intervention components will be assigned across time in response to the needs of each participant much like clinical practice [25]. This section will focus on how to use the decision rules and tailoring variables to adapt the intervention dosages to better help individuals achieve their goals.

2.6.1 Adaptive Interventions

Adaptive intervention is a promising approach to prevention and treatment. They are especially useful for prevention programs with numerous components aimed at different aspects for the treatment. Adaptive interventions individualize therapy by the use of decision rules for how the therapy level and type should vary according to measures of adherence, and response collected during past treatment [25, 28]. In fixed interventions, the same dosage is applied to all program participants without taking into account any of their individual characteristics. In an adaptive, time-varying intervention, the frequency or intensity of intervention dosages will change over time, based on the result of important outcomes of the intervention (also known as tailoring variables [25]). Decision rules operationalize these changes, which can correspond to eliminating or adding some intervention components based on participant response during the intervention, or altering the dosage of existing components (for example, increasing the number of physical activity sessions). As adaptive strategies play an increasingly important role as a methodological framework for many important prevention problems, it is evident that much research is needed on the analysis, design and effective implementation of these interventions.

Adaptive interventions have four key elements: sequence of decisions regarding participant's care, the set of treatment options at each decision point, tailoring variables and a sequence of decision rules [33]. They can help researchers better treat patients who do not have response to the initial treatment, increase the intervention effectiveness, deal with the relapses problem, and improve the patient's response [25].

2.6.2 Decision Rules

In our research, IF-THEN decision rules acting on values of tailoring variables (in this case, GWG) obtained from a dynamical systems model illustrate how adaptive intervention works for managing GWG. We implement the decision rules developed by Downs and

Savage [6] which work on IF-THEN condition in order to maintain appropriate GWG throughout pregnancy based on pre-pregnancy BMI status. The intervention starts at week 14. At the study entry, if the participant's GWG is outside the IOM guidelines, she will receive first augmentation from the base dosage; otherwise she will stay in the baseline program. The assessment for adaptive intervention occurs every three weeks for the second trimester, and every two weeks for the third trimester until week 35. Based on the outcome of the previous intervention, the dosage and the frequency of the intervention components will change according to the decision rules. The intervention level is maintained for three assessment cycles before stepping down, but as soon as the participant fails to meet the IOM guidelines at an assessment cycle, she is stepped up (Figure 2.10). We will mainly focus on the augmentation of two intervention components (HE and PA) in active learning session.

The baseline intervention (GWG Order 0) can be divided into two sessions. Session 1 includes education (printed HE, PA materials; additional online resources; HE/PA weekly plans; face-to-face delivery), goals (goal education; set GWG, HE, PA goals with implementation intentions; instructors review goals and provide feedback), and self-monitoring (instructor reviews GWG and HE/PA behaviors from past week; provides face-to-face discussion of problem-solving to overcome barriers), while session 2 contains active learning (give women a scale to weigh food at home; PA session guided by instructor). Based on the worst case under which the participant always fails to meet the GWG goal throughout the whole intervention, we set eight GWG step ups, listed in Table 2.6.

2.6.3 Illustration of the Overall GWG Dynamical Systems Model using Production-Inventory Systems

The overall GWG dynamical systems model in Figure 2.1 can also be illustrated with the concept of production-inventory systems, which is shown in Figure 2.11 for the energy

Table 2.6: Intervention Dosages for the Adaptive Intervention Decision Rules [6]

Dosage	**Description**
GWG Order -3	default dosage after week 35 when the intervention stops
GWG Order -2	reduce to 1 session per week with self-monitoring and active learning
GWG Order -1	change the delivery of education and goals from face-to-face to electronic (website/email), but still maintain 2 sessions per week
GWG Order 0	baseline intervention
GWG Order +1	add 30 min moderate vigorous physical activity (MVPA) guided by instructor to session 1 (PA active learning)
GWG Order +2	daily dietary monitoring
GWG Order +3	add 1 time out-of-session feedback from instructor monitoring progress via email/phone (Self-monitoring)
GWG Order +4	add 30 minutes walking with exercise buddy out-of-session to build social support (PA active learning)
GWG Order +5	add in personal meal preparation and add remaining day meal replacement progress via email/phone (HE active learning)
GWG Order +6	increase instructor out-of-session feedback monitoring progress via email/phone to every other day (Self-monitoring)
GWG Order +7	increase the length of session 1, and add 15 min MVPA (PA active learning)
GWG Order +8	add remaining day meal replacement to session 1 (HE active learning)

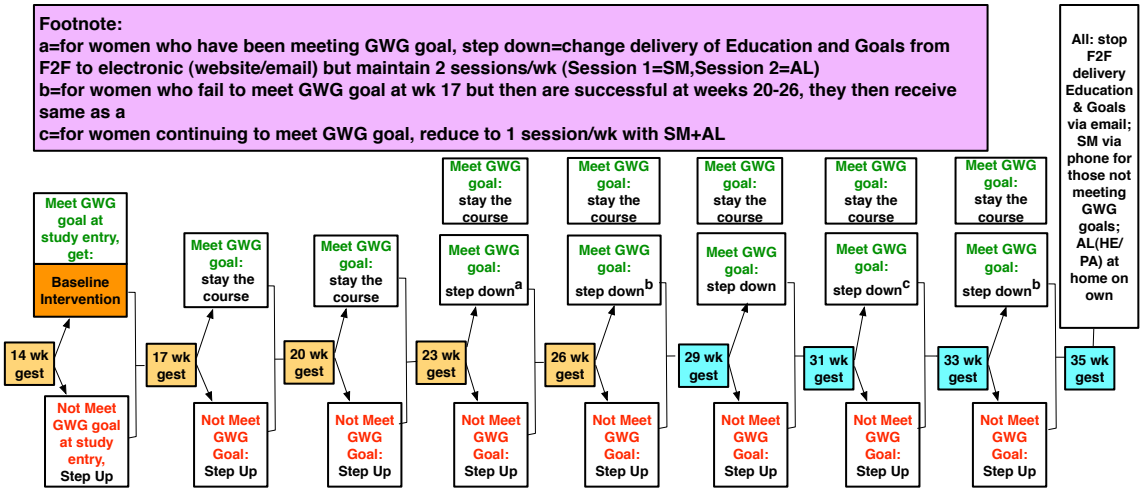

Figure 2.10: Flow Chart for IF-THEN Decision Rules (Adaptive Intervention) Developed by Downs and Savage [6].

intake loop. The outflow of EI-TPB model serves as the inputs to the energy balance model. There are two self-monitoring loops, dietary record and GWG measurement. The decision rules operationalize the changes of these measurements and assign the dosages of the intervention components that are the inflows to the intervention delivery dynamics, the outflows of which are the new inflows to the EI-TPB model.

2.7 Simulation Study

In this section, we consider two case studies that rely on our proposed dynamical systems model in this chapter, to illustrate the benefits of the simulation framework and the effect of self-regulation, and adaptive intervention operated by decision rules. All the simulations consider a 25-year-old pregnant woman with pre-gravid parameters of height (=1.6m) and her weight will change in different scenarios to illustrate how the adaptive interventions work for the participants in different BMI categories. The maternal age was selected using 2010 Data from the Center for Disease Control and Prevention illustrating mean age of mother at first birth is 25.4 years [71].

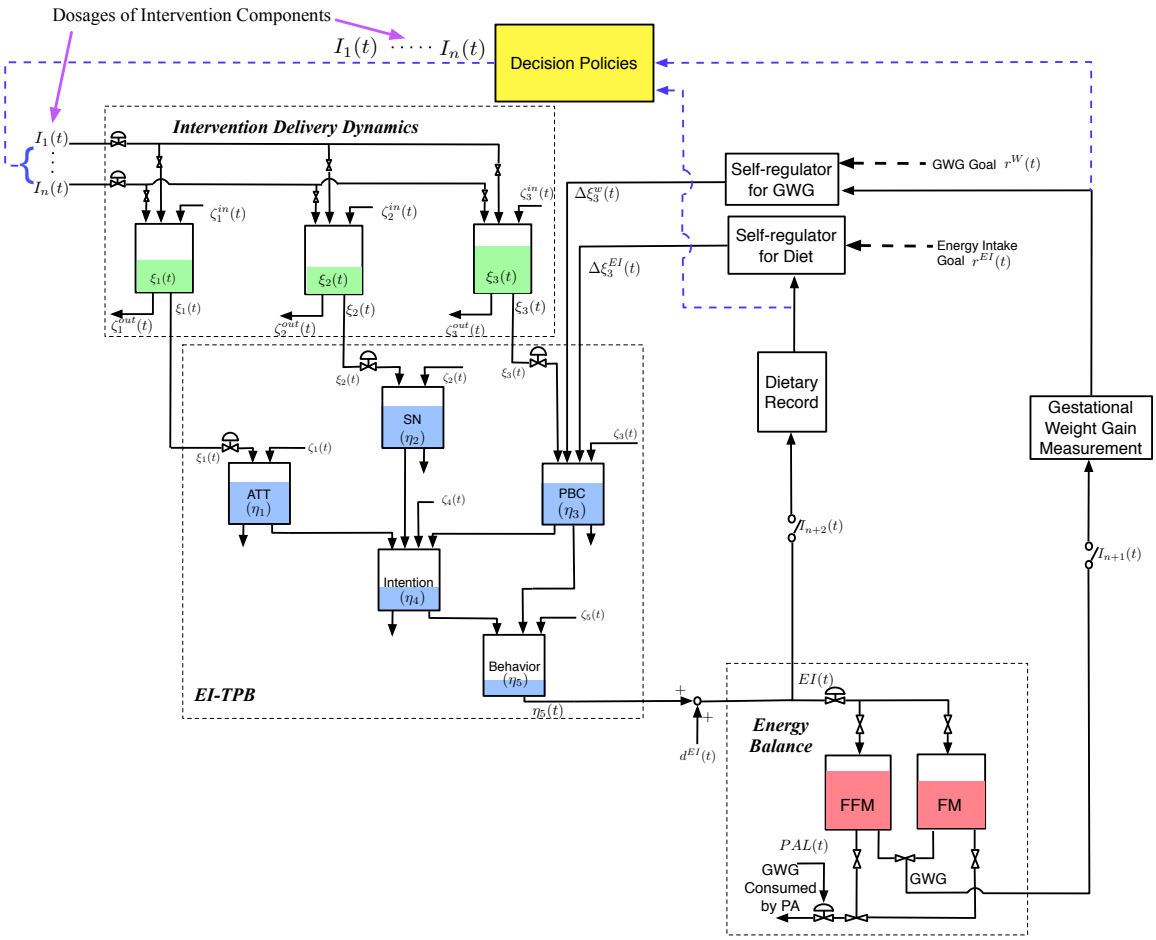

Figure 2.11: GWG System Illustration with the Concept of Production-inventory Systems for Energy Intake Loop.

The first case study includes two hypothetical simulation scenarios, the one without intervention (only self-regulation effect) and the other with the fixed behavioral intervention in the model. In the second case study, we will implement our decision rules and simulate the GWG adaptive interventions for OW/OBPW.

We assume that the participant will have a ramp increase in her EI from day 14 to day 91 (which approximates the energy intake increase with the time due to the pregnancy and is treated as the disturbance in the system) and her EI will keep constant from day 92 to

the delivery if there is no intervention.

$$slope = 15\% \times \frac{Initial\ EI}{91-13} = 15\% \times \frac{Initial\ EI}{78} \tag{2.45}$$

In order to mimic a natural trend within the participant to increase EI and reduce PA during the pregnancy, several external disturbance signals are considered in all simulations to apply to the model. The first one is the behavior disturbance variable ζ_5 within EI-TPB model. This disturbance will have little influence at the beginning, but will play a significant role later, because participant is more likely to refuse to reduce her EI at late pregnancy. This disturbance signal ζ_5 is represented in the simulation as sine wave function starting at day 14 and parametrized as follows:

$$\zeta_5(t) = A\sin[\omega(t-14) + \frac{\pi}{2}] - A \tag{2.46}$$

where A is the amplitude of the sine wave, while ω is the frequency. As output disturbance, this directly lowers the participant's EI behavior (top plot in Figure 2.12).

The next two disturbance signals are relevant with the natural PAL change during the pregnancy. The participant is potentially engaged in less PA from the second to third trimester as she gains weight without intervention (middle plot in Figure 2.12). The intervention can help improve her PAL in the second trimester, and however she will still decrease PA during her latter stage of pregnancy, especially one or two months prior to delivery. The bottom plot in Figure 2.12 is the PAL disturbance signal with intervention. Both disturbance signals above will directly lower PAL in the energy balance model in (2.9).

2.7.1 Self-Regulation and Intervention Effect

In this section, we will have two hypothetical simulation scenarios with the women having pre-gravid weight(=75kg), which places the participant (BMI=29.30) in the overweight BMI category. For the sake of simplicity, we will only focus on the effects that

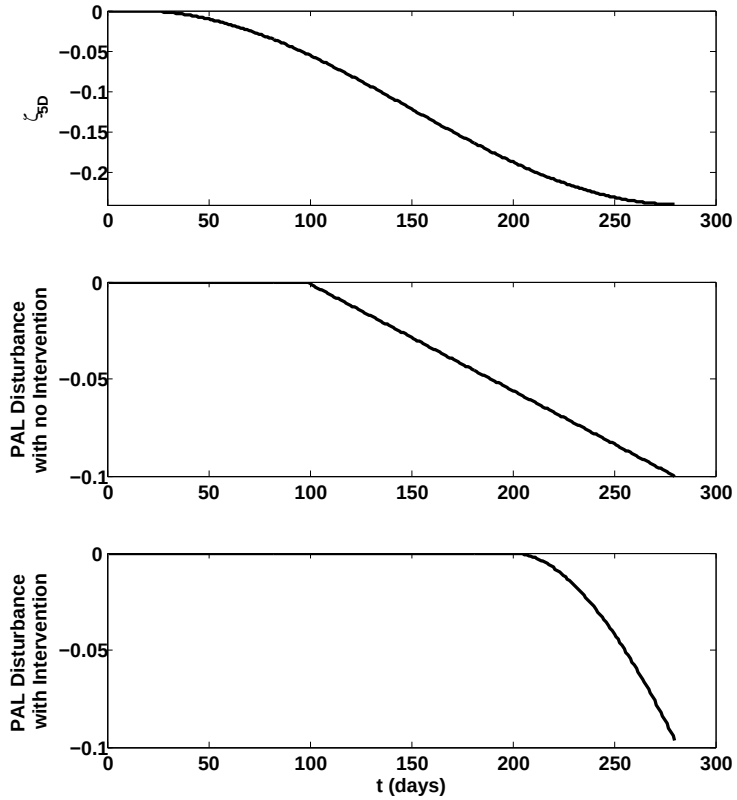

Figure 2.12: Disturbance Signals for ζ_5 in the EI-TPB (top), PAL with no Intervention and PAL (middle) with Intervention (bottom), respectively.

intervention components and self-regulation play on the inflow to PBC in the TPB models. The intervention gains for the inflow of PBC in EI-TPB are set to 0.001 for all relevant intervention components ($K^I_{31}, \ldots, K^I_{34}$=0.001), while the ones for the PA-TPB model are similarly fixed to 0.0075 ($K^I_{64}, \ldots, K^I_{67}$=0.0075). In this study, dosages for all intervention components are fixed according to the frequency stated in Table 2.5.

The decision on whether or not to start the intervention is made based on the discrepancy between a threshold value and the participant's weight. The threshold value in this section is set as 20% above the upper bound of the IOM guidelines. The intervention starts if the participant's weight exceeds a threshold, and stops once the participant's weight enters within the threshold.

Table 2.7 summarizes the model parameters in the simulation studies, including the behavioral parameters, time constants τ_i, time delays θ_i, gains assumed for the participant, and the disturbance signal parameters respectively. No time delay or disturbances are assumed in the intervention delivery dynamics. All these values are hypothetical but have been selected such that the simulated responses mimic those of an actual participant.

We assume that there is no self-regulation effect before the participant is aware of her pregnancy (prior to day 14), and the participant increases her energy intake substantially at day 14. Meanwhile, the self-regulation in this simulation will be associated with IOM guidelines only. When the participant's weight exceeds the threshold, K_e should have a small magnitude. On the contrary, when the participant's gestational weight is below the threshold, K_e should correspondingly increase as a result of the improvement that the participant has accomplished. The sign of K_e depends on the sign and magnitude of $\Delta e(t)$. Because for overweight and obese women with weight above IOM guidelines, a positive $\Delta e(t)$ indicates that the participant is not making as great progress as she did the day before, while a negative $\Delta e(t)$ indicates improvement. Therefore, K_e should be positive for (2.35) to be computed properly. Table 2.8 lists the values for K_e used in the simulations.

2.7.1.1 No Intervention Scenario

The simulation scenario described in this section consists of using the dynamical systems model summarized in Figure 2.1 to examine the scenario where the intervention is not applied. The assumption in this case is that the participant increases her energy intake once she is aware of her pregnancy at day 14. Figure 2.13 shows the participant's response for the EI-TPB model and PA-TPB model, while Figure 2.14 shows the changes in maternal body mass and the energy balance variables.

The scenario without intervention indicates that behavioral change is accomplished by the self-regulation effect on PBC in the TPB models. The simulation results indicate

Table 2.7: Model Parameters for the Simulation Studies. Time Constants (τ_i) are in Units of Days.

Parameter	EI-TPB	PA-TPB	Parameter	EI-TPB	PA-TPB
b_1	3	1	e_1	6	4
n_1	2	7	m_1	3	8
p_1	1	4	c_1	2	2
τ_1	1	30	γ_{11}	1	0.7
τ_2	1	30	γ_{22}	1	0.5
τ_3	1	10	γ_{33}	1	0.7
τ_4	1	20	β_{41}	1	0.34
τ_5	1	30	β_{42}	1	0.27
$\theta_1 \ldots \theta_3$	0	0	β_{43}	1	0.13
$\theta_4 \ldots \theta_6$	5	10	β_{53}	1	0.08
θ_7, θ_8	10	20	β_{54}	1	0.42
A	0.12	0	ω	$\frac{\pi}{270}$	0

Table 2.8: Tabulation for Self-regulatory Controller Gains K_e Applied in the Simulations in Section 2.7.1.

If-Else Condition	EI-TPB	PA-TPB
Day$\leq$14	0	0
Day $>$14 and BM $>$threshold value	2	1
Day $>$14 and BM $\leq$ threshold value	4	2

that the PBC inflow in the EI-TPB model will stay constant until day 14. Following the initial ramp increase in EI, the PBC inflow first ramps up (due to no weight increase at the very beginning), and soon diminishes, indicating that the participant is not confident of controlling her GWG. However, PBC inflow improves a little with the passage of time as the participant checks her weight daily, compares her weight with the target data, and realizes that the situation is not as bad as she expects. Because of self-regulation, the PBC and intention inventories η_3 and η_4 increase gradually. However, the behavior in PA does not improve overall as a consequence of the PAL disturbance in Figure 2.12 starting from

second to third trimester, which can be seen from the energy expenditure (EE) profile in Figure 2.14. In this scenario, we can see that the inflow of PBC eventually tries to reach the initial levels, with GWG remaining outside IOM guidelines from second trimester up until the time of delivery. This means that self-regulation alone has a limited effect on GWG control, especially for women classified as overweight or obese.

2.7.1.2 Fixed Intervention Scenario

In this section, we consider how the implementation of fixed intervention can help the participant adjust her GWG to remain within IOM guidelines. As noted previously, the assumption in this simulation is that dosages of intervention components are fixed once the intervention activation threshold is exceeded (body mass $>$ 20% above the upper bound set by the IOM guidelines). The intervention stops when the body mass is lower than the threshold.

The simulation results for the intervention scenario in Figure 2.13 and Figure 2.14 show that the intervention starts at day 106 and ends at day 227. The whole process can be divided into four stages. The first stage occurs during the first 14 days with constant PBC inflows and no significant weight changes. The second stage starts from day 15 to the day before the intervention. The participant increases her EI due to the pregnancy, which results in decreases in PBC, intention and behavior. When the participant weight exceeds the threshold value, the intervention starts; this is the third stage. In this stage, the PBC inflow increases almost linearly as a result of the integrator in the intervention delivery dynamics. When compared with the PBC curve for the intervention-only case in the TPB models, we can see that at early intervention, the self-regulation effect tries to counteract the effect of the intervention by lowering the expected increase in the PBC inflow, which means the participant does not have much faith believing that she can succeed in controlling her weight gain. However, as the intervention proceeds, the participant's confidence is greatly

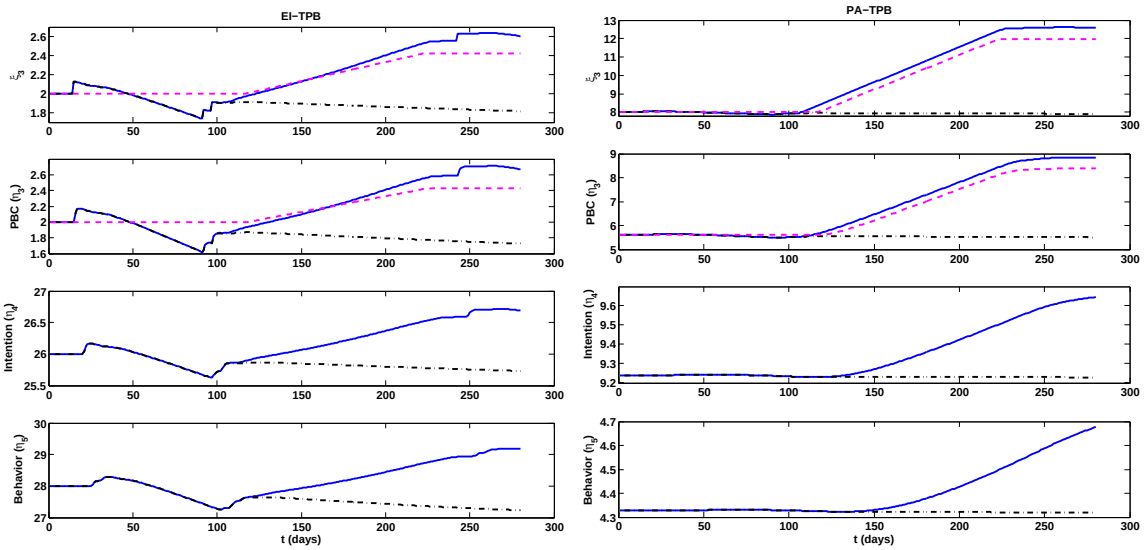

Figure 2.13: Simulation Responses for the Energy Intake Behavior (EI-TPB) Model (left) and Physical Activity Behavior (PA-TPB) Models (right). The Black Dashed Lines Represent the Case with no Intervention (Self-regulation only) while the Blue Solid Lines Represent the Case with the Intervention. The Magenta Dashdot Lines in the TPB Model Variables Show the Simulation Responses in these Variables when no Self-regulation is in Effect.

enhanced as a result of the improvement contributed by the intervention. Consequently, in the latter part of the third stage, self-regulation works together with the intervention to enable better GWG control despite the existence of external disturbances. The fourth stage occurs once the intervention stops. In this stage, the participant may feel initially aimless with the termination of intervention. Meanwhile, it is late third trimester when she is more likely to reduce her PA. However, the built-up PBC inflow during the intervention can still almost keep constant, and her EE profile is still above the initial EE despite of its decrease due to PAL disturbance. In this scenario, we can see that with the help of intervention and self-regulation, it is possible for a woman to manage her GWG within the IOM guidelines with the fixed intervention ending around two months before delivery, even in the presence of disturbances.

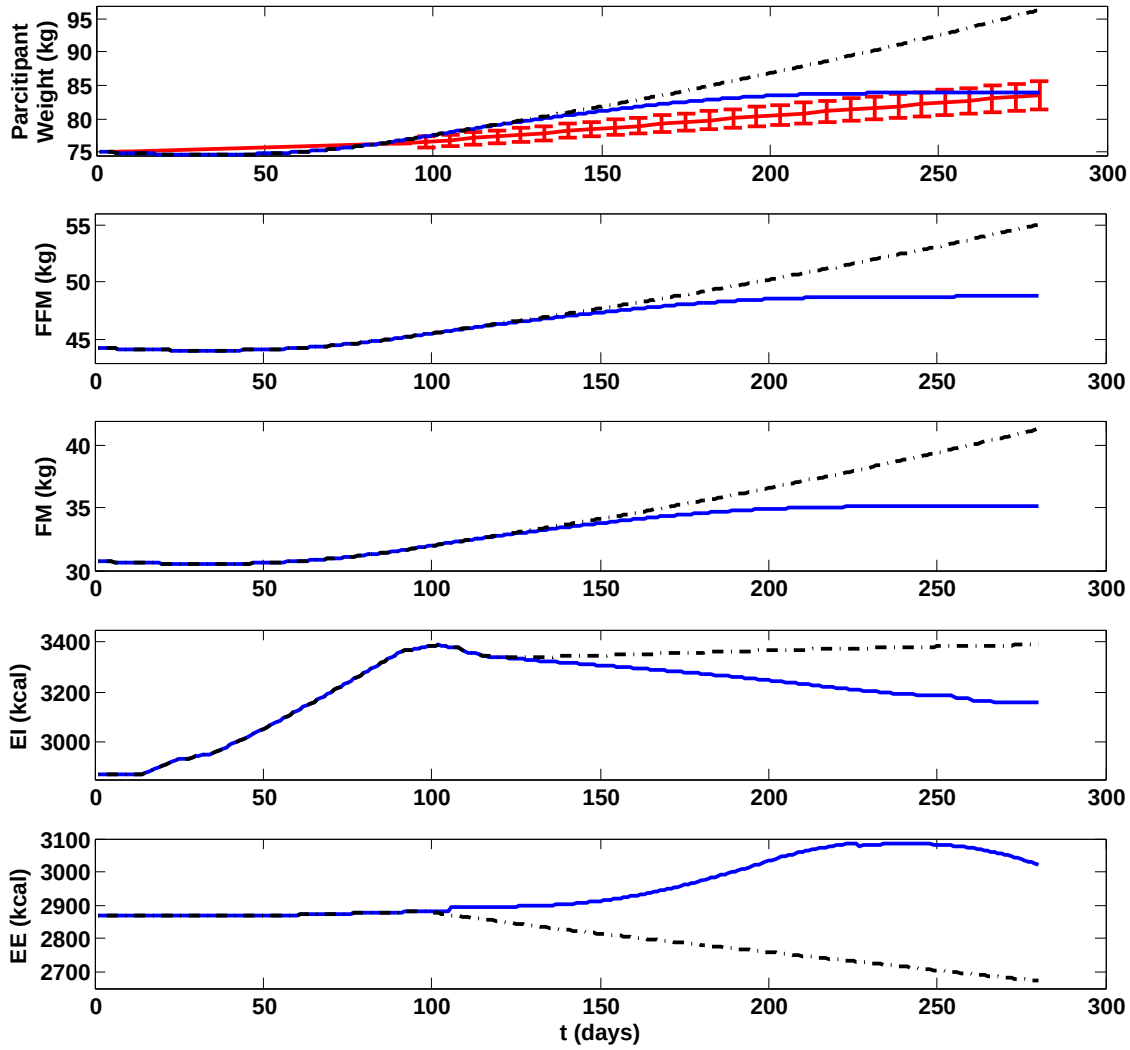

Figure 2.14: Simulation Responses for Maternal Energy Balance. Red Lines Represent the 2009 IOM Guidelines Applied a Daily Basis; the Black Dashed Lines Represent the Case with no Intervention (Self-regulation only) while the Blue Solid Line Represents the Case with the Intervention and Self-regulation.

2.7.2 *Adaptive Interventions via Decision Rules*

In the second part of the simulation, we will implement the decision rules discussed in Section 2.6. Because the intervention is targeted mainly to the OW/OBPW, we set the women pre-gravid weight as 70kg (BMI=27.34, overweight) and 80kg (BMI=31.25, obese) for the two scenarios in this section. This adaptive intervention will only have effect on the PBC inflows just as how it works in section 2.7.1, with the gains for the inflow of PBC in EI-TPB as (K^I_{31}, ..., K^I_{34}=0.0008), and the ones for the PA-TPB model fixed as (K^I_{64}, ..., K^I_{67}=0.006). We assume that the participant will have a ramp increase just like the one in (2.45) in Section 2.7.1.

The proposed hypothetical intervention aims to help the participant manage her GWG within the IOM guidelines. The case study assumes the participant enters the intervention with the baseline program at week 14 (day 98). The dosage of the intervention components is adapted every so many weeks (e.g. 3-week cycle in the second trimester and 2-week cycle in the third trimester) based on decision rules of whether she is meeting or not meeting her GWG goal until week 35 (day 245) as described in the Section 2.6.

For the self-regulation, we will include not only the weight reference but also the EI reference due to the self-monitoring components in the intervention, which is a little different from the one used in Section 2.7.1. The self-regulation will influence the PBC inflow of two TPB models. We assume self-regulation starts with the intervention when the counseling, the GWG target and self-monitoring data are available. Because we have two sets of reference values for the self-regulation, the corresponding gains K_e applied in the EI self-regulation model are also changed and are listed in Table 2.9. Since no PA reference data right now, the controller gains for PA self-regulation remain the same with the ones in Table 2.8.

Table 2.10 summarizes the intervention dosages applied in the models. According to

Table 2.9: Tabulation for Self-regulatory Controller Gains K_e Applied in the Simulations in Section 2.7.2.

If-Else Condition	**EI-TPB**	**PA-TPB**
Day$\leq$98	0	0
Day $>$98 and GWG $>$IOM threshold value	1	1
Day $>$98 and GWG $\leq$ IOM threshold value	2	2
Day$\leq$98	0	-
Day $>$98 and EI $>$EI threshold value	0.0025	-
Day $>$98 and EI $\leq$ EI threshold value	0.005	-

the flow chart of decision rules described in Figure 2.10 and intervention dosage in Table 2.5, we have 12 GWG order sequences (-3 to +8), where order 0 is baseline program, order -1 $\sim$ oder -3 represent three reductions below baseline program, and order +1 $\sim$ order +8 refer to eight augmentations above baseline program. The parameters for the intervention dosage in the decision rules are assigned to reflect how the dosages are changed according to the decision rules, the participant's response and outcome during the intervention. All the other parameters in the model are the same as the ones in Table 2.7.

2.7.2.1 Simulation Study for Overweight Group

Figure 2.15 and Figure 2.16 show the simulation results for the behavioral variables in EI-TPB and PA-TPB models, the dosage of the intervention components, the maternal body mass, energy intake and energy expenditure for overweight participant with the decision rules implemented. We can see that the participant has a ramp EI increase from day 14 - 91 (first trimester). As discussed above, the adaptive intervention starts at week 14 (day 98) with the participant engaging in self-regulatory behaviors. The intervention dosages (both healthy eating and physical activity) change according to the measured outcomes during the previous treatment. If we simulate the EI based on the IOM guideline (upper, lower bounds and average values), we can get the corresponding step EI inputs for all three

Table 2.10: Intervention Dosages for the Decision Rules (BS=Baseline value)

HE Intervention				PA Intervention					GWG Order
Edu	Plan	Meal Demon	GS	Edu	Plan	GS	PA Session	PA Input to EB	
1/4	1/3	1/3	1/4	1/4	1/3	1/4	1/3	BS/3	-3
1/3	1/2	1/2	1/3	1/3	1/2	1/3	1/2	BS/2	-2
1/2	1	1	1/2	1/2	1	1/2	1	BS	-1
1	1	1	1	1	1	1	1	BS	0
1	1	1	1	1	1	1	2	2BS	+1
1	1	1	1	1	1	1	2	2BS	+2
1	1	1	1	1	1	1	2	2BS	+3
1	1	1	1	1	1	1	3	3BS	+4
1	1	2	1	1	1	1	3	3BS	+5
1	1	2	1	1	1	1	3	3BS	+6
1	1	2	1	1	1	1	4	4BS	+7
1	1	3	1	1	1	1	4	4BS	+8

trimesters (red line) which make the GWG follow the average IOM guideline (under the assumption of zero change of PAL). With GWG energy balance model, the suggested EE, FFM and FM can also be obtained as depicted in Figure 2.16.

The EI plot shows that the participant increases her EI very quickly in the first trimester, and just before the intervention, the participant has already had higher EI than the EI reference values she should have for the third trimester suggested by IOM. This indicates that this participant's perceived control to control her GWG is low and explains why the PBC inflow to the EI-TPB model reduces a little at the beginning of the intervention. However, the PBC inflows to both TPB models improve as she progresses through her pregnancy with the help of intervention adapted to her needs and self-regulation. At the entry of the intervention, the participant's GWG is within IOM guidelines even though her EI is above the reference values. The initial dosage she receives is baseline program with order 0 (Figure 2.15). At this does of intervention, the participant still has high EI leading to GWG above the IOM guidelines at the time of her second assessment cycle (3 weeks later). Thus, her intervention is tailored and augmented (i.e., dose/components are increased). Her EI and EE responses show that the participant gradually lowers her EI and tries to do more PA, which leads to the increase of EE. At around day 245 (week 35) when the intervention stops, she starts to reduce her PAL slightly which is mainly played by the PAL disturbance in Figure 2.12, as most women (even those participating in interventions) tend to decrease their PA in the third trimester as they approach delivery. However, the final value of PAL is still above the initial PAL. As a result, with participation in the individually-tailored adaptive intervention, she is able to control her EI within the EI reference values, and manage her GWG within the IOM guidelines at late pregnancy. This simulation study also demonstrates how the interventions are adapted with decision rules applied to the model.

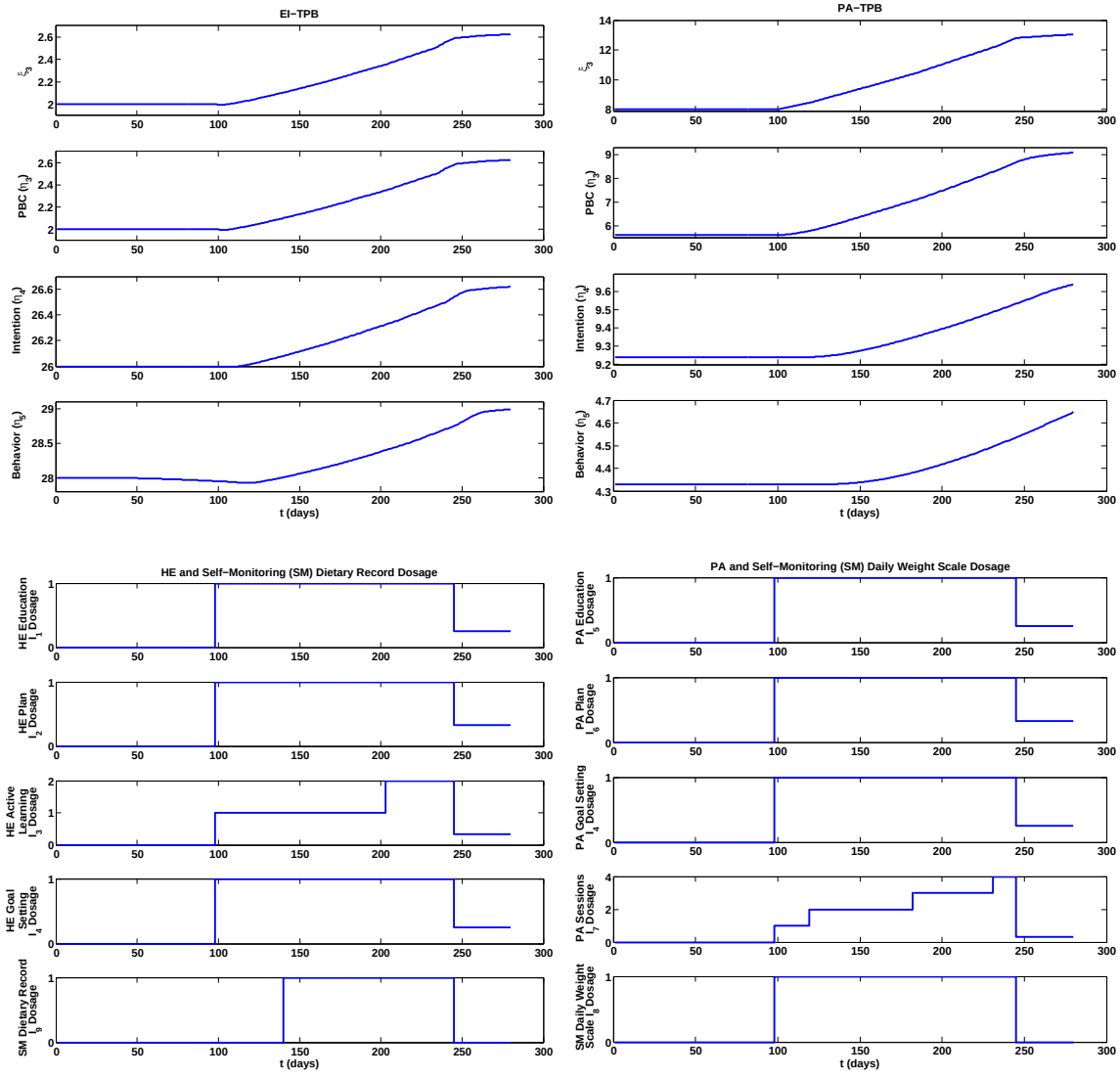

Figure 2.15: Simulation Result for the Behavioral Variables for Energy Intake TPB (EI-TPB) and Physical Activity TPB (PA-TPB) Models, and the Dosage of the Intervention Components for Overweight Participant with the Decision Rules Implemented.

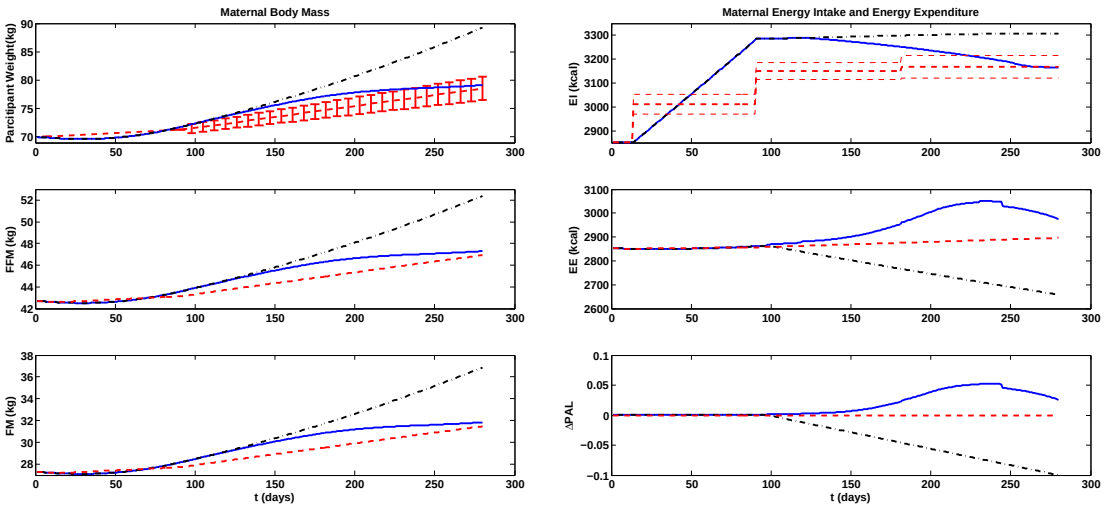

Figure 2.16: Simulation Responses for the Maternal Body Mass, Energy Intake and Energy Expenditure for Overweight Participants with the Decision Rules Implemented. Red Dashed Lines Represent the 2009 IOM Guidelines Applied on a Daily Basis, Black Dash-dot Lines Show the Simulation Response in these Variables in the Absence of an Intervention.

2.7.2.2 Simulation Study for Obese Group

Figure 2.17 and Figure 2.18 show the simulation responses for the obese group. There is no much big difference in the results between the overweight group and the obese one, except for the intervention dosages, the day when GWG and EI enter the reference value, and the ultimate body mass at delivery. The initial dosage she receives is augmentation +1, due to her GWG outside IOM guidelines at the entry of the intervention. This explains why she gets 2 levels as the initial dosage for PA sessions (I_7) in Figure 2.17 instead of 1 level dosage in the overweight case in Figure 2.15. The participant always has stepping up in

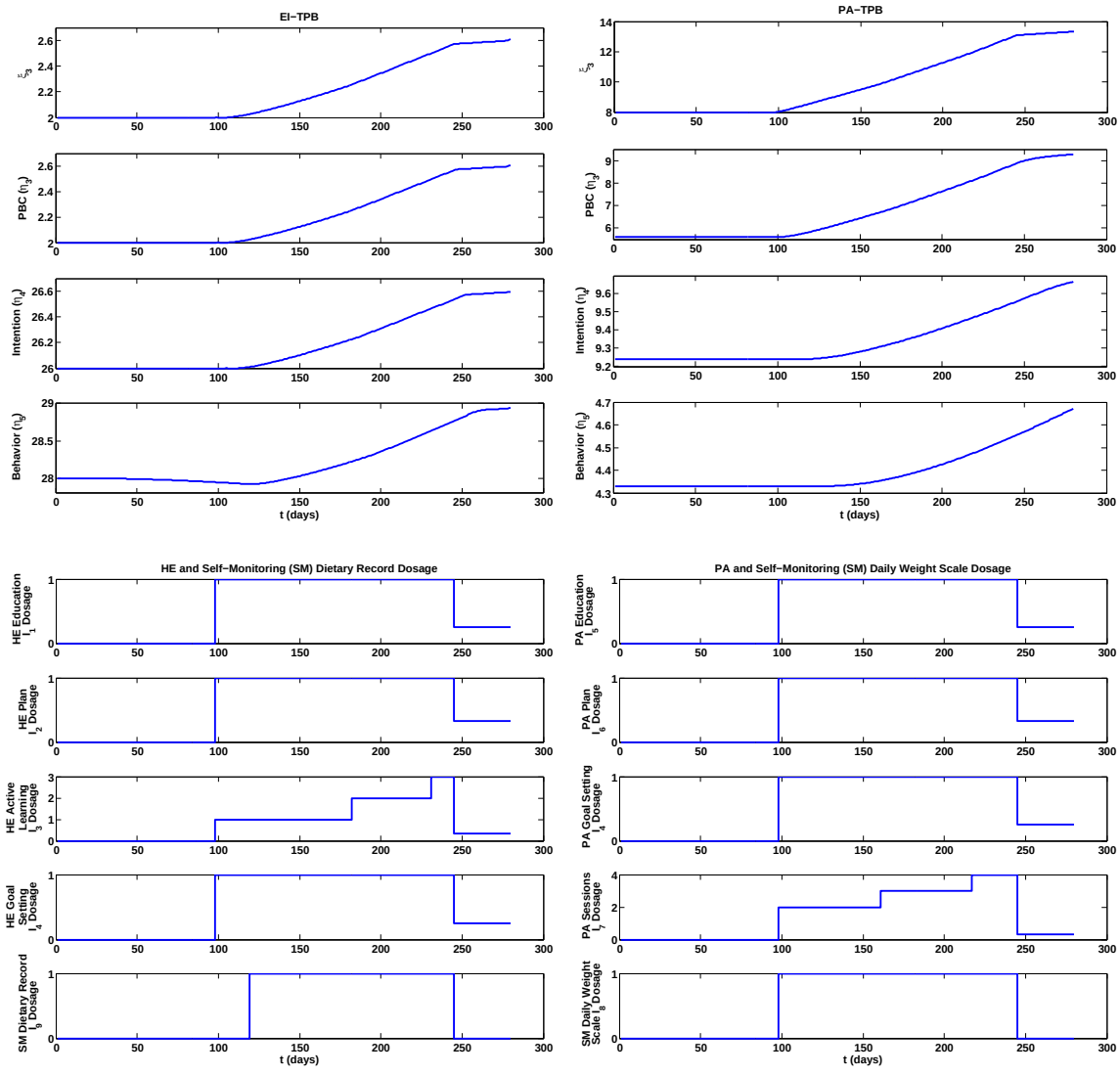

Figure 2.17: Simulation Result for the Behavioral Variables for Energy Intake TPB (EI-TPB) and Physical Activity TPB (PA-TPB) Models, and the Dosage of the Intervention Components for Obese Participant with the Decision Rules Implemented.

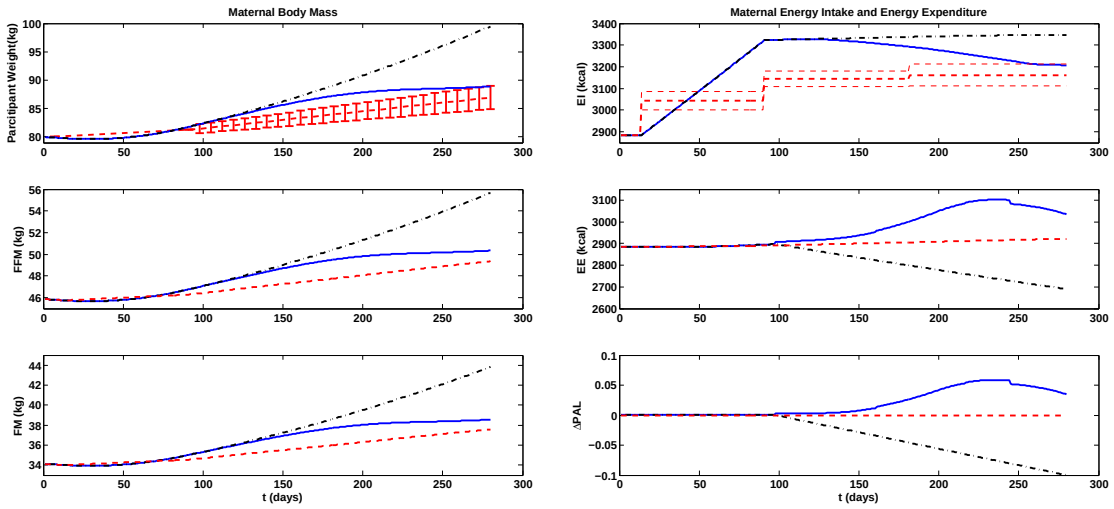

Figure 2.18: Simulation Responses for the Maternal Body Mass, Energy Intake and Energy Expenditure for Obese Participants with the Decision Rules Implemented. Red Dashed Lines Represent the 2009 IOM Guidelines Applied on a Daily Basis, Black Dash-dot Lines Show the Simulation Response in these Variables in the Absence of an Intervention.

dosage order, because her GWG is outside the IOM boundary throughout the whole intervention. However, after the intervention stops, the participant's built-up PBC and attitude inflows of both TPB models are still working. With the help of the self-regulation effect, the woman can both manage her GWG within the upper bound of the IOM guidelines and reduce her EI to make it reach the upper bound of the EI reference values before the time of delivery. The different simulation results between the overweight group and obese one are caused by the woman's pre-gravid weight. However, in the real life, there might be other external disturbances and individual variations that will undermine the intervention, and that is why the intervention does not always work on every participant. In this scenario, the participant has pre-gravid mass at 80kg, and with the help of intervention and

the self-regulation, she can still control her GWG within the IOM boundary at late third trimester. If the participant's pre-gravid weight is 95kg, the intervention fails to achieve the GWG goals with the same model parameters.

2.8 Fetal Birth Weight Model

The obesity epidemic is a major public health concern affecting all ages. In this section, we propose an intergenerational approach to prevent obesity. Dynamical systems modeling based on the previous sections is used to describe how an individually-tailored, behavioral intervention that adapts to the unique needs of each woman to reduce fetus exposure to an "obesogenic" intrauterine environment can impact gestational weight gain (GWG) and birth weight. This approach relies on integrating mechanistic energy balance, theory of planned behavior, and self-regulation models to describe how internal processes can be impacted by intervention dosages, and in turn, reinforce positive outcomes (engaging in healthy eating and physical activity) to moderate GWG and impact birth weight. A simulated hypothetical case study from MATLAB with Simulink is presented to illustrate the basic workings of the model and demonstrate how the proper design of an intervention that varies based on the needs of the participant can promote healthy GWG and infant birth weight.

2.8.1 Fetal Energy Balance Model

The energy balance model in Section 2.1 captures the weight change during the pregnancy for the mother. It addresses how the healthy diet (energy intake) and physical activity help reduce the growth of GWG. GWG has immediate and lifelong health benefits such as a reduced risk for postpartum weight retention in mother, adverse birth outcomes, and obesity in both mothers and offspring as we discussed before. Meanwhile, the childhood obesity epidemic is a major public health concern that is not limited to school age children and adolescents, but also affects infants and toddlers. Furthermore, the prenatal period is

an opportune time to intervene and break the intergenerational cycle of obesity by managing GWG. All these inspire us to integrate the fetal energy balance model into our current one. It is meaningful to show how GWG impacts infant birth weight by improving our current dynamical systems model which describes the influence of behavioral interventions on weight gain during pregnancy.

The fetal energy balance model [7] is obtained in a similar way as how we dealt with the maternal energy balance model [72]. It is based on a two-compartment (fat mass and fat-free mass) model. The fetal energy balance model will rely on the conservation of the energy, which is expressed as,

$$ES_f(t) = EI_f(t) - EE_f(t) \tag{2.47}$$

When expanding the ES_f into the instantaneous change of the sum of the two compartments (FFM and FM), the fetal fat mass can be calculated using the following full energy balance model,

$$\lambda_{FFMf}\frac{dFFM_f}{dt} + \lambda_{FMf}\frac{dFM_f}{dt} = EI_f(t) - EE_f(t) \tag{2.48}$$

where λ_{FMf} and λ_{FFMf} are the fetal caloric values of the fat and fat-free mass, both in kcal/kg. Fetal energy expenditure $EE_f(t)$ is modeled with μ as the proportion that fetal body mass contributes to energy expenditure ($\mu = 32$kcal/kg/d),

$$EE_f(t) = \mu(FFM_f(t) + FM_f(t)) \tag{2.49}$$

The formulation of fetal energy intake $EI_f(t)$ is expressed as a product of the total maternal calories consumed per day $EI(t)$ which will be changed due to the intervention, percentage factor of daily glycemic index of maternal diet $g_e(t)$ and placental volume $P(t)$.

$$EI_f(t) = \gamma g_e(t)P(t)EI(t) \tag{2.50}$$

where $\gamma = 0.000234$ which is introduced as a conversion constant measured in 1 ml^{-1}, $g_e(t)$ and $P(t)$ are both functions of mother's PAL.

The placental volume $P(t)$ is calculated as follows [72],

$$P(t) = \frac{P(140)K(t)exp(r(t-140))}{P(140)exp(r(t-140)) + K(t) - P(140))} \tag{2.51}$$

where r is the unrestricted growth rate, $K(t)$ is the carrying capacity, and $P(140)$ is the initial condition for the placental volume at day $t = 140$. The carrying capacity $K(t)$ is ranged from $K(t) = 424$ ml for non-exercising mothers to $K(t) = 522$ ml for high-intensity exercising mothers, and it can be estimated as a function of PAL as follows,

$$K(t) = 73.7PAL(t) + 337.8 \tag{2.52}$$

The initial placental volume ranges from $P(140) = 181$ ml for non-exercising mothers to $P(140) = 255$ ml for high-intensity exercising mothers and it can be estimated as a function of the baseline PAL ($PAL(0)$) as follows,

$$P(140) = 55.6PAL(0) + 115.9 \tag{2.53}$$

The percentage impact of the average daily glycemic index of maternal diet $g_e(t)$ depends on PAL, and is modeled as follows,

$$g_e = \frac{1}{PAL_{min} - PAL_{max}} + 1 \tag{2.54}$$

where $PAL_{min} = 1.17$ and $PAL_{max} = 2.55$.

Thus, the final fetal energy balance model is,

$$\lambda_{FFMf}\frac{dFFM_f}{dt} + \lambda_{FMf}\frac{dFM_f}{dt} = \gamma g_e(t)P(t)EI(t) - \mu(FFM_f(t) + FM_f(t)) \tag{2.55}$$

The change of mother's EI and PAL during the intervention will influence fetal EI, placental volume and ultimately fetal FM and birth weight.

2.8.2 Simulation Study

In this section, a simulated hypothetical case study will be presented illustrating the basic workings of this model and demonstrate proof of concept for how self-regulation and adaptive interventions with decision rules influence GWG during pregnancy, and in turn, impact infant birth weight. Exploratory simulations of our adaptive GWG intervention [10] will be generated from data based on an intergenerational fetal EB model [72] and artificial parameters to examine the effects of creating a healthy maternal-fetus eating and PA environment on infant birth weight.

Figure 2.19 summarizes the model diagrammatically, where the mechanistic energy balance leads to a dynamical model with EI and PAL as inputs; maternal fat mass FM_m, fat-free mass FFM_m, fetal fat mass FM_f and fat-free mass FFM_f as outputs. The outputs add up to total body masses BM_m and BM_f for mother and fetus, respectively. The fetal energy balance model will be the focus of this section as an extension of current GWG intervention model, when we integrate self-regulation, TPB, intervention delivery modules and decision framework. With this maternal-fetal energy balance model, the behavioral scientist can not only track the mother's GWG within the IOM guidelines, but also make sure the fetus' and infant's birth weight within the reasonable target.

The simulations in this section are based on a hypothetical 25-year-old female with pre-gravid body mass 75 kg, 160 cm in height, which classifies her as overweight (BMI=29.3). The participant is sedentary at the time of conception (PAL = 1.65) and potentially engaged in less PA from the second to third trimester as she gains weight. The intervention can help improve her PAL during pregnancy. In this section, decision rules developed by the R01 research team will be used to evaluate GWG every four weeks. If a woman is within her GWG goal, the intervention dosages will be sustained; however, if she is exceeding her GWG goal, the intervention is adapted (i.e., "stepped up") to increase potency. the case

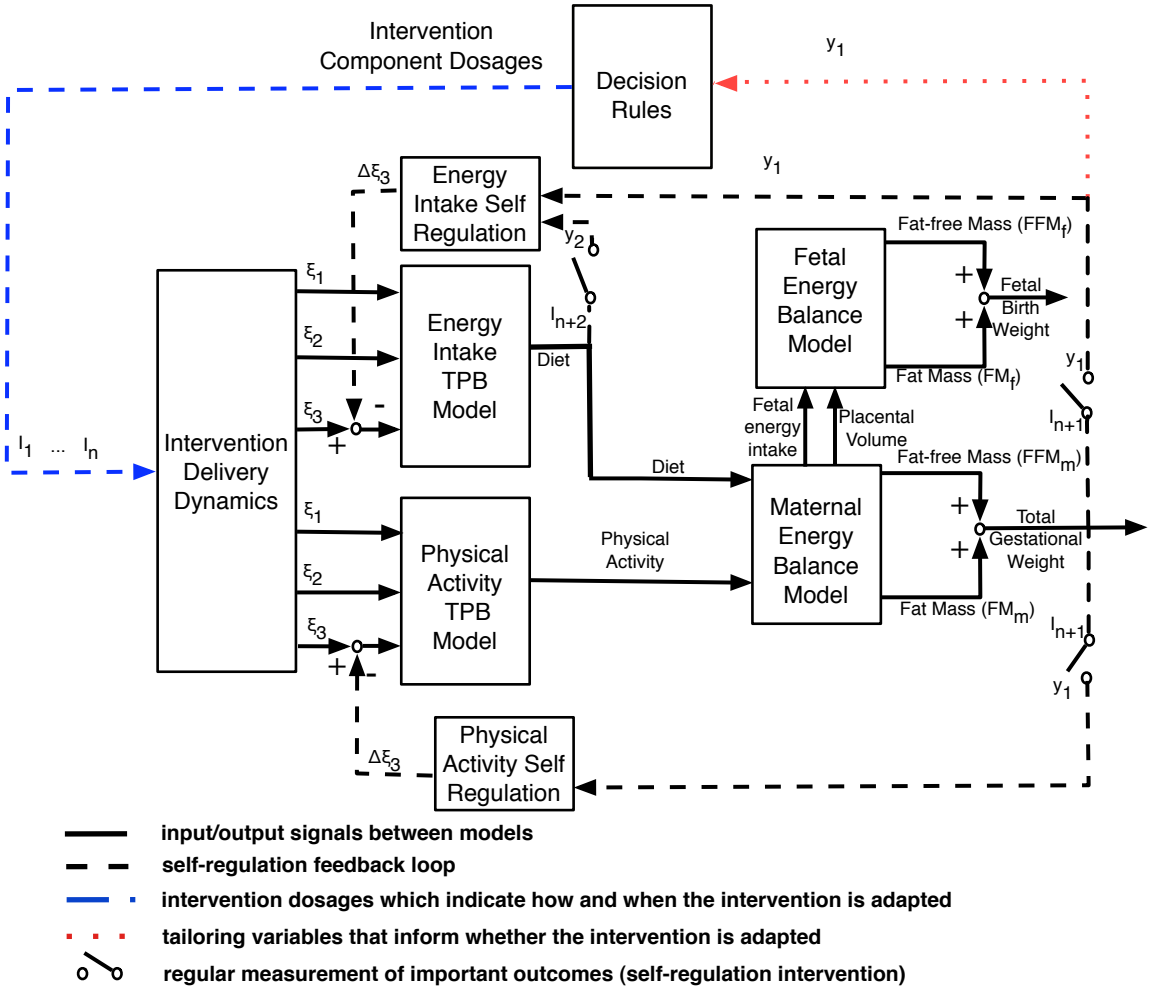

Figure 2.19: Schematic Representation for an Adaptive Fetal Birth Weight and Gestational Weight Gain Intervention.

Table 2.11: Summary of Dosage Augmentations per the IF-THEN Decision Rules on GWG and Fetal Weight Gain Control. (Notes: Baseline Intervention Includes Self-monitoring, Education and Guidance)

Options	**Adaptation**
Baseline intervention	NA
Step up 1	Baseline + healthy eating component
Step up 2	Baseline + 1 + PA component
Step up 3	Baseline + 1+2 + self-monitoring component
Step up 4	Baseline + 1 + 2 + 3 + healthy eating component
Step up 5	Baseline + 1 + 2 + 3 + 4 + PA component
Step up 6	Baseline + 1 + 2 + 3 + 4 + 5 + healthy eating component

study still assume the participant enters the intervention with the baseline program at week 14 as described in Table 2.11.

The model parameters in the behavioral models are same as the ones in Table 2.7, and the self regulatory controller gains are same as the ones in Table 2.9. The gains in intervention delivery modules are same as the ones in Section 2.7.2.

Figure 2.20 shows two hypothetical simulation scenarios for a 25 year old, overweight woman predicted maternal weight gain, EI, PAL, and fetal weight gain for the case study described above when she (a) receives our adaptive intervention and (b) does NOT receive our intervention. In both simulations, during the first trimester, we assume this overweight woman will increase her EI as she is aware of her pregnancy and she will remain sedentary with little or no activity (PAL is 1.65) throughout the first trimester. In the first scenario, the intervention starts around day 100 with the participant receiving the baseline intervention. At this dose of intervention, the participant still has high EI leading to GWG above the IOM guidelines at the time of her second assessment cycle. Thus, her intervention is augmented (i.e., dose/components are increased). Once the intervention is adapted, she gradually lowers her EI. Meanwhile, the intervention also forces her to be involved in PA, leading

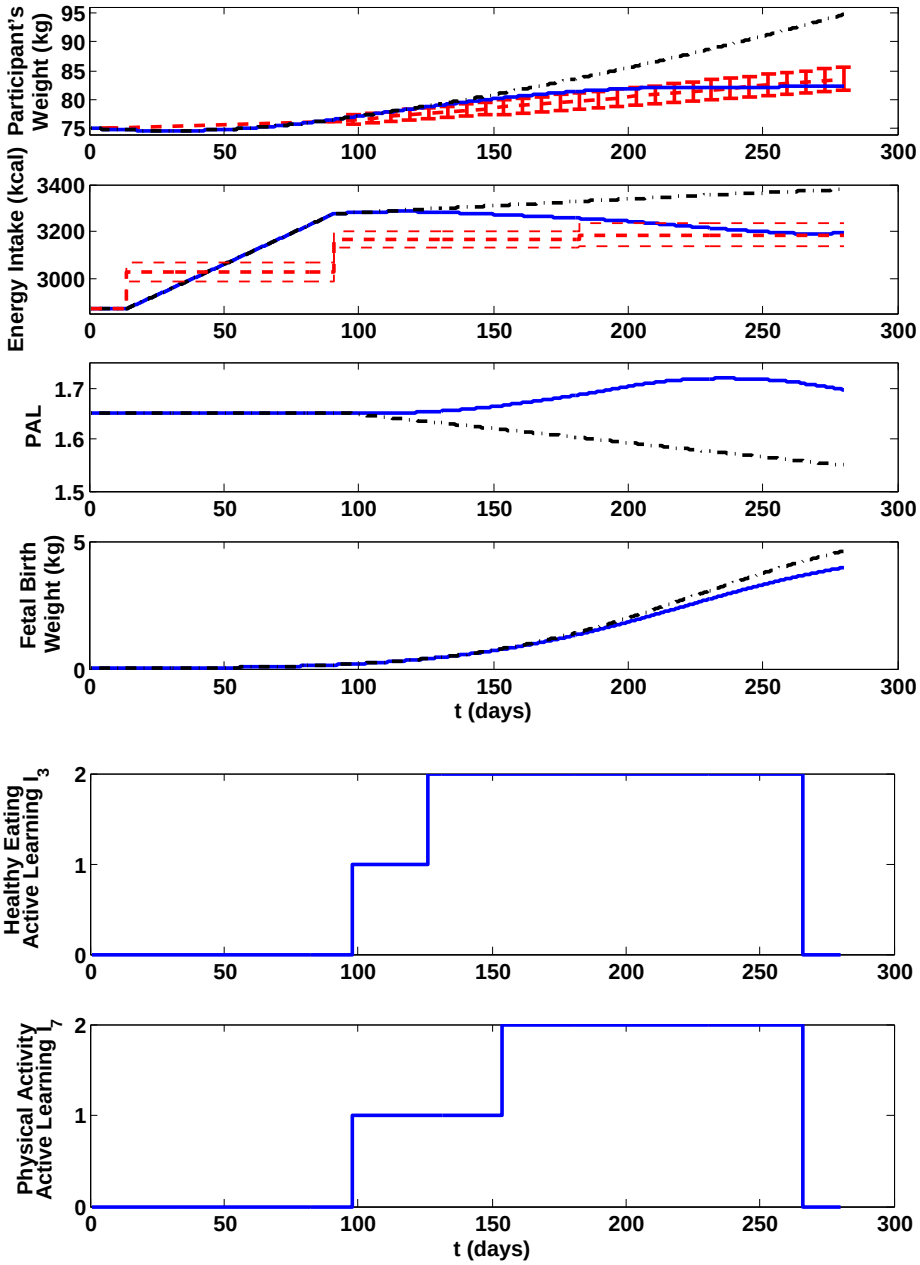

Figure 2.20: Simulation Responses for the Maternal Body Mass, Energy Intake (EI), Physical Activity Level (PAL) and Fetal Birth Weight. Red Lines Represent the 2009 IOM Guidelines Applied on a Daily Basis; the Blue Solid Lines Represent the Case with Intervention and Self-regulation, while the Black Dashed Lines Represent the Case with no Intervention.

to the increase of her PAL from sedentary (PAL = 1.65) at the start of the intervention to moderately active (PAL = 1.70) around day 196 (i.e., the start of her third trimester). The highest PAL that she achieves is 1.719 around day 230 (week 32), maintaining this level of activity until day 250 (week 35). Around this time, she starts to reduce her PAL slightly to 1.697 as most women (even those participating in interventions) tend to decrease their PA in the third trimester as they approach delivery. However this final value of PAL is not only still above the initial PAL 1.65, but also very close to the moderately active PAL range ($PAL = 1.7$). Because this intervention was adapted to this participant's specific needs, her EI decreased and PA increased during the intervention, and her rate or speed of weight gain slowed in the second trimester. As a result, with participation in the individually-tailored, adaptive intervention, she meets her GWG goal at day 190, and keeps her EI within the EI reference values at day 210. At time of delivery, she meets the IOM GWG guidelines based on her pre-pregnancy classification of overweight, gaining a total of 7.31 kg. Further, by modifying the intrauterine dietary intake and PA environment, her infant is born at 40 weeks gestation at 3.963 kg, which is within the range of normal and healthy birth weight.

The simulation result for the no-intervention case shows that without intervention, this same woman gradually increases her EI from the start of her second trimester (3300 kcals) to the end of her third trimester (3380 kcals). Without receiving an intervention, she increased her EI by about 500 kcal during pregnancy, which is about 150 kcals higher than recommended during the third trimester for an overweight (almost obese) woman. Also, from the beginning of the second trimester to the end of the third trimester, her PAL decreases from 1.65 to 1.55, making her even more sedentary. Without intervention, she gains 19.63 kg and exceeds the IOM GWG guidelines. Further, due to excessive GWG (high EI and low PA), this mother delivers an infant weighing 4.611 kg (10.166 pound). This infant would be considered macrosomic (birth weight greater than 90% for gestational age), which has negative health outcomes for both mother and infant, especially for those

born weighing more than 9 pounds 15 ounces as is in this case.

2.9 Chapter Summary

In this chapter, a comprehensive dynamical systems model for GWG adaptive behavioral interventions has been proposed, which deals with the application of control engineering theory in the field of psychology and behavioral health. The model provides a helpful and informative framework for better understanding, designing and optimizing interventions geared to reduce overweight problems during pregnancy, and hence prevent possible complications, both during and after delivery.

We showed two case studies, focusing on how self-regulation and intervention work in a fixed intervention and how the decision rules are implemented to get the dosage tailored according to participant's GWG needs as an adaptive intervention, respectively. The first study shows how self-regulation helps adjust PBC, which consequently changes the participant's intention and ultimately behavior with respect to healthy eating and physical activity during pregnancy. The self-regulation effect is strong when a participant feels confident in what she will do, and weak when she does not have faith in the success of the task. When the fixed intervention in involved, its effect is first offset by self-regulation; however, as the intervention outcomes improve, these two effects interact with each other to greatly increase the PBC inflow in the TPB models. Consequently, the resulting behavioral improvements counter the effect of natural disturbances that work to worsen behavior during the latter stage of pregnancy.

The incorporation of intervention dosage adaptations via decision rules with our comprehensive dynamical model to simulate the GWG intervention that adapts to the needs of OW/OBPW is the focus of the second case study. With the decision rules, the dosage changes with the increase of time. Based on the participant responses during the intervention, the existing intervention components are either augmented, diminished or kept

unchanged. The simulation responses for the overweight and obese scenarios are very similar. In this case study, if the parameters in behavioral models are same, the differences in the dosages assigned, the maternal body mass, the energy intake and energy expenditure are due to the pre-gravid weights. Meanwhile, the intervention does not guarantee that every participant can achieve her GWG goals in the real life due to the external unmeasured disturbances, and the individual variations in the responses to the intervention. In next chapter, we will evaluate how intra-individual and inter-individual variabilities play an important role in the intervention outcomes. Meanwhile, well-designed clinical trials will be required in order to accomplish the system identification tasks that will validate the model and enable future evaluation of the decision rules and implementation of hybrid model predictive control (HMPC) for this problem.

The chapter also extend GWG model to include fetal weight gain to simulate an intergenerational GWG intervention that could have substantial effects on maternal fetus eating and PA environment, GWG, and infant birth weight. The results from our case study simulations showed how in response to our intervention, self-regulation helps adjust PBC, which consequently changes the participant's intention and ultimately behavior with respect to healthy eating and PA during pregnancy, thereby impacting both GWG and infant birth weight. From these hypothetical simulations, we can better understand that OW/OBPW may need interventions tailored to their specific needs to create a healthy intrauterine environment in an effort to meet GWG goals, which in turn, moderate infant birth weight. Specifically in our simulation, after receiving two potential adaptations, this participant met her GWG goal, delivering a healthy sized baby whereas the participant who did not receive our intervention gained excessive weight and delivered a baby termed macrosomic (large for gestational age).

In conclusion, this chapter demonstrates the potential for real-world applications of an adaptive intervention to manage GWG in OW/OBPW and moderate infant birth weight and

provides a plausible proof of concept of our approach. The ultimate goal is to validate this simulation by examining the effectiveness of a real-life implementation of our intervention on both GWG and infant birth weight (i.e., short term effects).

Chapter 3

ADVANCED CONTROLLER FORMULATIONS FOR SELF-REGULATION

3.1 Overview

Self-regulation refers to the capacity of human beings to alter their behavioral response. It is the process by which people attempt to constrain unwanted urges in order to gain control of their behavior. Regulation means change, especially change to bring behavior to meet some standard such as a goal. One very useful form of self-regulation is to change one's behavior in order to follow rules, match ideals, or pursue goals [73].

As discussed in Section 2.4, many theories of self-regulation are conceptualized on the basis of negative feedback control systems. This is the basic regulator in control theory [9] as we illustrated in Section 2.4. The explicit statement of this idea goes back to [74] in psychobiologic homeostatic theories in 1991 and the cybernetic TOTE model presented by Miller, Galanter, and Pribram [75] in 1960, who were the first theorists to argue for the idea that feedback processes are important in macro-level human behavior. They presented a picture of human behavior guided by plans and goals and self-regulated by discrepancy-reducing feedback processes, which illustrated a feedback-based vision of behavior, and inspired others to consider its usefulness. Action to reduce the incongruity is triggered by perceived discrepancy between performance and an internal standard. In negative feedback control, if performance does not match the internal standard, the person could be inspired to take actions to improve his behavior; otherwise, he could not be stirred to action until he receives feedback of a shortcoming [51].

In this chapter, Internal Model Control (IMC) is applied to the mathematical formulation of self-regulation in which feedback processes are involved. Compared to the derivative-only controller for self-regulation shown in Section 2.4.2, the improved controller formulations will allow greater flexibility in the description of participant's different

self-regulation responses. It is an obvious fact that control system design is fundamentally determined by the steady state and dynamic behavior of the process to be controlled. The IMC viewpoint represents an alternative yet equivalent of the traditional feedback control algorithm. Its name denotes the fact that the process model becomes an important part for designing the controller.

This chapter will first introduce methods for designing feedback controllers as self-regulation algorithms based on IMC, followed by the different cascade control designs for inner and outer loops associated with corresponding setpoints in self-regulation. The simulations presented in this chapter not only illustrate the basic workings of the GWG model with improved self-regulation formulation, but also demonstrate proof of concept for how self-regulation and time-varying adaptive interventions influence GWG during pregnancy, and how intra-individual and inter-individual variabilities play an important role in the intervention outcomes.

It should be noted that self-regulation is ubiquitous in behavioral science, and hence, the controller formulations in this chapter are not limited to the GWG problem, but can also be applied to other behavioral intervention problems.

3.2 Internal Model Control (IMC)

The IMC structure [76] given in Figure 3.1 is central to the discussions on the design of controllers. Its conceptual usefulness lies in the fact that it allows us to concentrate on the controller design without having to be concerned with control system stability provided that the process model $\tilde{p}(s)$ is a perfect representation of a stable process $p(s)$.

While investigators have made use of concepts similar to those of IMC to design optimal feedback controller since the late 1950s when Newton, Gould and Kaiser [77] pointed out the transformation of the closed-loop structure into an open one in order to develop an H_2-optimal controller, it was Frank who was the first to anticipate the value of the control

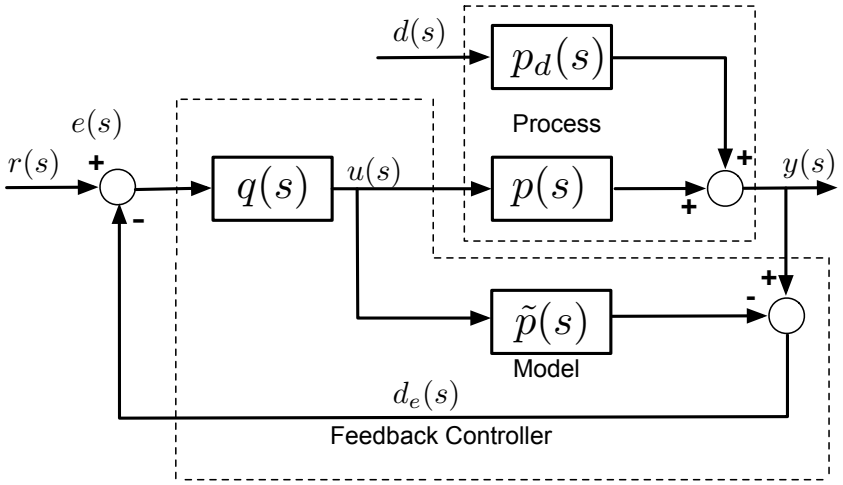

Figure 3.1: Schematic Representation of the Internal Model Control (IMC) Structure [12].

structure having in parallel the model and the plant and proposed utilization of the structure shown in Figure 3.1. However, it was Morari and García [76, 78–82] who brought the major contribution to this advanced control structure and placed the methodology in a sound theoretical framework.

3.2.1 Introduction

The IMC approach to controlling a process works in a very human style. When the controller tries to maintain a controlled variable close to a desired setpoint, it performs a simple calculation based on the model of the process in order to set the proper value of the manipulated variables. The controller calculates the difference between the actual value of the controlled output and an estimation of the effect of the intended value of the manipulated variable on the plant output. The calculation of this difference is the basic information on which decision is made to set the amplitude of the manipulated variable change that is sent to the plant. In fact, the controller determines the necessary change of the manipulated variable on a model-based estimation of the disturbance. Feedback signals of this procedure lead the closed loop system to have a desired behavior of the controlled

variable. This fundamental control approach serves as the core of IMC.

Figure 3.1 [12] presents a schematic representation of the IMC structure, in which $p(s)$ represents the process (plant) transfer function between the manipulated variable and the controlled variable, $p_d(s)$ the process transfer function between the disturbance and the controlled variable, $\tilde{p}(s)$ the mathematical model of the process, and $q(s)$ the transfer function of the IMC controller. From the block diagram in Figure 3.1, we can see that the role of the parallel path containing the model $\tilde{p}(s)$ is to generate the difference between the actual process output and an estimation of the manipulated variable effect on the process output. Assuming that there is no model/plant mismatch ($\tilde{p}(s) = p(s)$), the difference $d_e(s)$ is the estimated effect of the disturbances (both measured and unmeasured) on the controlled variable. If the process model is not perfect ($\tilde{p}(s) \neq p(s)$), the difference $d_e(s)$ includes both the effect of the disturbances on the output variable and the model-plant mismatch.

A simple way to connect the feedback controller $c(s)$ with the IMC controller $q(s)$ is to redraw Figure 3.1 as a simple feedback system, which is shown in Figure 3.2.

$$c(s) = \frac{u(s)}{e(s)} = \frac{q(s)}{1 - q(s)\tilde{p}(s)} \tag{3.1}$$

$$q(s) = \frac{c(s)}{1 + \tilde{p}(s)c(s)} \tag{3.2}$$

The closed-loop relationships between variables in Figure 3.2 are given by equations (3.3) - (3.5) below,

$$y(s) = \frac{p(s)q(s)r(s)}{1 + (p(s) - \tilde{p}(s))q(s)} + \frac{(1 - \tilde{p}(s)q(s))p_d(s)d(s)}{1 + (p(s) - \tilde{p}(s))q(s)} \tag{3.3}$$

$$u(s) = \frac{q(s)(r(s) - p_d(s)d(s))}{1 + (p(s) - \tilde{p}(s))q(s)} \tag{3.4}$$

$$e(s) = \frac{(1 - \tilde{p}(s)q(s))(r(s) - p_d(s)d(s))}{1 + (p(s) - \tilde{p}(s))q(s)} \tag{3.5}$$

In the absence of model-plant mismatch ($\tilde{p}(s) = p(s)$), these transfer functions simplify

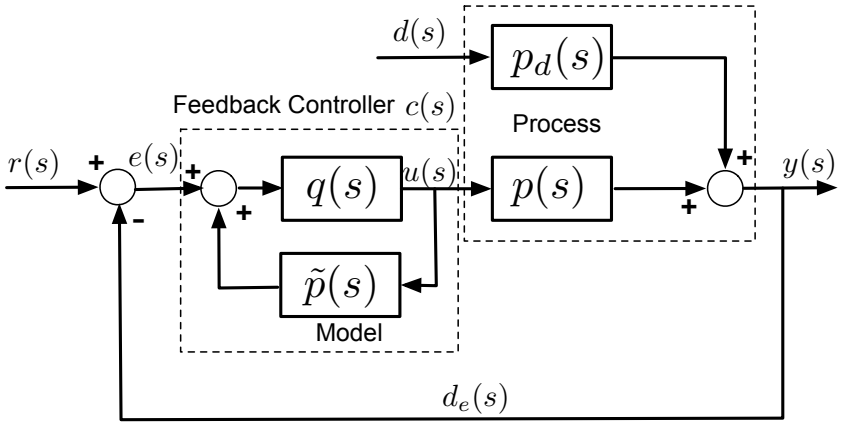

Figure 3.2: Alternate IMC Configuration Expressed as Classical Feedback System [12].

to,

$$y(s) = p(s)q(s)r(s) + (1 - \tilde{p}(s)q(s))p_d(s)d(s) \tag{3.6}$$

$$u(s) = q(s)(r(s) - p_d(s)d(s)) \tag{3.7}$$

$$e(s) = (1 - \tilde{p}(s)q(s))(r(s) - p_d(s)d(s)) \tag{3.8}$$

An ideal control system will make the process output follow its setpoint, and perfectly reject all disturbances so that they do not affect the output. Therefore, the ideal controller that could accomplish this requires that,

$$p(s)q(s) = 1 \quad \text{and} \quad \tilde{p}(s) = p(s) \tag{3.9}$$

This implies $q(s) = p(s)^{-1}$, which may not be physically realizable.

3.2.2 Two-Degree-of-Freedom (2 DoF) Internal Model Control

If both good tracking of setpoint *r* and good disturbance rejection *d* are important and if the dynamic characteristics of the two inputs *r* and *d* are substantially different, it is advantageous to introduce another controller block (Figure 3.3) [82]. The effect of *r* and *d* on the controlled variable, the manipulated variable and the control error can be described

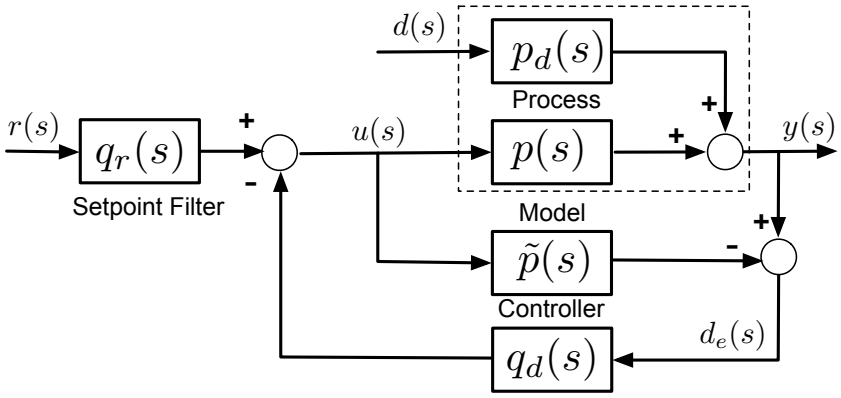

Figure 3.3: Two-Degree-of-Freedom (2 DoF) IMC [12].

as,

$$y(s) = \frac{pq_r}{1+q_d(p-\tilde{p})}r + \frac{1-\tilde{p}q_d}{1+q_d(p-\tilde{p})}p_d d \tag{3.10}$$

$$u(s) = \frac{q_r}{1+q_d(p-\tilde{p})}r - \frac{q_d}{1+q_d(p-\tilde{p})}p_d d \tag{3.11}$$

$$\begin{aligned} e(s) &= r(s) - y(s) \\ &= \left[1 - \frac{pq_r}{1+q_d(p-\tilde{p})}\right] r - \frac{1-\tilde{p}q_d}{1+q_d(p-\tilde{p})}p_d d \end{aligned} \tag{3.12}$$

For $p = \tilde{p}$, equation (3.10) - (3.12) become,

$$y(s) = pq_r r + (1-\tilde{p}q_d)p_d d \tag{3.13}$$

$$u(s) = q_r r - q_d p_d d \tag{3.14}$$

$$e(s) = (1-pq_r)r - (1-\tilde{p}q_d)p_d d \tag{3.15}$$

where q_d is designed for disturbance rejection and q_r for setpoint tracking.

3.2.3 2 DoF IMC Design for Self-Regulation

As introduced in the previous sections, IMC is a Q-parametrized, model-based controller design approach [82] which enables the user to adjust the shape and the speed of the closed-loop system response through the choice of IMC controller $q_x(s)$, where x corresponds to either a setpoint (r) or disturbance (d) response. In a two-degree-of-freedom

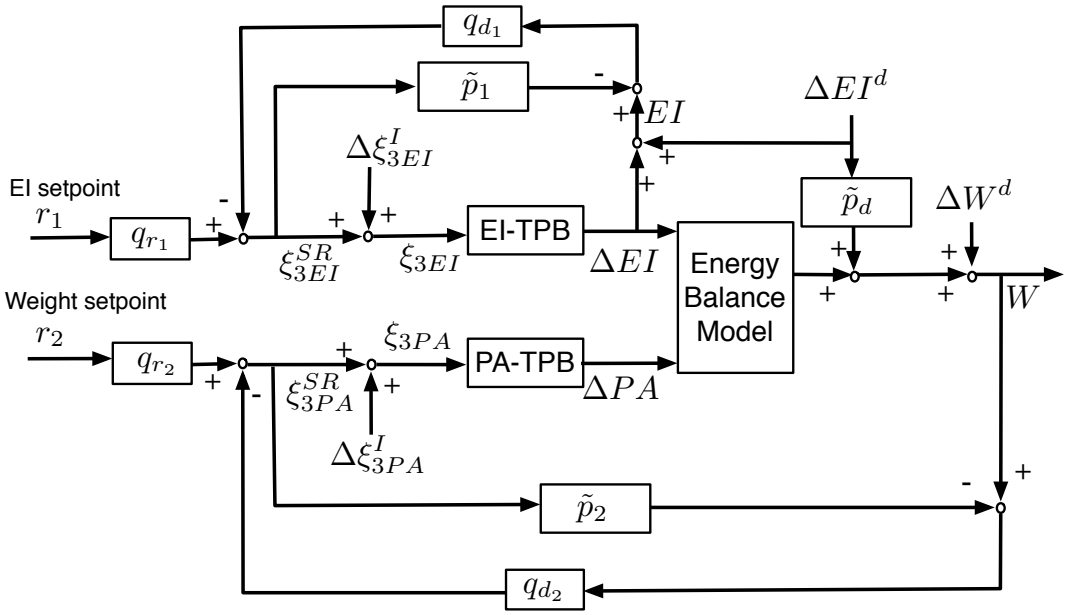

Figure 3.4: Closed-loop System Implemented with Self-regulation Designed by Two-Degree-of-Freedom (2 DoF) Internal Model Control (IMC).

(2 DoF) IMC implementation, the setpoint tracking and disturbance rejection responses are tuned independently. This implies that controller design through IMC offers significant flexibility in describing a participant's self-regulatory behavior through the tuning of controller adjustable parameters, and represents a substantial improvement to using a classical feedback control approach [10].

In this section, 2 DoF IMC approach [82] is applied to the modeling of self-regulation for EI and PA, respectively, which is shown in Figure 3.4. Self-regulation is implemented as a controller that adjusts the PBC inflows to the TPB models based on the discrepancies between reference values and measured outcomes (e.g., GWG or dietary record). There are two sets of reference trajectories applied to the model: EI reference values (r_1) and IOM guidelines (r_2) in Table 2.4, which are the setpoints for EI self-regulation and PA self-regulation, respectively. This self-regulation approach does not specify a PA setpoint target per se, but PA is adjusted to achieve a weight target (which is also influenced by the

EI controller). For simplicity, we consider the case where there is no time delay and no model-plant mismatch. Consequently, the Laplace transfer function between PBC inflow ($\xi_3(s)$) and behavior outflow ($\eta_5(s)$) in the TPB model is as follows,

$$\frac{\eta_{5x}(s)}{\xi_{3x}(s)} = [\frac{\beta_{54}^x \beta_{43}^x \gamma_{33}^x}{(\tau_5^x s+1)(\tau_4^x s+1)(\tau_3^x s+1)} + \frac{\beta_{53}^x \gamma_{33}^x}{(\tau_5^x s+1)(\tau_3^x s+1)}], \tag{3.16}$$

$$x = E \text{ (for EI) or } P \text{ (for PA)} \tag{3.17}$$

where η_{5EI} represents the participant's behavior EI, and η_{5PA} is the participant's behavior PA. Meanwhile, the EB model is reasonably approximated as the sum of two integrating systems, as noted below,

$$\Delta W(s) = \frac{K_E}{s}\Delta EI(s) + \frac{K_P}{s}\Delta PAL(s) \tag{3.18}$$

The closed-loop expressions for the manipulated variables (PBC inflows in EI-TPB and PA-TPB adjusted by self-regulation: ξ_{3EI}^{SR} and ξ_{3PA}^{SR}) and controlled variables (EI and W) are,

$$\begin{aligned}
\xi_{3EI}^{SR}(s) &= q_{r_1}(s)r_1(s) - q_{d_1}(s)(\Delta EI^d(s) + \tilde{p}_1(s)\Delta\xi_{3EI}^I(s)) && (3.19)\\
EI(s) &= \tilde{p}_1(s)q_{r_1}(s)r_1(s) \\
&+ (1-\tilde{p}_1(s)q_{d_1}(s))(\Delta EI^d(s) + \tilde{p}_1(s)\Delta\xi_{3EI}^I(s)) && (3.20)\\
\xi_{3PA}^{SR}(s) &= q_{r_2}(s)r_2(s) - q_{d_2}(s)\tilde{p}_2(s)\Delta\xi_{3PA}^I(s) - q_{d_2}(s)\tilde{p}_d(s)[\tilde{p}_1(s)q_{r_1}(s)r_1(s) \\
&+ (1-\tilde{p}_1(s)q_{d_1}(s))(\Delta EI^d(s) + \tilde{p}_1(s)\Delta\xi_{3EI}^I(s))] - q_{d_2}(s)\Delta W^d(s) && (3.21)\\
W(s) &= \tilde{p}_2(s)q_{r_2}(s)r_2(s) + (1-\tilde{p}_2(s)q_{d_2}(s))[\tilde{p}_d(s)\tilde{p}_1(s)q_{r_1}(s)r_1(s) \\
&+ \tilde{p}_2(s)\Delta\xi_{3PA}^I(s) + \Delta W^d(s) \\
&+ \tilde{p}_d(s)(1-\tilde{p}_1(s)q_{d_1}(s))(\Delta EI^d(s) + \tilde{p}_1(s)\Delta\xi_{3EI}^I(s))] && (3.22)
\end{aligned}$$

where $\tilde{p}_1(s)$ is the EI-TPB model, $\tilde{p}_d(s)$ is the approximated EB model for the EI input, $\tilde{p}_2(s)$ is the PA-TPB model cascading with the approximated EB model for the PA input,

and they are expressed as,

$$\tilde{p}_1(s) = \frac{\beta_{54}^E \beta_{43}^E \gamma_{33}^E}{(\tau_5^E s+1)(\tau_4^E s+1)(\tau_3^E s+1)} + \frac{\beta_{53}^E \gamma_{33}^E}{(\tau_5^E s+1)(\tau_3^E s+1)} \tag{3.23}$$

$$\tilde{p}_d(s) = \frac{K_E}{s} \tag{3.24}$$

$$\tilde{p}_2(s) = \frac{K_P}{s}[\frac{\beta_{54}^P \beta_{43}^P \gamma_{33}^P}{(\tau_5^P s+1)(\tau_4^P s+1)(\tau_3^P s+1)} + \frac{\beta_{53}^P \gamma_{33}^P}{(\tau_5^P s+1)(\tau_3^P s+1)}] \tag{3.25}$$

Meanwhile, in (3.19) - (3.22), $\Delta EI^d(s)$ is the EI increase due to pregnancy (a disturbance variable); $\Delta W^d(s)$ is the output weight disturbance; $\Delta\xi_{3EI}^I(s)$ and $\Delta\xi_{3PA}^I(s)$ are PBC inflow changes by intervention in EI-TPB and PA-TPB, respectively; $q_{r_1}(s)$, $q_{r_2}(s)$, $q_{d_1}(s)$, and $q_{d_2}(s)$ are the controllers that constitute the 2 DoF IMC and augmented with the filters in the closed loop system to follow setpoint changes and reject disturbances, which are defined as,

$$q_{r_1}(s) = \tilde{p}_1(s)^{-1} f_{r_1}(s) = \frac{1}{(\lambda_{r_1} s+1)^3} \tilde{p}_1(s)^{-1} \tag{3.26}$$

$$q_{r_2}(s) = \tilde{p}_2(s)^{-1} f_{r_2}(s) = \frac{1}{(\lambda_{r_2} s+1)^3} \tilde{p}_2(s)^{-1} \tag{3.27}$$

$$q_{d_1}(s) = \tilde{p}_1(s)^{-1} f_{d_1}(s) = \frac{1}{(\lambda_{d_1} s+1)^3} \tilde{p}_1(s)^{-1} \tag{3.28}$$

$$q_{d_2}(s) = \tilde{p}_2(s)^{-1} f_{d_2}(s) = \frac{4\lambda_{d_2} s+1}{(\lambda_{d_2} s+1)^4} \tilde{p}_2(s)^{-1} \tag{3.29}$$

where $q_{r_1}(s)$, $q_{r_2}(s)$, and $q_{d_1}(s)$ are augmented with Type I filters (no offset to steps) because the two setpoints and EI increase are all step changes; $q_{d_2}(s)$ is augmented with a Type II filter [82], because the EB model is approximated as a sum of integrators in (3.18), and this makes $\Delta EI^d(s)$ as a Type II (asymptotically ramp) output disturbance for the PA closed loop system. If q_{d_1} rejects EI disturbance ($\Delta EI^d(s)$) too slowly, then $q_{d_2}(s)$ can reject this Type II EI disturbance and output disturbance $\Delta W^d(s)$. λ_{r_1}, λ_{r_2}, λ_{d_1} and λ_{d_2} are the filter parameters, respectively. These parameters are all functions of personal characteristics or baseline conditions, such as age, social economic status, and social support.

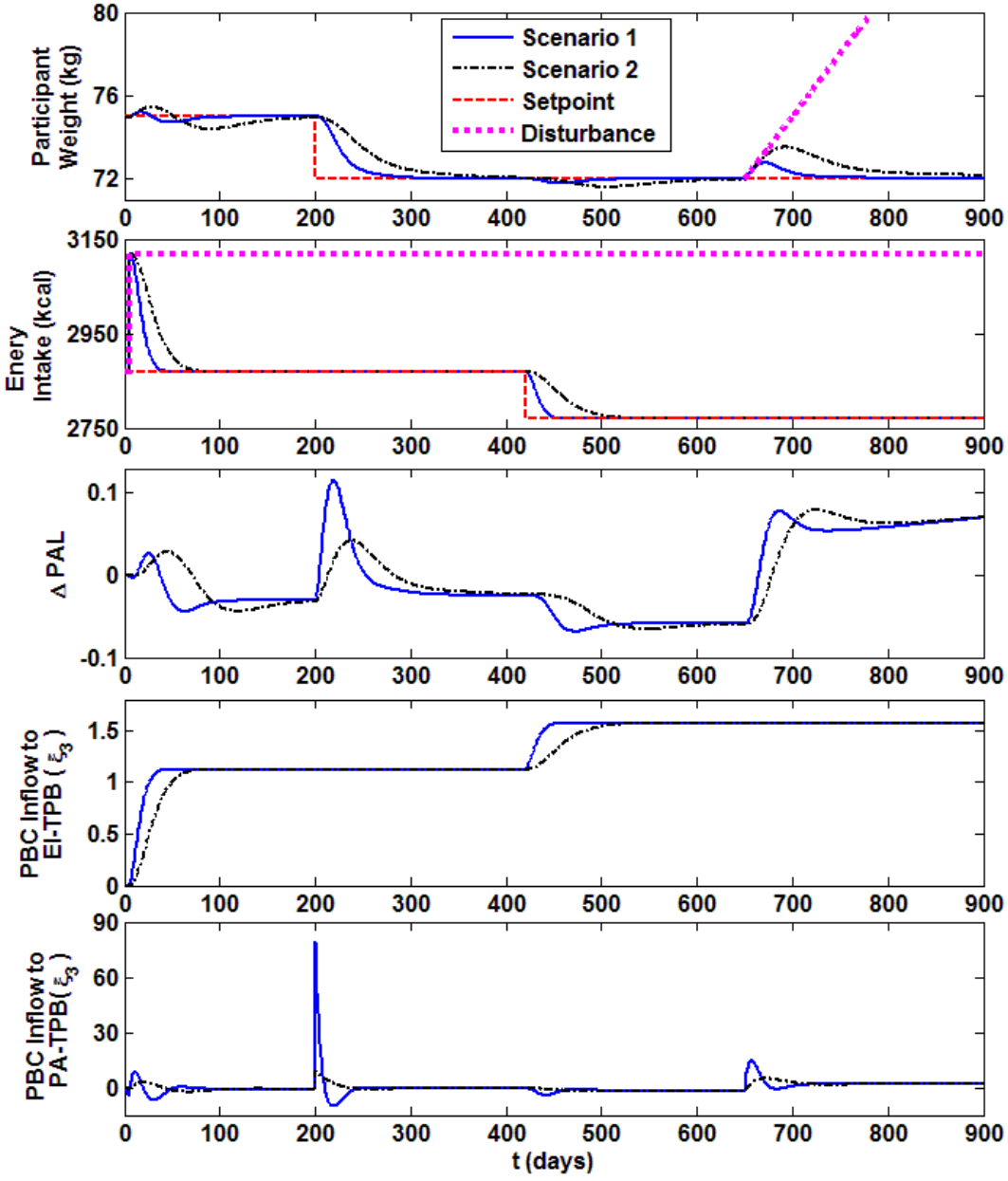

Figure 3.5: Example of Different Self-regulation Responses (Scenarios 1 and 2) Resulting from Changes in Tuning Parameters for the Self-regulation Structure of Figure 3.4. Red Dash Lines Represent Setpoints Applied on a Daily Basis; Blue Solid Lines and Black Dash-dot Lines Represent the Two Scenarios with Self-regulation, respectively; Pink Dot Lines Represent the Disturbance. Parameters for Scenario 1 are: $\lambda_{r_1} = 5, \lambda_{r_2} = 10, \lambda_{d_1} = 5, \lambda_{d_2} = 10$; Parameters for Scenario 2 are: $\lambda_{r_1} = 15, \lambda_{r_2} = 20, \lambda_{d_1} = 10, \lambda_{d_2} = 20$.

Figure 3.5 shows simulation examples with two different self-regulation responses for a participant in the absence of the intervention ($\Delta\xi^I_{3EI} = 0$, and $\Delta\xi^I_{3PA} = 0$). We examine how the controlled variables and manipulated variables respond to the step change disturbance in EI at day 5, a weight step setpoint change at day 200, an EI step setpoint at day 420, and a ramp disturbance change in weight at day 650, respectively. Different responses can be obtained by adjusting the parameters λ_{d_1}, λ_{d_2}, λ_{r_1}, and λ_{r_2}. Specifically, in the examples, Scenario 1 has lower values of λ_{d_1}, λ_{r_2}, λ_{r_1}, and λ_{d_2}, than Scenario 2; thus scenario 1 displays faster responses to rejecting EI disturbances, following weight and EI setpoint changes, and rejecting weight ramp disturbances, respectively. The IMC approach to defining self-regulation thus allows simulations to be readily defined for different types of dynamical systems responses, which in turn would describe individual participant responses.

3.3 Cascade Control

In the previous section, we use two one-loop control for each self-regulation associated with EI reference values and IOM guidelines, respectively. However, there are other scenarios where 1) both EI reference values and IOM guidelines are associated with EI self-regulation loop, or 2) not only IOM guidelines but also PA monitoring output might influence PA self-regulation loop. The former one constitutes the cascade control for the modeling of EI self-regulation, while the latter one requires the cascade control design for the modeling of PA self-regulation, both of which are the focus in this section.

3.3.1 Introduction

Cascade control can improve control system performance over single-loop control whenever either: (1) disturbances affect a measurable intermediate or secondary process output that directly affects the primary process output that we would like to control; or (2) the gain of the secondary process, including the actuator, is nonlinear [12]. The first case

corresponds more closely to the dynamical systems model for the GWG problem. The application of cascade control can help better limit the effect of the disturbances entering the secondary variable on the primary output.

Cascade control can be usefully applied to any process where a measurable secondary variable directly influences the primary controlled variable through some dynamics. Meanwhile, [12] states that it is not necessary for the inner loop dynamics to be faster than the outer loop dynamics.

3.3.2 Cascade Structures and Controller Designs

Figure 3.6 is the standard IMC cascade structure. This is a specific form of a 2 DoF control structure which can be used if in addition to the output to be controlled (y_1), another process output (y_2) can be measured. It is usually to design q_2 first with the out loop open and then design q_1 for the new plant consisting of the closed inner loop combined with p_1 [82].

The closed-loop relationship between variables in Figure 3.6 are given by equations (3.30) - (3.32) below,

$$u_1 = \frac{[1-(p_2-\tilde{p}_2)q_2]q_1(r-d_1)-q_1(p_1-\tilde{p}_1)(1-\tilde{p}_2q_2)d_2}{1+(p_2-\tilde{p}_2)q_2+q_1(p_1-\tilde{p}_1)p_2} \tag{3.30}$$

$$y_2 = \frac{p_2q_1(r-d_1)+(1-\tilde{p}_2q_2)d_2}{1+(p_2-\tilde{p}_2)q_2+q_1(p_1-\tilde{p}_1)p_2} \tag{3.31}$$

$$y_1 = \frac{p_1p_2q_1r+(1-\tilde{p}_2q_2)p_1d_2+[1-\tilde{p}_1p_2q_1+(p_2-\tilde{p}_2)q_2]d_1}{1+(p_2-\tilde{p}_2)q_2+q_1(p_1-\tilde{p}_1)p_2} \tag{3.32}$$

If there is no model-plant mismatch ($p_2=\tilde{p}_2$ and $p_1=\tilde{p}_1$), equations (3.30) - (3.32) can be simplified into,

$$u_1 = q_1(r-d_1) \tag{3.33}$$

$$y_2 = \tilde{p}_2q_1(r-d_1)+(1-\tilde{p}_2q_2)d_2 \tag{3.34}$$

$$y_1 = \tilde{p}_1\tilde{p}_2q_1r+(1-\tilde{p}_2q_2)\tilde{p}_1d_2+(1-\tilde{p}_1\tilde{p}_2q_1)d_1 \tag{3.35}$$

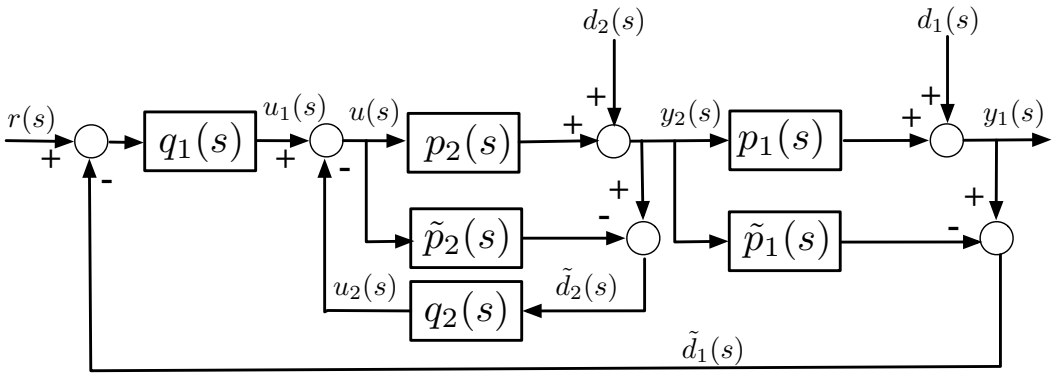

Figure 3.6: IMC Cascade Structure [12].

$$u_2 \quad = \quad u - u_1 = -q_2 d_2 \tag{3.36}$$

Based on the equations above, the inner loop controller q_2 should be chosen to invert $\tilde{p}_2$ as described in the previous section, while the outer loop controller q_1 should approximately invert the entire process model $\tilde{p}_1\tilde{p}_2$.

3.3.3 Cascade Control Design for Self-Regulation

There are two IMC design schemes associated with the EI self-regulation using cascade control proposed in this dissertation. In this section, we will first introduce each of them, and compare which one is better and simpler to design. After the cascade control is applied for the modeling of EI self-regulation, the weighted IMC cascade control for EI and PA self-regulations are explored and simulated with an illustration. Finally, this cascade control design will then also be implemented to the modeling of self-regulation using both PA monitoring output data and IOM guidelines, which will be discussed in Section 3.3.3.3.

3.3.3.1 IMC Cascade Control for Energy Intake Self-regulation Loop

Figure 3.7 is the two DoF IMC cascade control for both inner loop and outer loop in EI self-regulation. The inner loop is the standard 2 DoF IMC design, with q_{r_2} and q_{d_2} as the

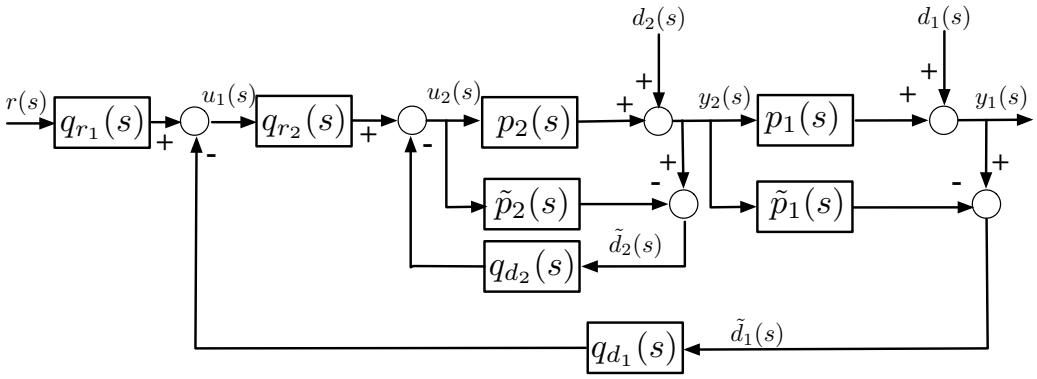

Figure 3.7: IMC Cascade Structure 1 for EI Self-regulation.

controllers to follow setpoint change and reject measured disturbance, respectively. When tuning the inner loop with the outer loop open, we use the EI reference values in Table 2.4 as the setpoint. When the outer loop is closed, it tries to change the setpoint (EI reference value) for the closed-loop system in the inner loop (u_1). The setpoint for the whole EI self-regulation r is the IOM guidelines, and q_{r_1} and q_{d_1} are 2 DoF IMC design for the outer loop to follow setpoint change and eliminate disturbance and model-plant mismatch. The closed-loop relationship between variables are given by,

$$y_2(s) = p_2u_2 + d_2 \tag{3.37}$$

$$\begin{aligned} u_2(s) &= q_{r_2}u_1 - q_{d_2}[(p_2-\tilde{p}_2)u_2 + d_2] \\ &= \frac{q_{r_2}u_1 - q_{d_2}d_2}{1+q_{d_2}(p_2-\tilde{p}_2)} \end{aligned} \tag{3.38}$$

$$\begin{aligned} y_1(s) &= p_1y_2 + d_1 \\ &= p_1p_2u_2 + p_1d_2 + d_1 \\ &= \frac{p_1p_2q_{r_2}u_1 - p_1\tilde{p}_2q_{d_2}d_2}{1+q_{d_2}(p_2-\tilde{p}_2)} + d_1 \end{aligned} \tag{3.39}$$

$$\begin{aligned} u_1(s) &= q_{r_1}r - q_{d_1}[(p_1-\tilde{p}_1)y_2 + d_1] \\ &= q_{r_1}r - q_{d_1}[(p_1-\tilde{p}_1)(p_2u_2+d_2) + d_1] \end{aligned} \tag{3.40}$$

where p_2 and $\tilde{p}_2$ are EI-TPB plant and model, d_2 are measured disturbance (EI increase with the time due to the pregnancy), u_2 and y_2 are manipulated variable (PBC inflow to EI-TPB) and secondary controlled variable (energy intake) in the inner loop, respectively. p_1 and $\tilde{p}_1$ are the energy balance model and the estimated energy balance model in (3.18) for the EI input, u_1 and y_1 are the manipulated variable (EI reference values recommended by the out loop IMC controllers) and primary controlled variable (GWG) in the outer loop.

Rearrange equations (3.38) and (3.40), the expression for the manipulated variable u_1 can be obtained,

$$\begin{aligned}[1+q_{d_2}(p_2-\tilde{p}_2) \quad &+ \quad q_{d_1}(p_1-\tilde{p}_1)p_1p_2q_{r_2}]u_1 = [1+q_{d_2}(p_2-\tilde{p}_2)]q_{r_1}r \\ &+ \quad q_{d_1}(p_1-\tilde{p}_1)(p_1p_2q_{d_2}-1)d_2 \\ &- \quad q_{d_1}[p_1-\tilde{p}_1+1+q_{d_2}(p_2-\tilde{p}_2)]d_1 \end{aligned} \tag{3.41}$$

Assume there is no model-plant mismatch ($p_1 = \tilde{p}_1$ and $p_2 = \tilde{p}_2$), then equation (3.41) simplifies to,

$$u_1(s) = q_{r_1}r - q_{d_1}d_1 \tag{3.42}$$

The other variables and control error are,

$$u_2(s) = q_{r_1}q_{r_2}r - q_{r_2}q_{d_1}d_1 - q_{d_2}d_2 \tag{3.43}$$

$$y_2(s) = q_{r_1}q_{r_2}\tilde{p}_2r - q_{r_2}q_{d_1}\tilde{p}_2d_1 - q_{d_2}\tilde{p}_2d_2 + d_2 \tag{3.44}$$

$$y_1(s) = q_{r_1}q_{r_2}\tilde{p}_1\tilde{p}_2r + (1-q_{r_2}q_{d_1}\tilde{p}_1\tilde{p}_2)d_1 + \tilde{p}_1(1-q_{d_2}\tilde{p}_2)d_2 \tag{3.45}$$

$$\begin{aligned} e(s) &= r - y_1 \\ &= (1-q_{r_1}q_{r_2}\tilde{p}_1\tilde{p}_2)r - (1-q_{r_2}q_{d_1}\tilde{p}_1\tilde{p}_2)d_1 - \tilde{p}_1(1-q_{d_2}\tilde{p}_2)d_2 \end{aligned} \tag{3.46}$$

The ideal controllers will make the closed-loop system track the setpoint change and reject disturbances, and therefore, the controllers in this IMC cascade structure 1 should be designed such that $q_{r_1}q_{r_2}$ invert the entire process model $\tilde{p}_1\tilde{p}_2$ (EI TPB model cascades

with the estimated energy balance model for EI input), $q_{r_2}q_{d_1}$ also invert the entire process model $\tilde{p}_1\tilde{p}_2$, and q_{d_2} inverts the estimated energy balance model for EI input $\tilde{p}_2$, which can be expressed below,

$$q_{d_2}(s) = \tilde{p}_2^{-1} f_{d_2} \tag{3.47}$$

$$q_{r_1}(s) = \tilde{p}_1^{-1} f_{r_1} \tag{3.48}$$

$$q_{r_2}(s) = \tilde{p}_2^{-1} f_{r_2} \tag{3.49}$$

$$q_{d_1}(s) = \tilde{p}_1^{-1} f_{d_1} \tag{3.50}$$

where f_{d_1}, f_{d_2}, f_{r_1} and f_{r_2} are either type I or type II low-pass filters, based on the types of the corresponding measured disturbances and setpoints.

Figure 3.8 is the another version of IMC cascade control for EI self-regulation. The difference between this one and the previous one is how the model is placed for the outer loop. The definition of the variables, the signals, the models and the plants are same with the one in Figure 3.7, except that $\tilde{p}$ is the model for the entire plant (closed- loop system in the inner loop cascading energy balance for EI input). The closed-loop relationship between variables in Figure 3.8 are,

$$y_2(s) = p_2 u_2 + d_2 \tag{3.51}$$

$$\begin{aligned} u_2(s) &= q_{r_2}u_1 - q_{d_2}[(p_2 - \tilde{p}_2)u_2 + d_2] \\ &= \frac{q_{r_2}u_1 - q_{d_2}d_2}{1 + q_{d_2}(p_2 - \tilde{p}_2)} \end{aligned} \tag{3.52}$$

$$\begin{aligned} y_1(s) &= p_1 y_2 + d_1 \\ &= p_1 p_2 u_2 + p_1 d_2 + d_1 \\ &= \frac{p_1 p_2 q_{r_2} u_1 - p_1 \tilde{p}_2 q_{d_2} d_2}{1 + q_{d_2}(p_2 - \tilde{p}_2)} + d_1 \end{aligned} \tag{3.53}$$

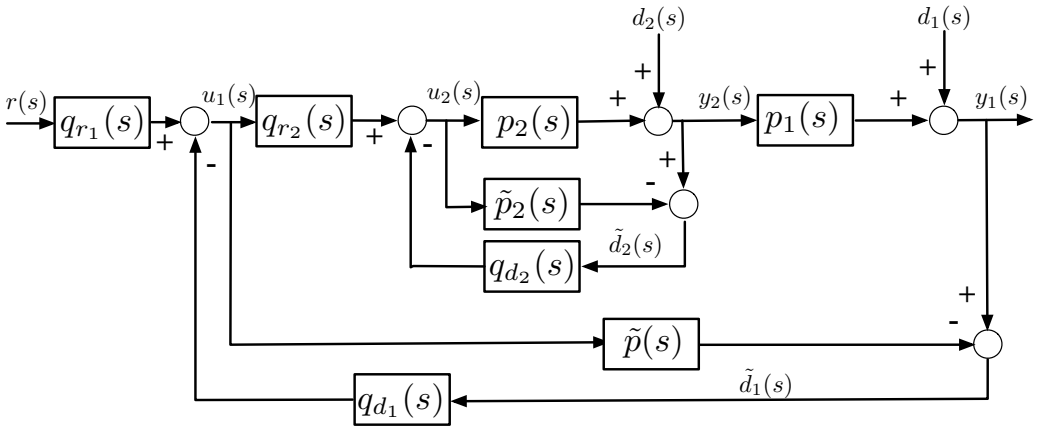

Figure 3.8: IMC Cascade Structure 2 for EI Self-regulation.

$$\begin{aligned} u_1(s) &= q_{r_1} r - q_{d_1}(y_1 - \tilde{p}u_1) \\ &= q_{r_1} r - q_{d_1}\left[\frac{p_1 p_2 q_{r_2} u_1 - p_1 \tilde{p}_2 q_{d_2} d_2}{1 + q_{d_2}(p_2 - \tilde{p}_2)} + d_1 - \tilde{p}u_1\right] \end{aligned} \tag{3.54}$$

Rearranging equation (3.54), the expression of u_1 without approximation can be obtained,

$$u_1(s) = \frac{[1 + q_{d_2}(p_2 - \tilde{p}_2)]q_{r_1} r + q_{d_1} p_1 p_2 q_{d_2} d_2 - q_{d_1}[1 + q_{d_2}(p_2 - \tilde{p}_2)](p_1 d_2 + d_1)}{[1 + q_{d_2}(p_2 - \tilde{p}_2)](1 - q_{d_1}\tilde{p}) + q_{d_1} p_1 p_2 q_{r_2}} \tag{3.55}$$

If there is no model-plant mismatch, we will get the expression for $\tilde{p}$ below,

$$\tilde{p}_2(s) = p_2 \tag{3.56}$$

$$\tilde{p}(s) = q_{r_2}\left[\frac{p_2}{1 + q_d(p_2 - \tilde{p}_2)}\right] p_1 = q_{r_2}\tilde{p}_1\tilde{p}_2 \tag{3.57}$$

The manipulated variables u_1, u_2, the controlled variables y_1, y_2, and the control error can be simplified as,

$$u_1(s) = q_{r_1} r + q_{d_1}\tilde{p}_1\tilde{p}_2 q_{d_2} d_2 - q_{d_1}\tilde{p}_1 d_2 - q_{d_1} d_1 \tag{3.58}$$

$$\begin{aligned} u_2(s) &= q_{r_2} u_1 - q_{d_2} d_2 \\ &= q_{r_1} q_{r_2} r + (q_{d_1} q_{d_2} q_{r_2}\tilde{p}_1\tilde{p}_2 - q_{d_1} q_{r_2}\tilde{p}_1 - q_{d_2}) d_2 - q_{d_1} q_{r_2} d_1 \end{aligned} \tag{3.59}$$

$$
\begin{aligned}
y_2(s) &= q_{r_1}q_{r_2}\tilde{p}_2 r + (q_{d_1}q_{d_2}q_{r_2}\tilde{p}_1\tilde{p}_2^2 - q_{d_1}q_{r_2}\tilde{p}_1\tilde{p}_2 - q_{d_2}\tilde{p}_2 + 1)d_2 \\
&\quad -q_{d_1}q_{r_2}\tilde{p}_2 d_1 \qquad (3.60)\\
y_1(s) &= q_{r_1}q_{r_2}\tilde{p}_1\tilde{p}_2 r + (1 - q_{d_1}q_{r_2}\tilde{p}_1\tilde{p}_2)d_1 \\
&\quad +(q_{d_1}q_{d_2}q_{r_2}\tilde{p}_1^2\tilde{p}_2^2 - q_{d_1}q_{r_2}\tilde{p}_1^2\tilde{p}_2 - q_{d_2}\tilde{p}_1\tilde{p}_2 + \tilde{p}_1)d_2 \qquad (3.61)\\
e(s) &= r - y_1 \\
&= (1 - q_{r_1}q_{r_2}\tilde{p}_1\tilde{p}_2)r - (1 - q_{d_1}q_{r_2}\tilde{p}_1\tilde{p}_2)d_1 \\
&\quad -(q_{d_1}q_{r_2}\tilde{p}_1\tilde{p}_2 - 1)(q_{d_2}\tilde{p}_2 - 1)\tilde{p}_1 d_2 \qquad (3.62)
\end{aligned}
$$

The ideal controllers to make the closed-loop system follow setpoint changes and decline disturbances should have control error equal to zero. If we compare the control error in equation (3.62) with the one in equation (3.46), we will see that the design of the controllers are same, which are listed in equations (3.47) - (3.50), except that the effect of disturbance d_2 on the control error will also be influenced by the tuning in d_1. In (3.46), d_2 is rejected by tuning the controller q_{d_2} to offset its effect on primary controlled variable, and control error, while in (3.62), d_2 is declined by tuning not only the controller q_{d_2}, but also $q_{d_1}q_{r_2}$.

Even though the designs of the controllers in these two IMC cascade control structures (Figure 3.7 and Figure 3.8) are similar, the structure 1 in Figure 3.7 is preferred. This is because it not only expresses the manipulated variables, controlled variables and the control error in a simpler manner, but also makes the model $\tilde{p}_1$ in Figure 3.7 independent of the closed-loop system in the inner loop, compared with $\tilde{p}$ in Figure 3.8 that will be designed relying on the tuning parameters in the controller q_{r_2} in the inner loop as indicated in (3.57).

3.3.3.2 Weighted IMC Cascade Control for Energy Intake and Physical Activity Self-Regulation

In the previous subsection, the two structures of the IMC cascade control for EI self-regulation are analyzed and compared. This section will mainly focus on the application of the IMC cascade structure 1 in Figure 3.7 to design the self-regulation in GWG model.

Figure 3.9 shows the IMC design for self-regulation loops in GWG model, where p_{EB} is the energy balance model, p_w is the model to split the output GWG based on the weight ($w\%$, w between 0 and 100) which shows how much weight loss is contributed by EI self-regulation and PA self-regulation, respectively. p_3 and $\tilde{p}_3$ are PA-TPB process and model respectively; $\tilde{p}_4$ is the estimated energy balance model for PA input, q_{d_3} and q_{r_3} are two controllers for the PA self-regulation to reject disturbances and follow setpoint $w\% \times r(s)$. The other blocks are same as what is illustrated in Figure 3.7. The expressions of these models are as follows,

$$\tilde{p}_1(s) = \frac{K_E}{s} \tag{3.63}$$

$$\tilde{p}_2(s) = \frac{\beta_{54}^E \beta_{43}^E \gamma_{33}^E}{(\tau_5^E s+1)(\tau_4^E s+1)(\tau_3^E s+1)} + \frac{\beta_{53}^E \gamma_{33}^E}{(\tau_5^E s+1)(\tau_3^E s+1)} \tag{3.64}$$

$$\tilde{p}_3(s) = \frac{\beta_{54}^P \beta_{43}^P \gamma_{33}^P}{(\tau_5^P s+1)(\tau_4^P s+1)(\tau_3^P s+1)} + \frac{\beta_{53}^P \gamma_{33}^P}{(\tau_5^P s+1)(\tau_3^P s+1)} \tag{3.65}$$

$$\tilde{p}_4(s) = \frac{K_P}{s} \tag{3.66}$$

Meanwhile, $q_{r_1}(s)$, $q_{r_2}(s)$, $q_{r_3}(s)$,$q_{d_1}(s)$, $q_{d_2}(s)$, and $q_{d_3}(s)$ are the IMC controllers augmented with the filters in the closed loop system to follow setpoint changes and reject disturbances, which are defined as,

$$q_{r_1}(s) = \tilde{p}_1(s)^{-1} f_{r_1}(s) = \frac{1}{(\lambda_{r_1} s+1)^2} \tilde{p}_1(s)^{-1} \tag{3.67}$$

$$q_{d_1}(s) = \tilde{p}_1(s)^{-1} f_{d_1}(s) = \frac{2\lambda_{d_1} s+1}{(\lambda_{d_1} s+1)^2} \tilde{p}_1(s)^{-1} \tag{3.68}$$

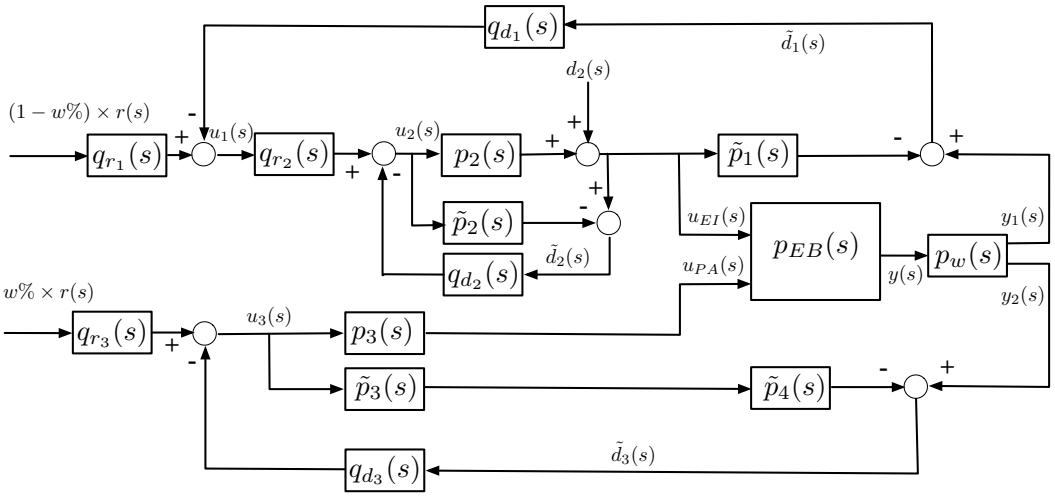

Figure 3.9: IMC Cascade Structure for Self-regulation Loops in GWG Model, with Weight Parameter Fraction *w%* for the Setpoint.

$$q_{r_2}(s) = \tilde{p}_2(s)^{-1} f_{r_2}(s) = \frac{3\lambda_{r_2}s+1}{(\lambda_{r_2}s+1)^3}\tilde{p}_2(s)^{-1} \tag{3.69}$$

$$q_{d_2}(s) = \tilde{p}_2(s)^{-1} f_{d_2}(s) = \frac{3\lambda_{d_2}s+1}{(\lambda_{d_2}s+1)^3}\tilde{p}_2(s)^{-1} \tag{3.70}$$

$$q_{r_3}(s) = (\tilde{p}_3(s)\tilde{p}_4(s))^{-1} f_{r_3}(s) = \frac{1}{(\lambda_{r_3}s+1)^4}(\tilde{p}_3(s)\tilde{p}_4(s))^{-1} \tag{3.71}$$

$$q_{d_3}(s) = (\tilde{p}_3(s)\tilde{p}_4(s))^{-1} f_{d_3}(s) = \frac{4\lambda_{d_3}s+1}{(\lambda_{d_3}s+1)^4}(\tilde{p}_3(s)\tilde{p}_4(s))^{-1} \tag{3.72}$$

where $q_{r_1}(s)$ and $q_{r_3}(s)$ are augmented with Type I filters (no offset to steps); $q_{d_1}(s)$, $q_{d_2}(s)$, $q_{d_3}(s)$, and $q_{r_2}(s)$ are augmented with Type II filters [82] in order to have no offset to ramp disturbance or setpoint change.

The cascade control (upper level) can better describe the two control loops in EI self-regulation with two setpoints (EI reference value for inner loop and IOM guidelines for outer loop), while the 2 DoF IMC design (lower level) is used to model PA self-regulation. If there is no intervention assumed, the increase of PBC in both EI-TPB and PA-TPB are contributed by self-regulation. The increase of PBC in EI-TPB leads to the decrease of EI and GWG, and the increase of PBC in PA-TPB results in the higher PAL and lower GWG.

Because the energy balance model does not indicate how much proportion of the reduced GWG is contributed by the change behavior of EI or PA, we have to rely on the weighted IMC cascade control structure to solve this problem. The weight parameter ($w\%$) is used to illustrate the percentage of the reduced GWG resulting from the improved PA behavior by self-regulation, which also serves as the setpoint for the PA self-regulation loop, and the setpoint for the EI self-regulation is therefore updated as $(1 - w\%) \times r(s)$ (both setpoints are shown in Figure 3.9). The sum of these two setpoints gives the IOM guidelines.

Figure 3.10 shows a simulation example of self-regulation responses for a participant in the absence of the intervention ($\Delta\xi^I_{3EI} = 0$, and $\Delta\xi^I_{3PA} = 0$) using the cascade IMC structure with weight parameter fraction ($w\% = 0.6$). In this examples, EI will have a step change disturbance at day 5, weight gain will a have step setpoint change at day 200, and a ramp disturbance at day 400. The EI reference values are now generated by the controllers q_{r_1} and q_{d_1}. With fast tuning of q_{r_2} ($q_{r_2} = 1$), the participant will be able to follow the EI setpoint assigned by the outer loop controllers. Meanwhile, the closed-loop system can also reject step EI disturbance and ramp weight disturbance by augmenting q_{d_2} with Type I filter, and q_{d_1} and q_{d_3} with Type II filters. The step change in weight step point is -5 kg, and the weight parameter $w\% = 0.6$, therefore, the behavior improvement in PA will lead to 3 kg weight loss, and the behavior improvement in EI will result in 2 kg weight loss. Although we do not have systematic guidelines to determine the weight parameter ($w\%$) so far, this information might be available after the clinical trial for this GWG intervention is performed.

3.3.3.3 IMC Cascade Control for Physical Activity Self-regulation Loop

If PA monitoring data is available, it can also help inform PA self-regulation, so as to motivate the participant to achieve her GWG goal. Because this PA self-regulation is associated with IOM guidelines, and PA monitoring data, this constitutes the cascade

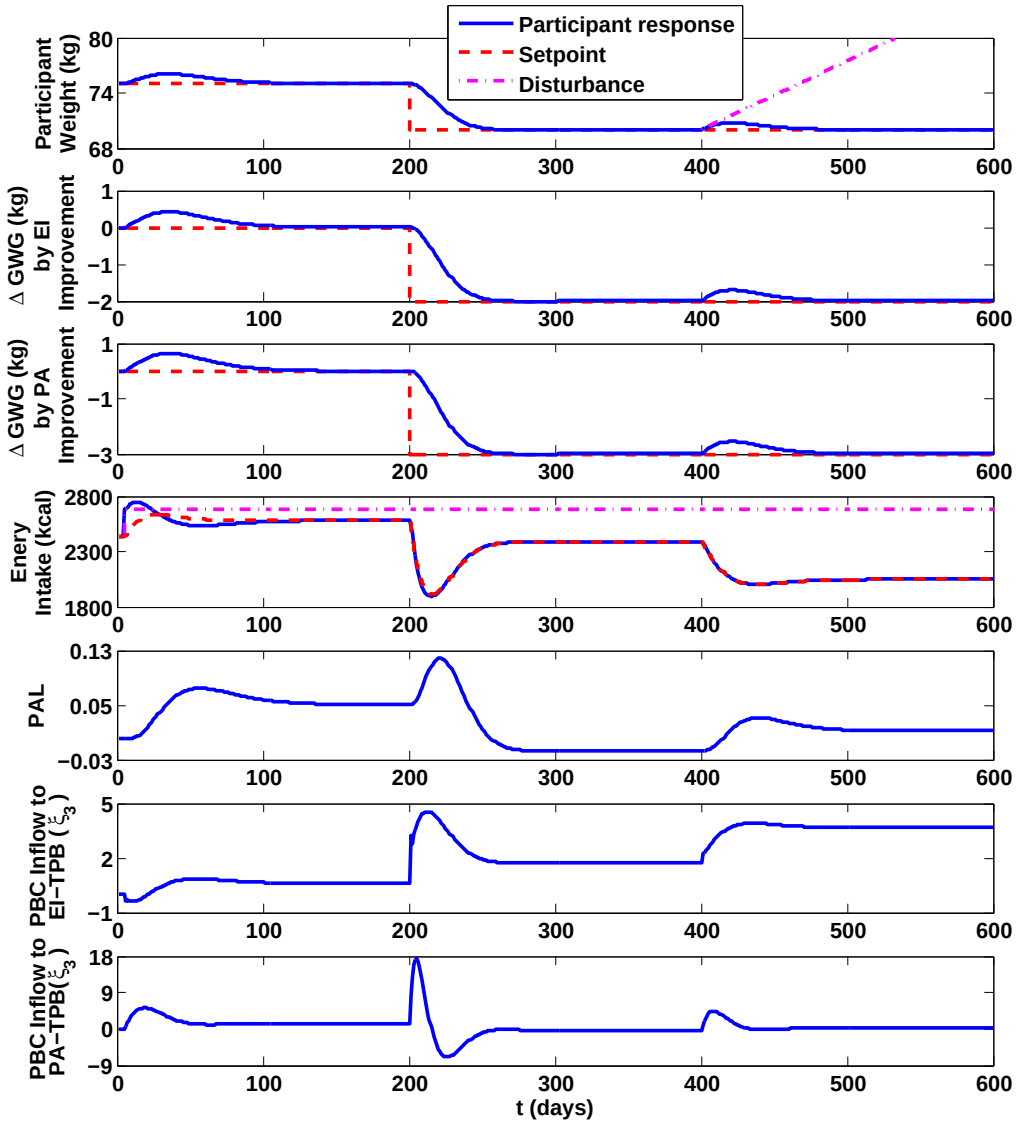

Figure 3.10: Example of Self-regulation Response Using the Cascade IMC Structure of Figure 3.9 with Weight Parameter Fraction ($w\% = 0.6$) for Selected Tuning Parameters. Red Dash Lines Represent Setpoints Applied on a Daily Basis; Blue Solid Lines Represent the Participant's Response with Self-regulation; Pink Dot-dash Lines Represent the Disturbance. Parameters for this Simulation are: $\lambda_{r_1} = 10, \lambda_{r_2} = 1, \lambda_{r_3} = 10, \lambda_{d_1} = 15, \lambda_{d_2} = 15, \lambda_{d_3} = 15$.

control for PA self-regulation, and it is very similar to the cascade control scheme for EI self-regulation depicted in Figure 3.7.

Figure 3.11 is the IMC cascade structure for GWG model, with PA self-regulation associated with PA monitoring data and IOM guidelines. Instead of having cascade control in EI self-regulation, this IMC cascade structure for GWG model will have IOM guidelines (r_2) as setpoint for the outer loop of PA self-regulation, while the PA setpoint (r_3) in the inner loop of PA self-regulation will be generated by the outer loop controller q_{r_2} and q_{d_2}. Meanwhile, additional PA disturbance (ΔPA^d) is added into this cascade control structure, which will have the same effect as the EI disturbance (ΔEI^d) in the EI self-regulation loop. The closed-loop expressions for the manipulated variables (PBC inflows in EI-TPB and PA-TPB adjusted by self-regulation inputs ξ_{3EI}^{SR} and ξ_{3PA}^{SR}) and controlled variables (EI, PA, and W) are,

$$\begin{aligned}
\xi_{3EI}^{SR}(s) &= q_{r_1}(s)r_1(s) - q_{d_1}(s)(\Delta EI^d(s) + \tilde{p}_1(s)\Delta\xi_{3EI}^{I}(s)) && (3.73)\\
\xi_{3PA}^{SR}(s) &= q_{r_3}(s)q_{r_2}(s)r_2(s) - q_{r_3}(s)q_{d_2}(s)\Delta W^d(s) \\
&- q_{r_3}(s)q_{d_2}(s)\tilde{p}_{d_1}(s)[(1-\tilde{p}_1(s)q_{d_1}(s))(\Delta EI^d(s) + \tilde{p}_1(s)\Delta\xi_{3EI}^{I}(s)) \\
&+ \tilde{p}_1(s)q_{r_1}(s)r_1(s)] - q_{d_3}(s)[\tilde{p}_3(s)\Delta\xi_{3PA}^{I}(s) + \Delta PA^d(s)] && (3.74)\\
EI(s) &= \tilde{p}_1(s)q_{r_1}(s)r_1(s) \\
&+ (1-\tilde{p}_1(s)q_{d_1}(s))(\Delta EI^d(s) + \tilde{p}_1(s)\Delta\xi_{3EI}^{I}(s)) && (3.75)\\
PA(s) &= \tilde{p}_3(s)q_{r_3}(s)q_{r_2}(s)r_2(s) - \tilde{p}_3(s)q_{r_3}(s)q_{d_2}(s)\Delta W^d(s) \\
&- \tilde{p}_3(s)q_{r_3}(s)q_{d_2}(s)\tilde{p}_{d_1}(s)[(1-\tilde{p}_1(s)q_{d_1}(s))(\Delta EI^d(s) + \tilde{p}_1(s)\Delta\xi_{3EI}^{I}(s)) \\
&+ \tilde{p}_1(s)q_{r_1}(s)r_1(s)] && (3.76)
\end{aligned}$$

$$
\begin{aligned}
W(s) &= (1-\tilde{p}_3(s)q_{r_3}(s)q_{d_2}(s)\tilde{p}_{d_2})[\tilde{p}_{d_1}(s)\tilde{p}_1(s)q_{r_1}(s)r_1(s)+\Delta W^d(s) \\
&+ \tilde{p}_{d_1}(s)(1-\tilde{p}_1(s)q_{d_1}(s)(\Delta EI^d(s)+\tilde{p}_1(s)\Delta\xi^I_{3EI}(s))] \\
&+ \tilde{p}_{d_2}(s)(1-\tilde{p}_3(s)q_{d_3}(s))[\tilde{p}_3(s)\Delta\xi^I_{3PA}(s)+\Delta PA^d(s)] \\
&+ \tilde{p}_3(s)q_{r_3}(s)q_{r_2}(s)\tilde{p}_{d_2}(s)r_2(s) \qquad (3.77)
\end{aligned}
$$

where $\tilde{p}_1(s)$ is the EI-TPB model, $\tilde{p}_3(s)$ is PA-TPB model, $\tilde{p}_{d_1}(s)$ is the approximated EB model for the EI input, $\tilde{p}_{d_2}(s)$ is the approximated PA model for the PA input, and they are expressed as,

$$
\begin{aligned}
\tilde{p}_1(s) &= \frac{\beta^E_{54}\beta^E_{43}\gamma^E_{33}}{(\tau^E_5 s+1)(\tau^E_4 s+1)(\tau^E_3 s+1)}+\frac{\beta^E_{53}\gamma^E_{33}}{(\tau^E_5 s+1)(\tau^E_3 s+1)} \qquad (3.78)\\
\tilde{p}_3(s) &= \frac{\beta^P_{54}\beta^P_{43}\gamma^P_{33}}{(\tau^P_5 s+1)(\tau^P_4 s+1)(\tau^P_3 s+1)}+\frac{\beta^P_{53}\gamma^P_{33}}{(\tau^P_5 s+1)(\tau^P_3 s+1)} \qquad (3.79)\\
\tilde{p}_{d_1}(s) &= \frac{K_E}{s} \qquad (3.80)\\
\tilde{p}_{d_2}(s) &= \frac{K_P}{s} \qquad (3.81)
\end{aligned}
$$

Meanwhile, in (3.73) - (3.77), $\Delta EI^d(s)$ is the EI increase due to pregnancy (a disturbance variable); $\Delta PA^d(s)$ is the PA disturbance (input disturbance for energy balance model); $\Delta W^d(s)$ is the output weight disturbance; $\Delta\xi^I_{3EI}(s)$ and $\Delta\xi^I_{3PA}(s)$ are PBC inflow changes by intervention in EI-TPB and PA-TPB, respectively; $q_{r_1}(s)$, $q_{r_2}(s)$, $q_{r_3}(s)$,$q_{d_1}(s)$, $q_{d_2}(s)$, and $q_{d_3}(s)$ are the controllers that constitute the 2 DoF IMC and augmented with the filters in the closed-loop system to follow setpoint changes and reject disturbances, which are

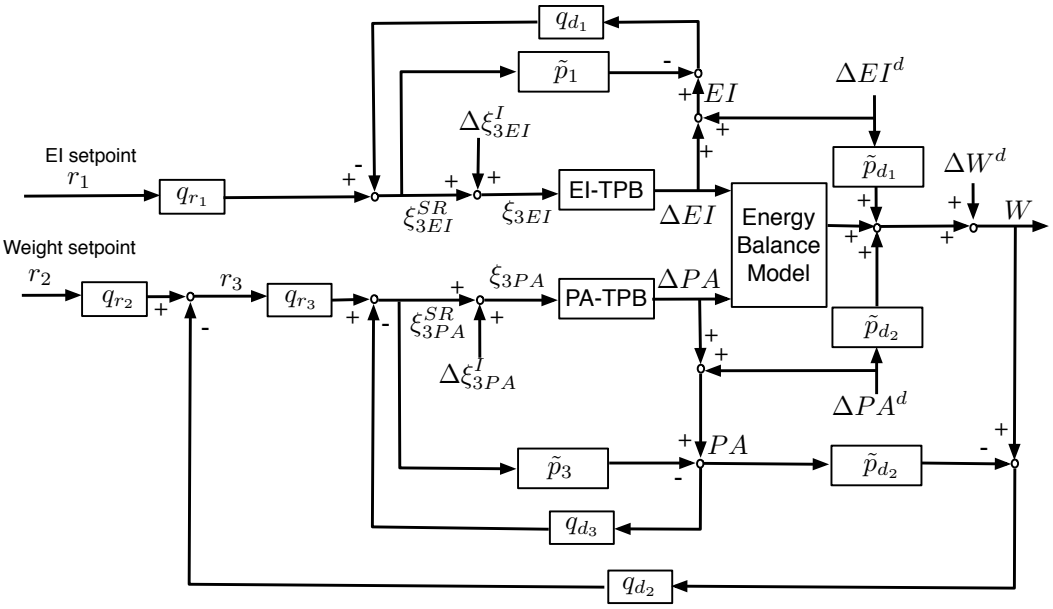

Figure 3.11: IMC Cascade Structure for GWG Model, with PA Self-regulation Loop Associated with PA Monitoring Results and IOM Guidelines.

defined as,

$$q_{r_1}(s) = \tilde{p}_1(s)^{-1} f_{r_1}(s) = \frac{1}{(\lambda_{r_1} s+1)^3} \tilde{p}_1(s)^{-1} \tag{3.82}$$

$$q_{r_2}(s) = \tilde{p}_{d_2}(s)^{-1} f_{r_2}(s) = \frac{1}{(\lambda_{r_2} s+1)^2} \tilde{p}_{d_2}(s)^{-1} \tag{3.83}$$

$$q_{r_3}(s) = \tilde{p}_3(s)^{-1} f_{r_3}(s) = \frac{1}{(\lambda_{r_3} s+1)^3} \tilde{p}_3(s)^{-1} \tag{3.84}$$

$$q_{d_1}(s) = \tilde{p}_1(s)^{-1} f_{d_1}(s) = \frac{1}{(\lambda_{d_1} s+1)^3} \tilde{p}_1(s)^{-1} \tag{3.85}$$

$$q_{d_2}(s) = \tilde{p}_{d_2}(s)^{-1} f_{d_2}(s) = \frac{3\lambda_{d_2} s+1}{(\lambda_{d_2} s+1)^3} \tilde{p}_{d_2}(s)^{-1} \tag{3.86}$$

$$q_{d_3}(s) = \tilde{p}_3(s)^{-1} f_{d_3}(s) = \frac{1}{(\lambda_{d_3} s+1)^3} \tilde{p}_3(s)^{-1} \tag{3.87}$$

where $q_{r_1}(s)$, $q_{r_2}(s)$, $q_{r_3}(s)$, $q_{d_1}(s)$ and $q_{d_3}(s)$ are augmented with Type I filters (no offset to steps) because the setpoints, EI and PA disturbance are all step changes; $q_{d_2}(s)$ is augmented with a Type II filter [82], because the EB model is approximated as a sum of integrators in (3.18), and this makes $\Delta EI^d(s)$ and $\Delta PA^d(s)$ as Type II (asymptotically ramp)

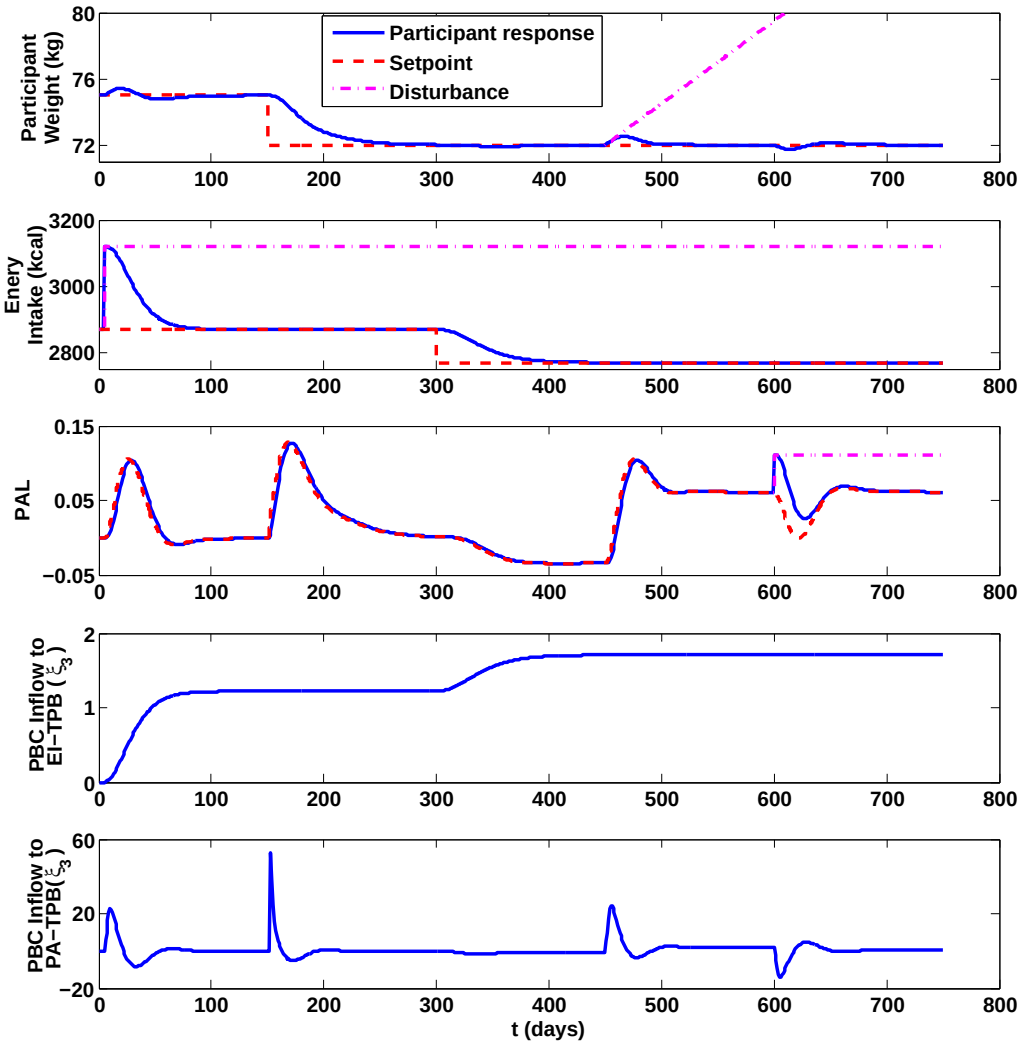

Figure 3.12: Example of Self-regulation Response Using the Cascade IMC Structure per Figure 3.11 with Selected Tuning Parameters for Fast Tuning of PA. Red Dash Lines Represent Setpoints Applied on a Daily Basis; Blue Solid Lines Represent the Participant's Response with Self-regulation; Pink Dot Lines Represent the Disturbance. Parameters for this Simulation are: $\lambda_{r_1} = 15, \lambda_{r_2} = 20, \lambda_{r_3} = 1, \lambda_{d_1} = 10, \lambda_{d_2} = 10, \lambda_{d_3} = 10$.

output disturbances for the PA closed loop system. If q_{d_1} and q_{d_3} rejects EI disturbance ($\Delta EI^d(s)$) and PA disturbance ($\Delta PA^d(s)$) too slowly, then $q_{d_2}(s)$ can reject these Type II disturbances and output disturbance $\Delta W^d(s)$.

Figure 3.12 and Figure 3.13 show two simulation examples of self-regulation responses

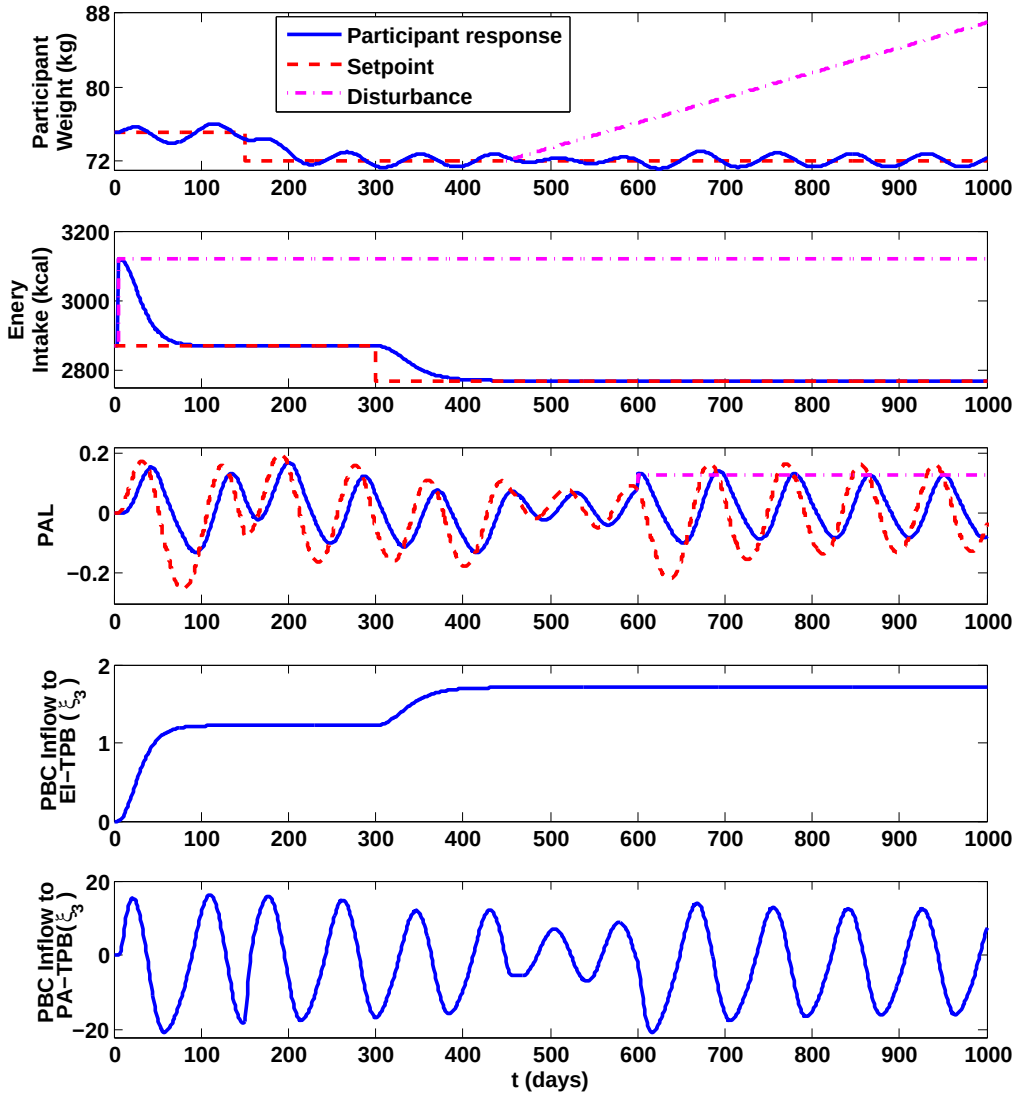

Figure 3.13: Example of Self-regulation Response Using the Cascade IMC Structure per Figure 3.11 with Selected Tuning Parameters for Slow Tuning of PA. Red Dash Lines Represent Setpoints Applied on a Daily Basis; Blue Solid Lines Represent the Participant's Response with Self-regulation; Pink Dot Lines Represent the Disturbance. Parameters for this Simulation are: $\lambda_{r_1} = 15, \lambda_{r_2} = 20, \lambda_{r_3} = 4, \lambda_{d_1} = 10, \lambda_{d_2} = 10, \lambda_{d_3} = 10$.

for a participant in the absence of the intervention ($\Delta\xi^I_{3EI} = 0$, and $\Delta\xi^I_{3PA} = 0$) using the cascade IMC structure in PA self-regulation discussed above. Specifically, in the examples, we can examine how the controlled variables and manipulated variables respond to the step change disturbance in EI at day 5, a weight step setpoint change at day 150, an EI step setpoint at day 300, a ramp disturbance change in weight at day 450, and a PA step disturbance at day 600 respectively. By introducing two additional controllers q_{r_3} and q_{d_3}, the formulation of this self-regulation can make use of PA monitoring data obtained in the real clinical trial, and the controllers in the outer loop will be able to calculate the PA setpoint (r_3) according to the weight setpoint (IOM guidelines r_2) in the PA self-regulation loop, and better decline the external PA disturbance ΔPA^d. When the participant can follow the PA setpoint assigned by the controller in a fast manner (Figure 3.12), she should also be able to achieve her weight gain goal. If the tuning parameter λ_{r_3} is greater, the participant could not completely follow PA setpoint change generated by the controller, which is the case in Figure 3.13. As a result, her PBC inflow to PA-TPB and PAL exhibits significant oscillatory responses, while her weight gain also displays relatively small oscillations around the GWG setpoint. The EI profile in both cases is not effected by the tuning of λ_{r_3}. From the comparison, we can also conclude that the simulation response for the controlled variables and the manipulated variables with fast tuning parameter λ_{r_3} in Figure 3.12 are very similar to the one shown in Figure 3.5. Therefore, for the sake of simplicity, the self-regulation formulation in Section 3.2.3 will be used.

3.4 Simulation Studies

The overall schematic representation of the GWG simulation model using 2 DoF IMC design for self-regulation depicted in Section 3.2.3 can also be visualized as a network of production-inventory systems that is akin to a supply chain, as shown in Figure 3.14. The outflows of the TPB models are an individual's behaviors (EI and PA), which serve then as

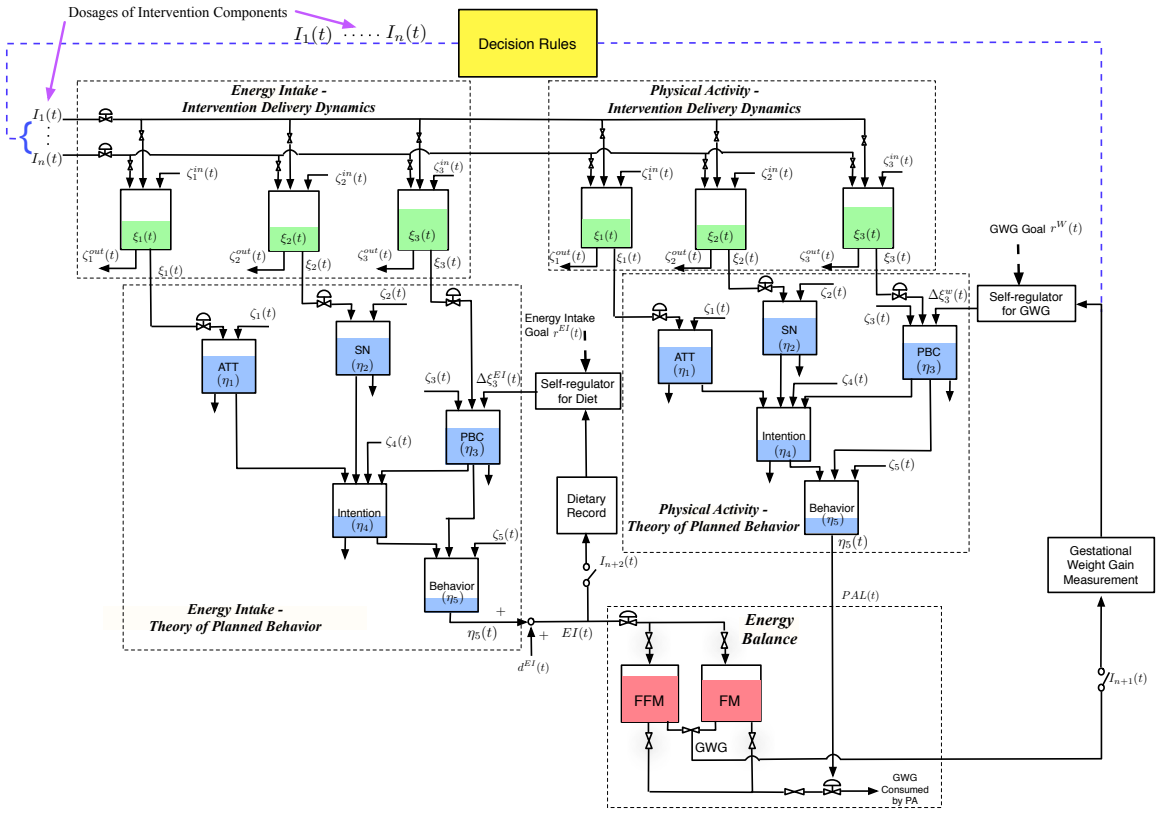

Figure 3.14: Adaptive Gestational Weight Gain Intervention Simulation Model, Represented as a Network of Production Inventory Systems.

the inflows to the EB model. There are two self-regulation loops associated with EI reference values and IOM guidelines, which adjust the PBC inventory in the two TPB models. Based on the measurements of important outcomes (in this case, GWG), decision rules adapt the intervention dosages which are the inflows to the intervention delivery dynamics, the outflows of which are the new inflows to the two TPB models.

In this section, we consider three hypothetical simulation scenarios that rely on our proposed simulation model in Figure 3.14. The first study focuses on the comparison of the responses of a participant among cases involving no intervention, a fixed intervention and an adaptive intervention; the latter illustrates how adaptive interventions adjust the levels

and types of intervention components determined by the decision rules in the response to individual's unique needs, and assist pregnant women in meeting the IOM GWG guidelines. The second simulation study is a participant-focused scenario where the main goal is to analyze the different behavioral responses due to intra-individual variability by changing the parameters in the behavioral models that allow the evaluation of various combination of self-regulation and behavioral improvements under the influence of intervention. The third study aims at understanding the inter-individual variability by assuming the participants all have the same EI increase but with different pre-gravid BMI categories, self-regulation responses, and behavioral improvements through PBC changes.

All the simulations are based on hypothetical 25-year-old females. Maternal age was selected using 2010 data from the Center for Disease Control and Prevention that indicates that the mean age of mothers at first birth is 25.4 years [71]. For the sake of simplicity, we will only focus on the effects that intervention components and self-regulation play on the PBC inflow to the TPB models. In both the intervention and non-intervention treatment, we assume the age of gestation at time of delivery to be 40 weeks. We stage a scenario that with no intervention, the participant will experience a ramp increase in her energy intake (EI) from day 35 to day 91, and her EI will keep constant throughout the remaining of the pregnancy. The participant is sedentary at the time of conception with $PAL = 1.65$, and potentially engaged in less PA from second to third trimester as she gains weight in the absence of intervention. Despite the fact that the intervention can help improve her PAL in the second trimester, we will consider that there will still be a decrease in her PA during the latter stage of pregnancy (especially one or two months prior to delivery) due to the fact that pregnant women can be reluctant to carry out PA at late third trimester. These are two PA disturbances that will be present in both the intervention and no intervention cases, and which will consequently lower her energy expenditure (EE) in the EB model.

The simulation study assumes that the participant enters the GWG intervention with the

Table 3.1: Summary of Dosage Augmentations for a Representative GWG Adaptive Intervention Consisting of IF-THEN Decision Rules in Section 3.4

Options	**Adaptation**
Baseline Intervention	NA
Step up 1	Baseline + HE Active Learning Component
Step up 2	Baseline + 1 + PA Active Learning Component
Step up 3	Baseline + 1+2 + HE Active Learning Componentt
Step up 4	Baseline + 1 + 2 + 3 + PA Active Learning Component
Step up 5	Baseline + 1 + 2 + 3 + 4 + HE Active Learning Component

baseline program at week 14 (day 98); at this time she starts engaging in self-regulatory behavior (e.g., weighing herself to monitor GWG, and using dietary records to monitor EI and a pedometer to monitor PAL). The dosage of the intervention components is adapted every four weeks based on decision rules of whether she is meeting her GWG goal or not until the end of week 37 (day 265). We focus on the augmentation of two of the intervention components previously described in [10]; these are HE and PA active learning which are shown in Table 3.1.

3.4.1 Contrasting Fixed versus Adaptive Interventions

This portion of the simulation study described in this section consists of an evaluation of the adaptive intervention via IF-THEN decision rules depicted in Table 3.1, and a comparison of the response of a given participant to the adaptive intervention, a traditional fixed intervention, and a scenario involving no intervention. For the fixed intervention case, only the baseline portion of the adaptive intervention is provided to the participant along with self-regulation; there occurs no augmentation on either the HE or PA active learning components. For the case of no intervention, we consider that there is no significant self-regulation at work; the assumption in this case is that this participant is not actively monitoring her weight, EI, or PA.

Table 3.2: Model Parameters for the Simulation Studies in Section 3.4.1. Time Constants (τ_i), Delays (θ_i), and Self-regulation Adjustable Parameters (λ_r, λ_d) are in Units of Days.

Parameter	EI-TPB	PA-TPB	Parameter	EI-TPB	PA-TPB
b_1	3	1	e_1	6	4
n_1	2	7	m_1	3	8
p_1	1	4	c_1	2	2
τ_1	1	30	γ_{11}	1	0.7
τ_2	1	30	γ_{22}	1	0.5
τ_3	1	10	γ_{33}	1	0.7
τ_4	1	20	β_{41}	1	0.34
τ_5	1	30	β_{42}	1	0.27
$\theta_1 \cdots \theta_3$	0	0	β_{43}	1	0.15
$\theta_4 \cdots \theta_6$	0	0	β_{53}	0	0.08
θ_7, θ_8	0	0	β_{54}	1	0.42
$k_{11} \cdots k_{17}$	0	-	$\theta_{11} \cdots \theta_{17}$	0	-
$k_{21} \cdots k_{27}$	0	-	$\theta_{21} \cdots \theta_{27}$	0	-
k_{31}	0.001	-	θ_{31}	0	-
k_{32}	0.001	-	θ_{32}	0	-
k_{33}	0.003	-	θ_{33}	0	-
k_{34}	0.001	-	θ_{34}	0	-
$k_{35} \cdots k_{37}$	0	-	$\theta_{35} \cdots \theta_{37}$	0	-
$k_{41} \cdots k_{47}$	-	0	$\theta_{41} \cdots \theta_{47}$	-	0
$k_{51} \cdots k_{57}$	-	0	$\theta_{51} \cdots \theta_{57}$	-	0
$k_{61} \cdots k_{63}$	-	0	$\theta_{61} \cdots \theta_{63}$	-	0
$k_{64} \cdots k_{66}$	-	0.005	$\theta_{64} \cdots \theta_{66}$	-	0
k_{67}	-	0.015	θ_{67}	-	0.015
λ_r	80	100	λ_d	90	140

The simulation is based on a participant with pre-gravid parameters of height 170 cm and weight 80 kg, which classifies her as overweight (BMI=27.68). Table 3.2 summarizes the model parameters in the simulation study, including the behavioral parameters, time constants τ_i, time delays θ_i, gains for the participant, and filter parameters in IMC design, respectively. All these values are hypothetical but have been selected such that the simulated responses mimic those of an actual participant. For all three scenarios, the participant has a ramp increase in her EI in the first trimester, and she will remain sedentary throughout the first trimester.

Figure 3.15 shows the participant's response in the PBC inflows to the EI-TPB and PA-TPB models, the participant's weight, EI, the change of PAL, EE, and the dosages of HE active learning and PA active learning for the cases with an adaptive intervention via IF-THEN decision rules, a fixed intervention, and no intervention, respectively. The interventions (adaptive and fixed) start at week 14 with the participant receiving the baseline program; this remains unchanged in the fixed intervention case. However, this baseline intervention is not enough for this participant due to her high EI , which leads to her GWG outside the IOM guidelines at the time of her second assessment circle (week 18). The intervention dosage gets augmented in the adaptive case, as dictated by the decision rules and her past and current responses. Meanwhile, because of her increased dosage, the participant's PBC inflows to the TPB models increase almost linearly as a result of the integrating action from the intervention delivery dynamics. The slope of PBC profile in both EI-TPB and PA-TPB is steeper in the adaptive intervention than the fixed intervention because of dose augmentation. Therefore, the participant experiences a faster decrease in EI, and increases her EE by involving herself in more PA, leading to an increase of her PAL from sedentary (PAL=1.65) at the start of the intervention to moderately active (PAL=1.70) around day 200, remaining at around this level throughout her pregnancy even in the face of PA disturbances. All these lead to her GWG increasing more slowly in the

adaptive intervention case. Therefore, the participant is able to meet her GWG goal at day 215, and keep her EI within the IOM guidelines by day 230. At late pregnancy, the participant achieves her GWG and EI targets just a little below the average settings. The fixed intervention can only help this participant meet her GWG goal at day 240, but she cannot manage her EI within the reference values prior to the end of the pregnancy.

In the scenario with no intervention, the participant will not experience a change in PBC inflows to the TPB models during the pregnancy. Because the increases in EI are not corrected in any way, her weight gain increases very fast. Starting from the second trimester, she is not willing increase her PA; her PAL and EE decrease, which accelerates the increase of her GWG. At the time of delivery, this participant increases her GWG by around 20 kg; meanwhile her EI is also outside the EI reference values.

The following conclusions can be drawn from the simulation results in this study:

- If no intervention is offered during pregnancy, most overweight and obese participants will not be able to regulate their GWG within the IOM guidelines due to difficulty engaging in healthy eating and physical activity.

- Traditional fixed interventions can offer some degree of effectiveness; nevertheless, they assign the same dosage to participants without considering their personal needs and individual response. As will be shown in Sections 7.2 and 7.3, fixed interventions are sometimes efficient and useful in the preventing excessive GWG among overweight pregnant women who have strong self-regulation and high PBC change, while most overweight and obese pregnant women may require an intensive intervention to manage their weight over the course of pregnancy; fixed interventions with lower dosage sometimes are insufficient for them.

- In adaptive interventions, IF-THEN decision rules use measurements of important outcomes to address the individual's needs. The tailoring variables (GWG) are as-

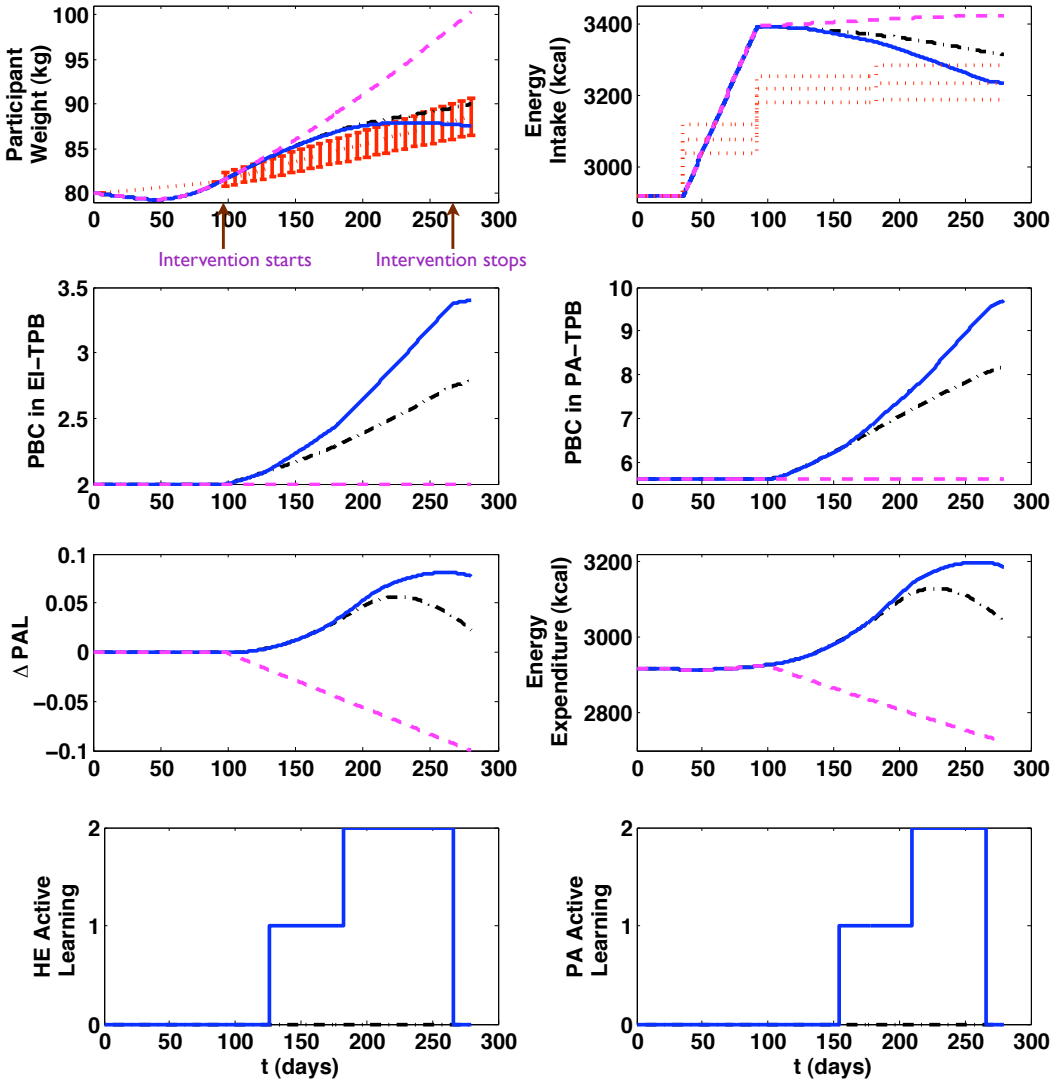

Figure 3.15: Simulation Responses Contrasting Adaptive, Fixed, and no Intervention for a Given Participant (Section 7.1). Red Dot Lines Represent the 2009 IOM Guidelines Applied on a Daily Basis; the Blue Solid Lines Represent the Case with Adaptive Interventions via IF-THEN Decision Rules, the Black Dash-dot Lines Represent the Case with Fixed Interventions, and the Dash Pink Lines Represent the Case with no Intervention.

sessed periodically and therefore, the intervention is adjusted on an ongoing basis if it is necessary. Thus, adaptive interventions can provide individually-tailed dosages to the participant according to her unique needs and responses collected via self-monitoring, which leads to better intervention effectiveness and results.

3.4.2 Understanding within Participant Variability

The simulations in this section focus on understanding intra-individual variability by examining the effects of both adaptive and fixed interventions on a participant exhibiting various types of behavioral responses. The participant considered is overweight with pre-gravid body mass 75 kg, 160 cm in height. By changing some of the parameters in the TPB and self-regulation behavioral models, the participant will display differing GWG profiles as a consequence of the differences in the speed and shape of the behavioral responses, which ultimately influences her GWG through the energy balance model. We consider the following four scenarios:

1. The participant shows strong self-regulation response and behavioral improvement through the intervention.

2. The participant has strong self-regulation response, but does not show as much behavioral improvement as she does in the first scenario.

3. The participant has high behavioral improvement through the influence of the intervention on PBC, intention and behavior, but shows weak self-regulation through a very slow response in this facet of the model.

4. The participant shows weak self-regulation response as in the earlier case, and does not improve her behavior as much as she does in the first and third scenarios as a consequence of the intervention.

Table 3.3: Model Parameter Changes for the Within-individual Variability Simulation Study in Section 3.4.2.

Scenario	Parameter	EI-TPB	PA-TPB
1	Table 3.2	Table 3.2	Table 3.2
2	$\Delta\tau_3$	4	10
	$\Delta\beta_{43}$	-0.2	-0.09
3	$\Delta\lambda_d$	20	70
4	$\Delta\tau_3$	4	10
	$\Delta\beta_{43}$	-0.2	-0.09
	$\Delta\lambda_d$	20	70

The model parameters in Table 3.2 are selected in the first (base) scenario, except that $\lambda_d = 80$ in the EI-TPB model so that the participant exhibits strong EI self-regulation. The parameters for the remaining three scenarios involve selected parameter deviations from the first scenario, which is summarized in Table 3.3.

Figure 3.16 shows the participant's response for the maternal body mass, EI and EE for the four scenarios under the influence of adaptive interventions (blue lines) and fixed interventions (black lines); Figure 3.17 presents the dosages of HE active learning and PA active learning for the four adaptive intervention scenarios, respectively. The simulation results indicate that when the participant has both strong self-regulation and behavioral improvement resulting from the intervention (scenario 1), she is able to manage her GWG within the IOM guidelines with either a fixed or adaptive interventions. However, her EI is almost barely within the reference values at the time of her delivery for the fixed intervention case. If the intervention does not have much influence on this same participant by reducing the gain and increasing the time constant in TPB models (scenario 2), she is still able to control her GWG with strong self-regulation responses during the interventions, but her EI is outside the reference values for fixed interventions. Because adaptive interventions augment dosages to meet the participant's need, her EI reaches the average bound of

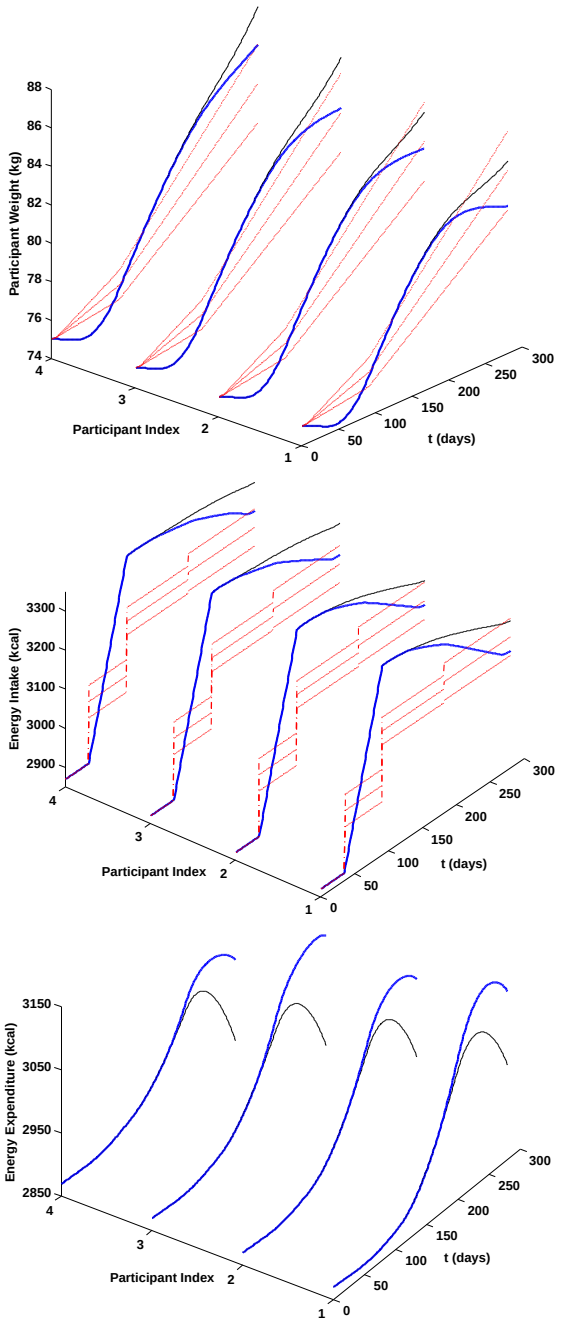

Figure 3.16: Simulation Response for the Participant's Weight, Energy Intake and Energy Expenditure for the Four Scenarios with Parameters Listed in Table 3.3. The Red Dashed-dotted Lines Represent the 2009 IOM Guidelines Applied on a Daily Basis; the Blue Thick Solid Lines Represent the Scenarios with Adaptive Interventions via IF-THEN Decision Rules, and Black Thin Dashed Lines are the Scenarios with Fixed Interventions.

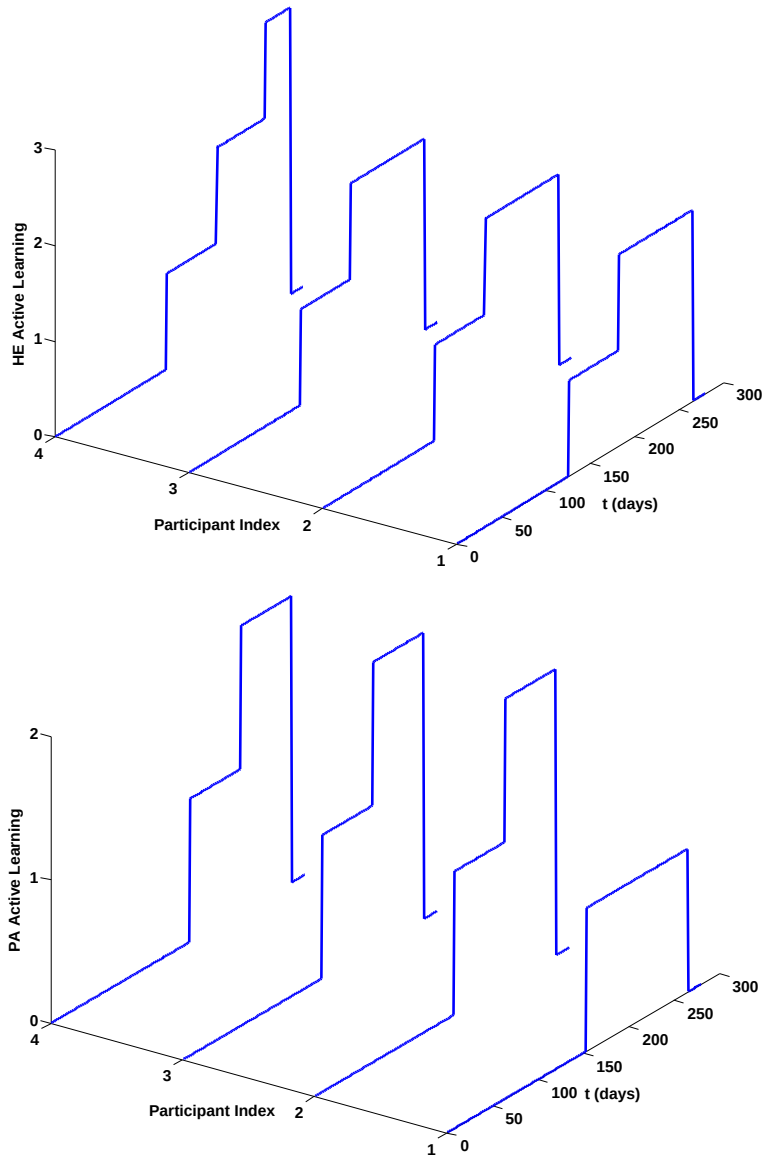

Figure 3.17: Simulation Response for the Intervention Components Dosages in Adaptive Interventions for the Four Scenarios with Parameters Listed in Table 3.3.

the reference values at late pregnancy. The third scenario demonstrates the importance of self-regulation during the interventions by showing that the participant cannot achieve either her GWG or EI goals with a fixed intervention with slow self-regulation, even though the intervention helps improve her PBC and behavior. Meanwhile, as a consequence of the increased potency provided by an adaptive intervention, the participant succeeds in regulating her GWG and EI within its corresponding reference values, respectively. Nonetheless, the improvements she makes in the adaptive intervention are not as efficient and effective as the ones in the first and second scenarios. As is seen in Figure 3.16, her GWG and EI start to reach the upper bound of the reference values in the late third trimester, while these occur in the early third trimester in the first two scenarios. The fourth scenario combines the bad elements of the second and third scenarios as a worst case situation which might happen to a participant with sluggish self-regulation and poor behavioral improvement as a result of the intervention. The fixed intervention fails to assist this participant in achieving her GWG and EI goals in this scenario as well. In the adaptive intervention, the participant receives the maximum dosage at late of the pregnancy by having her dosages augmented at each assessment cycle, as is shown in Figure 3.17, which leads to her GWG and EI reaching the upper bound of the reference values towards the end of her pregnancy.

In closing, this section has sought to understand variability within a participant by considering different behavioral and self-regulation responses that may occur during the intervention. Although a fixed intervention may be helpful and sufficient for an overweight pregnant woman who possesses both strong self-regulation and behavioral response, it fails to prevent excessive GWG when the participant demonstrates any weak response during the intervention. Adaptive interventions may enable delivery of interventions with greater degree of efficacy and personalization, which is demonstrated in all four evaluated scenarios. Meanwhile, self-regulation is as important as the influence of intervention dosages on the participant's behavioral change through PBC and intention during the interventions.

3.4.3 Understanding Variability between Participants

The simulations in this section are intended to explore variability between participants that are distinguished not only by different self-regulation and intervention effects, but also by having different pre-pregnancy BMI categories. By assuming that all participants experience the same EI increase in their first trimester, we can observe how weight gain and EI differs between these participants during the second and third trimesters, and better understand how fixed and adaptive interventions will work for women with different BMI, overweight and obese in particular. This section examines the following four hypothetical participants:

1. overweight with pre-gravid weight 75 kg, height 160 cm (BMI=29.30), strong self-regulation responses and high PBC change resulting from an intervention.

2. overweight with pre-gravid weight 80 kg, height 170 cm (BMI=27.68), weak self-regulation responses and low PBC change resulting from an intervention.

3. obese with pre-gravid weight 90 kg, height 165 cm (BMI= 33.06), strong self-regulation responses and high PBC change resulting from an intervention.

4. obese with pre-gravid weight 80 kg, height 160 cm (BMI= 31.25), weak self-regulation responses and low PBC change resulting from an intervention.

As was illustrated in the intra-participant variability study of Section 7.2, the model parameters in Table 3.2 are used to define the characteristics of the first participant, except that $\lambda_d = 80$ in the EI-TPB model so that the participant exhibits strong EI self-regulation. Meanwhile, the parameters for the other three participants are based on deviations for selected parameters from the first participant, as summarized in Table 3.4.

Table 3.4: Model Parameter Changes for the Inter-individual Variability Simulation Study in Section 3.4.3

Participant	Parameter	EI-TPB	PA-TPB
1 (BMI=29.30)	Table 3.2	Table 3.2	Table 3.2
2 (BMI=27.68)	$\Delta\lambda_d$	20	60
3 (BMI=33.06)	$\Delta\tau_3$	0	-2
	$\Delta\gamma_{33}$	0	0.1
	$\Delta\gamma_{53}$	0	0.01
	$\Delta\lambda_d$	5	30
4 (BMI=31.25)	$\Delta\tau_3$	0	2
	$\Delta\gamma_{33}$	0	0.1
	$\Delta\lambda_d$	20	60
	p_1	1	0

Figure 3.18 shows the participants' responses for weight and EI, Figure 3.19 is the participants' response for PBC from the EI-TPB and PA-TPB models, while Figure 3.20 shows the dosages of HE and PA active learning for the four overweight and obese participants under the influence of adaptive and fixed interventions, respectively.

The simulation results demonstrate how different participants respond to a similar increase in EI in the first trimester while subject to a fixed or adaptive intervention with self-regulation. When we compare the simulation results for the first and second participants who belong to the same BMI category (but have different self-regulation responses and pregravid parameters) we can see that both participants increase their EI by approximately 470 kcal in the first trimester which is much higher than they are supposed to increase as per the IOM EI reference values. The first participant has stronger self-regulation response, but one less dosage augmentation in PA active learning than the second participant. This means that the higher PBC increase witnessed in the EI-TPB model is contributed by her strong EI self-regulation. The PBC increase in the PA-TPB model is almost the same for both participants, because the first participant's stronger self-regulation is equivalent to the

influence of one more augmented PA active learning dose assigned to the second participant during the intervention. Thus, the first participant is able to control her weight gain earlier and faster within the IOM guidelines as a consequence of her strong self-regulation and high PBC influence, even though she receives less augmentation from the intervention than the second participant. A fixed intervention can enable the first participant to achieve her GWG goal within the guideline with the help of strong self-regulation and high PBC change from the influence of the intervention. However, it fails to assist the second participant in meeting her GWG goal.

The third participant is not in the same BMI category as the second participant, because of her high pre-pregnancy weight. Given the same amount of energy intake increase in the first trimester, the obese participant needs to reduce her weight gain (IOM guidelines: 4.4 - 7.0 kg) as well as have a greater EI reduction (EI increase reference values: 227 - 326 kcal) than the overweight participants (6.0-8.6 kg for GWG and 269 - 364 kcal for EI), as is indicated in Table 2.4. From the simulation results, we can see that the third participant receives the same dosages as the second participant who is overweight during the adaptive intervention. Therefore, the difference in PBC changes between these two participants is a consequence of their differing behavioral and self-regulation responses during the intervention. As is shown in the PBC inflow figures, the third participant increases her PBC inflows faster in both TPB models as a result of her stronger self-regulation, high gains and low time constant in the PA-TPB model. This explains why both her GWG and EI achieve the corresponding reference values earlier than the second participant. This comparison with an adaptive intervention illustrates that self-regulation and the behavioral improvements under the influences of intervention play a key role in the outcome of the interventions, and strong self-regulation and high PBC changes enable the participants to outperform the other peers who have better pre-gravid condition than them. Nevertheless, fixed interventions do not succeed in supporting both participants to meet their GWG goals.

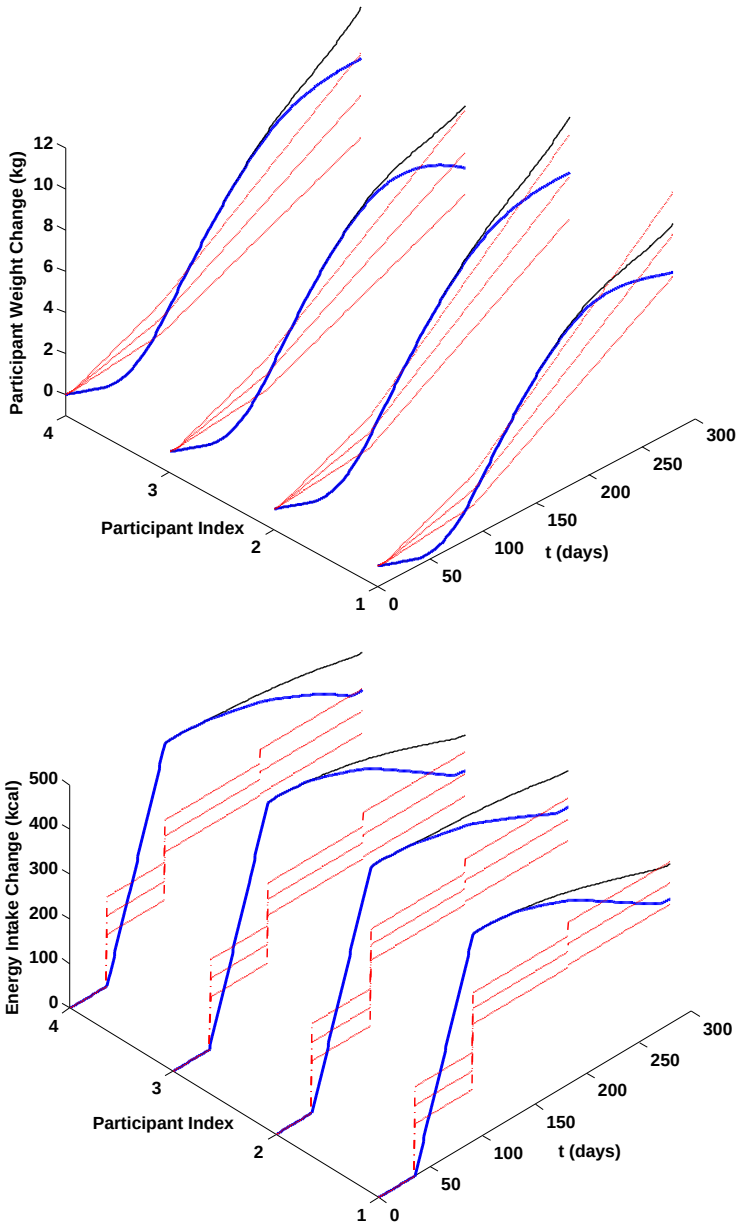

Figure 3.18: Simulation Response for the Participant's Weight Change, and Energy Intake Change for the four Participants with Parameters Listed in Table 3.4. The Red Dashed-dotted Lines Represent the 2009 IOM Guidelines Applied on a Daily Basis; the Blue Thick Solid Lines Represent the Scenarios with an Adaptive Intervention via IF-THEN Decision Rules, and the Black Thin Dashed Lines are the Scenarios with a Fixed Intervention.

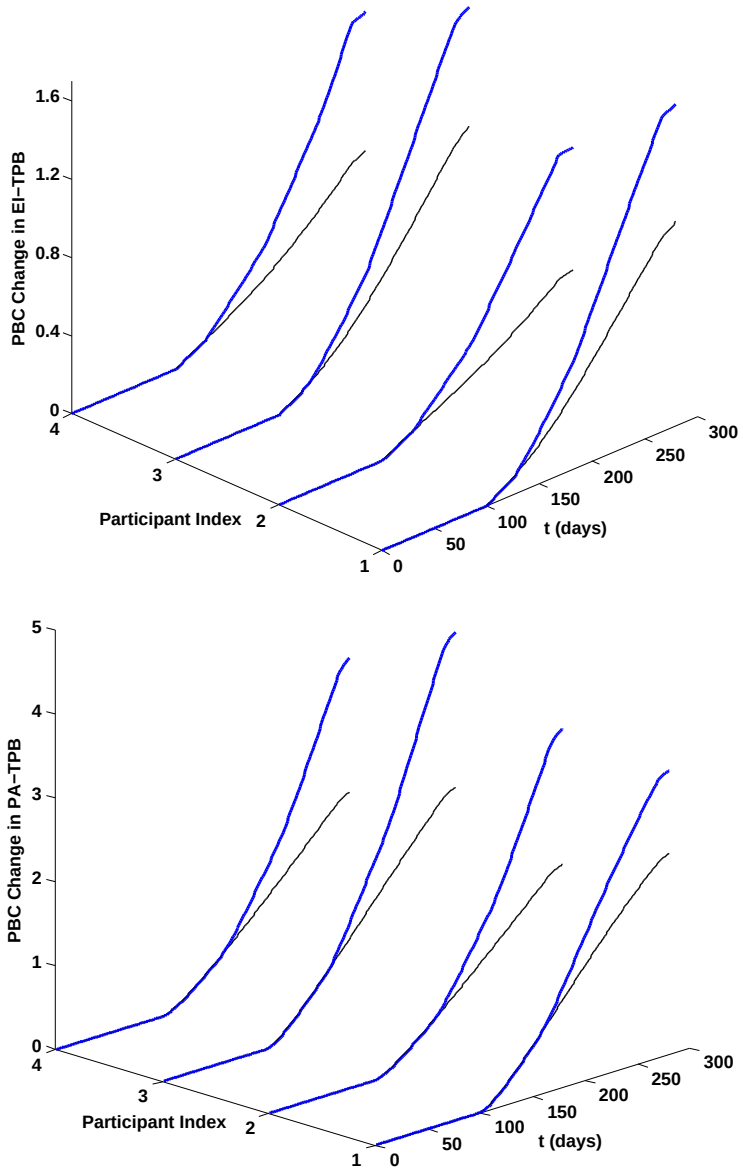

Figure 3.19: Simulation Response for the Participant's PBC Inflow Changes to EI-TPB Model and PA-TPB Model for the Four Participants with Parameters Listed in Table 3.4. The Blue Thick Solid Lines Represent the Scenarios with an Adaptive Intervention via IF-THEN Decision Rules, and Black Thin Dashed Lines are the Scenarios with a Fixed Intervention.

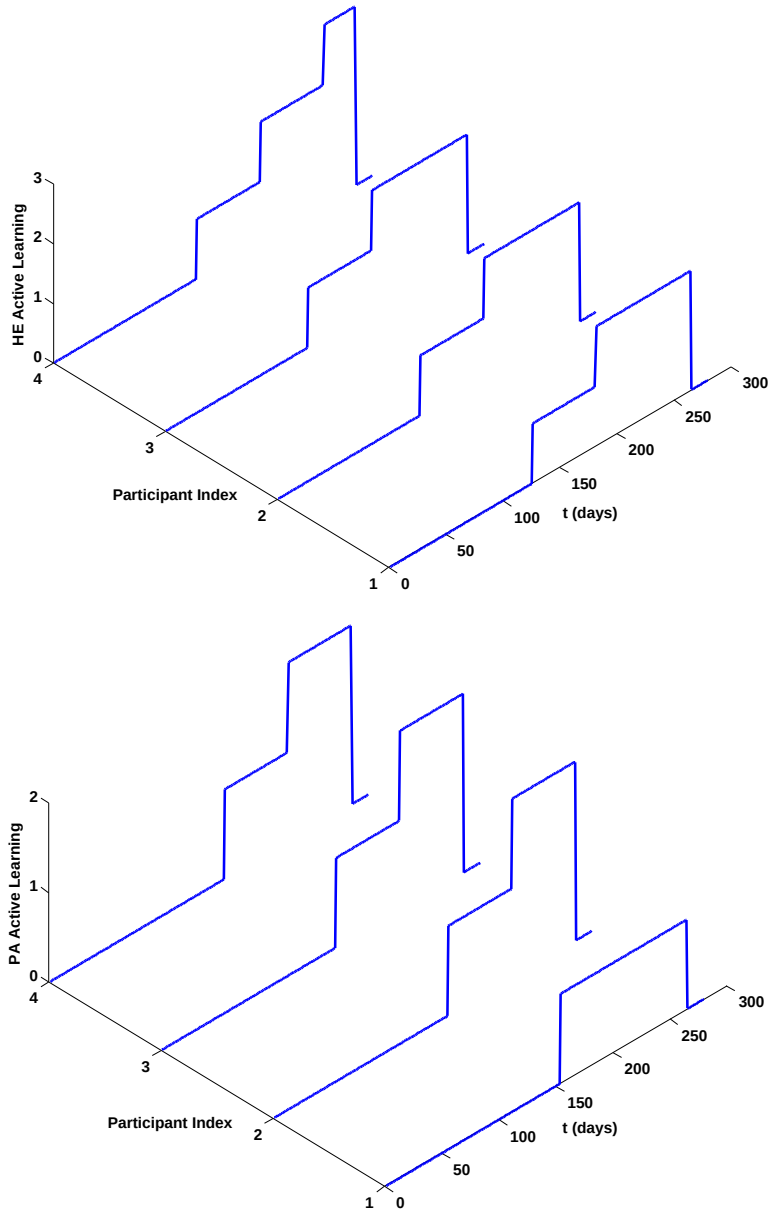

Figure 3.20: Simulation Response for the Participant's Intervention Components Dosages for the Four Participants with Parameters Listed in Table 3.4. The Blue Lines Represent the Scenarios with Adaptive Interventions via IF-THEN Decision Rules, and Black Lines are the Scenarios with Fixed Interventions.

Even though both are obese, the fourth participant actually has a better pre-pregnancy condition (with lower BMI and higher baseline value for the PBC inflow to EI-TPB model) than the third participant. With the same EI profile in the first trimester, their weight gains are same at the beginning of the intervention, and their GWG IOM guidelines and EI reference values are also same. However, the fourth participant has weak self-regulation, a little greater time constant and smaller gain in the TPB models which decelerates the behavioral response. This is indicated by her slower PBC inflow increase in both EI-TPB and the PA-TPB models although she receives one more HE active learning dose than the third participant during the intervention. As a result, she receives the strongest dosages by getting her intervention augmented at each assessment cycle, as is shown in Figure 3.20. But this is still barely able to help her achieve GWG goal, with her GWG and EI reaching the upper bound of the corresponding reference values at the very late of her pregnancy. Fixed interventions fail to help her control GWG and EI at all.

The comparison of simulation results between the first participant (overweight) and the third participant (obese) indicates the effect that pre-pregnancy condition has on the intervention outcomes. When both participants have strong self-regulation responses and high PBC changes during the intervention, even though the first participant receives one less augmentation in PA active learning which results in her lower PBC changes in PA-TPB model, she is still able to achieve GWG goal and EI reference values earlier than the third participant. This concludes that the pre-pregnancy BMI will determine if the participant can perform better during the intervention only when they both have similar self-regulation and behavioral response.

Through the different responses from these diverse participants, we can better understand why fixed interventions do not succeed in the prevention of excessive GWG among overweight and obese pregnant women, and why adaptive interventions represent a promising approach to prevention and treatment. While the pre-gravid BMI is an important index

to indicate if the participant has healthy diet and active exercise life before pregnancy, high BMI does not mean the participant will fail to manage her GWG during the interventions. The key factors which determine if adaptive interventions are efficient, effective and successful for a particular overweight or obese participant are the strong self-regulation and fast behavioral improvement through high PBC change during the intervention. Only when both participants display same self-regulation and behavioral responses during the intervention, does pre-gravid BMI play an important role in the speed of the improvements and effectiveness of the interventions.

3.5 Chapter Summary

The aim of this chapter is to introduce how to use advanced control engineering approaches to design self-regulation schemes in behavioral systems, and the GWG problem in particular. Various control-oriented formulations were proposed, in order to find the most suitable one for this GWG dynamical system.

To accomplish this goal, we first introduced internal model control (IMC) and its 2 DoF design structure by the use of nominal model (estimated model). The control results are shown in the simulation examples and these illustrate the flexibility to tune the controllers to achieve different speed of setpoint tracking and disturbances rejection by varying the tuning parameters. On the basis of this 2 DoF IMC design, we extend the formulation of self-regulation by the use of cascade control, in order to better make use of all the measurements which might be available in the real-life clinical trial. Two different IMC design schemes for EI self-regulation using cascade control were first proposed, developed and analyzed, so that it is convenient and straightforward for the user to pick which one is easy to design and implement. After PA self-regulation is integrated into the control system, a new weight parameter fraction is introduced to illustrate how much each self-regulation contributes to tracking setpoint change. The formulation of this self-regulation

will be useful once we have a systematic way to get the estimation of the weight parameter fraction through the clinical trial. The second formulation of self-regulation using cascade control involves the measurements of PA monitoring data. The outer loop of PA self-regulation using IOM guidelines as setpoint will inform the inner loop of PA setpoint, which allows the participant to achieve her GWG goal, while making both EI and PA follow the corresponding reference values. When the tuning parameters in the inner loop for PA self-regulation is smaller, the participant is able to track the PA setpoint generated by the outer loop PA self-regulation quickly, and the corresponding simulation result in this formulation is very similar to the one in 2 DoF IMC design of self-regulation.

With the significant flexibility in describing a participant's self-regulatory behavior through the tuning of contorller adjustable parameters, the simulation studies in this chapter focus on the evaluation and comparison between fixed versus adaptive interventions, and the understanding of variability within and between participants. The simulation results not only illustrate how adaptive interventions deliver greater degrees of efficacy according to a participant's changing needs and responses (leading to overall improved and more effective interventions) but also indicate why fixed interventions may have limited success among overweight and obese pregnant women in the prevention of excessive GWG.

We expect pilot testing and clinical trials to inform the refinement of some structural aspects of the simulation model, such as the proper structure of the self-regulation problem, and how additional measurements (e.g., physical activity) can influence the problem as illustrated in Section 3.3.3.3. The GWG model integrating IMC design for self-regulation in this chapter can be used by behavioral scientists to evaluate decision rules for adaptive interventions, to understand the optimal choices on the level and duration of intervention components, or as the open-loop model for the implementation of Hybrid Model Predictive Control (HMPC) algorithms acting as decision frameworks for such interventions.

Chapter 4

OPTIMIZED ADAPTIVE BEHAVIORAL INTERVENTIONS WITH SEQUENTIAL DECISION POLICIES USING HYBRID MODEL PREDICTIVE CONTROL

4.1 Overview

As introduced in Chapter 2, in an adaptive, time-varying intervention, the frequency or intensity of intervention dosages will change over time, based on the result of important outcomes of the intervention (also known as tailoring variables [25]). Decision rules operationalize these changes, eliminating / adding some intervention components based on participant response during the intervention, or altering the dosage of existing components.

Control engineering can offer a systematic and efficient approach to optimizing the effectiveness of such individually tailored treatment and prevention policies, which is also known as "just-in-time" behavioral interventions. In a control engineering approach to optimizing an adaptive time-varying intervention, the controller assigns the dosages of the intervention components to the participant as dictated by model dynamics, problem constraints, and disturbances. This chapter presents a control-oriented approach to the problem using Model Predictive Control (MPC) algorithm which offers an appealing framework for designing optimized, time-varying adaptive interventions. The discrete magnitude nature of the intervention dosage assignment dictates the need for Hybrid Model Predictive Control (HMPC) schemes. The clinical and resource considerations in these behavioral health problem settings (e.g., the augmentation/reduction of the components follow a certain predefined dosage sequence) are significant challenges which have remained largely unexplored in literature. The goal of this chapter is to develop an HMPC-based intervention decision algorithm that can automatically assign optimized intervention dosages to modify individual's behavior while systematically addressing these unique clinical considerations and constraints, relying on a Mixed Logical Dynamical (MLD) structure with constraints

as an HMPC formulation to control the linear hybrid systems. This control algorithm makes use of feedback and feedforward control action by online optimization of a cost function using a receding horizon strategy, which is well suited for designing behavioral interventions.

In order to achieve this goal, the dynamical systems model developed for GWG intervention in the previous chapters is used as an illustration to exemplify how to design HMPC algorithm acting as a sequential decision framework for adaptive interventions. Figure 4.1 shows the overall schematic representation for GWG intervention in this chapter. It is very similar to Figure 2.1 in Chapter 2, except that the decision policy is accomplished by hybrid model predictive control (HMPC) in lieu of "IF-THEN" decision rules to optimize the behavioral intervention and improve participant response. The individual self-regulation strategies described in Figure 3.4 in Chapter 3 remain in this chapter as well.

The simulation studies are presented to demonstrate the effectiveness for implementing adaptive behavioral interventions involving multiple components by the use of HMPC, the proper generation of postulated dosage sequence, and the potential benefits of HMPC framework for optimized adaptive interventions in contrast to adaptive intervention using simple decision rules.

4.2 Hybrid Dynamical Systems

Hybrid systems are dynamical systems that involve the interaction between continuous and discrete dynamics. The term hybrid has also been applied to describe processes that involve continuous dynamics and discrete (logical) decisions, such as for instance on/off switches or valves, gears or speed selectors, evolutions dependent on if-then-else rules [23,42]. These binary or discrete behaviors can be expressed by binary constraints that can be a part of the state, output, input and the like. Below are some examples of such hybrid dynamical systems, summarized from [42].

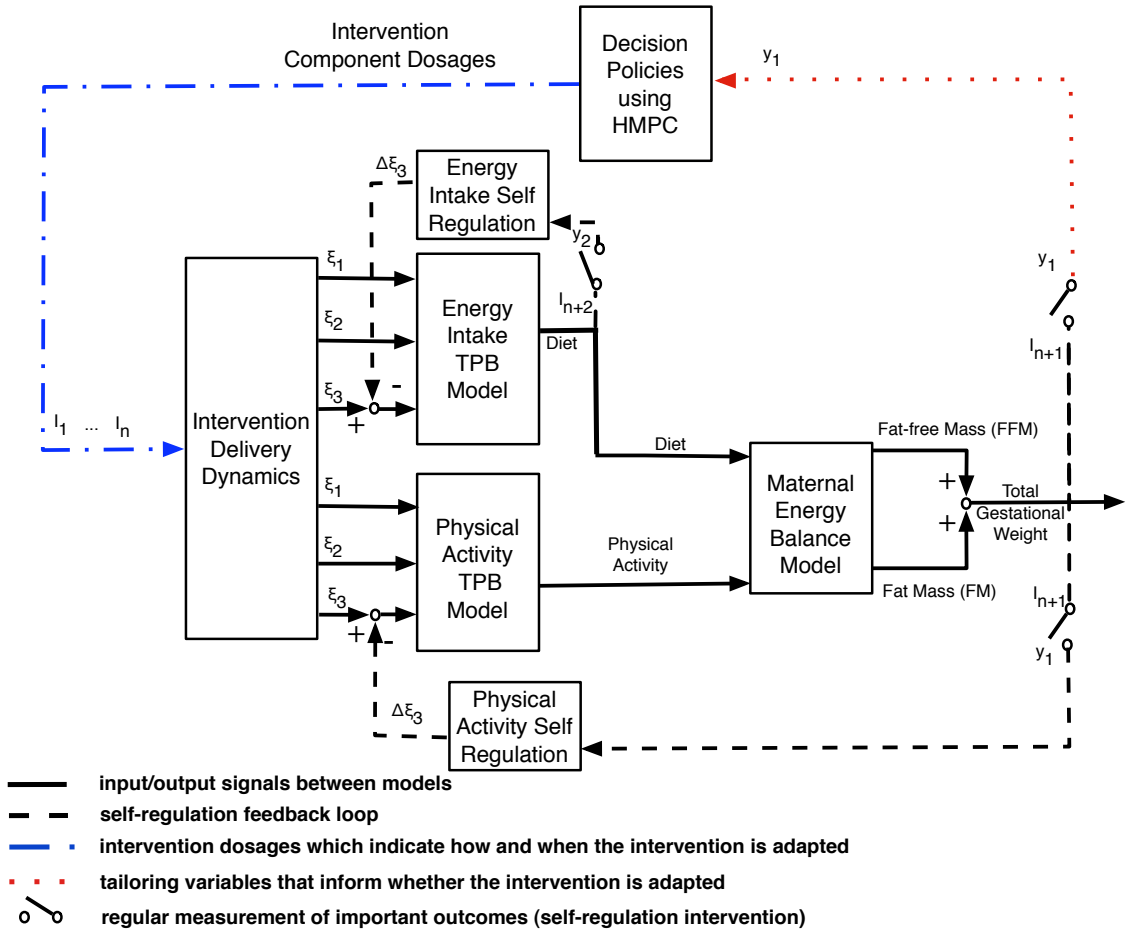

Figure 4.1: Schematic Representation for an "Adaptive" Optimized Gestational Weight Gain (GWG) Intervention by Hybrid Model Predictive Control (HMPC) [1].

1. Piecewise linear dynamic systems

   Consider the following piecewise linear time-invariant dynamic system in which the state equation is updated relying on binary variables δ_i,

$$x(t+1) = \begin{cases} A_1 x(t) + B_1 u(t) & \text{if } \delta_1(t) = 1 \\ \vdots & \\ A_n x(t) + B_n u(t) & \text{if } \delta_n(t) = 1 \end{cases} \tag{4.1}$$

$$y(t) = Cx(t) + Du(t) \tag{4.2}$$

where δ_i are 0-1 binary variables ($i = 1, 2, \cdots, n$), and $\delta_1 + \delta_2 + \cdots + \delta_n = 1$.

2. Piecewise linear output functions

   In practical applications, it frequently happens that a process can be modeled as a linear dynamic system cascaded by a nonlinear output function. Think of the case where the output from a linear system may be under conditions like saturations, for example. In other words, y can take only certain values which can be described by boolean logic. An example is shown below,

$$x(t+1) = Ax(t) + Bu(t) \tag{4.3}$$

$$y(t) = \begin{cases} C_1 x(t) + D_1 u(t) & \text{if } \delta = 0 \\ C_2 x(t) + D_2 u(t) & \text{if } \delta = 1 \end{cases} \tag{4.4}$$

3. Discrete inputs

   Control laws typically provide command inputs ranging on a continuum. However, in application frequently one has to deal with command inputs which are inherently discrete. Such cases include the dosage the doctor prescribes for the patients, and the number of intervention sessions in the behavioral interventions. Consider, for instance, the following system:

$$x(t+1) = Ax(t) + Bu(t) \tag{4.5}$$

$$u(t) = \begin{cases} u_1 & \text{if } \delta = 0 \\ u_2 & \text{if } \delta = 1 \end{cases} \tag{4.6}$$

4. Qualitative outputs

   Some systems have qualitative (i.e., categorical) outputs based on a certain criteria. Consider the following example, in which, y has qualitative outputs based on

different values of the state x.

$$x(t+1) = Ax(t)+Bu(t) \tag{4.7}$$

$$y(t) = \begin{cases} \text{Excellent} & \text{if } x(t) \leq x_1 \\ \text{Good} & \text{if } x_1 \leq x(t) \leq x_2 \\ \text{Acceptable} & \text{if } x_2 \leq x(t) \leq x_3 \\ \text{Fail} & \text{if } x_3 \leq x(t) \leq x_4 \end{cases} \tag{4.8}$$

where x_i is the constant within the boundary of the state $x(t)$, $(i = 1,2,3,4)$.

Hybrid systems have been the topic of intense research activity in recent years, primarily because of their importance in applications [83]. For this class of systems, several control approaches have been proposed in the literature. However, optimal control approaches for hybrid systems are the most promising ones at the moment, and have been thoroughly investigated in recent years [84, 85]. Many results can be found in the control-engineering literature. A computational approach based on ideas from dynamic programming and convex optimization is presented in [85]. [42,86] address a model predictive control technique for hybrid systems, which is able to stabilize the mixed logical dynamical (MLD) system on desired reference trajectories, and solves the online optimization procedures through *Mixed Integer Quadratic Programming* (MIQP).

In this chapter, we study and discuss the solution to an MPC for linear hybrid systems with discrete inputs only, where the system is described as a *mixed logical dynamical* (MLD) system.

4.2.1 Mixed Logical Dynamical (MLD) Systems

Hybrid systems represent a combination of logic, finite-state machines, linear discrete-time dynamic systems and constraints [42]. The mixed logical dynamical (MLD) modeling framework is based on the idea of translating logic relations, discrete/logic dynamics, A/D

(analog to digital (logic)), D/A conversion and logic constraints into mixed integer linear inequalities. These inequalities are combined with the continuous dynamical part which is described by linear difference equations. The resulting MLD-based model framework is described by the following equations,

$$x(k+1) = Ax(k) + B_1 u(k) + B_2 \delta(k) + B_3 z(k) + B_d d(k) \tag{4.9}$$

$$y(k) = Cx(k) + d'(k) + \nu(k) \tag{4.10}$$

$$E_2 \delta(k) + E_3 z(k) \leq E_5 + E_4 y(k) + E_1 u(k) - E_d d(k) \tag{4.11}$$

where $x = [x_c^T \quad x_d^T]^T$, $x_c \in \mathbb{R}^{n_c}$, $x_d \in \{0, 1\}^{n_d}$, $n \stackrel{\triangle}{=} n_c + n_d$ is the state of the system including continuous x_c and 0-1 x_d; $u = [u_c^T \quad u_d^T]^T$, $u_c \in \mathbb{R}^{m_c}$, $u_d \in \{0, 1\}^{m_d}$, $m \stackrel{\triangle}{=} m_c + m_d$ represents m inputs of the system (both continuous commands u_c and discrete commands u_d). y is the output and d, d' and ν represent measured disturbances, unmeasured disturbances and measurement noise signals, respectively. $\delta \in \{0,1\}$ and $z \in \mathbb{R}^{r_c}$ are discrete and continuous auxiliary variables that are introduced in order to convert logical/discrete decisions into their equivalent linear inequality constraints. The dimension of these auxiliary variables and the number of linear constraints in (4.11) depends on the specific character of the discrete logical / discrete decisions that would be enforced in the particular hybrid system. This framework permits the user to include and prioritize constraints and the general rules in the description of the model. The MLD system (4.9) - (4.11) is assumed to be well posed if for a given state $x(k)$ and a given input $u(k)$, the inequalities (4.11) have a unique solution for $\delta(k)$ and $z(k)$. Relying on propositional logic, one can convert boolean logic and discrete decisions into linear inequalities (4.11). The detail description of MLD form and the conversion techniques can be found in [42].

4.2.2 MPC Prediction

Equations (4.9) - (4.11) extend the MLD framework shown in [42] through the inclusion of both measured and unmeasured disturbances. Here, we consider a stochastic disturbance model for unmeasured disturbance d',

$$x_w(k) = A_w x_w(k-1) + B_w w(k-1) \tag{4.12}$$

$$d'(k) = C_w x_w(k) \tag{4.13}$$

We consider differenced forms of the disturbance and system models as follows,

$$\begin{aligned} \Delta x(k) &= A\Delta x(k-1) + B_1\Delta u(k-1) + B_2\Delta\delta(k-1) + B_3\Delta z(k-1) \\ &+ B_d\Delta d(k-1) \end{aligned} \tag{4.14}$$

$$\Delta x_w(k) = A_w\Delta x_w(k-1) + B_w\Delta w(k-1) \tag{4.15}$$

The following equations can be obtained if propagating equations (4.10), (4.14), and (4.15),

$$\begin{aligned} X(k) &= \tilde{A}X(k-1) + \tilde{B}_1\Delta u(k-1) + \tilde{B}_2\Delta\delta(k-1) + \tilde{B}_3\Delta z(k-1) \\ &+ \tilde{B}_d\Delta d(k-1) + \tilde{B}_w\Delta w(k-1) \end{aligned} \tag{4.16}$$

$$y(k) = \tilde{C}X(k) + \nu(k) \tag{4.17}$$

where

$$\begin{aligned} X(k) &= [\Delta x^T(k) \quad \Delta x_w^T(k) \quad y^T(k)]^T \\ \tilde{A} &= \begin{bmatrix} A & 0 & 0 \\ 0 & A_w & 0 \\ CA & A_w & I \end{bmatrix};\ \tilde{B}_i = \begin{bmatrix} B_i \\ 0 \\ CB_i \end{bmatrix},\ i = 1, d; \\ \tilde{B}_w &= \begin{bmatrix} 0 \\ I \\ I \end{bmatrix};\ \tilde{C} = [0 \quad 0 \quad I] \end{aligned}$$

Here $\Delta*(k) = *(k) - *(k-1)$ and $\Delta w(k)$ is a white noise sequence.

If the prediction horizon of this MPC model is p, the moving horizon is m, the future value of output $y(k+1)$ is,

$$\begin{aligned} y(k+1) &= \tilde{C}X(k+1) \\ &= \tilde{C}\tilde{A}X(k) + \tilde{C}\tilde{B}_1\Delta u(k) + \tilde{C}\tilde{B}_2\Delta\delta(k) + \tilde{C}\tilde{B}_3\Delta z(k) + \tilde{C}\tilde{B}_d\Delta d_{flt}(k) \\ &= \tilde{C}\tilde{A}X(k) + \tilde{C}\tilde{B}_1 u(k) + \tilde{C}\tilde{B}_2\delta(k) + \tilde{C}\tilde{B}_3 z(k) + \tilde{C}\tilde{B}_d d_{flt}(k) - \tilde{C}\tilde{B}_1 u(k-1) \\ &- \tilde{C}\tilde{B}_2\delta(k-1) - \tilde{C}\tilde{B}_3 z(k-1) - \tilde{C}\tilde{B}_d d_{flt}(k-1) \end{aligned} \tag{4.18}$$

The future value of output $y(k+2)$,

$$\begin{aligned} y(k+2) &= \tilde{C}\tilde{A}X(k+1) + \tilde{C}\tilde{B}_1\Delta u(k+1) + \tilde{C}\tilde{B}_2\Delta\delta(k+1) \\ &+ \tilde{C}\tilde{B}_3\Delta z(k+1) + \tilde{C}\tilde{B}_d\Delta d_{flt}(k+1) \\ &= \tilde{C}\tilde{A}^2X(k) + [(\tilde{C}\tilde{A}\tilde{B}_1 - \tilde{C}\tilde{B}_1)u(k) + \tilde{C}\tilde{B}_1 u(k+1)] \\ &+ [(\tilde{C}\tilde{A}\tilde{B}_2 - \tilde{C}\tilde{B}_2)\delta(k) + \tilde{C}\tilde{B}_2\delta(k+1)] + [(\tilde{C}\tilde{A}\tilde{B}_3 - \tilde{C}\tilde{B}_3)z(k) \\ &+ \tilde{C}\tilde{B}_3 z(k+1)] + [(\tilde{C}\tilde{A}\tilde{B}_d - \tilde{C}\tilde{B}_d)d_{flt}(k) + \tilde{C}\tilde{B}_d d_{flt}(k+1)] \\ &- \tilde{C}\tilde{A}\tilde{B}_1 u(k-1) - \tilde{C}\tilde{A}\tilde{B}_2\delta(k-1) - \tilde{C}\tilde{A}\tilde{B}_3 z(k-1) - \tilde{C}\tilde{A}\tilde{B}_d d_{flt}(k-1) \end{aligned} \tag{4.19}$$

The prediction equations for the future output over the prediction horizon p are obtained similarly, with the assumption that $\Delta u(k+i) = 0, i > m-1$, therefore, the future value of output $y(k+m+1)$ is as follows,

$$\begin{aligned} y(k+m+1) &= \tilde{C}\tilde{A}^{m+1}X(k) + [\tilde{C}\tilde{A}^m\tilde{B}_1\Delta u(k) + \tilde{C}\tilde{A}^{m-1}\tilde{B}_1\Delta u(k+1) + \cdots \\ &+ \tilde{C}\tilde{A}\tilde{B}_1\Delta u(k+m-1)] + [\tilde{C}\tilde{A}^m\tilde{B}_2\Delta\delta(k) + \tilde{C}\tilde{A}^{m-1}\tilde{B}_2\Delta\delta(k+1) \\ &+ \cdots + \tilde{C}\tilde{B}_2\Delta\delta(k+m)] + [\tilde{C}\tilde{A}^m\tilde{B}_3\Delta z(k) + \tilde{C}\tilde{A}^{m-1}\tilde{B}_3\Delta z(k+1) \\ &+ \cdots + \tilde{C}\tilde{B}_3\Delta z(k+m)] + [\tilde{C}\tilde{A}^m\tilde{B}_d\Delta d_{flt}(k) + \tilde{C}\tilde{A}^{m-1}\tilde{B}_d\Delta d_{flt}(k+1) \\ &+ \cdots + \tilde{C}\tilde{B}_d\Delta d_{flt}(k+m)] \end{aligned} \tag{4.20}$$

Rearranging equation above, and expressing it with the terms related to control efforts, auxiliary binary variables, auxiliary continuous variables and measured disturbance.

$$
\begin{aligned}
y(k+m+1) &= \tilde{C}\tilde{A}^{m+1}X(k) + [(\tilde{C}\tilde{A}^{m}\tilde{B}_1 - \tilde{C}\tilde{A}^{m-1}\tilde{B}_1)u(k) + (\tilde{C}\tilde{A}^{m-1}\tilde{B}_1 \\
&- \tilde{C}\tilde{A}^{m-2}\tilde{B}_1)u(k+1) + \cdots + (\tilde{C}\tilde{A}^{2}\tilde{B}_1 - \tilde{C}\tilde{A}\tilde{B}_1)u(k+m-2) \\
&+ \tilde{C}\tilde{A}\tilde{B}_1 u(k+m-1)] + [(\tilde{C}\tilde{A}^{m}\tilde{B}_2 - \tilde{C}\tilde{A}^{m-1}\tilde{B}_2)\delta(k) + (\tilde{C}\tilde{A}^{m-1}\tilde{B}_2 \\
&- \tilde{C}\tilde{A}^{m-2}\tilde{B}_2)\delta(k+1) + \cdots + (\tilde{C}\tilde{A}\tilde{B}_2 - \tilde{C}\tilde{B}_2)\delta(k+m-1) \\
&+ \tilde{C}\tilde{B}_2\delta(k+m)] + [(\tilde{C}\tilde{A}^{m}\tilde{B}_3 - \tilde{C}\tilde{A}^{m-1}\tilde{B}_3)z(k) + (\tilde{C}\tilde{A}^{m-1}\tilde{B}_3 \\
&- \tilde{C}\tilde{A}^{m-2}\tilde{B}_3)z(k+1) + \cdots + (\tilde{C}\tilde{A}\tilde{B}_3 - \tilde{C}\tilde{B}_3)z(k+m-1) \\
&+ \tilde{C}\tilde{B}_3 z(k+m)] + [(\tilde{C}\tilde{A}^{m}\tilde{B}_d - \tilde{C}\tilde{A}^{m-1}\tilde{B}_d)d_{flt}(k) + (\tilde{C}\tilde{A}^{m-1}\tilde{B}_d \\
&- \tilde{C}\tilde{A}^{m-2}\tilde{B}_d)d_{flt}(k+1) + \cdots + (\tilde{C}\tilde{A}\tilde{B}_d - \tilde{C}\tilde{B}_d)d_{flt}(k+m-1) \\
&+ \tilde{C}\tilde{B}_d d_{flt}(k+m)] - \tilde{C}\tilde{A}^{m}\tilde{B}_1 u(k-1) - \tilde{C}\tilde{A}^{m}\tilde{B}_2\delta(k-1) \\
&- \tilde{C}\tilde{A}^{m}\tilde{B}_3 z(k-1) - \tilde{C}\tilde{A}^{m}\tilde{B}_d d_{flt}(k-1) \qquad (4.21)
\end{aligned}
$$

The future value of output $y(k+p)$ is

$$\begin{aligned}
y(k+p) &= \tilde{C}\tilde{A}^{p}X(k)+[(\tilde{C}\tilde{A}^{p-1}\tilde{B}_1-\tilde{C}\tilde{A}^{p-2}\tilde{B}_1)u(k)+(\tilde{C}\tilde{A}^{p-2}\tilde{B}_1 \\
&- \tilde{C}\tilde{A}^{p-3}\tilde{B}_1)u(k+1)+\cdots+(\tilde{C}\tilde{A}^{p-m+1}\tilde{B}_1-\tilde{C}\tilde{A}^{p-m}\tilde{B}_1)u(k+m-2) \\
&+ \tilde{C}\tilde{A}^{p-m}\tilde{B}_1u(k+m-1)]+[(\tilde{C}\tilde{A}^{p-1}\tilde{B}_2-\tilde{C}\tilde{A}^{p-2}\tilde{B}_2)\delta(k) \\
&+ (\tilde{C}\tilde{A}^{p-2}\tilde{B}_2-\tilde{C}\tilde{A}^{p-3}\tilde{B}_2)\delta(k+1)+\cdots+(\tilde{C}\tilde{A}\tilde{B}_2-\tilde{C}\tilde{B}_2) \\
&\quad \delta(k+p-2)+\tilde{C}\tilde{B}_2\delta(k+p-1)]+[(\tilde{C}\tilde{A}^{p-1}\tilde{B}_3-\tilde{C}\tilde{A}^{p-2}\tilde{B}_3)z(k) \\
&+ (\tilde{C}\tilde{A}^{p-2}\tilde{B}_3-\tilde{C}\tilde{A}^{p-3}\tilde{B}_3)z(k+1)+\cdots+(\tilde{C}\tilde{A}\tilde{B}_3-\tilde{C}\tilde{B}_3) \\
&\quad z(k+p-2)+\tilde{C}\tilde{B}_3z(k+p-1)]+[(\tilde{C}\tilde{A}^{p-1}\tilde{B}_d-\tilde{C}\tilde{A}^{p-2}\tilde{B}_d)d_{flt}(k) \\
&+ (\tilde{C}\tilde{A}^{p-2}\tilde{B}_d-\tilde{C}\tilde{A}^{p-3}\tilde{B}_d)d_{flt}(k+1)+\cdots+(\tilde{C}\tilde{A}\tilde{B}_d-\tilde{C}\tilde{B}_d) \\
&\quad d_{flt}(k+p-2)+\tilde{C}\tilde{B}_dd_{flt}(k+p-1)]-\tilde{C}\tilde{A}^{p-1}\tilde{B}_1u(k-1) \\
&- \tilde{C}\tilde{A}^{p-1}\tilde{B}_3\delta(k-1)-\tilde{C}\tilde{A}^{p-1}\tilde{B}_3z(k-1)-\tilde{C}\tilde{A}^{p-1}\tilde{B}_dd_{flt}(k-1) \qquad (4.22)
\end{aligned}$$

Now the p step ahead prediction equations of MPC can be obtained by propagating (4.18) - (4.22), along with linear inequality constraints described in (4.11), resulting in the following prediction equations,

$$\begin{aligned}
Y(k+1) &= \Phi X(k)+H_1U(k)+H_2\bar{\delta}(k)+H_3Z(k)+H_dD(k)-H_{11}u(k-1) \\
&- H_{21}\delta(k-1)-H_{31}z(k-1)-H_{d1}d_{flt}(k-1) \qquad (4.23) \\
\bar{E}_5 &\geq \bar{E}_2\bar{\delta}(k)+\bar{E}_3Z(k)+\bar{E}_4Y(k)+\bar{E}_1U(k)+\bar{E}_dD(k) \qquad (4.24)
\end{aligned}$$

Equation (4.24) can be further simplified if we substitute $Y(k)$ and rewrite as,

$$\begin{aligned}
\tilde{E}_5 &\geq \tilde{E}_2\bar{\delta}(k)+\tilde{E}_3Z(k)+\tilde{E}_4X(k)+\tilde{E}_1U(k)+\tilde{E}_dD(k) \\
&\quad -\tilde{E}_{41}u(k-1)-\tilde{E}_{42}\delta(k-1)-\tilde{E}_{43}z(k-1)-\tilde{E}_{4d}d_{flt}(k-1) \qquad (4.25)
\end{aligned}$$

where d_{flt} represents the filtered value of the measured disturbance obtained using a discrete time filter, which will be described later in the presentation of three-Degree-of-Freedom (3 DoF) tuning approach in Section 4.3.4. $Y(k+1)$, $U(k)$, $\bar{\delta}(k)$, $Z(k)$ and $D(k)$ are

future values of outputs, inputs, auxiliary binary variables, auxiliary continuous variables and filtered measured disturbances as given below:

$$Y(k+1) = [y^T(k+1)\, y^T(k+2) \cdots y^T(k+p)]^T \tag{4.26}$$

$$U(k) = [u^T(k) \cdots u^T(k+m-1)]^T \tag{4.27}$$

$$\bar{\delta}(k) = [\delta^T(k) \cdots \delta^T(k+p-1)]^T \tag{4.28}$$

$$Z(k) = [z^T(k) \cdots z^T(k+p-1)]^T \tag{4.29}$$

$$D(k) = [{d_{flt}}^T(k) \cdots {d_{flt}}^T(k+p-1)]^T \tag{4.30}$$

Φ, H_{**}, H_*, $\bar{E}_*$, and $\tilde{E}_*$ are the appropriate coefficients matrices that can be generated from the equations (4.11), (4.18) - (4.22) above. They are given below,

$$\Phi = \begin{bmatrix} \tilde{C}\tilde{A} \\ \tilde{C}\tilde{A}^2 \\ \vdots \\ \tilde{C}\tilde{A}^p \end{bmatrix} \tag{4.31}$$

$$H_{i1} = \begin{bmatrix} \tilde{C}\tilde{B}_i \\ \tilde{C}\tilde{A}\tilde{B}_i \\ \tilde{C}\tilde{A}^2\tilde{B}_i \\ \vdots \\ \tilde{C}\tilde{A}^{p-1}\tilde{B}_i \end{bmatrix} \quad i = 1,\ 2,\ 3,\ d \tag{4.32}$$

$$H_1 = \begin{bmatrix} \tilde{C}\tilde{B}_1 & 0 & \cdots & 0 & 0 \\ \tilde{C}\tilde{A}\tilde{B}_1 - \tilde{C}\tilde{B}_1 & \tilde{C}\tilde{B}_1 & \cdots & 0 & 0 \\ \tilde{C}\tilde{A}^2\tilde{B}_1 - \tilde{C}\tilde{A}\tilde{B}_1 & \tilde{C}\tilde{A}\tilde{B}_1 - \tilde{C}\tilde{B}_1 & \ddots & \vdots & \vdots \\ \vdots & \vdots & \ddots & \tilde{C}\tilde{B}_1 & \vdots \\ \tilde{C}\tilde{A}^{m-1}\tilde{B}_1 - \tilde{C}\tilde{A}^{m-2}\tilde{B}_1 & \tilde{C}\tilde{A}^{m-2}\tilde{B}_1 - \tilde{C}\tilde{A}^{m-3}\tilde{B}_1 & \cdots & \tilde{C}\tilde{A}\tilde{B}_1 - \tilde{C}\tilde{B}_1 & \tilde{C}\tilde{B}_1 \\ \tilde{C}\tilde{A}^{m}\tilde{B}_1 - \tilde{C}\tilde{A}^{m-1}\tilde{B}_1 & \tilde{C}\tilde{A}^{m-1}\tilde{B}_1 - \tilde{C}\tilde{A}^{m-2}\tilde{B}_1 & \cdots & \tilde{C}\tilde{A}^2\tilde{B}_1 - \tilde{C}\tilde{A}\tilde{B}_1 & \tilde{C}\tilde{A}\tilde{B}_1 \\ \vdots & \vdots & \vdots & \vdots & \vdots \\ \tilde{C}\tilde{A}^{p-1}\tilde{B}_1 - \tilde{C}\tilde{A}^{p-2}\tilde{B}_1 & \tilde{C}\tilde{A}^{p-2}\tilde{B}_1 - \tilde{C}\tilde{A}^{p-3}\tilde{B}_1 & \cdots & \tilde{C}\tilde{A}^{p-m+1}\tilde{B}_1 - \tilde{C}\tilde{A}^{p-m}\tilde{B}_1 & \tilde{C}\tilde{A}^{p-m}\tilde{B}_1 \end{bmatrix} \tag{4.33}$$

$$\tilde{H}_i = \begin{bmatrix} \tilde{C}\tilde{B}_d & 0 & \cdots & 0 & 0 \\ \tilde{C}\tilde{A}\tilde{B}_d - \tilde{C}\tilde{B}_d & \tilde{C}\tilde{B}_d & \cdots & 0 & 0 \\ \tilde{C}\tilde{A}^2\tilde{B}_d - \tilde{C}\tilde{A}\tilde{B}_d & \tilde{C}\tilde{A}\tilde{B}_d - \tilde{C}\tilde{B}_d & \cdots & \vdots & \vdots \\ \vdots & \vdots & \ddots & \vdots & \vdots \\ \tilde{C}\tilde{A}^{p-1}\tilde{B}_d - \tilde{C}\tilde{A}^{p-2}\tilde{B}_d & \tilde{C}\tilde{A}^{p-2}\tilde{B}_d - \tilde{C}\tilde{A}^{p-3}\tilde{B}_d & \cdots & \tilde{C}\tilde{A}\tilde{B}_d - \tilde{C}\tilde{B}_d & \tilde{C}\tilde{B}_d \end{bmatrix} \quad i = 2,\ 3,\ d \tag{4.34}$$

$$\bar{E}_i = \text{diag}\{E_i, \cdots, E_i\},\ i = 2,\ 3,\ d \tag{4.35}$$

$$\bar{E}_4 = \text{diag}\{-E_4, \cdots, -E_4\} \tag{4.36}$$

$$\bar{E}_5 = [E_5 \quad E_5 \ \cdots \ E_5]^T \tag{4.37}$$

$$\bar{E}_1 = \begin{bmatrix} -E_1 & 0 & \cdot & 0 \\ 0 & \ddots & \cdot & \vdots \\ \vdots & \cdots & \cdot & -E_1 \\ \vdots & \vdots & \vdots & \vdots \\ 0 & \cdots & \cdot & -E_1 \end{bmatrix} \tag{4.38}$$

$$\tilde{E}_i = (\bar{E}_4 \bar{H}_i + \bar{E}_i),\ i = 1,\ 2,\ 3,\ d \tag{4.39}$$

$$\tilde{E}_4 = \bar{E}_4 \bar{\Phi} \tag{4.40}$$

$$\tilde{E}_{4i} = \bar{E}_4 \bar{H}_{i1},\ i = 1,\ 2,\ 3,\ d \tag{4.41}$$

$$\tilde{E}_5 = \bar{E}_5 \tag{4.42}$$

$$\bar{H}_j = \begin{bmatrix} [0]_{n_y} \\ H_j(1:(p-1)n_y, :) \end{bmatrix}, j = 1,\ 2,\ 3,\ d,\ 11,\ 21,\ 31,\ d1 \tag{4.43}$$

$$\bar{\Phi} = \begin{bmatrix} \tilde{C} \\ \Phi(1:(p-1)n_y, :) \end{bmatrix} \tag{4.44}$$

Here n_y is number of outputs, $[0]_{n_y}$ denotes matrix with n_y rows that have all the elements 0 and $*(1:(p-1)n_y, :)$ is read as row 1 to row $(p-1)n_y$ of the matrix $*$ with all the columns.

4.3 Hybrid Model Predictive Control (HMPC)

As is illustrated in Figure 4.2, MPC solves a finite horizon optimal control problem using the model prediction to obtain the control move over a finite horizon under given constraints. Hybrid model predictive control (HMPC) works the same way as MPC, except

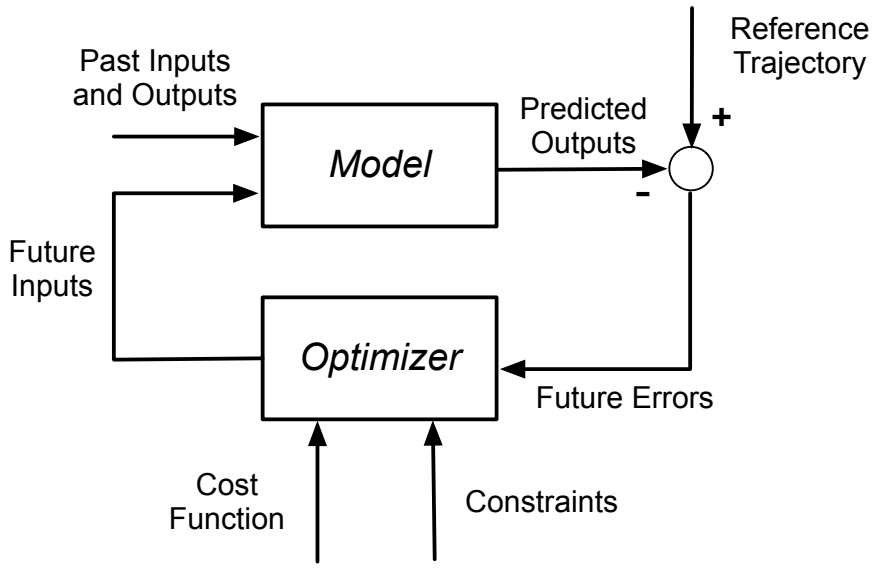

Figure 4.2: Basic Structure of MPC [13].

that the model used is the linear hybrid dynamical system. Here, we rely on the MLD model to generate the prediction equations of future outputs, which is shown in the previous section.

4.3.1 Objective Functions

In this work, we rely on a quadratic cost function of the form

$$\begin{aligned} J \stackrel{\triangle}{=} \quad & \sum_{i=1}^{p} \|(y(k+i)-y_r)\|_{Q_y}^2 + \sum_{i=0}^{m-1} \|(\Delta u(k+i))\|_{Q_{\Delta u}}^2 + \sum_{i=0}^{m-1} \|(u(k+i)-u_r)\|_{Q_u}^2 \\ & + \sum_{i=0}^{p-1} \|(\delta(k+i)-\delta_r)\|_{Q_d}^2 + \sum_{i=0}^{p-1} \|(z(k+i)-z_r)\|_{Q_z}^2 \end{aligned} \tag{4.45}$$

The optimization problem consists of finding the sequence of control actions $u(k), \cdots, u(k+m-1), \delta(k), \cdots, \delta(k+p-1)$ and $z(k), \cdots, z(k+p-1)$ that minimize J

$$\min_{\{[u(k+i)]_{i=0}^{m-1},\, [\delta(k+i)]_{i=0}^{p-1},\, [z(k+i)]_{i=0}^{p-1}\}} J \tag{4.46}$$

subject to mixed integer constraints according to (4.11) and various process constraints. In (4.45), Q_y, $Q_{\Delta u}$, Q_u, Q_d and Q_z are penalty weights on the control error, move size, control

signal, auxiliary binary variables and auxiliary continuous variables, respectively. Therefore, the first term is used to minimize the prediction error, the second term is the move suppression, the third to the fifth terms are to keep control signal, auxiliary binary variables and auxiliary continuous variables at their setpoint, respectively. In most practical problems, only the first three terms of the objective function (control error, move size, control signal) are considered. However, in order to maintain generality of the MPC formulation, we include the last two terms.

4.3.2 General Process Constraints

The general process constraints in HMPC include the manipulated variable constraints, manipulated variable rate constraints, and output variables constraints, which are listed below,

$$y_{\min} \leq \quad y(k+i) \quad \leq y_{\max},\ 1 \leq i \leq p \tag{4.47}$$

$$u_{\min} \leq \quad u(k+i) \quad \leq u_{\max},\ 0 \leq i \leq m-1 \tag{4.48}$$

$$\Delta u_{\min} \leq \quad \Delta u(k+i) \quad \leq \Delta u_{\max},\ 0 \leq i \leq m-1 \tag{4.49}$$

The objective function in (4.45) and the linear hybrid system described by the MLD model (4.9) - (4.11) are governed by both binary and continuous variables. Therefore, (4.45) along with the linear hybrid system dynamics (4.9) - (4.11) , and linear inequality constraints described in (4.47) - (4.49), the solution to this optimization problem forms a mixed integer quadratic program (MIQP).

4.3.3 Hybrid MPC Controller Move

By the use of vector and matrices form, the MPC problem in (4.45) - (4.49) can be rewritten as,

$$\begin{aligned}\min_{\{U(k),\bar{\delta}(k),Z(k)\}} J \;\triangleq\; & \|(Y(k+1)-Y_r)\|^2_{\widehat{Q}_y} + \|(R_u U(k) - R_{u0}u(k-1))\|^2_{\widehat{Q}_{\Delta u}} \\ + \; & \|(U(k)-U_r)\|^2_{\widehat{Q}_u} + \|(\bar{\delta}(k)-\bar{\delta}_r)\|^2_{\widehat{Q}_d} + \|(Z(k)-Z_r)\|^2_{\widehat{Q}_z}\end{aligned} \tag{4.50}$$

subject to mixed integer constraints according to (4.25) and various process constraints,

$$Y_{\min} \leq \quad Y(k+1) \quad \leq Y_{\max} \tag{4.51}$$

$$U_{\min} \leq \quad U(k) \quad \leq U_{\max} \tag{4.52}$$

$$\Delta U_{\min} \leq \quad \Delta U(k) \quad \leq \Delta U_{\max} \tag{4.53}$$

where,

$$\widehat{Q}_* = \begin{bmatrix} Q_* & 0 & \cdot & 0 \\ \vdots & \ddots & \cdot & \vdots \\ 0 & \cdots & \cdot & Q_* \end{bmatrix};\; R_u = \begin{bmatrix} I & 0 & \cdots & 0 & 0 \\ -I & I & \cdots & 0 & 0 \\ 0 & -I & \ddots & \vdots & \vdots \\ \vdots & \vdots & \ddots & \ddots & \vdots \\ 0 & 0 & \cdots & -I & I \end{bmatrix};\; R_{u0} = \begin{bmatrix} I \\ 0 \\ \vdots \\ 0 \end{bmatrix}$$

Y_r, U_r, $\bar{\delta}_r$ and Z_r are the reference vectors for the outputs, inputs, auxiliary binary variables and auxiliary continuous variables as given below,

$$Y_r = [y_r^T(k+1) \quad y_r^T(k+2) \cdots y_r^T(k+p)]^T \tag{4.54}$$

$$U_r = [u_r^T(k) \quad u_r^T(k+1) \cdots u_r^T(k+m-1)]^T \tag{4.55}$$

$$\bar{\delta}_r = [\delta_r^T(k) \quad \delta_r^T(k+1) \cdots \delta_r^T(k+p-1)]^T \tag{4.56}$$

$$Z_r = [z_r^T(k) \quad z_r^T(k+1) \cdots z_r^T(k+p-1)]^T \tag{4.57}$$

Substituting (4.23) for $Y(k+1)$ into (4.50), and rearranging the cost function in (4.55) so that one group having all the quadratic terms of the decision variables $U(k)$, $\bar{\delta}(k)$, $Z(k)$; while the other group consisting of the linear terms with constraints in (4.25), (4.51) - (4.53) resulting in the definition of MPC problem into a standard mixed integer quadratic program (MIQP) as follows:

$$\min_{\Xi(k)} J \stackrel{\triangle}{=} \frac{1}{2}\Xi(k)^T H \Xi(k) + G^T \Xi(k) \tag{4.58}$$

$$S\Xi(k) \leq b \tag{4.59}$$

where $\Xi(k) = [U(k)^T \quad \bar{\delta}(k)^T \quad Z(k)^T]^T$ is the vector of the decision variables, H and G are coefficient matrices for the quadratic and linear terms of the objective function, respectively, and S and b represent the coefficient matrices for the linear constraints. The coefficient matrices H, G, S and b are defined using Φ, H_*, H_{**}, $\tilde{E}_*$, and $\bar{E}_*$, and they can be obtained below.

Let all the other terms that are unrelated with $U(k)$, $\bar{\delta}(k)$ and $Z(k)$ as R_1 in (4.23), which gives,

$$Y(k+1) = H_1 U(k) + H_2 \bar{\delta}(k) + H_3 Z(k) + R_1 \tag{4.60}$$

where $R_1 = \Phi X(k) + H_d D(k) - H_{11} u(k-1) - H_{21}\delta(k-1) - H_{31} z(k-1) - H_{d1} d_{flt}(k-1)$. Substituting (4.60) into (4.50), we have,

$$\begin{aligned} \min_{\Xi(k)} J \stackrel{\triangle}{=} & \|(H_1 U(k) + H_2 \bar{\delta}(k) + H_3 Z(k) + R_1 - Y_r)\|^2_{\widehat{Q}_y} \\ + & \|(R_u U(k) - R_{u0} u(k-1))\|^2_{\widehat{Q}_{\Delta u}} + \|(U(k) - U_r)\|^2_{\widehat{Q}_u} + \|(\bar{\delta}(k) - \bar{\delta}_r)\|^2_{\widehat{Q}_d} \\ + & \|(Z(k) - Z_r)\|^2_{\widehat{Q}_z} \end{aligned} \tag{4.61}$$

Let $R = R_1 - Y_r$, (4.61) becomes,

$$
\begin{aligned}
\min_{\Xi(k)} J &\triangleq \|(H_1U(k)+H_2\bar{\delta}(k)+H_3Z(k)+R)\|^2_{\widehat{Q}_y}+\|(R_uU(k)-R_{u0}u(k-1))\|^2_{\widehat{Q}_{\Delta u}} \\
&+ \|(U(k)-U_r)\|^2_{\widehat{Q}_u}+\|(\bar{\delta}(k)-\bar{\delta}_r)\|^2_{\widehat{Q}_d}+\|(Z(k)-Z_r)\|^2_{\widehat{Q}_z} \qquad (4.62) \\
&= [U(k)^TH_1^T+\bar{\delta}(k)^TH_2^T+Z(k)^TH_3^T+R^T]\widehat{Q}_y^2[H_1U(k)+H_2\bar{\delta}(k) \\
&+ H_3Z(k)+R]+[U(k)^TR_u^T-u(k-1)^TR_{u0}^T]\widehat{Q}_{\Delta u}^2[R_uU(k)-R_{u0}u(k-1)] \\
&+ [U(k)^T-U_r^T]\widehat{Q}_u^2[U(k)-U_r]+[\bar{\delta}(k)^T-\bar{\delta}_r^T]\widehat{Q}_d^2[\bar{\delta}(k)-\bar{\delta}_r] \\
&+ [Z(k)^T-Z_r^T]\widehat{Q}_z^2[Z(k)-Z_r] \qquad (4.63) \\
&= R^T\widehat{Q}_yR+U(k)^TH_1^T\widehat{Q}_yR+\bar{\delta}(k)^TH_2^T\widehat{Q}_yR+Z(k)^TH_3^T\widehat{Q}_yR \\
&+ R^T\widehat{Q}_yH_1U(k)+U(k)^TH_1^T\widehat{Q}_yH_1U(k)+\bar{\delta}(k)^TH_2^T\widehat{Q}_yH_1U(k) \\
&+ Z(k)^TH_3^T\widehat{Q}_yH_1U(k)+R^T\widehat{Q}_yH_2\bar{\delta}(k)+U(k)^TH_1^T\widehat{Q}_yH_2\bar{\delta}(k) \\
&+ \bar{\delta}(k)^TH_2^T\widehat{Q}_yH_2\bar{\delta}(k)+Z(k)^TH_3^T\widehat{Q}_yH_2\bar{\delta}(k)+R^T\widehat{Q}_yH_3Z(k) \\
&+ U(k)^TH_1^T\widehat{Q}_yH_3Z(k)+\bar{\delta}(k)^TH_2^T\widehat{Q}_yH_3Z(k)+Z(k)^TH_3^T\widehat{Q}_yH_3Z(k) \\
&+ U(k)^TR_u^T\widehat{Q}_{\Delta u}R_uU(k)-u(k-1)^TR_{u0}^T\widehat{Q}_{\Delta u}R_uU(k) \\
&- U(k)^TR_u^T\widehat{Q}_{\Delta u}R_{u0}u(k-1)+u(k-1)^TR_{u0}^T\widehat{Q}_{\Delta u}R_{u0}u(k-1) \\
&+ U(k)^T\widehat{Q}_uU(k)-U_r^T\widehat{Q}_uU(k)-U(k)^T\widehat{Q}_uU_r \\
&+ U_r^T\widehat{Q}_uU_r+\bar{\delta}(k)^T\widehat{Q}_d\bar{\delta}(k)-\bar{\delta}_r^T\widehat{Q}_d\bar{\delta}(k)-\bar{\delta}(k)^T\widehat{Q}_d\bar{\delta}_r+\bar{\delta}_r^T\widehat{Q}_d\bar{\delta}_r \\
&+ Z(k)^T\widehat{Q}_zZ(k)-Z_r^T\widehat{Q}_zZ(k)-Z(k)^T\widehat{Q}_zZ_r+Z_r^T\widehat{Q}_dZ_r \qquad (4.64)
\end{aligned}
$$

In (4.64), all the terms that do not contain $U(k)$, $\bar{\delta}(k)$, or $Z(k)$ can be treated as constant, because they are not the decision variables $\Xi(k)$ in the optimization problem. Rearranging (4.64), we can have the following equation with quadratic terms in (4.66) as the first part, linear terms in (4.67) as the second part, constant terms as the third part, as expressed in (4.65).

$$
\min_{\Xi(k)} J \triangleq \text{Quadratic Terms} + \text{Linear Terms} + \text{Constant Terms} \qquad (4.65)
$$

where

$$\begin{aligned}
\text{Quadratic Terms} &= U(k)^T(H_1^T\widehat{Q}_yH_1 + R_u^T\widehat{Q}_{\Delta u}R_u + \widehat{Q}_u)U(k) \\
&+ \bar{\delta}(k)^T(H_2^T\widehat{Q}_yH_2 + \widehat{Q}_d)\bar{\delta}(k) + \bar{\delta}(k)^TH_2^T\widehat{Q}_yH_1U(k) \\
&+ Z(k)^T(H_3^T\widehat{Q}_yH_3 + \widehat{Q}_z)Z(k) + Z(k)^TH_3^T\widehat{Q}_yH_1U(k) \\
&+ U(k)^TH_1^T\widehat{Q}_yH_2\bar{\delta} + Z(k)^TH_3^T\widehat{Q}_yH_2\bar{\delta}(k) \\
&+ U(k)^TH_1^T\widehat{Q}_yH_3Z(k) + \bar{\delta}(k)^TH_2^T\widehat{Q}_yH_3Z(k) \qquad (4.66)
\end{aligned}$$

$$\begin{aligned}
\text{Linear Terms} &= 2[R^T\widehat{Q}_yH_1 - u(k-1)^TR_{u0}^T\widehat{Q}_{\Delta u}R_u - U_r^T\widehat{Q}_u]U(k) \\
&+ 2[R^T\widehat{Q}_yH_2 - \bar{\delta}_r^T\widehat{Q}_d]\bar{\delta}(k) + 2[R^T\widehat{Q}_yH_3 - Z_r^T\widehat{Q}_z]Z(k) \qquad (4.67)
\end{aligned}$$

Now the expression for the coefficient matrix H are obtained based on (4.66),

$$H = 2\begin{bmatrix}
H_1{}^T\widehat{Q}_yH_1 + \widehat{R}_u\widehat{Q}_{\Delta u}\widehat{R}_u + \widehat{Q}_u & H_1{}^T\widehat{Q}_yH_2 & H_1{}^T\widehat{Q}_yH_3 \\
H_2{}^T\widehat{Q}_yH_1 & H_2{}^T\widehat{Q}_yH_2 + \widehat{Q}_d & H_2{}^T\widehat{Q}_yH_3 \\
H_3{}^T\widehat{Q}_yH_1 & H_3{}^T\widehat{Q}_yH_2 & H_3{}^T\widehat{Q}_yH_3 + \widehat{Q}_z
\end{bmatrix} \qquad (4.68)$$

The linear terms in (4.67) has constant R,

$$R = \Phi X(k) + H_dD(k) - H_{11}u(k-1) - H_{21}\delta(k-1) - H_{31}z(k-1) - H_{d1}d_{flt}(k-1) - Y_r \qquad (4.69)$$

Substituting the expression of R into (4.67), the expressions for the coefficient matrices of G are,

$$G = 2[g_1 \;\; g_2 \;\; g_3]^T \qquad (4.70)$$

where,

$$
\begin{aligned}
g_1 &= X(k)^T \Phi^T \widehat{Q}_y H_1 - Y_r{}^T \widehat{Q}_y H_1 - U_r{}^T \widehat{Q}_u + D(k)^T H_d{}^T \widehat{Q}_y H_1 - \\
&\quad u(k-1)^T (R_{u0}{}^T \widehat{Q_{\Delta u}} R_u + H_{11}{}^T \widehat{Q}_y H_1) - \delta(k-1)^T H_{21}{}^T \widehat{Q}_y H_1 - \\
&\quad z(k-1)^T H_{31}{}^T \widehat{Q}_y H_1 - d_{flt}(k-1)^T H_{d1}{}^T \widehat{Q}_y H_1 \qquad (4.71) \\
g_2 &= X(k)^T \Phi^T \widehat{Q}_y H_2 - Y_r{}^T \widehat{Q}_y H_2 - \bar{\delta}_r^T \widehat{Q}_d + D(k)^T H_d{}^T \widehat{Q}_y H_2 - \\
&\quad u(k-1)^T H_{11}{}^T \widehat{Q}_y H_2 - \delta(k-1)^T H_{21}{}^T \widehat{Q}_y H_2 - z(k-1)^T H_{31}{}^T \widehat{Q}_y H_2 - \\
&\quad d_{flt}(k-1)^T H_{d1}{}^T \widehat{Q}_y H_2 \qquad (4.72) \\
g_3 &= X(k)^T \Phi^T \widehat{Q}_y H_3 - Y_r{}^T \widehat{Q}_y H_3 - Z_r{}^T \widehat{Q}_z + D(k)^T H_d{}^T \widehat{Q}_y H_3 - \\
&\quad u(k-1)^T H_{11}{}^T \widehat{Q}_y H_3 - \delta(k-1)^T H_{21}{}^T \widehat{Q}_y H_3 - z(k-1)^T H_{31}{}^T \widehat{Q}_y H_3 \\
&\quad - d_{flt}(k-1)^T H_{d1}{}^T \widehat{Q}_y H_3 \qquad (4.73)
\end{aligned}
$$

Similarly, substituting equation (4.23) into (4.51), $\Delta U(k) = R_u U(k) - R_{u0} u(k-1)$ into (4.53) give,

$$
\begin{aligned}
Y_{\min} &\leq \Phi X(k) + H_1 U(k) + H_2 \bar{\delta}(k) + H_3 Z(k) + H_d D(k) - H_{11} u(k-1) \\
&\quad - H_{21} \delta(k-1) - H_{31} z(k-1) - H_{d1} d_{flt}(k-1) \leq Y_{\max} \qquad (4.74)
\end{aligned}
$$

$$
\Delta U_{\min} \leq R_u U(k) - R_{u0} u(k-1) \leq \Delta U_{\max} \qquad (4.75)
$$

Rearranging the linear inequality in MLD framework (4.24), the process constraints in (4.74), (4.52), and (4.75), the expression for S and b can be obtained,

$$S = \begin{bmatrix} s_1 \\ s_2 \\ -s_2 \end{bmatrix} \tag{4.76}$$

where,

$$s_1 = [\tilde{E}_1 \;\; \tilde{E}_2 \;\; \tilde{E}_3] \tag{4.77}$$

$$s_2 = \begin{bmatrix} H_1 & H_2 & H_3 \\ I_{m(nu)} & [0]_{m(nu)\times p(nd)} & [0]_{m(nu)\times p(nz)} \\ R_u & [0]_{m(nu)\times p(nd)} & [0]_{m(nu)\times p(nz)} \end{bmatrix} \tag{4.78}$$

4.3.4 MPC with Three-Degree-of-Freedom (3 DoF)

The conventional MPC tuning rules rely on changing p (the prediction horizon), m (the control horizon) and penalty weights (such as $Q_{\Delta u}$, (move suppression)) which may not be very intuitive. The MPC formulation in this chapter features three-degree-of-freedom (3 DoF) tuning in which it allows the user to meet the performance requirements such as adjusting the speed of setpoint tracking, anticipated measured disturbance rejection and unmeasured disturbance rejection independently [23] in the closed-loop system by varying parameters α_r, α_d and f_a, respectively. These parameters can be adjusted between values 0 and 1, which in turn alter the response of Type I or Type II filters which supply filtered signal to the controller (for setpoint tracking and measured disturbance rejection) or adjust the observer gain (for unmeasured disturbance rejection). Therefore, the controller can be detuned relative to optimal but is more robust. Figure 4.3 shows a 3 DoF controller block diagram of MPC where P, P_d are the system plant and measured disturbance plant, the observer block has tuning parameter f_a for tuning unmeasured disturbance rejection, model block is used to predict the future values of controlled variables, $f(q,\alpha_r)$, $f(q,\alpha_r)$ are the filters for reference and measured disturbance signals, and optimizer block is to

$$b = \begin{bmatrix} \tilde{E}_5 - \tilde{E}_4 X(k) - \tilde{E}_d D(k) + \tilde{E}_{41} u(k-1) + \tilde{E}_{42} \delta(k-1) + \tilde{E}_{43} z(k-1) + \tilde{E}_{4d} d_{flt}(k-1) \\ Y_{\max} - \Phi X(k) - H_d D(k) + H_{11} u(k-1) + H_{21} \delta(k-1) + H_{31} z(k-1) + H_{d1} d_{flt}(k-1) \\ U_{\max} \\ \Delta U_{\max} + R_{u0} u(k-1) \\ -Y_{\min} + \Phi X(k) + H_d D(k) - H_{11} u(k-1) - H_{21} \delta(k-1) - H_{31} z(k-1) - H_{d1} d_{flt}(k-1) \\ -U_{\min} \\ -\Delta U_{\min} - R_{u0} u(k-1) \end{bmatrix} \tag{4.79}$$

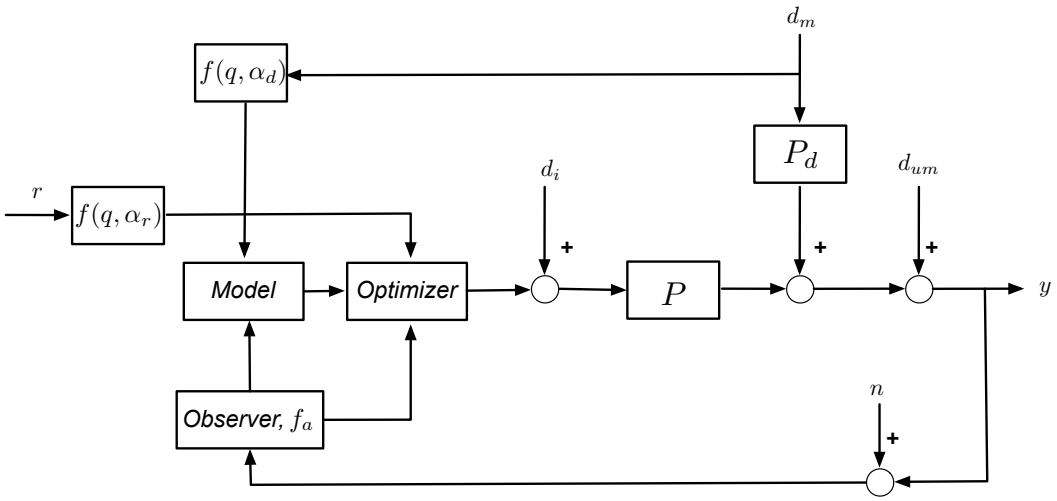

Figure 4.3: Three-Degree-of-Freedom (3 DoF) Controller Block Diagram of MPC.

generate the control signal based on future predicted errors, and constraints.

4.3.4.1 Reference Trajectory and Setpoint Tracking

The output reference trajectory Y_r is generated using the filter $f(q,\alpha_r^j)$, with which one can detune a controller to vary the speed and the shape of the closed-loop response. Based on the system in this work, we can use a Type I filter as shown below,

$$f(q,\alpha_r^j) \quad = \quad \frac{(1-\alpha_r^j)q}{q-\alpha_r^j},\ 1 \leq j \leq n_y \tag{4.80}$$

where q is the forward shift operator. The speed of setpoint tracking can be adjusted by choosing α_r^j between [0, 1) for each individual output j. The smaller the value for α_r^j, the faster the output response for setpoint tracking. This adjustment is more intuitive and convenient than adjusting move suppression weights ($Q_{\Delta u}$) that directly affect the manipulated variables and consequently, the effect on a specific controlled variable response is more difficult to predict.

4.3.4.2 Measured Disturbance Rejection

The proposed formulation relies on an externally generated forecast of the measured disturbance as in (4.30); this forecast is filtered and provided as an anticipated signal to the control algorithm. The speed desired to reject measured disturbances can be adjusted independently by using a filter $f(q,\alpha_d^j),\ 1 \leq j \leq n_{dist}$ for each measured disturbance signal, where n_{dist} is the number of measured disturbances and α_d^j is a tuning parameter between [0, 1) for each j-th measured disturbance. The lower the value for α_d^j, the faster the speed of measured disturbance rejection. The type of measured disturbance will determine the form of the transfer function $f(q,\alpha_d^j)$. Type I filter in the form of equation (4.80) is used to decline step disturbance signal, while Type II filter is used to reject ramp disturbance signal [82], which is defined in (4.81) - (4.83) below. Type II filter structure should also be used when integrating system dynamics are present [22].

$$f(q,\alpha_d^j) = (\beta_0 + \beta_1 q^{-1} + \cdots + \beta_\omega q^{-\omega}) \times \frac{(1-\alpha_d^j)q}{q-\alpha_d^j} \tag{4.81}$$

$$\beta_k = \frac{-6k\alpha_d^j}{(1-\alpha_d^j)\omega(\omega+1)(2\omega+1)},\ 1 \leq k \leq \omega \tag{4.82}$$

$$\beta_0 = 1 - (\beta_1 + \cdots + \beta_\omega) \tag{4.83}$$

4.3.4.3 Unmeasured Disturbance Rejection

It is necessary to calculate the coefficient matrix G for the linear term of the objective function (4.58) and b at the right-hand side of constraint equation (4.59) at each time step in the proposed MPC problem described in (4.58) - (4.59). This requires initial states $X(k)$ of the augmented system at each time instance. The augmented states $X(k)$ can be estimated from the current measurements $y(k)$ with unmeasured disturbance rejection achieved by a suitably designed state observer / filter. The unmeasured disturbances can be applied externally and can also come from the model-plant mismatch. In this formulation, the separation of the effect of measured and unmeasured disturbance of the state estimation

is required in order to have true multiple-degree-of-freedom tuning for these controller modes. Reference tracking is not a part of the prediction equation and hence, by definition, is independent of both α_d and f_a. To decouple the effects of measured and unmeasured disturbance rejection, we track the measured disturbance and filtered measured disturbance separately, and propose a two-step procedure for estimating the augmented states $X(k)$. In the first step, state estimation is accomplished utilizing the model, the actual (unfiltered) measured disturbance signal d, and a filter K_f as follows,

$$X(k|k-1) = \tilde{A}X(k-1|k-1) + \tilde{B}_1\Delta u(k-1) + \tilde{B}_d\Delta d(k-1) \quad (4.84)$$

$$X(k|k) = X(k|k-1) + K_f(y(k) - \tilde{C}X(k|k-1)) \quad (4.85)$$

Since we rely on the unfiltered measured disturbance d in (4.84), the second term in (4.85) represents the effect of unmeasured disturbances only; the choice for K_f will define the speed and character of unmeasured disturbance rejection. In the second step, we estimate an augmented state of the system by considering the filtered measured disturbance signal d_{flt} and the contribution of the unmeasured disturbance (i.e., the prediction error) from (4.85) as follows,

$$X_{flt}(k|k-1) = \tilde{A}X_{flt}(k-1|k-1) + \tilde{B}_1\Delta u(k-1) + \tilde{B}_d\Delta d_{flt}(k-1) \quad (4.86)$$

$$X_{flt}(k|k) = X_{flt}(k|k-1) + K_f(y(k) - \tilde{C}X(k|k-1)) \quad (4.87)$$

where $X_{flt}(k|k)$ in (4.87) is the estimate corresponding to both filtered measured disturbance and unmeasured disturbance, with its first term capturing the effect of the filtered measured disturbances and its second term capturing the effect of the unmeasured disturbances. This approach allows the tuning for measured disturbances specified through α_d^j does not influence unmeasured disturbance rejection, while the unmeasured disturbance filter matrix K_f does not affect measured disturbance rejection. $X_{flt}(k|k)$ is used in (4.70)

and (4.79) to calculate the coefficient matrices G and b that appear in the MPC problem (4.58) - (4.59).

The optimal value of the filter gain K_f could be found by solving an algebraic Riccati equation which requires the estimation of covariance matrices for the unmeasured disturbance. However, such information is not available and known accurately. Therefore, we apply the parametrization of the filter gain in [87], which enables specifying the speed of unmeasured disturbance rejection for each output channel independently by the user while keeping with the setpoint tracking and measured disturbance modes. For the case of $A_w = diag\{\alpha_1,\ \alpha_2,\ \cdots,\ \alpha_{n_y}\}$, we rely on the following parametrization of the filter gain,

$$K_f = \begin{bmatrix} 0 \\ F_b \\ F_a \end{bmatrix} \tag{4.88}$$

where

$$F_a = \text{diag}\{(f_a)_1, \cdots, (f_a)_{n_y}\} \tag{4.89}$$

$$F_b = \text{diag}\{(f_b)_1, \cdots, (f_b)_{n_y}\} \tag{4.90}$$

$$(f_b)_j = \frac{{(f_a)_j}^2}{1+\alpha_j-\alpha_j(f_a)_j},\ 1 \le j \le n_y \tag{4.91}$$

$(f_a)_j$ is a tuning parameter that lies between 0 and 1; the speed of unmeasured disturbance rejection is proportional to the tuning parameter $(f_a)_j$. As $(f_a)_j$ approaches zero, the state estimator increasingly ignores the prediction error correction, and the control solution is mainly determined by the deterministic model (4.84) and the the feedforward anticipation signal. On the other hand, the state estimator tries to compensate for all prediction error as $(f_a)_j$ approaches 1, and hence the controller becomes extremely aggressive. Thus, the adjustment of $(f_a)_j$ allows the user to directly influence unmeasured disturbance rejection for each output response individually, which is more intuitive and convenient than tuning with move suppression in the traditional MPC formulation.

4.4 HMPC Algorithm for Sequential Decision Policies

This section presents the design procedure for an HMPC-based intervention which have multiple intervention components featuring sequential decision policies. We will use GWG interventions to illustrate how to design the logical specification associated with proposed dosage sequence. Meanwhile, other clinical considerations and constraints which are common in adaptive interventions will also be examined and addressed, so that this HMPC algorithm for sequential decision policies can work for any other adaptive sequential interventions. This problem relies on the use of Mixed Logical Dynamical (MLD) for the control of hybrid systems that we introduced earlier in this chapter, and the improved three-degree-of-freedom (3 DoF) tuning formulation of Nandola and Rivera [23] is implemented.

4.4.1 Clinical Considerations and Constraints

As we discussed in Chapter 2, the adaptive intervention for GWG features multiple intervention components, emphasizing health eating (HE) habits and physical activity (PA). The control design problem presented in this chapter is based on the practical operational constraints and clinical considerations. In order to illustrate how to analyze these constraints and requirements, GWG adaptive intervention using "IF-THEN" decision rules is illustrated in Figure 4.4, with its postulated sequenced rules depicted in Table 4.1, which will act on the values of tailoring variables (in this case, GWG) measured through self-monitoring by the participant. The decision rules are used to evaluate GWG every two weeks from week 14 through week 36 during pregnancy. If a participant is achieving her GWG goal, the intervention dosage will be sustained or reduced. However if her GWG exceeds the IOM guidelines, a more intensive intervention is necessary for her to increase potency, and therefore, her intervention gets augmented.

The adaptation rules in Table 4.1 play an important role in deriving the following clinical constraints and considerations when we design the HMPC-based GWG intervention

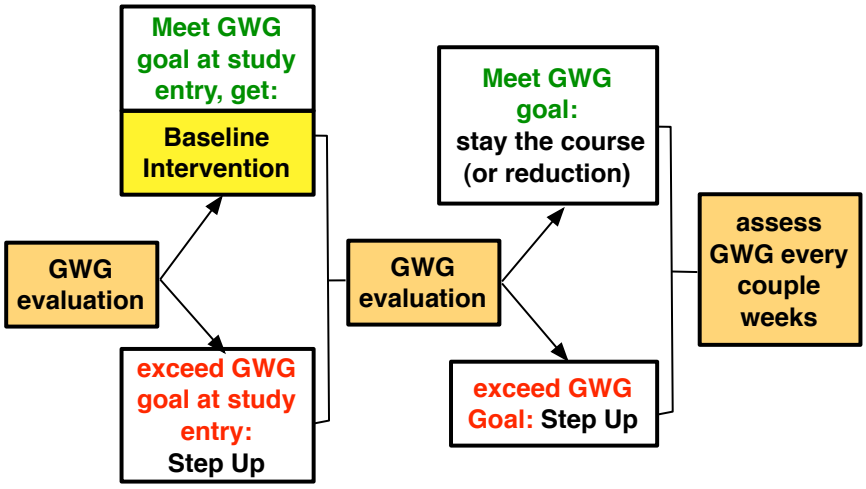

Figure 4.4: IF-THEN Decision Rules for Time-varying GWG Intervention Evaluation for Adapting Intervention.

strategy:

1. This adaptive intervention aims to personalizing the intervention in order to prevent excessive GWG. Therefore, GWG is controlled variable in this design problem where the overall goal is to support the participant to meet the GWG IOM guidelines (setpoint).

2. Intervention adjustment based on the participant's changing needs is facilitated by feedback of the measured GWG daily in the self-monitoring process.

3. The intervention components are delivered in pre-determined discrete doses, with HE active learning in $\{0, 1, 2, 3\}$, PA active learning in $\{0, 1, 2, 3, 4\}$, and other components in $\{0, 1\}$.

4. The intervention should be patient-friendly, and therefore, its change or adaptation cannot be too aggressive. This can be readily enforced by the use of move size constraints, and the high and low limits on manipulated variables.

Table 4.1: Summary of Dosage Augmentations and Reductions per the IF-THEN Decision Rules for GWG Adaptive Intervention [1] for the Simulations in Section 4.5.1 and Section 4.5.2.

Options	**Adaptation**
Step down 3	reduction of other components
Step down 2	reduction of healthy eating active learning
Step down 1	reduction of physical activity active learning
Baseline	base dose for all components
Step up 1	first augmentation of healthy eating active learning
Step up 2	second augmentation of healthy eating active learning
Step up 3	first augmentation of physical activity active learning
Step up 4	second augmentation of physical activity active learning
Step up 5	third augmentation of physical activity active learning

5. The intervention starts at week 14, and is adapted every two weeks, which means that the intervention decisions ($T_{\text{sw}} = 14$) are made at frequencies other than the regular sampling intervals (e.g., daily weight scale, $T_{\text{s}} = 1$).

6. Only one component can have dosage change at each decision point.

7. The augmentation and/or reduction of the intervention is specified in a certain predefined dosage sequence, rather than the arbitrary change of the dosages within the limits.

The ensuing subsections will develop a procedure to formulate HMPC for this optimized GWG intervention and illustrate how to address these requirements and rules above.

4.4.2 Discrete Magnitude of Dosages

The discrete values of the intervention components in the system for this GWG intervention can be represented logically through binary $\delta(k)$ and continuous $z(k)$ auxiliary variables:

$$\delta_i(k) = 1 \Leftrightarrow z_i(k) = i-1;\ \ i \in \{1,2,3,4\} \tag{4.92}$$

$$u_1(k) = \sum_{i=1}^{4} z_i(k) \quad \sum_{i=1}^{4} \delta_i(k) = 1 \tag{4.93}$$

$$\delta_j(k) = 1 \Leftrightarrow z_j(k) = j-5;\ \ j \in \{5,6,7,8,9\} \tag{4.94}$$

$$u_2(k) = \sum_{j=5}^{9} z_j(k) \quad \sum_{j=5}^{9} \delta_j(k) = 1 \tag{4.95}$$

$$\delta_\ell(k) = 1 \Leftrightarrow z_\ell(k) = \ell-10;\ \ \ell \in \{10,11\} \tag{4.96}$$

$$u_n(k) = \sum_{\ell=10}^{11} z_\ell(k) \quad \sum_{\ell=10}^{11} \delta_\ell(k) = 1;\ \ n \in \{3,4,5,6,7\} \tag{4.97}$$

where (4.92) and (4.93) describe that one of four possible levels (0, 1, 2, 3) of HE active learning component ($u_1(k)$) must be assigned for each participant; (4.94) and (4.95) state that one of five levels (0, 1, 2, 3, 4) of PA active learning component ($u_2(k)$) are available to be assigned to the participants; and (4.96) and (4.97) represents two discrete doses (0, 1) of all the other five components (i.e., goal setting $u_3(k)$, HE education $u_4(k)$, PA education $u_5(k)$, HE weekly plan $u_6(k)$, PA weekly plan $u_7(k)$). (4.92) - (4.97) can be converted into linear inequalities as E_i matrices ($i \in \{1,2,3,4,5,d\}$) in (4.11).

4.4.3 Switching Time Strategy

As a result of clinical and resource considerations, it is often desirable to make decisions at frequencies other than the regular sampling interval. For example, in Figure 4.5, the participant visits the clinic only on the days which are marked in red, and however the measurements are still taken on a daily basis. Therefore, it is necessary for the controller to recognize at which time points the intervention can be adapted, and during which time frames the intervention has to stay the course. In other words, the control decisions are required to be made at an *a priori* known integer multiple T_{sw} of the system sample time T_{s}, in addition to the previously discussed constraints. This requirement is different from specifications of multirate control as all variables in this work are sampled at the same

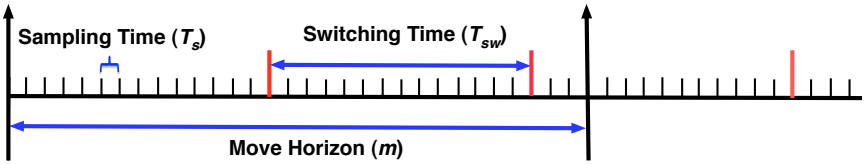

Figure 4.5: Diagrammatic Illustration of the Switching Time Strategy in Section 4.4.3.

rate. It is also distinct from move blocking strategies [88] used for computational burden reduction. This algorithm is referred to in this work as a switching time strategy [29]. It is achieved by enforcing control move size constraints $\Delta u(k)$ to be zero over the control horizon except when decisions have to be made, as indicated in Figure 4.5. By taking the receding horizon nature of HMPC into account, this can be written as time-dependent linear equality constraint: $A_{T_{\text{sw}}}(k)u(k) = 0, i \in \{0,\ 1,\ \ldots\ ,\ m-1\}$. The matrix $A_{T_{\text{sw}}}(k)$ has a block-diagonal structure, for example,

$$\begin{bmatrix} \star & & & & & & & & & \\ \star & \star & & & & & & & & \\ \star & & \star & & & & & & & \\ & & \mathbf{0} & & & & & & & \\ & & & \star & \star & & & & & \\ & & & \star & & \star & & & & \\ & & & \star & & & \star & & & \\ & & & & & & \ddots & & & \\ & & & & & & & \mathbf{0} & & \\ & & & & & & & & \star & \star \\ & & & & & & & & \star & \star \end{bmatrix} \begin{bmatrix} u(k) \\ u(k+1) \\ \vdots \\ u(k+m-1) \end{bmatrix} = \begin{bmatrix} \star \\ 0 \\ \vdots \\ 0 \end{bmatrix} \tag{4.98}$$

where rows with $\star$ entries and $\mathbf{0}$ are assigned by the algorithm. The rest of the entries in the matrix are zero. This matrix is generated dynamically at each sampling instant k using the following steps:

1. Given the control horizon m and switching time $T_{\text{sw}}(\leq m)$, calculate the number of blocks $\texttt{numblocks} = \lfloor \frac{m-1}{T_{\text{sw}}} \rfloor + 1$. If the $\texttt{numblocks} \geq 3$, define number of block excluding the first and last block: $\texttt{midblocks} = \texttt{numblocks} - 2$. The term 'switching sample' will be used to denote sample when the control is allowed to change its value i.e. $\texttt{iff}\ \texttt{rem}(\frac{k}{T_{\text{sw}}}) = 0$, where $\texttt{rem}$ is the remainder.

2. The matrix $A_{T_{\text{sw}}}(k)$ is populated by $0, 1$ or -1 to implement the move size restriction, and its size is determined by length of control horizon and size of $\texttt{numblocks}$: $A_{T_{\text{sw}}}(k) \in \mathbb{R}^{(T_{\text{sw}}+\texttt{midblocks}\times(T_{\text{sw}}-1)+\texttt{rem}(\frac{m-1}{T_{\text{sw}}})+1)\times m}$.

3. The rows in $A_{T_{\text{sw}}}(k)$ corresponding to switching samples will be set to zero; otherwise the rows will be populated to implement $\Delta u(k+i) = 0$.

4. Finally, the first sample $u(k)$ is assigned the previously calculated optimal value i.e. $u(k) = u^*$ when k does not corresponds to the switching sample (as per the receding horizon framework).

While mathematically the switching time strategy described in this section is similar to move blocking strategies used in MPC [88], the difference, besides the process of generating the matrix $A_{T_{\text{sw}}}(k)$, lies in the fact that in move blocking, the goal is to reduce the computational burden by decreasing the dimensions of the decision variable, whereas here the requirement is to apply controls only at specified samples, while the dimension of the decision variable remains the same. This is enforced as a constraint in the optimization problem shown in (4.45).

4.4.4 Sequential Decision Policies

Adaptive behavioral interventions are usually made up of many intervention components $(u_1, ..., u_n)$, the dosages of which are treated as manipulated variables. As an illustration, we assume there are seven $(n = 7)$ components $(u_1,\ u_2,\ \cdots\ u_7)$ which are aug-

mented or reduced during the GWG intervention, as described in Table 4.1. They are Healthy Eating (HE) active learning (as $u_1(k) \in \{0,1,2,3\}$), Physical Activity (PA) active learning (as $u_2(k) \in \{0,1,2,3,4\}$), and all the other five components (goal setting $u_3(k)$, HE/PA eduction $u_4(k), u_5(k)$, and HE/PA weekly plan $u_6(k), u_7(k)$) which serve as part of baseline program, are augmented and reduced at the same time, and are only available in two doses ($u_3(k) = u_4(k) = \cdots = u_7(k) \in \{0,1\}$). Therefore, we can simply use the dosage of goal setting $u_3(k)$ to represent these five components. Meanwhile, in the baseline program, all these seven components enter at the same time with a base dosage as $u_j(k) = 1, j \in \{1,2,\cdots,7\}$.

The multiple intervention components in this problem require the need to address the decision regarding which component should be first augmented or reduced at each decision point (considered in this illustration as on a bi-weekly basis) when the dosage can be updated per the individual's measured outcomes and performance. There can be many predefined dosage sequences available according to the requirements of different intervention programs. In this dissertation, we assume that the augmentation and/or reduction of the GWG intervention follows the dosage sequences specified in Table 4.1. Therefore, u_2 will be augmented from its base dose only after u_1 reaches its maximum dose, while u_1 will not be reduced from full dosage until u_2 returns back to its base dose (augmentation and reduction sequence above baseline). When the participant's response and performance is very optimistic during the intervention, the intervention can also be reduced from the baseline program, with u_2 eliminated first, followed by u_1 and u_3; the augmentation sequence for the components to be added from zero dose to base dose will be in the opposite order, with u_3 added first, followed by u_1 and u_2 (augmentation and reduction sequence below baseline). Meanwhile, the patient-friendly requirement that only one component can be altered at each intervention decision indicates the necessity to involve the functionality of allowing the selection of one input change (if $\Delta u_i(k) \neq 0$, then $\Delta u_j(k) = 0$ for $j \neq i$;

$i, j \in \{1, 2, ..., n\}$, where n is the number of intervention components, k is the sampling time). In this GWG problem as an example, because dosages of $u_3(k), u_4(k), \cdots, u_7(k)$ remain the same throughout the intervention, we can assume $n = 3$. The logic in the sequential decision policies restricts how the future dosage can be specified over time based on the current dosage the participants receive, and their performance during the intervention. The decision on how to properly assign the dosages will be dictated by the HMPC controller with user-specified objective function, and the clinical considerations and constraints associated with these logical conditions embedded into the dynamical model. The underlying logical specification can be converted into linear inequalities relying on the generation of a sequence table and the selection of a single input in multi-input scenario [29]. This section mainly focuses on the design procedure for how to handle the logical specifications associated with sequential decision policies relying on MLD structure with constraints as HMPC formulation, and the design of such an HMPC controller is illustrated on a GWG intervention involving several components with a clinically proposed dosage sequence illustrated earlier in Table 4.1.

4.4.4.1 Generation of a Sequence Table

Table 4.2 is the sequence table derived from augmentation/reduction rule table (Table 4.1). It summarizes the proposed dosage sequence according to the description mentioned previously, which elucidates how the dosages will change during the intervention. For instance, if the participant is currently receiving the intervention with dosage sequence 2, then in the next decision point (two weeks later), her intervention can have three options: (1) it can be augmented to sequence 3, 4, or 5 based on the move size $\Delta u_2(k)$; (2) it can get reduced to sequence 1 or 0 according to the move size $\Delta u_1(k)$; or (3) it can remain unchanged. The HMPC controller should be able to determine the optimized discrete dosages according to the participant's response and the user-specified objective function,

Table 4.2: Dosage Sequence Table for the GWG Behavioral Intervention Example in Section 4.5.1 and Section 4.5.2.

Dosage Sequence	**Healthy Eating Active Learning u_1**	**Physical Activity Active Learning u_2**	**Other Components $u_3 \cdots u_7$**	**Description**	**Propositional Logic**
-3	0	0	0	Reduction of $u_3 \cdots u_7$	$\delta_1 \wedge \delta_5 \wedge \delta_{10}$
-2	0	0	1	Reduction of u_1	$\delta_1 \wedge \delta_5 \wedge \delta_{11}$
-1	1	0	1	Reduction of u_2	$\delta_2 \wedge \delta_5 \wedge \delta_{11}$
0	1	1	1	Baseline	$\delta_2 \wedge \delta_6 \wedge \delta_{11}$
1	2	1	1	First augmentation of u_1	$\delta_3 \wedge \delta_6 \wedge \delta_{11}$
2	3	1	1	Second augmentation of u_1	$\delta_4 \wedge \delta_6 \wedge \delta_{11}$
3	3	2	1	First augmentation of u_2	$\delta_4 \wedge \delta_7 \wedge \delta_{11}$
4	3	3	1	Second augmentation of u_2	$\delta_4 \wedge \delta_8 \wedge \delta_{11}$
5	3	4	1	Third augmentation of u_2	$\delta_4 \wedge \delta_9 \wedge \delta_{11}$

and subject to the general process constraints in (4.51) - (4.53) and the clinical constraints associated with the dosage sequence.

With the help of information in Table 4.2, the following logical conditions are generated and embedded into the dynamical model using binary variables ($\delta(k)$) in MLD model, so that only the dosage combinations in Table 4.2 are selected,

$$\begin{aligned}\Omega = \quad & (\delta_1 \wedge \delta_5 \wedge \delta_{10}) \oplus (\delta_1 \wedge \delta_5 \wedge \delta_{11}) \oplus (\delta_2 \wedge \delta_5 \wedge \delta_{11}) \oplus \\ & (\delta_2 \wedge \delta_6 \wedge \delta_{11}) \oplus (\delta_3 \wedge \delta_6 \wedge \delta_{11}) \oplus (\delta_4 \wedge \delta_6 \wedge \delta_{11}) \oplus \\ & (\delta_4 \wedge \delta_7 \wedge \delta_{11}) \oplus (\delta_4 \wedge \delta_8 \wedge \delta_{11}) \oplus (\delta_4 \wedge \delta_9 \wedge \delta_{11}) \end{aligned} \tag{4.99}$$

where $(\delta_1 \wedge \delta_5 \wedge \delta_{10})$ stands for dosage sequence -3 in Table 4.2 ($u_1 = u_2 = \cdots = u_7 = 0$), in which $\delta_1 = 1$ means $u_1 = 0$ is selected, $\delta_5 = 1$ means $u_2 = 0$, and $\delta_{10} = 1$ means $u_n = 0$ (n $\in \{3,4,5,6,7\}$); $(\delta_1 \wedge \delta_5 \wedge \delta_{11})$ represents dosage sequence -2 in Table 4.2; $(\delta_2 \wedge \delta_5 \wedge \delta_{11})$ represents dosage sequence -1 in Table 4.2; and the like. The nine combinations in (4.99) above are the nine dosage sequences in Table 4.2. Ω in (4.99) can be expressed in the linear inequalities in (4.11). This limits the possibilities of the dosage combinations to nine instead of a possible $\binom{4}{1} \times \binom{5}{1} \times \binom{2}{1} = 40$ combinations. For problems with larger dimensions than those shown in this example, the generation of Table 4.2 and its corresponding logical conditions in (4.99) can be efficiently automated.

4.4.4.2 Manipulating One Input at a Time when Move Size $\mid \Delta u \mid \leq 1$

The GWG adaptive interventions require that at each intervention decision, there is only one component being altered. This is necessary, because it can prevent the participant from being uncomfortable due to any dramatic intervention adaptation and hence unable to follow up with the pace of the intervention. For example, when the participant is having intervention with dosage "step up 1", in the next assessment cycle, her intervention can only be augmented to "step up 2" instead of "step up 3", even though the adaptation

from"step up 1" to "step up 3" meet combination constraint in (4.99), the manipulated variable bounds and move size constraint that we specified so far. This basically implies that the controller can only choose one component to be altered at each intervention decision.

Therefore, with the logical specification for Ω in (4.99), we can rely on the mathematical explanation in either (4.100) or (4.101) to achieve "one input change at a time" logical condition when the move size constraints are ± 1 ($\mid \Delta u(k) \mid \leq 1$),

$$\mid u_1(k) \mid + \mid u_2(k) + \mid u_3(k) \mid \quad \leq \quad 1 \tag{4.100}$$

$$\Delta u_1(k)^2 + \Delta u_2(k)^2 + \Delta u_3(k)^2 \quad \leq \quad 1 \tag{4.101}$$

Because the change in u_3 is same as the change in $u_4, \cdots, u_7$, one only needs to put this constraint on three inputs, although we have seven manipulated variables. Equation (4.100), or the quadratic inequality (4.101) can both be expressed as linear inequalities which shall have the same constraint effect on the MLD model as (4.100) and (4.101) do. Hence, the following linear inequalities are considered,

$$\Delta u_1(k) + \Delta u_2(k) \quad \leq \quad 1 \tag{4.102}$$

$$\Delta u_1(k) + \Delta u_2(k) \quad \geq \quad -1 \tag{4.103}$$

$$\Delta u_2(k) + \Delta u_3(k) \quad \leq \quad 1 \tag{4.104}$$

$$\Delta u_2(k) + \Delta u_3(k) \quad \geq \quad -1 \tag{4.105}$$

$$\Delta u_3(k) + \Delta u_1(k) \quad \leq \quad 1 \tag{4.106}$$

$$\Delta u_3(k) + \Delta u_1(k) \quad \geq \quad -1 \tag{4.107}$$

Linear inequalities (4.102) - (4.107) are not mathematically equivalent to (4.100) or (4.101). However, because the possibilities of dosage combinations for intervention components in (4.99) are already limited, there is no chance for one component to be augmented while the other to be reduced, which is exactly the exception that meets (4.102)

- (4.107) but does not satisfy either (4.100) or (4.101). Therefore, the linear inequalities above are equivalent with (4.100) or the quadratic inequality (4.101) when they are implemented with the constraints in (4.99) and when the move size constraints are ± 1 ($| \Delta u(k) | \leq 1$).

4.4.4.3 Manipulating One Input Signal at a Time for Arbitrary Move Size

The previous section demonstrates how to address the logical specification associated with manipulating one input at a time when move size is ± 1. However, for an arbitrary move size (as might also be the case in adaptive interventions) the constraints postulated in (4.100) and (4.101) are inadequate to make sure that only one component incurs a dosage change at each intervention decision. This section extends the HMPC formulation for sequential behavioral interventions with arbitrary move sizes, and hence to make it more generalizable.

In order to achieve this, an extension of the traditional MLD framework for HMPC is presented. Additional binary variables ϕ and its associated logical specifications are introduced to the MLD equation to generate corresponding constraints on the basis of the sequence table in Table 4.2. They are converted into linear inequalities, and are implemented by either appending them to (4.11) or by overwriting the move size constraints in (4.53). The number of the additional binary variables corresponds to the number of the manipulated inputs.

For example, in the GWG intervention illustrated above, three binary variables (ϕ_1, ϕ_2 and ϕ_3) are used to augment the vector of binary variables δ in (4.11). The selection of one

input change can be logically expressed as follows,

$$\phi_1(k) = 1 \Leftrightarrow \begin{cases} |\ \Delta u_1(k)\ | > 0, \\ \Delta u_2(k)\ = \Delta u_3(k) = 0 \end{cases} \tag{4.108}$$

$$\phi_2(k) = 1 \Leftrightarrow \begin{cases} |\ \Delta u_2(k)\ | > 0, \\ \Delta u_1(k)\ = \Delta u_3(k) = 0 \end{cases} \tag{4.109}$$

$$\phi_3(k) = 1 \Leftrightarrow \begin{cases} |\ \Delta u_3(k)\ | > 0, \\ \Delta u_1(k)\ = \Delta u_2(k) = 0 \end{cases} \tag{4.110}$$

$$\phi(k) \odot \Delta u(k)_{\min} \leq \Delta u(k) \leq \phi(k) \odot \Delta u(k)_{\max} \tag{4.111}$$

$$\phi_1(k) + \phi_2(k) + \phi_3(k) \leq 1 \tag{4.112}$$

$$\text{where } \phi(k) = [\phi_1(k) \quad \phi_2(k) \quad \phi_3(k)]^T \tag{4.113}$$

$$\Delta u(k) = [\Delta u_1(k) \quad \Delta u_2(k) \quad \Delta u_3(k)]^T \tag{4.114}$$

$$\Delta u(k)_{\max} = [\Delta u_1(k)_{\max} \quad \Delta u_2(k)_{\max} \quad \Delta u_3(k)_{\max}]^T \tag{4.115}$$

$$\Delta u(k)_{\min} = [\Delta u_1(k)_{\min} \quad \Delta u_2(k)_{\min} \quad \Delta u_3(k)_{\min}]^T \tag{4.116}$$

and $\odot$ is the Hadamard product, k is the sampling time. In (4.108), the selection of $\phi_1(k)$ means $u_1(k)$ will be altered, while the other components $u_2(k), \cdots, u_7(k)$ remain unchanged; (4.109) and (4.110) have the similar logical meaning. (4.111) redefines the move size constraints at each decision point, and (4.112) makes sure that only one binary variable from $\phi_1(k)$, $\phi_2(k)$ and $\phi_3(k)$ will be selected if it is necessary. The logical specifications in (4.108) - (4.111) can be expressed as linear inequalities related with initial control effort $u_0(k)$, $u(k)$ over the m control horizon, and $\phi(k)$ over the p prediction horizon; (4.112) is augmented after the linear inequalities of binary variables $\delta(k)$ in (4.11) over the p prediction horizon. Please note that the move size constraints in (4.115) and

(4.116) are defined as time-varying vectors in order to maintain generality; this can also help address the fact that the decision to assign the dosage is made less frequent than the daily sampling time of output measurement through self-monitoring process, (which has been discussed in the switching time strategy in Section 4.4.3).

4.5 Simulation Studies

In this section, we consider three simulation scenarios taken from GWG intervention with sequential decision polices. The first study focuses on the examination of how the improved HMPC framework assigns the optimized dosages, the change of which follows the proposed sequenced rules in Table 4.1. The extension of the traditional MLD framework introduced in Section 4.4.4.3 will be used in this study, and the corresponding logical specifications associated with clinical constraints and consideration discussed in the previous section are implemented to address the sequential decision policies. This study aims to validate the optimal decision policies generated by HMPC framework when the move size limits are arbitrary. The second case study intends to better understand why HMPC-based adaptive intervention offers an appealing and valuable framework for optimized behavioral intervention by the comparison with the adaptive intervention via "IF-THEN" decision rules. The GWG sequential behavioral intervention with move size ± 1 is used as an example to illustrate this, and the HMPC framework relying on traditional MLD model with constraints in Section 4.4.4.2 is implemented to generate the sequential decision policies in Table 4.1. The objective of the third case study is to illustrate that the HMPC algorithm developed in this section is not limited to the particular proposed dosage sequence in Table 4.1. By proposing a new set of sequential decision policies in Table 4.4, the design procedure of HMPC controller is analyzed and demonstrated, and the simulation results help not only verify that the dosage assigned by HMPC controller follows the new sequenced rules, but also demonstrate again why HMPC-based intervention is a promising

approach to design adaptive sequential interventions.

The simulations are based on a hypothetical 25-year-old female with 75 kg in pregravid body mass, 160 cm in height, which classifies her as overweight (BMI=29.30). Maternal age was selected using 2010 Data from the Center for Disease Control and Prevention illustrating mean age of mother at first birth is 25.4 years [71]. The open-loop model for GWG interventions is depicted in Figure 4.1. Two-degree-of-freedom (2 DoF) Internal Model Control (IMC) is used to formulate self-regulation, as illustrated in Section 3.2.3. For the sake of simplicity, we only focus on the effects that intervention components and self-regulation play on the perceived behavioral control (PBC) inflow to the Theory of Planned Behavior (TPB) models. In both the intervention and non-intervention treatments, we assume the age of gestation at time of delivery to be 40 weeks. We claim that the participant will have a ramp increase in her energy intake (EI) from day 35 to day 91. The participant is sedentary at the time of conception, and she potentially engages in less physical activity (PA) from the second to third trimester as she gains more weight in the absence of intervention. The intervention can help improve her physical activity level (PAL) in the second trimester, and however she will still decrease her PA during her latter stage of pregnancy, especially one or two months prior to delivery. These are two PA disturbances for intervention and no intervention case, which will lower her energy expenditure (EE) in the energy balance model.

4.5.1 Validation for the Proposed Dosage Sequence Formulation

The simulation in this section focuses on the evaluation of adaptive interventions administered by HMPC controller with arbitrary move size, and the illustration of how the optimized dosages featuring sequential decision rules in Table 4.2 are assigned by HMPC. The scenario in the absence of intervention is also presented so as to illustrate how much improvement the participant has made under the influence of HMPC-based adaptive inter-

ventions. The participant will not engage in self-regulation when there is no intervention.

Table 4.3 summarizes the model parameters in this simulation study, including the behavioral parameters, time constants τ_i, time delay θ_i, gains assumed for the participant in the TPB model and intervention delivery dynamics module, and filter parameters in the internal model control design for self-regulation, respectively. All these parameter values are hypothetical but have been selected such that the simulated responses mimic those of an actual participant. The parameters for the HMPC are as follows: $p = 30$ and $m = 28$, $Q_y = 100$, $\alpha_r = 0.9$, $\alpha_d = 0$, $f_a = 0.5$, and sampling time $T_s = 1$ (the participant measures her GWG and monitors dietary record daily), and the switching time $T_{\text{sw}} = 14$ (intervention decisions are made every two weeks). The move size constraints for the manipulated variables at the intervention decision are $\Delta u(k)_{\max} = [1 \quad 2 \quad 1]^T$, and $\Delta u(k)_{\min} = [-1 \quad -2 \quad -1]^T$ to illustrate that this improved HMPC no longer limits the move size to be ± 1.

Figure 4.6 shows the simulation result with a participant's responses for maternal body mass, EI, EE, the intervention component dosages, and the PBC inflows to the two TPB models. The dosage of goal setting $u_3(k)$ is same as the other four dosages $u_4(k), \cdots, u_7(k)$ throughout the intervention, therefore, only $u_3(k)$ is plotted to represent these other four dosages as well. The whole process can be divided into four stages. The first stage occurs before the intervention begins. For both intervention and no-intervention case, the participant has a ramp increase in her EI due to her pregnancy, and she remains sedentary throughout the first trimester. The second stage starts at week 14 when the intervention is initialized with the baseline program ($u_1(k) = u_2(k) = u_3(k) = 1$) assigned to the participant. Although the participant's weight gain is within the IOM guidelines at the beginning of the intervention, her high EI increase in the first trimester soon leads her weight outside the reference values (around day 125), and this indicates the necessity for a more intensive intervention. As a result, $u_1(k)$ is the first to be augmented step by step at each interven-

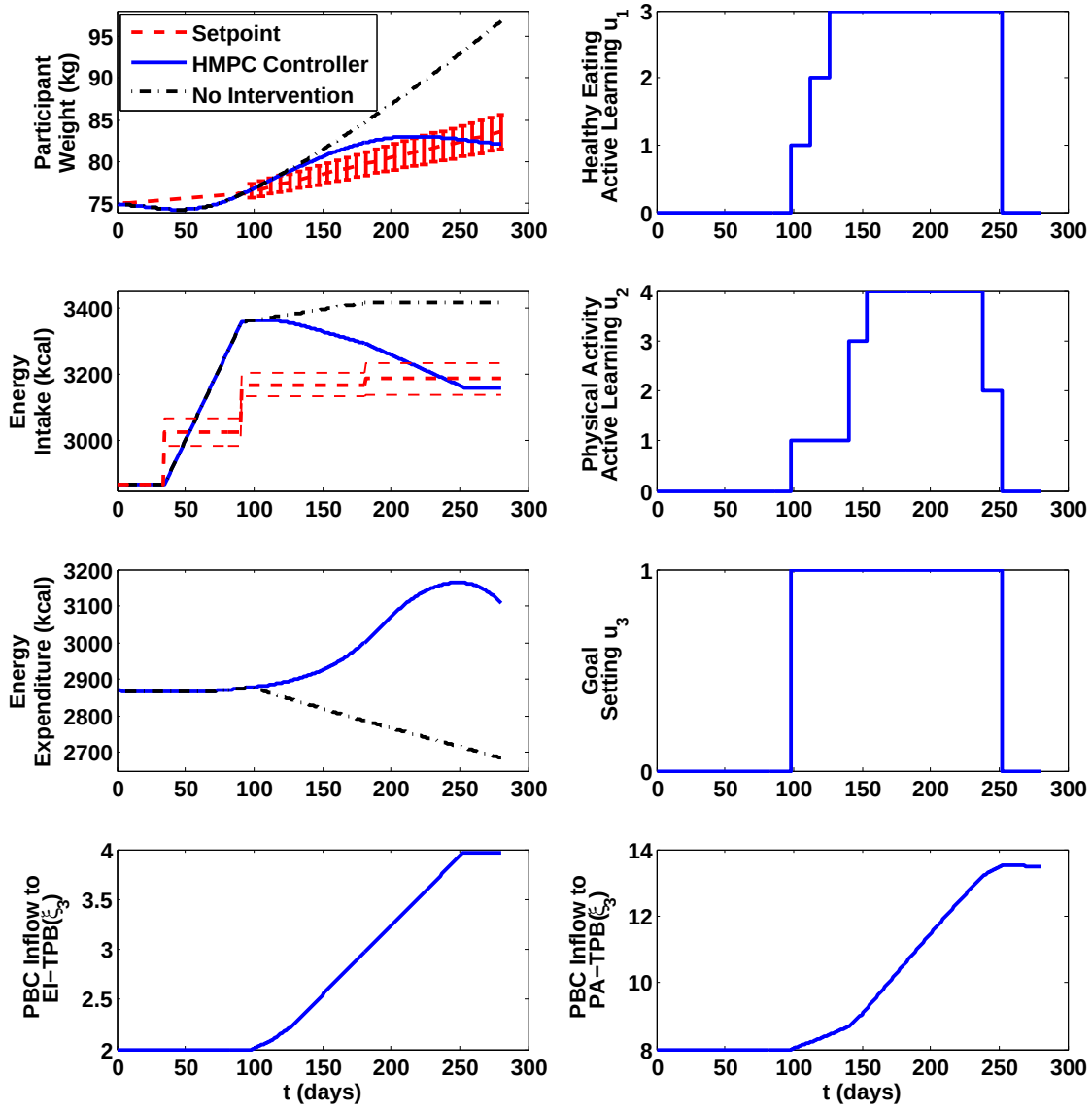

Figure 4.6: Simulation Responses in Section 4.5.1 for Maternal Body Mass, Energy Intake (EI), Energy Expenditure (EE), the Intervention Component Dosages, and the Perceived Behavioral Control (PBC) Inflows to the Theory of Planned Behavior (TPB) Models. Red Dashed Lines Represent the 2009 IOM Guidelines in Table 2.4 Applied on a Daily Basis; the Blue Solid Lines are the Case with Adaptive GWG Intervention Using HMPC Framework Corresponding to the Dosage Sequence Table 4.2; and the Black Dashed-dotted Lines are the Case in the Absence of the Interventions.

Table 4.3: Model Parameters for the Simulation Studies in Section 4.5.1. Time Constants (τ_i), Delays (θ_i), and Self-regulation Adjustable Parameters (λ_r, λ_d) are in Units of Days.

Parameter	EI-TPB	PA-TPB	Parameter	EI-TPB	PA-TPB
b_1	3	1	e_1	6	4
n_1	2	7	m_1	3	8
p_1	1	4	c_1	2	2
τ_1	1	30	γ_{11}	1	0.7
τ_2	1	30	γ_{22}	1	0.5
τ_3	1	10	γ_{33}	1	0.7
τ_4	1	20	β_{41}	1	0.34
τ_5	1	30	β_{42}	1	0.27
$\theta_1 \dots \theta_3$	0	0	β_{43}	1	0.13
$\theta_4 \dots \theta_6$	0	0	β_{53}	0	0.08
θ_7, θ_8	0	0	β_{54}	1	0.42
k_{u_1}	0.004	0	θ_{u_1}	0	0
k_{u_2}	0	0.01	θ_{u_2}	0	0
k_{u_3}	0.002	0.006	θ_{u_3}	0	0
λ_r	70	100	λ_d	90	155

tion decision with move size constraint $-1 \leq \Delta u_1(k) \leq 1$. $u_2(k)$ will not get augmented until two weeks after $u_1(k)$ reaches its maximum dose ($u_1(k)_{\max} = 3$). This helps verify that the HMPC controller will only allow one manipulated variable to incur the change at each time. The move size constraint on $u_2(k)$ is ± 2, and hence this component is first augmented by two doses from its base value at week 20, followed by one dose augmentation at week 22 when $u_2(k)$ reaches its maximum doses ($u_2(k)_{\max} = 4$). This stage mainly involves the augmentation above the baseline program ($u_n(k) \geq 1, n \in \{1,2,3\}$), and the adaptation of the intervention between the week 14 and week 22 shows that it follows the proposed sequential decision policies above the baseline. This full dosages of all these components are assigned to the participant and sustained for five intervention decisions. The third stage begins at day 220, the participant meets her GWG goal; HMPC controller reduces the intervention by decreasing $u_2(k)$ by two doses, while still keeping $u_1(k)$ at its

maximum dosage. The adapted intervention in this stage also indicates that it follows the proposed reduction sequence above the baseline program in Table 4.1. The fourth stage starts with the termination of the intervention at week 36. The previous effects of intervention and self-regulation keep the participant engaging in a healthy diet and active exercise life style. At the same time, the participant's PA starts gradually reducing, due to the fact that pregnant woman is reluctant to do PA at late third trimester, which leads to the decrease of EE. Despite of her reduced EE, the final EE is still above its initial value. At late pregnancy, the participant is able to control her EI at a stable level, while controlling her GWG within the IOM guideline.

4.5.2 HMPC versus Decision Rules

This section presents a hypothetical scenario focusing on the understanding of why HMPC structure offers a potentially valuable framework for adaptive interventions by comparison with the intervention using "IF-THEN" decision rules for GWG problem.

Simple "IF-THEN" decision rules for time-varying GWG adaptive intervention are depicted in Figure 4.4. They act on the result of important outcomes of the intervention (also known as tailoring variables [25]). In this GWG intervention, the decision rules evaluate GWG every two weeks (same as $T_{\text{sw}} = 14$ in HMPC-based intervention) from week 14. If a participant is within the IOM guidelines, the intervention dosage will be sustained for two intervention decisions every time before it gets reduced. However, as soon as the participant fails to meet the IOM guidelines at any intervention decision, her intervention gets augmented to increase potency. The augmentation and reduction of the intervention components also follows the corresponding sequenced rules described in Table 4.1, with the dosage change taking place only one step at a time for all the components, which indicates that move size constraints on all manipulated variables are ± 1 in HMPC-based intervention. Therefore, in this case study, the constraints for manipulating one input at a time in

Section 4.4.4.2 will be used and examined.

In the simulation study, we assume the anticipated disturbance occurs in the late of the participant's second trimester, and continues until her delivery when there is no intervention. The intervention will help the participant attenuate this EI increase. For the sake of simplicity, the model parameters in Table 4.3 are used for this simulation study. The parameters for the HMPC are also same as the ones used in Section 4.5.1, except that $f_a = 1$, $\alpha_r = 0.9$, and move size constraints are set to $\Delta u(k)_{\max} = [1 \quad 1 \quad 1]^T$, and $\Delta u(k)_{\min} = [-1 \quad -1 \quad -1]^T$ at each intervention decision, in order to match the ones in "IF-THEN" decision rules.

The simulation responses for maternal body mass, EI, EE, the intervention component dosages, and the PBC inflows to Theory of Planned Behavior (TPB) models under different scenarios (HMPC-based intervention, adaptive intervention using decision rules, and no intervention) are shown in Figure 4.7. The scenario in the absence of the intervention is presented in the simulation result in order to illustrate how the interventions play an important role on the participant's improvement in behavior: EI and PA under the influences of strong disturbance. From the EI profile without the intervention, we can see that the participant will increase her EI not only in the first trimester before the intervention due to her awareness of the pregnancy, but only in the late of the second trimester after the intervention starts. At the beginning of the intervention, the participant's weight is again within the IOM guidelines, although her EI (3302 kcal/day) is already 100 kcal higher than the EI reference values (3202 kcal/day) assumed for the third trimester. Therefore, for both HMPC-based intervention and intervention using decision rules, the initial dosage this participant receives is the baseline program.

In HMPC-based intervention, this participant's weight is always within the IOM guidelines after the intervention starts. In order not to have this participant reduce too much weight which might be even below the lower bound of IOM guidelines, the HMPC con-

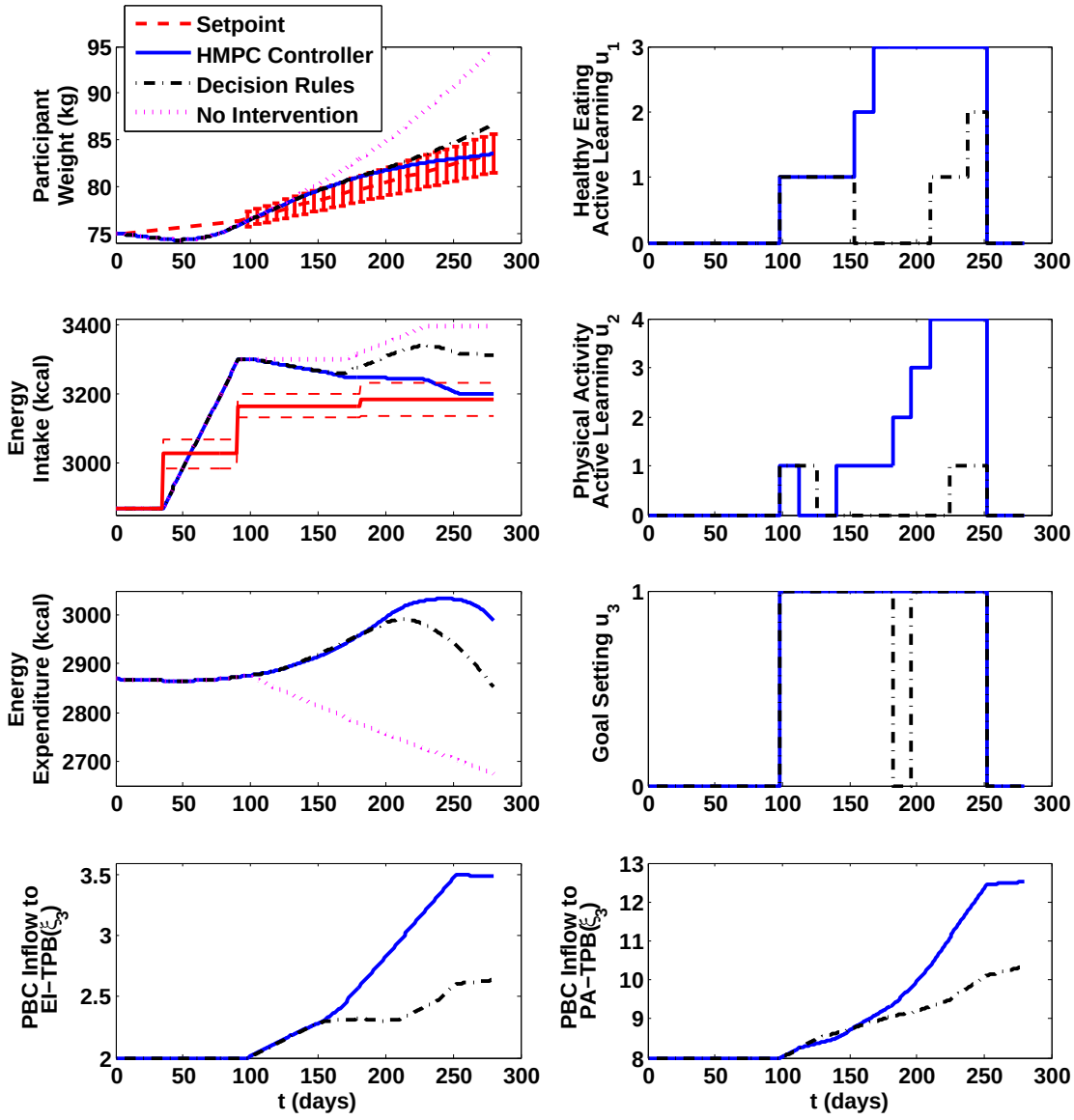

Figure 4.7: Simulation Results in Section 4.5.2 for the Participant's Responses for Maternal Body Mass, Energy Intake (EI), Energy Expenditure (EE), the Intervention Component Dosages, and the Perceived Behavioral Control (PBC) Inflows to the Theory of Planned Behavior (TPB) Models for the HMPC-based Intervention, the Adaptive Intervention Using Decision Rules, and no Intervention Case. The Red Dashed Lines Represent the 2009 IOM Guidelines in Table 2.4 Applied on a Daily Basis; the Blue Solid Lines are the Case with HMPC-based Intervention Corresponding to the Dosage Sequence Table 4.2; the Black Dashed-dotted Lines Represent the Case with Adaptive Intervention Using "IF-THEN" Decision Rules in Sequenced Rules Table 4.1; and the Pink Dotted Lines are the Case in the Absence of the Interventions.

troller first reduces the intervention for this participant by setting dosage to zero for component $u_2(k)$ at week 16. At this reduced intervention, the other two components at their base doses can still maintain this participant within the IOM guidelines during the week 16-20 when there is no extra EI increase (disturbance). At week 20, HMPC controller augments the intervention by adding this component $u_2(k)$, which makes the intervention restored to the baseline program. The EI anticipated disturbance occurs at day 170, and therefore the HMPC controller continues augmenting the intervention at week 22 (day 154) by increasing the dose for $u_1(k)$, considering the prediction horizon $m = 30$. The component $u_2(k)$ does not get augmented until week 26, which is two weeks after $u_1(k) = 3$. The move size constraint on $u_2(k)$ in this scenario is also ± 1 in order to match the case using decision rules for the comparison. The intervention reaches the maximum dosages for all the components at week 30, and the intervention remains unchanged until the end of the intervention. This hypothetical participant with the HMPC-based intervention is able to keep her weight within the IOM guidelines throughout her whole pregnancy, no matter whether there exists an EI increase as disturbance. This participant also manages to control her EI within the reference values in the mid-third trimester. The participant's PBC inflows to the TPB models increase faster when the intervention gets augmented, and more slowly when the intervention gets reduced.

Examining the case of adaptive intervention using decision rules, this same participant will receive the same baseline program at the entry of the intervention due to her weight is within the IOM guideline. Because she is able to meet her GWG goal under the baseline program for two intervention decisions (4 weeks), her intervention gets reduced by setting the dosage of component $u_2(k)$ to zero at week 18 first. With this reduced intervention, for the next four weeks, this participant's weight gain continues staying inside the IOM guidelines, and therefore, the dosage of component $u_1(k)$ gets reduced to zero at week 22 when only the component $u_3(k)$ with base dose is assigned to this participant. This

participant still succeeds maintaining her weight gain within the IOM guidelines for the next 4 weeks, and hence, at week 26, the dosage of $u_3(k)$ is also decreased to zero. The EI increase occurs at day 170 (late second trimester). With this EI disturbance, her high EI increase in the first trimester, and her reduced less intensive (or even no) intervention, her weight gain starts to be outside the IOM guidelines around day 195 when her intervention finally gets initialized again with component $u_3(k)$ added first at week 28, $u_1(k)$ second at week 30, and $u_2(k)$ at week 32. At week 34, her intervention is augmented above the baseline by increasing $u_1(k)$ to dose 2, and the intervention stops at week 36 with no possibility for further augmentation to reduce her weight gain. Therefore, all these augmented actions are not taken place in a timely manner before or immediately after EI disturbance in the second trimester, even though this participant's weight in within the IOM guidelines for the first several intervention decisions. As a result, this participant's GWG is outside the IOM guidelines at her late pregnancy, and her EI is always above the reference values throughout her pregnancy. The improvements in her PBC inflows to the TPB models are only around half of those using HMPC-based intervention.

This case study illustrates that the feedforward control action in HMPC controller is very useful in addressing anticipated disturbances which may be a priori or can be measured / predicted in the course of the intervention, while the feedback control action can response to unmeasured disturbance. HMPC controller will assign the future dosages based on not only the participant's past and current dosages, but also the predicted measured outcomes over the prediction horizon, while the decision rules adapt the intervention only based on the participant's current and past responses. Hence, when the anticipated disturbance is available, HMPC-based intervention can better predict the future responses of the participant, and make the dosage adjustment earlier than the intervention using decision rules which may or may not provide the augmentation in time.

4.5.3 Alternate Sequenced Rules

In this section, another set of sequenced rule for GWG interventions is proposed to demonstrate how the HMPC algorithm developed earlier can be applied to the design of different sequential decision policies. The alternate sequenced rules conform to the ones in real-life GWG interventions designed by Penn State collaborators. The goal of the simulation in this section is to illustrate that the HMPC algorithm is not only useful for one particular set of the sequenced rules in Table 4.1 for the GWG interventions, it can also serve as a basic framework of designing other sequential decision policies.

The adaptation rules used in this simulation are described in Table 4.4. This new set of sequenced rules states that:

1. The intervention starts at week 14, and is adapted every four weeks, which means switching time $T_{\text{sw}} = 28$.

2. The baseline program is make up of five components (HE/PA education, HE/PA weekly plan, and goal setting), and will be sustained throughout the intervention, while the other two components (HE component and PA component) are not offered during the baseline program.

3. Among all the seven components, there are two components (HE component u_1 and PA component u_2) which will be augmented from the baseline program. They are delivered in pre-determined discrete doses, with HE component (u_1) in $\{0, 1, 2, 3\}$, PA (u_2) component in $\{0, 1, 2\}$.

4. The augmentation of each component can only occur one step at a time, and there is no reduction of the components for the sake of cost saving (move size constraints: $0 \leq \Delta u \leq 1$).

Table 4.4: Summary of Dosage Augmentations per the IF-THEN Decision Rules for GWG Adaptive Interventions [7] for the Simulation in Section 4.5.3.

Options	Adaptation
Baseline Intervention	Education, Goal setting, plans, and self-monitoring
Step up 1	Baseline + HE component[a]
Step up 2	Baseline + 1 + PA component[b]
Step up 3	Baseline + 1+ 2 + HE component
Step up 4	Baseline + 1 + 2 + 3 + PA component
Step up 5	Baseline + 1 + 2 + 3 + 4 + HE component

[a]augmentation of healthy eating (HE) active learning.

[b]augmentation of physical activity (PA) active learning.

5. The adaptation of the intervention has to follow a certain pre-defined dosage sequence described in Table 4.4, which incrementally increases the HE and PA components in an alternating pattern.

Consequently, the discrete values of the components as system's manipulated variables (u_1, u_2) can be expressed as follows,

$$\begin{aligned}
\delta_i(k) &= 1 \Leftrightarrow z_i(k) = i;\ \ i \in \{0,\ 1,\ 2,\ 3\} && (4.117)\\
u_1(k) &= \sum_{i=0}^{3} z_i(k) \quad \sum_{i=0}^{3} \delta_i(k) = 1 && (4.118)\\
\delta_j(k) &= 1 \Leftrightarrow z_j(k) = j-4;\ \ j \in \{4,\ 5,\ 6\} && (4.119)\\
u_2(k) &= \sum_{j=4}^{6} z_j(k) \quad \sum_{j=4}^{6} \delta_j(k) = 1 && (4.120)\\
\delta_\ell(k) &= 1 \Leftrightarrow z_\ell(k) = \ell-6;\ \ \ell = 7 && (4.121)\\
u_n(k) &= \sum_{\ell=7}^{7} z_\ell(k) \quad \sum_{\ell=7}^{7} \delta_\ell(k) = 1;\ \ n \in \{3,4,5,6,7\} && (4.122)
\end{aligned}$$

where (4.117) and (4.118) specify that one of four possible levels (0, 1, 2, 3) of HE active learning component (u_1) must be assigned for each participant; (4.119) and (4.120) state that one of three levels (0, 1, 2) of PA active learning component (u_2) are available to be assigned to the participants, as indicated in Table 4.4; (4.121) and (4.122) represent the

dosages of the five components included in the baseline program. Meanwhile, according to the sequenced rules in Table 4.4, the sequence table can be generated, and they are listed in Table 4.5.

Again, with the information provided in Table 4.5, the propositional logic can be used to generate the following logical conditions which will be embedded into the dynamical model, and this can be guarantee that only the dosage combinations in Table 4.5 are selected.

$$\begin{aligned}\Omega = \quad & (\delta_0 \wedge \delta_4 \wedge \delta_7) \oplus (\delta_1 \wedge \delta_4 \wedge \delta_7) \oplus (\delta_1 \wedge \delta_5 \wedge \delta_7) \oplus \\ & (\delta_2 \wedge \delta_5 \wedge \delta_7) \oplus (\delta_2 \wedge \delta_6 \wedge \delta_7) \oplus (\delta_3 \wedge \delta_6 \wedge \delta_7)\end{aligned} \tag{4.123}$$

where $(\delta_0 \wedge \delta_4 \wedge \delta_7)$ is the dosage assigned to the participant in the baseline program ($u_1 = u_2 = 0$, $u_3 = \cdots = u_7 = 1$), in which $\delta_0 = 1$ means $u_1 = 0$ is selected, $\delta_4 = 1$ means $u_2 = 0$, $\delta_7 = 1$ means $u_3 = \cdots = u_7 = 1$; $(\delta_1 \wedge \delta_4 \wedge \delta_7)$ represents dosage sequence 1 in Table 4.5; $(\delta_1 \wedge \delta_5 \wedge \delta_7)$ represents dosage sequence 2 in Table 4.5; and the like. The six combinations in (4.123) are the six dosage sequences in Table 4.5. Ω in (4.123) can be expressed in the linear inequalities in (4.11). This limits the possibilities of the dosage combinations to six instead of a possible $\binom{4}{1} \times \binom{3}{1} = 12$ combinations.

Table 4.6 summarizes the model parameters in this simulation study. The parameters for the HMPC are as follows: the prediction horizon $p = 60$, the control horizon $m = 30$, the penalty weight on the control error $Q_y = 10$; the 3-DoF tuning parameters: $\alpha_r = 0$, $\alpha_d = 0$, and $f_a = 1$. The sampling time for the participant to measure her GWG and monitor dietary record is $T_s = 1$ day, and the intervention decision (assessment cycle) is made every four weeks ($T_{\text{sw}} = 28$ days).

Figure 4.8 shows the simulation comparison of the participant's responses for the case with HMPC-based intervention (blue lines) and the case with adaptive intervention via decision rules (black lines). For the sake of better illustrating how the interventions have

Table 4.5: Dosage Sequence Table for the GWG Behavioral Intervention Simulation in Section 4.5.3.

Dosage Sequence	**Healthy Eating Active Learning u_1**	**Physical Activity Active Learning u_2**	**Other Components $u_3 \cdots u_7$**	**Description**	**Propositional Logic**
0	0	0	1	Baseline	$\delta_0 \wedge \delta_4 \wedge \delta_7$
1	1	0	1	First augmentation of u_1	$\delta_1 \wedge \delta_4 \wedge \delta_7$
2	1	1	1	First augmentation of u_2	$\delta_1 \wedge \delta_5 \wedge \delta_7$
3	2	1	1	Second augmentation of u_1	$\delta_2 \wedge \delta_5 \wedge \delta_7$
4	2	2	1	Second augmentation of u_2	$\delta_2 \wedge \delta_6 \wedge \delta_7$
5	3	2	1	Third augmentation of u_1	$\delta_3 \wedge \delta_6 \wedge \delta_7$

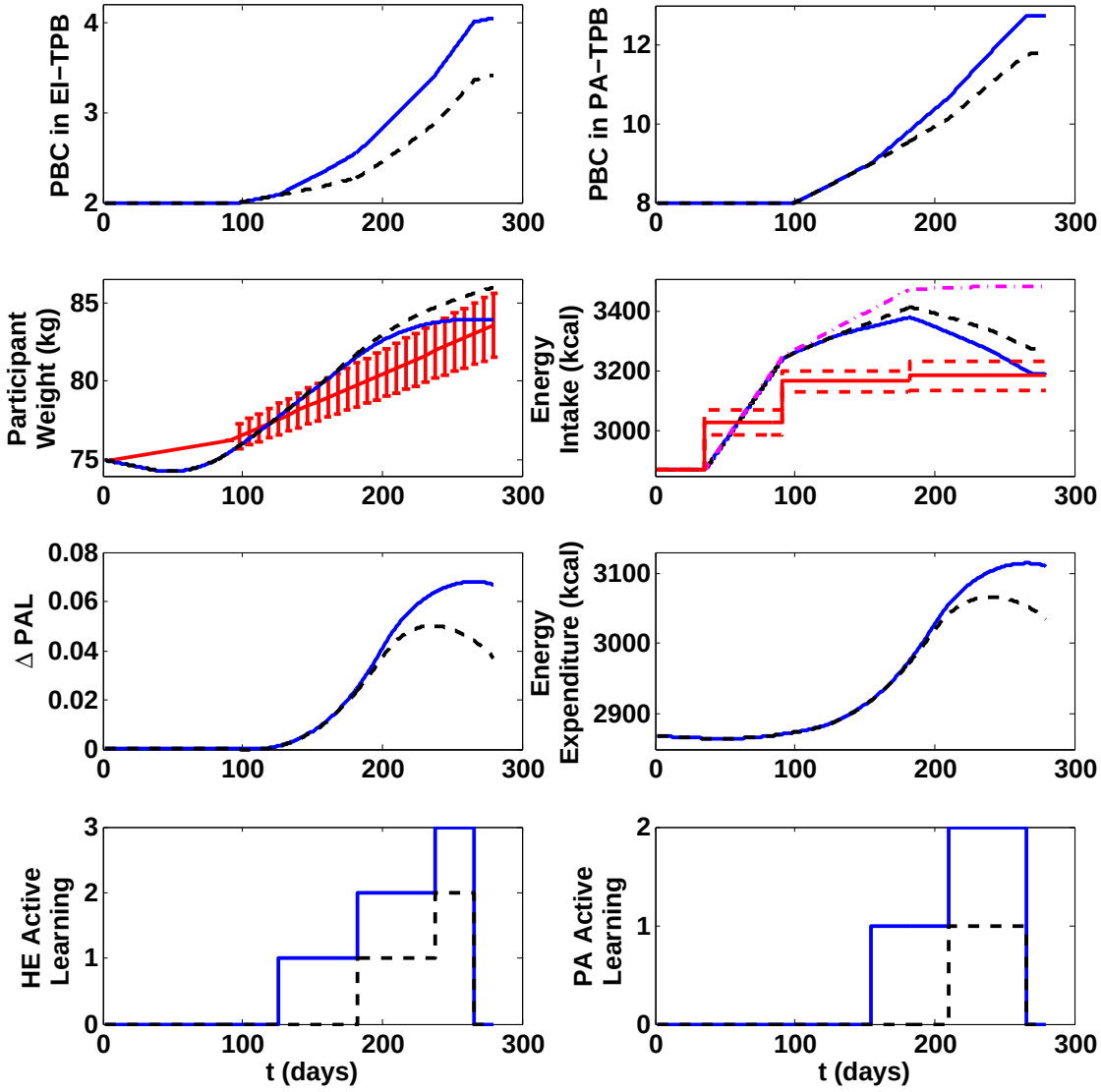

Figure 4.8: Simulation Responses in Section 4.5.3 for the PBC Inflows to the Two TPB Models, Maternal Body Mass, Energy Intake, PAL Change, Energy Expenditure, and the Dosages of Two Augmented Intervention Components. Red Line Represent the 2009 IOM Guidelines Applied on a Daily Basis; the Blue Solid Lines Represent the Case with Optimized Adaptive Interventions Using HMPC Corresponding to the Dosage Sequence Table in Table 4.5, the Black Dash Lines are Adaptive Interventions via "IF-THEN" Decision Rules in Sequenced Rules Table 4.4, and the Pink Dash-dot Line is the Energy Intake Profile with no Interventions.

Table 4.6: Model Parameters for the Simulation Study in Section 4.5.3. Time Constants (τ_i) are in Units of Days.

Parameter	EI-TPB	PA-TPB	Parameter	EI-TPB	PA-TPB
b_1	3	1	e_1	6	4
n_1	2	7	m_1	3	8
p_1	1	4	c_1	2	2
τ_1	1	30	γ_{11}	1	0.7
τ_2	1	30	γ_{22}	1	0.5
τ_3	1	30	γ_{33}	0.95	0.9
τ_4	1	30	β_{41}	1	0.34
τ_5	1	36	β_{42}	1	0.27
$\theta_1 \dots \theta_3$	0	0	β_{43}	1	0.18
$\theta_4 \dots \theta_6$	0	0	β_{53}	0	0.12
θ_7, θ_8	0	0	β_{54}	1	0.42
k_{u_1}	0.005	0	θ_{u_1}	0	0
k_{u_2}	0	0.01	θ_{u_2}	0	0
k_{u_3}	0.001	0.005	θ_{u_3}	0	0
λ_r	80	100	λ_d	90	155

an effect on the participant's improvement in her energy intake, the energy intake profile in the absence of intervention (pink dotted-dash line) is presented as well. First, the simulation result for the dosages of augmented intervention components can help validate if the HMPC controller assigns the optimized dosages based on the sequenced rules that were mentioned earlier. When the intervention starts, the baseline program is offered to the participant because her weight is within the IOM guidelines. HMPC controller augments HE active learning and PA active learning incrementally in an alternating pattern, as required in the sequenced rules. In this particular intervention, there is no reduction for cost saving purposes, as discussed earlier. This figure also illustrates why HMPC controller serves an appealing framework for adaptive intervention in contrast with the case using decision rules. As mentioned previously in Section 4.5.2, when the anticipated or measured disturbance is available, HMPC-based intervention can take action to make the dosage adjustment in a timely manner according to the model dynamics and prediction

over the receding horizon, compared with the intervention via decision rules which may or may not provide the augmentation in time.

4.6 Chapter Summary

This chapter has presented the formulation and the application of HMPC to the design of adaptive sequential behavioral interventions. Because the GWG problem is an excellent example of a sequential intervention, the open-loop model developed in Chapter 2 and Chapter 3 serves as the basis to implement HMPC algorithms acting as decision framework in an GWG intervention. The behavioral health setting defines the difference in this problem from the conventional control engineering applications, and it requires us to take into account the clinical and resource considerations when the control system is designed. Specifically, the HMPC framework is formulated to address the discrete-valued nature of the manipulated variables, the difference in the frequency between an intervention decision and the sampling interval, and the patient-friendly dosage assignment which follows the pre-defined dosage sequence, thus creating the functionality needed by the control algorithm to make sequential decisions within a receding horizon framework.

The greatest challenge described in this chapter is to design the linear inequalities to meet the logical conditions associated with dosage sequence. Propositional logic can enforce constraints between variables only at the current sampling time, however the dosage sequence requires the constraints between manipulated variables in a time-varying manner. In this chapter, for the sake of simplicity, we first assume the move size constraints of all the manipulated variables are ± 1, the process constraints and extra constraints are embedded into the MLD framework to address this logical specification associated with the dosage sequence. Later, we present an extension of the traditional MLD-based HMPC scheme which can address a more generalized case with arbitrary move size. Relying on the additional binary variables introduced to the MLD structure, and the user-specified

sequence table, the logical specifications associated with the sequential decision policies in adaptive interventions can be easily generated, and embedded into HMPC formulation using MLD structure with constraints.

Three simulation studies were presented, focusing on the assessment of how adaptive intervention with sequential decision policies using HMPC framework assigns the optimized dosages with its change following the proposed dosage sequence, the illustration of how HMPC-based intervention is able to adjust the dosages of the intervention components "just-in-time" through the comparison with adaptive intervention using decision rules, and the exemplification of how to generate different sequential decision policies using the proposed HMPC algorithm. This offers a "proof-of-concept" demonstration of the potential that HMPC-based interventions can provide in improving the participant's response, increasing the effectiveness of the intervention, and enabling less waste of resources by relying on a dynamical model, measured outcomes, and predicted measured disturbance (if available).

This work is proof of concept as well focusing on the application of control-oriented approaches in the field of behavioral health and medicine. The HMPC algorithm proposed in this chapter was illustrated on an intervention for managing weight gain during pregnancy; however, as we can see in Section 4.5.3, it can be applied to any other adaptive behavioral intervention problem featuring multiple intervention components which also require a pre-defined dosage sequence.

Chapter 5

ENHANCEMENTS TO THE GWG ADAPTIVE INTERVENTION

5.1 Overview

In earlier chapters, a dynamical systems model for the behavioral interventions to prevent excessive GWG was presented, which was used to formulate the controllers for self-regulation, and decision policies that generate optimized discrete dosages with pre-defined dosage sequence, respectively. This dissertation addresses the application of control theory in the field of psychology and behavioral health, and has provided valuable insights for the demonstration of how to use dynamical systems and control-oriented methods to design, implement and optimize the adaptive sequential behavioral interventions.

This chapter extends the prior simulation work to allow us to examine some real-life scenarios, that will ultimately be important in pilot testing and clinical trials of this research. We focus on two enhancements to the existing application in this dissertation: one is the linear time-varying system for GWG adaptive intervention using gain-scheduling parameter varying control as an initial approach; and the other is filter design for multi-rate digital control that addresses the difference in the frequency of measurement of the self-monitoring components. The latter can be achieved by introducing an additional filter for the slow measurements, which together with the one in 3 DoF tuning approach constitute the cascade filters for dual-rate system, as described in [14]. Numerical examples are shown using GWG adaptive intervention as discussed in the previous chapters for these two enhancements.

The rest of the chapter is organized as follows. Section 5.2 describes the algorithm for how to implement gain-scheduling parameter varying control under HMPC framework. Section 5.3 presents the design procedure of cascade filter for multi-rate control system. Section 5.4 gives the summary of this chapter.

5.2 Gain-Scheduling Parameter Varying Control for GWG Intervention

The behavioral model - Theory of Planned Behavior (TPB) introduced in Section 2.3 is generated by the use of the principle of conservation of mass based on the relationship between fluid analogies and path diagrams from structural equation modeling. For reasons of simplicity, we earlier assume it was a first-order linear time-invariant model. However, the variations of participant's attitude and behavior during pregnancy indicate the potential parameter changes in the model in real life, leading to the linear time-varying model,

$$\tau_1(t)\frac{d\eta_1}{dt} = \gamma_{11}(t)\xi_1(t-\theta_1(t)) - \eta_1(t) + \zeta_1(t) \tag{5.1}$$

$$\tau_2(t)\frac{d\eta_2}{dt} = \gamma_{22}(t)\xi_2(t-\theta_2(t)) - \eta_2(t) + \zeta_2(t) \tag{5.2}$$

$$\tau_3(t)\frac{d\eta_3}{dt} = \gamma_{33}(t)\xi_3(t-\theta_3(t)) - \eta_3(t) + \zeta_3(t) \tag{5.3}$$

$$\begin{aligned}\tau_4(t)\frac{d\eta_4}{dt} &= \beta_{41}(t)\eta_1(t-\theta_4(t)) + \beta_{42}(t)\eta_2(t-\theta_5(t)) + \beta_{43}(t)\eta_3(t-\theta_6(t)) \\ &\quad -\eta_4(t) + \zeta_4(t)\end{aligned} \tag{5.4}$$

$$\tau_5(t)\frac{d\eta_5}{dt} = \beta_{54}(t)\eta_4(t-\theta_7(t)) + \beta_{53}(t)\eta_3(t-\theta_8(t)) - \eta_5(t) + \zeta_5(t) \tag{5.5}$$

where the time constants τ_i, gains β_{ij}, γ_{ij} and time delay θ_i will be changing with time in this time-varying system model. For example, the time constants can have several different values during the intervention or pregnancy. We can address these problems using gain scheduling parameter varying control, which will help better improve the prediction of controlled variables over the receding horizon using an HMPC strategy.

Gain scheduling is perhaps one of the most popular nonlinear control design approaches which have been widely and successfully applied in various fields, ranging from aerospace to process control. Gain scheduling design typically employs a "divide and conquer" approach whereby the nonlinear design task is decomposed into a number of linear sub-tasks. Such a decomposition depends on establishing a relationship between a nonlinear system and a family of linear systems. One or more observable variables are used to determine

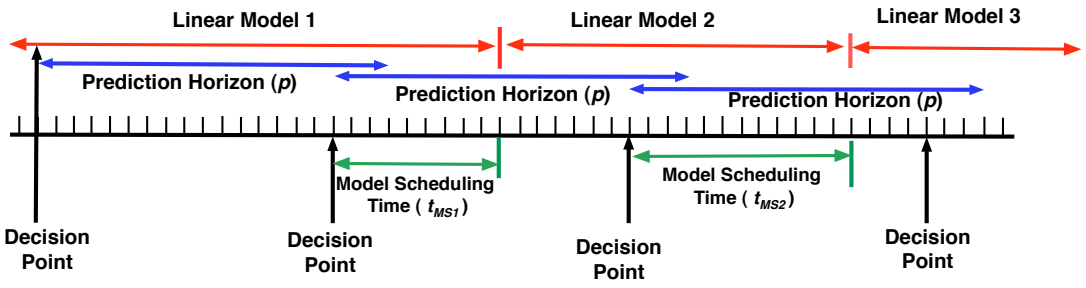

Figure 5.1: Illustration of the Gain Scheduling Strategy for a GWG Intervention Developed in this Chapter

what operating region the system is currently in and to enable the appropriate linear controller [89].

In this work, we assume that there are several different linear models to describe a participant's behavioral change during the intervention, and the gain scheduling will switch the model according to preset times (also called scheduling signals, or scheduling variables). For example, there are three linear models as illustrated in Figure 5.1. The intervention will be adapted at each decision point. For the first decision, there is no model change over the prediction horizon p, and therefore, the MPC will schedule linear model 1 which will predict the future values of controlled variables. At the second decision point, the prediction horizon spans between the model scheduling time for linear model 1 and linear model 2. Hence, at the time to make the intervention decision, it is very important for the HMPC controller to understand that linear model 2 will be used t_{MS1} days after the intervention decision is made. One can reach a similar conclusion when the third intervention decision is made: HMPC should switch from linear model 2 to linear model 3 t_{MS2} days after the new dosage is assigned. If each scheduling model is very close to our real process, then the predicted values of the controlled variables from HMPC will be more accurate, compared with using only one fixed linear model (e.g., linear model 1). The difference between the model scheduling time and the switching time that is illustrated in Section 4.4.3 is that

model scheduling time t_{MS} is changing at every decision point, while the switching time refers to the frequency when the participant visits the clinics, and it is usually a constant.

In order to implement this gain scheduling strategy for GWG intervention in Figure 5.1, we have to introduce additional variable (model scheduling time t_{MS}) to our HMPC algorithm every time when the intervention is adapted during the model scheduling time. Therefore, the p step ahead prediction equations of MPC have to be updated, especially the matrices related with the state space model parameters, to show this model scheduling strategy. For the convenience, we re-state the process model, the disturbance model, and the differenced forms of the disturbance and system models that were previously described in Chapter 4. The MLD-based model framework is expressed as follows,

$$\begin{aligned} x(k+1) &= Ax(k)+B_1u(k)+B_2\delta(k)+B_3z(k)+B_dd(k) && (5.6)\\ y(k) &= Cx(k)+d'(k)+\nu(k) && (5.7)\\ E_2\delta(k)+E_3z(k) &\leq E_5+E_4y(k)+E_1u(k)-E_dd(k) && (5.8) \end{aligned}$$

Here, the stochastic disturbance model for unmeasured disturbance d' that we consider is,

$$\begin{aligned} x_w(k) &= A_wx_w(k-1)+B_ww(k-1) && (5.9)\\ d'(k) &= C_wx_w(k) && (5.10) \end{aligned}$$

The differenced forms of the disturbance and system models are as follows,

$$\begin{aligned} \Delta x(k) &= A\Delta x(k-1)+B_1\Delta u(k-1)+B_2\Delta\delta(k-1)+B_3\Delta z(k-1)\\ &+ B_d\Delta d(k-1) && (5.11)\\ \Delta x_w(k) &= A_w\Delta x_w(k-1)+B_w\Delta w(k-1) && (5.12) \end{aligned}$$

The following equations can be obtained if propagating equations (5.7), (5.11), and (5.12),

$$
\begin{aligned}
X(k) &= \tilde{A}X(k-1)+\tilde{B}_1\Delta u(k-1)+\tilde{B}_2\Delta\delta(k-1)+\tilde{B}_3\Delta z(k-1) \\
&+ \tilde{B}_d\Delta d(k-1)+\tilde{B}_w\Delta w(k-1) \qquad (5.13) \\
y(k) &= \tilde{C}X(k)+\nu(k) \qquad (5.14)
\end{aligned}
$$

where

$$
\begin{aligned}
X(k) &= [\Delta x^T(k) \quad \Delta x_w^T(k) \quad y^T(k)]^T \\
\tilde{A} &= \begin{bmatrix} A & 0 & 0 \\ 0 & A_w & 0 \\ CA & A_w & I \end{bmatrix};\ \tilde{B}_i = \begin{bmatrix} B_i \\ 0 \\ CB_i \end{bmatrix},\ i=1,d; \\
\tilde{B}_w &= \begin{bmatrix} 0 \\ I \\ I \end{bmatrix};\ \tilde{C} = [0 \quad 0 \quad I]
\end{aligned}
$$

Here $\Delta*(k) = *(k) - *(k-1)$ and $\Delta w(k)$ is a white noise sequence.

Therefore, when different linear model is scheduled according to preset time, the matrices in (5.13) and (5.14) are different, and this will impact the p step ahead prediction below, which is also shown in (4.23) - (4.24).

$$
\begin{aligned}
Y(k+1) &= \Phi X(k)+H_1U(k)+H_2\bar{\delta}(k)+H_3Z(k)+H_dD(k)-H_{11}u(k-1) \\
&- H_{21}\delta(k-1)-H_{31}z(k-1)-H_{d1}d_{flt}(k-1) \qquad (5.15) \\
\bar{E}_5 &\geq \bar{E}_2\bar{\delta}(k)+\bar{E}_3Z(k)+\bar{E}_4Y(k)+\bar{E}_1U(k)+\bar{E}_dD(k) \qquad (5.16)
\end{aligned}
$$

In order to derive the expressions of new matrices in (5.15) and (5.16), let us assume that $t_{MS} = 4$ as an example first. The second model is expressed as,

$$
\begin{aligned}
X(k) &= \hat{A}X(k-1) + \hat{B}_1\Delta u(k-1) + \hat{B}_2\Delta\delta(k-1) + \hat{B}_3\Delta z(k-1) \\
&+ \hat{B}_d\Delta d(k-1) + \hat{B}_w\Delta w(k-1) \qquad (5.17) \\
y(k) &= \hat{C}X(k) + \nu(k) \qquad (5.18)
\end{aligned}
$$

If the prediction horizon of the MPC model is p, the moving horizon is m, the future value of output $y(k+1)$ is

$$
\begin{aligned}
y(k+1) &= \tilde{C}X(k+1) \\
&= \tilde{C}\tilde{A}X(k) + \tilde{C}\tilde{B}_1\Delta u(k) + \tilde{C}\tilde{B}_2\Delta\delta(k) + \tilde{C}\tilde{B}_3\Delta z(k) + \tilde{C}\tilde{B}_d\Delta d_{flt}(k) \\
&= \tilde{C}\tilde{A}X(k) + \tilde{C}\tilde{B}_1 u(k) + \tilde{C}\tilde{B}_2\delta(k) + \tilde{C}\tilde{B}_3 z(k) + \tilde{C}\tilde{B}_d d_{flt}(k) \\
&- \tilde{C}[\tilde{B}_1 u(k-1) + \tilde{B}_2\delta(k-1) + \tilde{B}_3 z(k-1) + \tilde{B}_d d_{flt}(k-1)] \qquad (5.19)
\end{aligned}
$$

The future value of output $y(k+2)$

$$
\begin{aligned}
y(k+2) &= \tilde{C}\tilde{A}^2X(k) + [(\tilde{C}\tilde{A}\tilde{B}_1 - \tilde{C}\tilde{B}_1)u(k) + \tilde{C}\tilde{B}_1 u(k+1)] \\
&+ [(\tilde{C}\tilde{A}\tilde{B}_2 - \tilde{C}\tilde{B}_2)\delta(k) + \tilde{C}\tilde{B}_2\delta(k+1)] + [(\tilde{C}\tilde{A}\tilde{B}_3 - \tilde{C}\tilde{B}_3)z(k) \\
&+ \tilde{C}\tilde{B}_3 z(k+1)] + [(\tilde{C}\tilde{A}\tilde{B}_d - \tilde{C}\tilde{B}_d)d_{flt}(k) + \tilde{C}\tilde{B}_d d_{flt}(k+1)] \\
&- \tilde{C}\tilde{A}[\tilde{B}_1 u(k-1) + \tilde{B}_2\delta(k-1) + \tilde{B}_3 z(k-1) + \tilde{B}_d d_{flt}(k-1)]
\end{aligned}
\qquad (5.20)
$$

Similarly, the future value of output $y(k+3)$

$$
\begin{aligned}
y(k+3) &= \tilde{C}\tilde{A}^3X(k) \\
&+ [(\tilde{C}\tilde{A}^2\tilde{B}_1 - \tilde{C}\tilde{A}\tilde{B}_1)u(k) + (\tilde{C}\tilde{A}\tilde{B}_1 - \tilde{C}\tilde{B}_1)u(k+1) + \tilde{C}\tilde{B}_1u(k+2)] \\
&+ [(\tilde{C}\tilde{A}^2\tilde{B}_2 - \tilde{C}\tilde{A}\tilde{B}_2)\delta(k) + (\tilde{C}\tilde{A}\tilde{B}_2 - \tilde{C}\tilde{B}_2)\delta(k+1) + \tilde{C}\tilde{B}_2\delta(k+2)] \\
&+ [(\tilde{C}\tilde{A}^2\tilde{B}_3 - \tilde{C}\tilde{A}\tilde{B}_3)z(k) + (\tilde{C}\tilde{A}\tilde{B}_3 - \tilde{C}\tilde{B}_3)z(k+1) + \tilde{C}\tilde{B}_3z(k+2)] \\
&+ [(\tilde{C}\tilde{A}^2\tilde{B}_d - \tilde{C}\tilde{A}\tilde{B}_d)d_{flt}(k) + (\tilde{C}\tilde{A}\tilde{B}_d - \tilde{C}\tilde{B}_d)d_{flt}(k+1) + \tilde{C}\tilde{B}_dd_{flt}(k+2)] \\
&- \tilde{C}\tilde{A}^2[\tilde{B}_1u(k-1) + \tilde{B}_2\delta(k-1) + \tilde{B}_3z(k-1) + \tilde{B}_dd_{flt}(k-1)] \qquad (5.21)
\end{aligned}
$$

The future value of output $y(k+4)$ will involve the second model (5.17) - (5.18), because we assume $t_{MS} = 4$,

$$
\begin{aligned}
y(k+4) &= \hat{C}X(k+4) \\
&= \hat{C}\hat{A}X(k+3) + \hat{C}\hat{B}_1\Delta u(k+3) + \hat{C}\hat{B}_2\Delta\delta(k+3) \\
&+ \hat{C}\hat{B}_3\Delta z(k+3) + \hat{C}\hat{B}_d\Delta d_{flt}(k+3) \\
&= \hat{C}\hat{A}\tilde{A}^3X(k) + [\hat{C}\hat{A}(\tilde{A}^2\tilde{B}_1 - \tilde{A}\tilde{B}_1)u(k) + \hat{C}\hat{A}(\tilde{A}\tilde{B}_1 - \tilde{B}_1)u(k+1) \\
&+ \hat{C}(\hat{A}\tilde{B}_1 - \hat{B}_1)u(k+2) + \hat{C}\hat{B}_1u(k+3)] \\
&+ [\hat{C}\hat{A}(\tilde{A}^2\tilde{B}_2 - \tilde{A}\tilde{B}_2)\delta(k) + \hat{C}\hat{A}(\tilde{A}\tilde{B}_2 - \tilde{B}_2)\delta(k+1) \\
&+ \hat{C}(\hat{A}\tilde{B}_2 - \hat{B}_2)\delta(k+2) + \hat{C}\hat{B}_2\delta(k+3)] \\
&+ [\hat{C}\hat{A}(\tilde{A}^2\tilde{B}_3 - \tilde{A}\tilde{B}_3)z(k) + \hat{C}\hat{A}(\tilde{A}\tilde{B}_3 - \tilde{B}_3)z(k+1) \\
&+ \hat{C}(\hat{A}\tilde{B}_3 - \hat{B}_3)z(k+2) + \hat{C}\hat{B}_3z(k+3)] \\
&+ [\hat{C}\hat{A}(\tilde{A}^2\tilde{B}_d - \tilde{A}\tilde{B}_d)d_{flt}(k) + \hat{C}\hat{A}(\tilde{A}\tilde{B}_d - \tilde{B}_d)d_{flt}(k+1) \\
&+ \hat{C}(\hat{A}\tilde{B}_d - \hat{B}_d)d_{flt}(k+2) + \hat{C}\hat{B}_dd_{flt}(k+3)] \\
&- \hat{C}\hat{A}\tilde{A}^2[\tilde{B}_1u(k-1) + \tilde{B}_2\delta(k-1) + \tilde{B}_3z(k-1) + \tilde{B}_dd_{flt}(k-1)]
\end{aligned}
$$

(5.22)

Similarly, the future value of output $y(k+5)$ will also involve the second model, and can be expressed as,

$$\begin{aligned}
y(k+5) &= \hat{C}\hat{A}^2\tilde{A}^3X(k) \\
&+ [\hat{C}\hat{A}^2(\tilde{A}^2\tilde{B}_1-\tilde{A}\tilde{B}_1)u(k)+\hat{C}\hat{A}^2(\tilde{A}\tilde{B}_1-\tilde{B}_1)u(k+1) \\
&+ \hat{C}\hat{A}(\hat{A}\tilde{B}_1-\hat{B}_1)u(k+2)+\hat{C}(\hat{A}\hat{B}_1-\hat{B}_1)u(k+3)+\hat{C}\hat{B}_1u(k+4)] \\
&+ [\hat{C}\hat{A}^2(\tilde{A}^2\tilde{B}_2-\tilde{A}\tilde{B}_2)\delta(k)+\hat{C}\hat{A}^2(\tilde{A}\tilde{B}_2-\tilde{B}_2)\delta(k+1) \\
&+ \hat{C}\hat{A}(\hat{A}\tilde{B}_2-\hat{B}_2)\delta(k+2)+\hat{C}(\hat{A}\hat{B}_2-\hat{B}_2)\delta(k+3)+\hat{C}\hat{B}_2\delta(k+4)] \\
&+ [\hat{C}\hat{A}^2(\tilde{A}^2\tilde{B}_3-\tilde{A}\tilde{B}_3)z(k)+\hat{C}\hat{A}^2(\tilde{A}\tilde{B}_3-\tilde{B}_3)z(k+1) \\
&+ \hat{C}\hat{A}(\hat{A}\tilde{B}_3-\hat{B}_3)z(k+2)+\hat{C}(\hat{A}\hat{B}_3-\hat{B}_3)z(k+3)+\hat{C}\hat{B}_3z(k+4)] \\
&+ [\hat{C}\hat{A}^2(\tilde{A}^2\tilde{B}_d-\tilde{A}\tilde{B}_d)d_{flt}(k)+\hat{C}\hat{A}^2(\tilde{A}\tilde{B}_d-\tilde{B}_d)d_{flt}(k+1) \\
&+ \hat{C}\hat{A}(\hat{A}\tilde{B}_d-\hat{B}_d)d_{flt}(k+2)+\hat{C}(\hat{A}\hat{B}_d-\hat{B}_d)d_{flt}(k+3)+\hat{C}\hat{B}_dd_{flt}(k+4)] \\
&- \hat{C}\hat{A}^2\tilde{A}^2[\tilde{B}_1u(k-1)+\tilde{B}_2\delta(k-1)+\tilde{B}_3z(k-1)+\tilde{B}_dd_{flt}(k-1)]
\end{aligned} \tag{5.23}$$

Under the assumption that $\Delta u(k+i)=0,\ i>m-1$, the future value of output $y(k+m+1)$ is as follows,

$$
\begin{aligned}
y(k+m+1) &= \hat{C}\hat{A}^{m-2}\tilde{A}^3X(k) \\
&+ [\hat{C}\hat{A}^{m-2}(\tilde{A}^2\tilde{B}_1-\tilde{A}\tilde{B}_1)u(k)+\hat{C}\hat{A}^{m-2}(\tilde{A}\tilde{B}_1-\tilde{B}_1)u(k+1) \\
&+ \hat{C}\hat{A}^{m-3}(\hat{A}\tilde{B}_1-\hat{B}_1)u(k+2)+\hat{C}\hat{A}^{m-4}(\hat{A}\hat{B}_1-\hat{B}_1)u(k+3) \\
&+ \hat{C}\hat{A}^{m-5}(\hat{A}\hat{B}_1-\hat{B}_1)u(k+4)+\cdots+\hat{C}\hat{A}\hat{B}_1u(k+m-1)] \\
&+ [\hat{C}\hat{A}^{m-2}(\tilde{A}^2\tilde{B}_2-\tilde{A}\tilde{B}_2)\delta(k)+\hat{C}\hat{A}^{m-2}(\tilde{A}\tilde{B}_2-\tilde{B}_2)\delta(k+1) \\
&+ \hat{C}\hat{A}^{m-3}(\hat{A}\tilde{B}_2-\hat{B}_2)\delta(k+2)+\hat{C}\hat{A}^{m-4}(\hat{A}\hat{B}_2-\hat{B}_2)\delta(k+3) \\
&+ \hat{C}\hat{A}^{m-5}(\hat{A}\hat{B}_2-\hat{B}_2)\delta(k+4)+\cdots \\
&+ \hat{C}\hat{A}\hat{B}_2\delta(k+m-1)+\hat{C}\hat{B}_2\delta(k+m)] \\
&+ [\hat{C}\hat{A}^{m-2}(\tilde{A}^2\tilde{B}_3-\tilde{A}\tilde{B}_3)z(k)+\hat{C}\hat{A}^{m-2}(\tilde{A}\tilde{B}_3-\tilde{B}_3)z(k+1) \\
&+ \hat{C}\hat{A}^{m-3}(\hat{A}\tilde{B}_3-\hat{B}_3)z(k+2)+\hat{C}\hat{A}^{m-4}(\hat{A}\hat{B}_3-\hat{B}_3)z(k+3) \\
&+ \hat{C}\hat{A}^{m-5}(\hat{A}\hat{B}_3-\hat{B}_3)z(k+4)+\cdots \\
&+ \hat{C}\hat{A}\hat{B}_3z(k+m-1)+\hat{C}\hat{B}_3z(k+m)] \\
&+ [\hat{C}\hat{A}^{m-2}(\tilde{A}^2\tilde{B}_d-\tilde{A}\tilde{B}_3)d_{flt}(k)+\hat{C}\hat{A}^{m-2}(\tilde{A}\tilde{B}_d-\tilde{B}_d)d_{flt}(k+1) \\
&+ \hat{C}\hat{A}^{m-3}(\hat{A}\tilde{B}_d-\hat{B}_d)d_{flt}(k+2)+\hat{C}\hat{A}^{m-4}(\hat{A}\hat{B}_d-\hat{B}_d)d_{flt}(k+3) \\
&+ \hat{C}\hat{A}^{m-5}(\hat{A}\hat{B}_d-\hat{B}_d)d_{flt}(k+4)+\cdots \\
&+ \hat{C}\hat{A}\hat{B}_dd_{flt}(k+m-1)+\hat{C}\hat{B}_dd_{flt}(k+m)] \\
&- \hat{C}\hat{A}^{m-2}\tilde{A}^2[\tilde{B}_1u(k-1)+\tilde{B}_2\delta(k-1)+\tilde{B}_3z(k-1)+\tilde{B}_dd_{flt}(k-1)]
\end{aligned}
\tag{5.24}
$$

The future value of output $y(k+p)$ is

$$
\begin{aligned}
y(k+p) &= \hat{C}\hat{A}^{p-3}\tilde{A}^3X(k) \\
&+ [\hat{C}\hat{A}^{p-3}(\tilde{A}^2\tilde{B}_1-\tilde{A}\tilde{B}_1)u(k)+\hat{C}\hat{A}^{p-3}(\tilde{A}\tilde{B}_1-\tilde{B}_1)u(k+1) \\
&+ \hat{C}\hat{A}^{p-4}(\hat{A}\tilde{B}_1-\hat{B}_1)u(k+2)+\hat{C}\hat{A}^{p-5}(\hat{A}\hat{B}_1-\hat{B}_1)u(k+3) \\
&+ \hat{C}\hat{A}^{p-6}(\hat{A}\hat{B}_1-\hat{B}_1)u(k+4)+\cdots+\hat{C}\hat{A}\hat{B}_1u(k+m-1)] \\
&+ [\hat{C}\hat{A}^{p-3}(\tilde{A}^2\tilde{B}_2-\tilde{A}\tilde{B}_2)\delta(k)+\hat{C}\hat{A}^{p-3}(\tilde{A}\tilde{B}_2-\tilde{B}_2)\delta(k+1) \\
&+ \hat{C}\hat{A}^{p-4}(\hat{A}\tilde{B}_2-\hat{B}_2)\delta(k+2)+\hat{C}\hat{A}^{p-5}(\hat{A}\hat{B}_2-\hat{B}_2)\delta(k+3) \\
&+ \hat{C}\hat{A}^{p-6}(\hat{A}\hat{B}_2-\hat{B}_2)\delta(k+4)+\cdots \\
&+ \hat{C}\hat{A}\hat{B}_2\delta(k+m-1)+\hat{C}\hat{B}_2\delta(k+m)] \\
&+ [\hat{C}\hat{A}^{p-3}(\tilde{A}^2\tilde{B}_3-\tilde{A}\tilde{B}_3)z(k)+\hat{C}\hat{A}^{p-3}(\tilde{A}\tilde{B}_3-\tilde{B}_3)z(k+1) \\
&+ \hat{C}\hat{A}^{p-4}(\hat{A}\tilde{B}_3-\hat{B}_3)z(k+2)+\hat{C}\hat{A}^{p-5}(\hat{A}\hat{B}_3-\hat{B}_3)z(k+3) \\
&+ \hat{C}\hat{A}^{p-6}(\hat{A}\hat{B}_3-\hat{B}_3)z(k+4)+\cdots \\
&+ \hat{C}\hat{A}\hat{B}_3z(k+m-1)+\hat{C}\hat{B}_3z(k+m)] \\
&+ [\hat{C}\hat{A}^{p-3}(\tilde{A}^2\tilde{B}_d-\tilde{A}\tilde{B}_3)d_{flt}(k)+\hat{C}\hat{A}^{p-3}(\tilde{A}\tilde{B}_d-\tilde{B}_d)d_{flt}(k+1) \\
&+ \hat{C}\hat{A}^{p-4}(\hat{A}\tilde{B}_d-\hat{B}_d)d_{flt}(k+2)+\hat{C}\hat{A}^{p-5}(\hat{A}\hat{B}_d-\hat{B}_d)d_{flt}(k+3) \\
&+ \hat{C}\hat{A}^{p-6}(\hat{A}\hat{B}_d-\hat{B}_d)d_{flt}(k+4)+\cdots \\
&+ \hat{C}\hat{A}\hat{B}_dd_{flt}(k+m-1)+\hat{C}\hat{B}_dd_{flt}(k+m)] \\
&- \hat{C}\hat{A}^{p-3}\tilde{A}^2[\tilde{B}_1u(k-1)+\tilde{B}_2\delta(k-1)+\tilde{B}_3z(k-1)+\tilde{B}_dd_{flt}(k-1)]
\end{aligned}
\tag{5.25}
$$

Therefore, the appropriate coefficients matrices Φ, H_{**}, and H_* in the p step ahead prediction equations of MPC in (5.15) and (5.16) can be generated from the equations

(5.8), (5.19) - (5.25) above. They are given below,

$$\Phi = \begin{bmatrix} \tilde{C}\tilde{A} \\ \tilde{C}\tilde{A}^2 \\ \vdots \\ \tilde{C}\tilde{A}^{t_{MS}-1} \\ \hat{C}\hat{A}\tilde{A}^{t_{MS}-1} \\ \hat{C}\hat{A}^2\tilde{A}^{t_{MS}-1} \\ \vdots \\ \hat{C}\hat{A}^{p-t_{MS}+1}\tilde{A}^{t_{MS}-1} \end{bmatrix} \tag{5.26}$$

$$H_{i1} = \begin{bmatrix} \tilde{C}\tilde{B}_i \\ \tilde{C}\tilde{A}\tilde{B}_i \\ \vdots \\ \tilde{C}\tilde{A}^{t_{MS}-3}\tilde{B}_i \\ \hat{C}\hat{A}\tilde{A}^{t_{MS}-2}\tilde{B}_i \\ \hat{C}\hat{A}^2\tilde{A}^{t_{MS}-2}\tilde{B}_i \\ \vdots \\ \hat{C}\hat{A}^{p-t_{MS}+1}\tilde{A}^{t_{MS}-2}\tilde{B}_i \end{bmatrix} \quad i = 1,\ 2,\ 3,\ d \tag{5.27}$$

The remaining coefficients matrices are expressed in the same way described in (4.35) - (4.44), with the new matrices derived in (5.26) - (5.29).

This model scheduling strategy for HMPC control algorithm can be demonstrated with an example of the GWG intervention which is shown in Figure 5.2. For the sake of simplicity, we assume there are only two components (HE and PA active learning (u_1 and u_2, respectively)) involved in the intervention adaptation. The simulation aims to compare the intervention effectiveness between the scenario using model scheduling strategy depicted in Figure 5.1 and the one using single linear model. Because the model scheduling strat-

$$H_1 = \begin{bmatrix} \tilde{C}\tilde{B}_1 & 0 & \cdots & 0 & 0 \\ \tilde{C}\tilde{A}\tilde{B}_1 - \tilde{C}\tilde{B}_1 & \tilde{C}\tilde{B}_1 & \cdots & 0 & 0 \\ \tilde{C}\tilde{A}^2\tilde{B}_1 - \tilde{C}\tilde{A}\tilde{B}_1 & \tilde{C}\tilde{A}\tilde{B}_1 - \tilde{C}\tilde{B}_1 & \ddots & \vdots & \vdots \\ \vdots & \vdots & \ddots & \vdots & \vdots \\ \tilde{C}\tilde{A}^{t_{MS}-2}\tilde{B}_1 - \tilde{C}\tilde{A}^{t_{MS}-3}\tilde{B}_1 & \tilde{C}\tilde{A}^{t_{MS}-3}\tilde{B}_1 - \tilde{C}\tilde{A}^{t_{MS}-4}\tilde{B}_1 & \cdots & \vdots & \vdots \\ \hat{C}\hat{A}(\tilde{A}^{t_{MS}-2}\tilde{B}_1 - \tilde{A}^{t_{MS}-3}\tilde{B}_1) & \hat{C}\hat{A}(\tilde{A}^{t_{MS}-3}\tilde{B}_1 - \tilde{A}^{t_{MS}-4}\tilde{B}_1) & \cdots & \vdots & \vdots \\ \hat{C}\hat{A}^2(\tilde{A}^{t_{MS}-2}\tilde{B}_1 - \tilde{A}^{t_{MS}-3}\tilde{B}_1) & \hat{C}\hat{A}^2(\tilde{A}^{t_{MS}-3}\tilde{B}_1 - \tilde{A}^{t_{MS}-4}\tilde{B}_1) & \cdots & \vdots & \vdots \\ \vdots & \vdots & \ddots & \hat{C}\hat{B}_1 & \vdots \\ \hat{C}\hat{A}^{m-t_{MS}+1}(\tilde{A}^{t_{MS}-2}\tilde{B}_1 - \tilde{A}^{t_{MS}-3}\tilde{B}_1) & \hat{C}\hat{A}^{m-t_{MS}+1}(\tilde{A}^{t_{MS}-3}\tilde{B}_1 - \tilde{A}^{t_{MS}-4}\tilde{B}_1) & \cdots & \hat{C}(\hat{A}\hat{B}_1 - \hat{B}_1) & \hat{C}\hat{B}_1 \\ \hat{C}\hat{A}^{m-t_{MS}+2}(\tilde{A}^{t_{MS}-2}\tilde{B}_1 - \tilde{A}^{t_{MS}-3}\tilde{B}_1) & \hat{C}\hat{A}^{m-t_{MS}+2}(\tilde{A}^{t_{MS}-3}\tilde{B}_1 - \tilde{A}^{t_{MS}-4}\tilde{B}_1) & \cdots & \hat{C}\hat{A}(\hat{A}\hat{B}_1 - \hat{B}_1) & \hat{C}\hat{A}\hat{B}_1 \\ \vdots & \vdots & \vdots & \vdots & \vdots \\ \hat{C}\hat{A}^{p-t_{MS}+1}(\tilde{A}^{t_{MS}-2}\tilde{B}_1 - \tilde{A}^{t_{MS}-3}\tilde{B}_1) & \hat{C}\hat{A}^{p-t_{MS}+1}(\tilde{A}^{t_{MS}-3}\tilde{B}_1 - \tilde{A}^{t_{MS}-4}\tilde{B}_1) & \cdots & \hat{C}\hat{A}^{p-m}(\hat{A}\hat{B}_1 - \hat{B}_1) & \hat{C}\hat{A}^{p-m}\hat{B}_1 \end{bmatrix} \quad (5.28)$$

$$H_i = \begin{bmatrix} \tilde{C}\tilde{B}_i & 0 & \cdots & 0 & 0 \\ \tilde{C}\tilde{A}\tilde{B}_i - \tilde{C}\tilde{B}_i & \tilde{C}\tilde{B}_i & \cdots & 0 & 0 \\ \tilde{C}\tilde{A}^2\tilde{B}_i - \tilde{C}\tilde{A}\tilde{B}_i & \tilde{C}\tilde{A}\tilde{B}_i - \tilde{C}\tilde{B}_i & \ddots & \vdots & \vdots \\ \vdots & \vdots & \ddots & \vdots & \vdots \\ \tilde{C}\tilde{A}^{t_{MS}-2}\tilde{B}_i - \tilde{C}\tilde{A}^{t_{MS}-3}\tilde{B}_i & \tilde{C}\tilde{A}^{t_{MS}-3}\tilde{B}_i - \tilde{C}\tilde{A}^{t_{MS}-4}\tilde{B}_i & \cdots & \vdots & \vdots \\ \hat{C}\hat{A}(\tilde{A}^{t_{MS}-2}\tilde{B}_i - \tilde{A}^{t_{MS}-3}\tilde{B}_i) & \hat{C}\hat{A}(\tilde{A}^{t_{MS}-3}\tilde{B}_i - \tilde{A}^{t_{MS}-4}\tilde{B}_i) & \cdots & \vdots & \vdots \\ \hat{C}\hat{A}^2(\tilde{A}^{t_{MS}-2}\tilde{B}_i - \tilde{A}^{t_{MS}-3}\tilde{B}_i) & \hat{C}\hat{A}^2(\tilde{A}^{t_{MS}-3}\tilde{B}_i - \tilde{A}^{t_{MS}-4}\tilde{B}_i) & \cdots & \vdots & \vdots \\ \vdots & \vdots & \ddots & \hat{C}\hat{B}_i & \vdots \\ \hat{C}\hat{A}^{p-t_{MS}+1}(\tilde{A}^{t_{MS}-2}\tilde{B}_i - \tilde{A}^{t_{MS}-3}\tilde{B}_i) & \hat{C}\hat{A}^{p-t_{MS}+1}(\tilde{A}^{t_{MS}-3}\tilde{B}_i - \tilde{A}^{t_{MS}-4}\tilde{B}_i) & \cdots & \hat{C}(\hat{A}\hat{B}_i - \hat{B}_i) & \hat{C}\hat{B}_i \end{bmatrix} \quad i = 2,\ 3,\ d \quad (5.29)$$

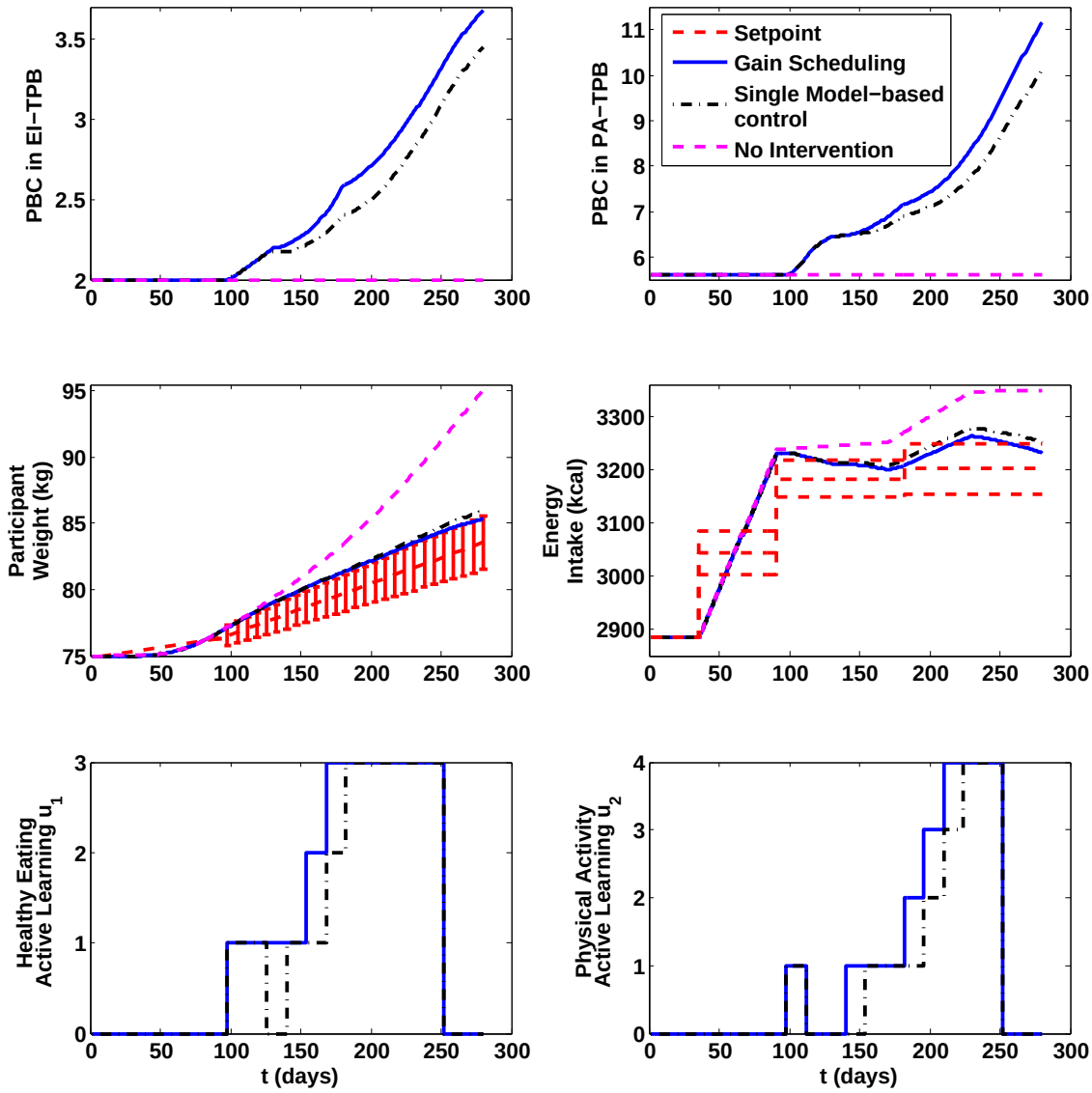

Figure 5.2: Example of Simulation Responses Using Gain-scheduling Parameter Varying Control in Figure 5.1 and the Single-model Based Control Strategy. Red Dash Lines Represent Setpoint Applied on a Daily Basis; Blue Solid Lines Represent the Participant's Response Using Model Scheduling Strategy; Black Dash-dot Lines Represents the Participant's Response Using Single Model-based Control, and the Pink Dash Lines are the Case with no Intervention.

Table 5.1: Model Parameters for the Simulation Studies in Section 5.2. Time Constants (τ_{i_j} where j Refers to the j-th Model), Delays (θ_i), and Self-regulation Adjustable Parameters (λ_r, λ_d) are in Units of Days.

Parameter	**EI-TPB**	**PA-TPB**	**Parameter**	**EI-TPB**	**PA-TPB**
b_1	3	1	e_1	6	4
n_1	2	7	m_1	3	8
p_1	1	2	c_1	2	2
τ_{1_1}	1	30	τ_{1_2}	1	30
τ_{2_1}	1	30	τ_{2_2}	1	30
τ_{3_1}	1	10	τ_{3_2}	10	60
τ_{4_1}	1	20	τ_{4_2}	10	70
τ_{5_1}	1	30	τ_{5_2}	10	80
τ_{1_3}	1	30	γ_{11}	1	0.7
τ_{2_3}	1	30	γ_{22}	1	0.5
τ_{3_3}	50	160	γ_{33}	1	0.7
τ_{4_3}	50	170	β_{41}	1	0.34
τ_{5_3}	50	180	β_{42}	1	0.27
$\theta_1 \ldots \theta_3$	0	0	β_{43}	1	0.13
$\theta_4 \ldots \theta_6$	0	0	β_{53}	0	0.08
θ_7, θ_8	0	0	β_{54}	1	0.42
k_{u_1}	0.006	0	θ_{u_1}	0	0
k_{u_2}	0	0.06	θ_{u_2}	0	0
λ_r	80	100	λ_d	80	110

egy will switch the model based on preset time, the predicted controlled variables over the receding horizon can be obtained more accurate than the ones using single linear model. Specifically, in this simulation example, three linear models are preset to describe the participant's behavioral response for three time frames during the intervention. The parameters of the model are listed in Table 5.1. The changes of the time constants in TPB models occur at day 130 and day 180, respectively, to make the participant's response in behavioral change more slowly. The change of the PBC inflows to the two TPB models indicate these parameter varying phenomenon. In this example, the scenario using gain-scheduling strategy understands and predicts that the participant's behavioral improvement is deteriorated

during the intervention due to the increase of the time constants in the TPB model, and that is why the controller using model scheduling strategy assigns the dosages of the intervention components more aggressive compared with the one using single model-based control strategy after the baseline program. As a result of the difference in dosage assignment, the PBC inflows to both TPB models increase faster in the scenario using gain scheduling strategy than the one using single model-based control, and the participant shows less weight increase and energy intake increase in the first scenario. At late pregnancy, the same participant is able to manage her weight gain and energy intake to be within the upper bound of IOM guidelines and EI reference values, respectively, with this more intensive intervention; while she can not achieve either her GWG goal or EI goal if she receives the dosage assigned by single model-based MPC controller. This gain-scheduling strategy is very useful for the future implementation of the GWG intervention, once more information and data is available through the pilot study and clinical trials to inform us of the nonlinearity within this GWG model.

5.3 Multi-Rate Digital Control

The filter design for multi-rate digital control is inspired by the fact that the measurement of energy intake might take place once a week, while other self-monitoring components, such as weight gain and PAL, are still measured daily. This has been pointed out to us by the behavioral scientists in this R01 funded research group who are currently implementing the pilot study and designing the clinical trial for the GWG adaptive behavioral intervention. The difference of the frequency in the measurement of self-monitoring components indicates the existence of noise and other inaccuracies. Thus, this section focuses on how to estimate these unknown variables or missing measurement data by the use of the filter design for this multi-rate sampled-data system.

Multi-rate systems are encountered when some signals of interest are sampled at a

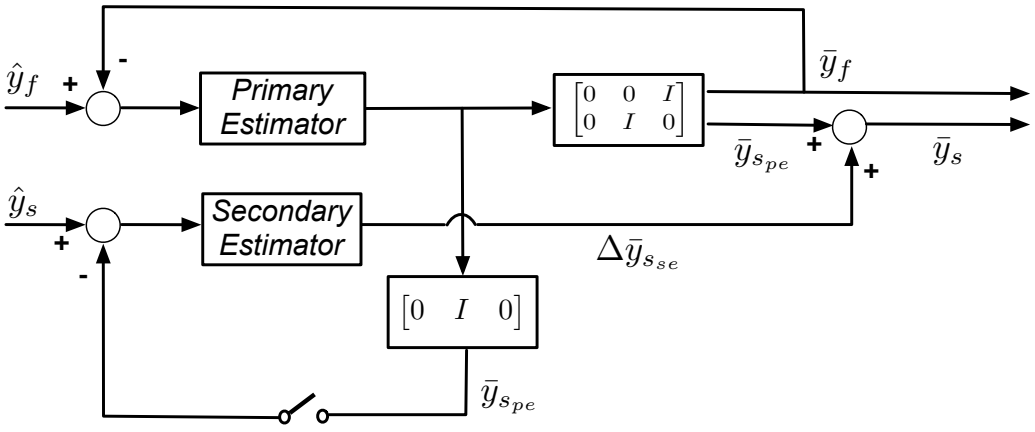

Figure 5.3: Cascade Structure of the Multi-rate Filter [14], where $\hat{y}_f$ and $\hat{y}_s$ Refer to the Controlled Variables Measured at Faster Sampling and Slower Sampling, respectively; $\bar{y}_f$ and $\bar{y}_s$ Represent the Estimations of Controlled Variables Sampled at Higher and Lower Frequency, respectively.

different rate than others. This situation is likely to occur when it is impossible for us to sample all the physical variables of a system at a single rate. It is expected that multi-rate controllers would give better performance than single-rate controllers, because of the extra degrees of freedom they allow in manipulating control variables [90].

The formulation of multi-rate sampled data system using MPC is developed based on the one described in [14], and however some changes are necessary in order to fit our existing 3 DoF HMPC algorithm in behavioral intervention problem settings. Figure 5.3 shows the cascade filtering strategy for the multi-rate system. We assume that $\hat{y}_f$ is the measurement with faster sampling (i.e., in this case, GWG daily measurements); and $\hat{y}_s$ is the measurements with slow frequency (i.e., in this case, EI weekly measurements). The main principle in this cascade structure for multi-rate filter is that we use the faster measurement to estimate all the state variables, while the slower measurement will be used to do the adjustment on that particular output variable with slow sampling.

Let us assume that the following equations are used to describe the model,

$$x(k,j) = Ax(k,j-1) + B_u u(k,j-1) + B_d d(k,j-1) \tag{5.30}$$

$$y_f(k,j) = C_f x(k,j) + w(k,j-1) \tag{5.31}$$

$$y_s(k,j) = C_s x(k,j) \tag{5.32}$$

where y_f is the controlled variable with fast sampling, y_s is the controlled variable with slow sampling, u is the manipulated variable, d is the disturbance variable, w is the output disturbance, respectively. We declare that τ_f is the sampling time of measurements for y_f, τ_s is the sampling time of measurements for y_s. Therefore, for each sampling of y_s, $N = \frac{\tau_s}{\tau_f}$ measurements of y_f will be available. k notates the k-th time measurement of variable y_s, and j denotes the j-th time measurement of variable y_f, where $j \in 0, 1, \cdots, N-1$. When $j = 0$, it indicates that the measurements of both y_f and y_s are available.

The available measurements are described as follows:

$$\hat{y}_f(k,j) = C_f x(k,j) + w(k,j-1) + \upsilon_f(k,j) \tag{5.33}$$

$$\hat{y}_s(k,j) = C_s x(k,j) + \upsilon_s(k,j) \tag{5.34}$$

where $\hat{y}_f$ and $\hat{y}_s$ represent the measurements for fast sampling and slow sampling, respectively. $\upsilon_f(k,j)$ and $\upsilon_s(k,j)$ are the measurement noises.

For convenience of notation, we use the differenced form of the disturbance and system models that are similar to (5.13) and 5.14, which are described as follows,

$$X(k,j) = \tilde{A}X(k,j-1) + \tilde{B}_u \Delta u(k,j-1) + \tilde{B}_d \Delta d(k,j-1) \tag{5.35}$$

$$\hat{Y}(k,j) = \tilde{C}X(k,j) + V(k,j) \tag{5.36}$$

where

$$
\begin{aligned}
X(k,j) &= [\Delta x^T(k,j) \quad y_s^T(k,j) \quad y_f^T(k,j)]^T \\
\hat{Y}(k,j) &= [y_s^T(k,j) \quad y_f^T(k,j)]^T \\
V(k,j) &= [\upsilon_s^T(k,j) \quad \upsilon_f^T(k,j)]^T \\
\tilde{A} &= \begin{bmatrix} A & 0 & 0 \\ C_sA & 0 & 0 \\ C_fA & 0 & 0 \end{bmatrix};\ \tilde{B}_i = \begin{bmatrix} B_i \\ C_sB_i \\ C_fB_i \end{bmatrix},\ i = u,d; \\
\tilde{C} &= \begin{bmatrix} 0 & I & 0 \\ 0 & 0 & I \end{bmatrix};
\end{aligned}
$$

Here $\Delta * (k) = *(k) - *(k-1)$.

The multirate system shown in Figure 5.3 features cascade structure. It can be written in the following standard form.

$$\bar{X}(k,j|k,j-1) = \tilde{A}\bar{X}(k,j-1|k,j-1) + \tilde{B}_u\Delta u(k,j-1) + \tilde{B}_d\Delta d(k,j-1) \tag{5.37}$$

$$\bar{X}(k,j|k,j) = \bar{X}(k,j|k,j-1) + K_{cas}(j)\{\hat{Y}(k,j) - \tilde{C}\bar{X}(k,j|k,j-1)\} \tag{5.38}$$

where

$$K_{cas}(j) = K_f = \begin{bmatrix} K_{fx} \\ K_{fys} \\ K_{fyf} \end{bmatrix} \quad \text{for } j = 1,2,\cdots,N-1 \tag{5.39}$$

$$K_{cas}(0) = \left[\begin{array}{c|c} 0 & K_{fx} \\ K_s & (I-K_s)K_{fys} \\ 0 & K_{fyf} \end{array}\right]; \tag{5.40}$$

Table 5.2: Model Parameters for the Simulation Studies in Section 5.3. Time Constants (τ_i), Delays (θ_i), and Self-regulation Adjustable Parameters (λ_r, λ_d) are in Units of Days.

Parameter	**EI-TPB**	**PA-TPB**	**Parameter**	**EI-TPB**	**PA-TPB**
b_1	3	1	e_1	6	4
n_1	2	7	m_1	3	8
p_1	1	2	c_1	2	2
τ_1	1	30	γ_{11}	1	0.7
τ_2	1	30	γ_{22}	1	0.5
τ_3	1	10	γ_{33}	1	0.7
τ_4	1	10	β_{41}	1	0.34
τ_5	1	20	β_{42}	1	0.27
$\theta_1 \ldots \theta_3$	0	0	β_{43}	1	0.13
$\theta_4 \ldots \theta_6$	0	0	β_{53}	0	0.08
θ_7, θ_8	0	0	β_{54}	1	0.42
k_{u_1}	0.003	0	θ_{u_1}	0	0
k_{u_2}	0	0.015	θ_{u_2}	0	0
k_{u_3}	0.001	0.005	θ_{u_3}	0	0
λ_r	80	100	λ_d	100	155

K_s can be tuned between the values 0 and 1. The greater K_s is, the secondary state estimator relies more on the measurements of y_s, and this also means the controller will be more aggressive. When the measurements of y_f and y_s are both available, (5.40) can be used to estimate the state variables and the controlled variables. However, if the measurements of y_s are not accurate or not obtained, which means $K_s = 0$, (5.40) reduces to (5.39) without approximation. In this case, only the fast sampling measurements y_f will be used for the state estimation. The details of how to derive the formulation of estimators can also be found in [14].

This cascade filter design for the dual-rate control system can be demonstrated using the GWG example considered earlier. The simulation uses the same controller design for the sequential decision policies that described in Section 4.4.4 with move size constraints $| \Delta u(k) | \leq 1$. All simulations are using parameters listed in Table 5.2. The parameters for

the HMPC are as follows: $p = 25$, $m = 22$, $Q_y = [1; 50]$, $\alpha_r = [0; 0]$, $\alpha_d = 0$, and $f_a = 1$.

Figure 5.4 shows the case for slow tuning of secondary estimator with $K_s = 0.3$, while Figure 5.5 shows the case for fast tuning with $K_s = 0.8$. From the comparison of both cases, we can see that the smaller K_s is, the less aggressive the controller will be. In Figure 5.4, u_1 is reduced from base dose to zero at the beginning of the intervention, even though the participant's EI and weight are outside the setpoints, respectively. The intervention does not get augmented back to the baseline until week 18, and stays the course for another four weeks. In order to make sure the participant will achieve her GWG goal, both u_1 and u_2 are augmented above the baseline program step by step at each intervention decision starting from week 22, and then u_2 gets reduced at week 34 when the controller predicts that the participant will be able to achieve her GWG goals very soon. This simulation helps verify again that the augmentations and reductions of the intervention components follow the sequential decision policies described in Section 4.4.4. For the scenario with $K_s = 0.8$ in Figure 5.5, the controller is a little more aggressive compared with the one in Figure 5.4. Because the controller does not reduce the intervention components at the beginning of the intervention, this participant is able to manage her GWG within the IOM guidelines, and control her EI within the reference values, earlier than the scenario depicted in Figure 5.4, respectively. Meanwhile, the intervention starts to get reduced around week 30 in order to avoid the overdose scenario for this particular participant.

Figure 5.6 shows the simulation responses using single-rate control system. This can be achieved by setting $K_s = 0$. In this example, only GWG measurement is available to estimate both the state variables and the controlled variables. This simulation result illustrates that this participant is still able to achieve the goal with adaptive intervention, and however, the result is not as satisfactory as the ones in Figure 5.4 and Figure 5.5. Specifically, this participant was not able to achieve her GWG goal even before the intervention stops. Meanwhile, the missing EI measurements makes the estimation of EI not accurate

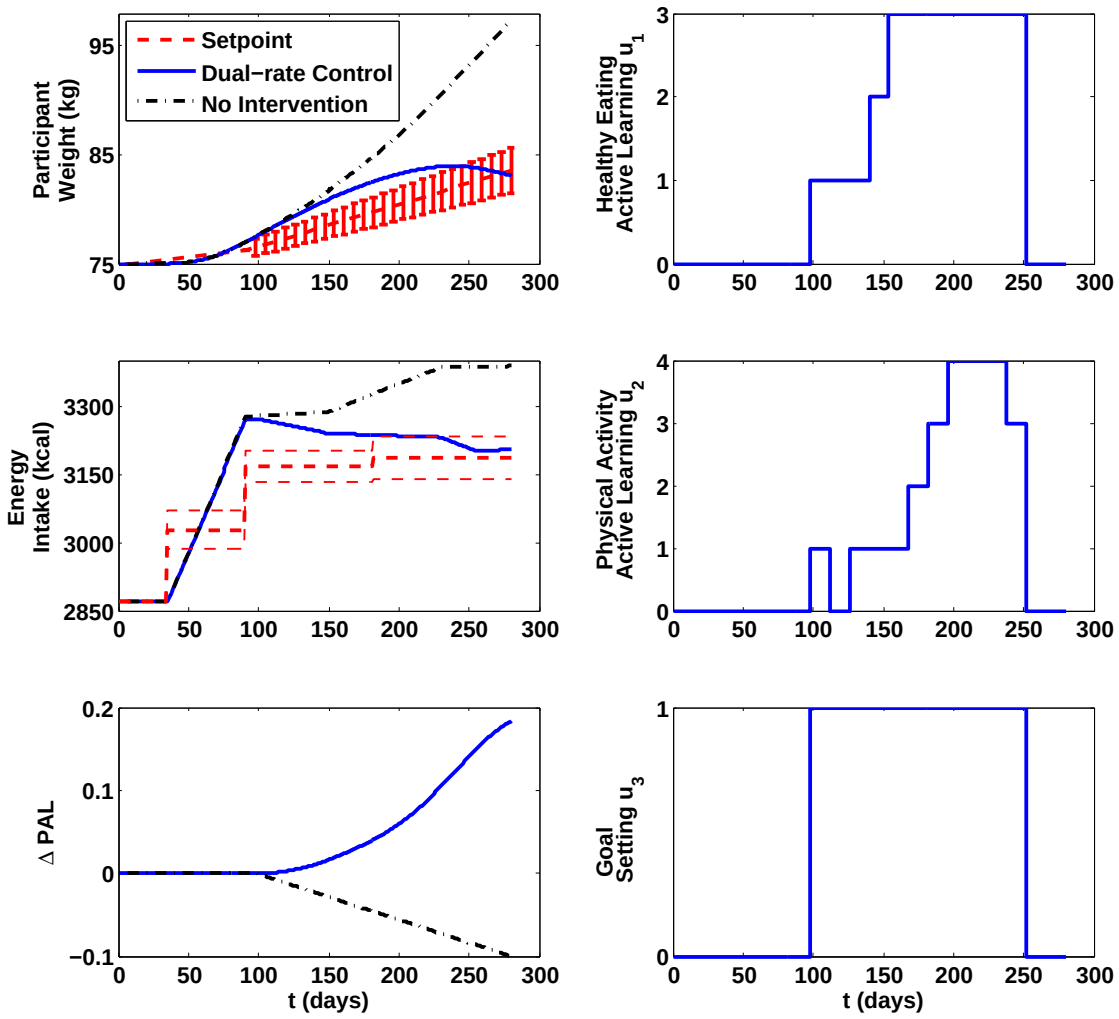

Figure 5.4: Example of Simulation Responses Using Cascade Structure of the Multi-rate Filter per Figure 5.3 with $K_s = 0.3$ for Slow Tuning of the Secondary Estimator. Red Dash Lines Represent Setpoint applied on a Daily Basis; Blue Solid Lines Represent the Participant's Response for Maternal Body Mass, Energy Intake (EI), Physical Activity Level (PAL), and the Intervention Component Dosages; Black Dash-dot Lines Represents the Case with no Intervention.

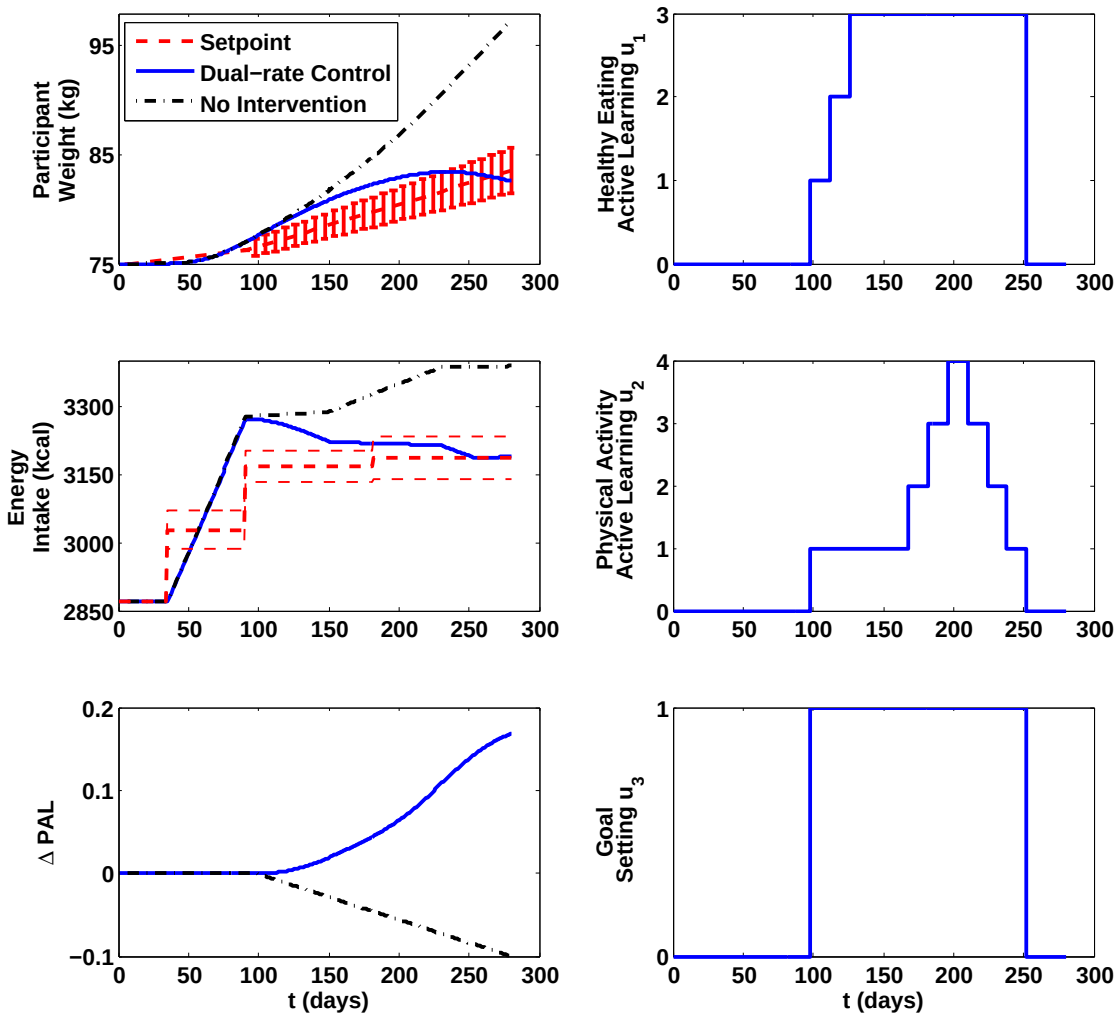

Figure 5.5: Example of Simulation Responses Using Cascade Structure of the Multi-rate Filter per Figure 5.3 with $K_s = 0.8$ for Fast Tuning of the Secondary Estimator. Red Dash Lines Represent Setpoint applied on a Daily Basis; Blue Solid Lines Represent the Participant's Response for Maternal Body Mass, Energy Intake (EI), Physical Activity Level (PAL), and the Intervention Component Dosages; Black Dash-dot Lines Represents the Case with no Intervention.

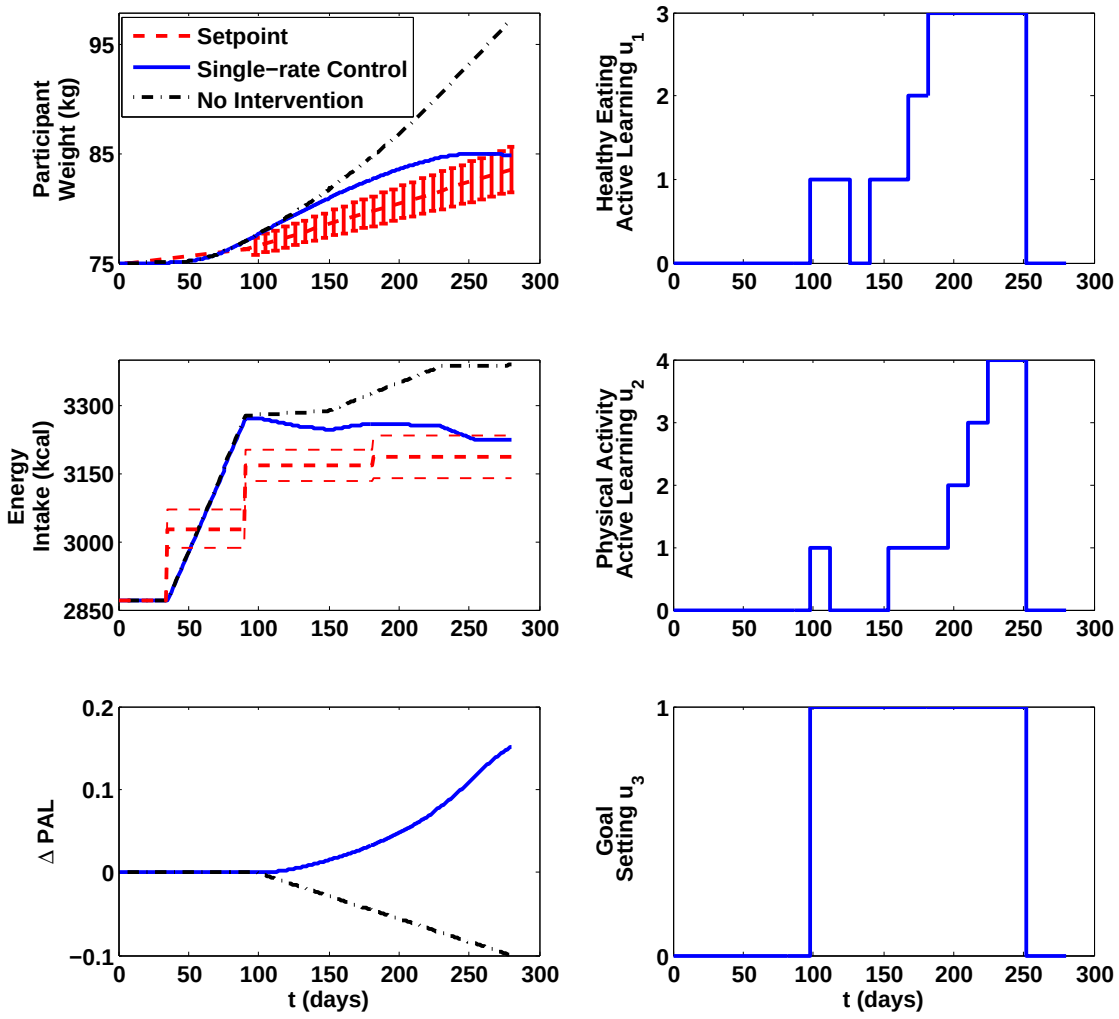

Figure 5.6: Example of Simulation Responses Using Single-rate Control System with $K_s = 0$. Red Dash Lines Represent Setpoint Applied on a Daily Basis; Blue Solid Lines Represent the Participant's Response for Maternal Body Mass, Energy Intake (EI), Physical Activity Level (PAL), and the Intervention Component Dosages; Black Dash-dot Lines Represents the Case with no Intervention.

enough, compared with the two scenarios using dual-rate control system illustrated in Figure 5.4 and Figure 5.5, which is the reason why the intervention is still less aggressive, even though the participant's initial condition is not promising.

The simulation examples in this section demonstrate the tuning rules of the cascade structure of the multi-rate filter depicted in Figure 5.3. In contrast to the simulation result using single-rate control system, it is easy to conclude that the cascade filter design for the dual-rate control system developed in this chapter offers extra degree of freedom, and usually leads to better and more effective intervention results in this GWG intervention. Furthermore, when the EI measurements are available and accurate, one can rely more on those measurements, get more accurate estimation of the controlled variables, and thus take more appropriate control action.

5.4 Summary

In summary, this chapter has introduced two specific enhancements to the simulation to address real-life scenarios in the GWG intervention using: gain-scheduling parameter varying control, and the cascade filter design for multi-rate control system. Both improvements are proposed on the basis of hybrid model predictive control (HMPC) framework implemented with 3 DoF tuning rules. For the gain-scheduling parameter varying control scenario, the simulation example is presented to show that the model scheduling strategy is able to provide more accurate prediction of controlled variables over the prediction horizon, and thus take more appropriate and earlier actions to assign the dosage when compared with the scenario using single linear model. The simulation examples using cascade structure of the multi-rate filter not only demonstrate how the secondary estimator works with the primary estimator using fast sampling measurements to better estimate the controlled variables sampled at low frequency, but also illustrate how the secondary estimator can be tuned to influence the control system, and particularly why this multi-rate control system

is preferable to the single-rate control system for GWG problem.

The two improvements presented in this chapter aim to address the real-life scenarios in the GWG intervention. Whether and how to integrate these strategies will largely depend on the implementation of the pilot studies, the clinical trials and their corresponding results obtained by our Penn State collaborators.

Chapter 6

SUMMARY AND CONCLUSIONS

6.1 Conclusions

This dissertation has demonstrated how dynamical systems modeling and control engineering methods can be useful for better understanding, designing, and ultimately optimizing the performance of sequential behavioral interventions through a time-varying adaptive framework, with the goal of increasing intervention effectiveness and improving participant response. Excessive gestational weight gain is a very serious public health concern in the USA, and is a perfect representative example involving multiple intervention components and featuring pre-defined sequential decision policies; therefore it is used to exemplify the design procedure for sequential behavioral interventions in this dissertation.

The comprehensive dynamical systems model for a behavioral intervention to manage GWG and regulate fetal weight gain developed in this dissertation relies on a mechanistic energy balance model and the dynamical behavioral models which incorporate some well-accepted concepts in psychology and behavioral science, such as the Theory of Planned Behavior (TPB), self-regulation theory, intervention delivery dynamics and hypothetical "IF-THEN" decision rules recommended by behavioral scientists. The fluid analogy for the TPB inspires to conceptualize and establish the overall schematic representation for the adaptive intervention in terms of a network of production inventory systems in supply chain management which is a classical problem in enterprise systems that has application in many problem arenas. This conceptualization allows us to build a bridge between traditional process control problem settings with this unconventional one, and facilitates the application of classical control engineering and modern control engineering approaches to design the intervention. Self-regulation is postulated as a feedback controller to reflect the capacity of individuals to alter the behavior, and it is initially parametrized as

derivative-only controller to show that the improvements of the outcome during the intervention strengthen individual's confidence in aiming to achieve the intervention goal. The overall dynamical model illustrates the preliminary design and theoretical implementation of an adaptive behavioral intervention based on a set of hypothetical decision rules. It can play a useful role in the evaluation of decision policies, and the corresponding simulations can aid the intervention scientists to test and select the decision rules.

From the control engineering perspective, a comprehensive dynamical systems model can facilitate the understanding of the intervention "process" dynamics, and therefore, the formulation of the controller can be achieved on the basis of the nominal model of this intervention. Self-regulation in adaptive interventions is the first feedback control process that catches our attention. In Chapter 3, the manner in which self-regulation is modeled in the system was revisited and reevaluated. The advanced controller formulations used in Chapter 3 are model-based control involving two-degree-of-freedom (2 DoF) Internal Model Control (IMC), the cascade control relying on IMC strategy, and the weighted cascade control. The controller design through these formulations allows significant flexibility in depicting a participant's self-regulatory behavior by tuning the controller adjustable parameters, and represents a substantial improvement to using a classical feedback control approach. The comparison of these algorithms was made based on the analysis of the advantages and disadvantages these controllers showed in the design procedures and simulation examples. The simulation studies demonstrate how adaptive interventions offer greater degrees of efficacy according to a participant's changing needs and responses, indicate why fixed interventions may have limited success among overweight and obese pregnant women in the prevention of excessive GWG, and illustrate how intra-individual variabilities and inter-individual variabilities play an important role in the intervention outcomes.

With the integration of the improved formulation of self-regulation developed in Chap-

ter 3 into the dynamical systems model, the "open-loop" model that serves as the basis for the design of optimized adaptive sequential behavioral intervention was obtained. Chapter 4 presented a novel intervention paradigm using Hybrid Model Predictive Control (HMPC) algorithm to systematically tailor treatment policies over time. The HMPC algorithm relied on the use of an MLD structure with constraints. Due to the unique resource considerations and clinical constraints, such as sequential decision making, the patient-friendly intervention and discrete-valued nature of the intervention components, the user-specified dosage sequence tables were proposed, the algorithm enforcing the manipulation of one input at a time was developed, and the switching time strategy to assign the dosages at time intervals less frequent than the measurement sampling intervals was introduced. The mixed-integer linear constraints were utilized to account for all these new improvements which can then be incorporated into the HMPC framework. The design procedure of HMPC controller was illustrated on a GWG problem involving multiple components with different sets of clinically proposed dosage sequence. The potential usefulness of such an intervention framework was demonstrated through case studies, and the comparison between HMPC-based intervention and adaptive intervention relying on "IF-THEN" rules was made to prove the benefits of hybrid predictive control for optimized adaptive interventions. Although the HMPC controller design is based on the adaptive sequential behavioral interventions to prevent excessive GWG, it is also applicable to other similar adaptive behavioral intervention programs featuring multiple intervention components with sequential decision policies.

This dissertation also extended the simulation work for the GWG intervention to address scenarios which may potentially be necessary in a real-life clinical trial. The gain scheduling parameter control algorithm featuring the model scheduling strategy was developed to address the nonlinearities in the model; this was readily embedded into the HMPC framework. The cascade filter for dual-rate control system was introduced in order

to address the differences in frequency for measurements. Numerical examples illustrated the basic working of these two enhancements.

6.2 Future Research Directions

As this dissertation presents an initial demonstration of the potential for real-world applications of adaptive sequential behavioral interventions and provides a plausible "proof of concept" of the approach, there are several interesting directions for future work.

6.2.1 System Identification Modeling

The original work was funded by a roadmap R21 grant (R21 DA024266) and K25 grant (K25 DA021173) from the National Institute on Drug Abuse (NIDA) and the Office of Behavioral and Social Sciences Research (OBSSR). This research has now been funded to examine this topic in particular with an R01 grant (R01 HL119245) from the National Heart, Lung, and Blood Institute (NHLBI).

As a result of this R01, various aspects of this work are being piloted during 2014, and a novel design of clinical trial will be implemented in the year 2015. The data from the pilot study and the clinical trial will allow us to perform system identification of the TPB and self-regulation models, and the evaluation of the GWG energy balance model. With the experimental validation of the model, the future evaluation of decision rules is enabled by examining the effectiveness of the intervention framework. Furthermore, the pilot testing and clinical trials are expected to inform the refinement of some structural aspects of the simulation model, such as the proper structure of the self-regulation problem as described in Section 3.3.3, and how additional measurements (e.g., physical activity) can influence the problem. The ultimate goal is to better use control systems engineering approach to optimize the adaptive sequential behavioral interventions by developing a real-life implementation of the HMPC-based intervention.

6.2.2 Experimental Validation of the Control Scheme

As this work presents a novel intervention paradigm using a control-oriented approach, it is important to validate the HMPC control scheme. Notably, variability between the participants and in dose-response dynamics pose a major challenge for widespread use of such an intervention framework. Consequently, with the clinical trials implemented and model obtained from system identification, it is critical to examine and enhance robustness to plant-model mismatch. Meanwhile, including the features of gain-scheduling MPC strategy as discussed in Section 5.2 in an intervention will better personalize the decision policies, especially for the intra-individual variability case. However, more information regarding the scheduling variables will be obtained from the clinical trials and it needs further experimental validation as well.

6.2.3 Incorporating Infrequent Measurements in Kalman Filter

In Section 5.3, the cascade filter for dual-rate control system was introduced in order to address the differences in frequency for measurements. The real-life GWG clinical trials inform us that there may exist some infrequent but accurate measurements for energy intake or other variables which are sampled at irregular intervals instead of daily or even weekly. Therefore, future work on designing kalman filter to incorporate such infrequent measurements so that the control system can fully make use of these data in decision making is very important.

6.2.4 Hybrid Model Predictive Control with Temporal Logic

In Chapter 4, propositional logic was used to generate the linear inequalities associated with pre-defined dosage sequence, which can be embedded into the Mixed Logical Dynamical (MLD) systems for the hybrid systems. However, propositional logic can not specify the following situations between variables, such as “proposition P will eventually

be true at some future time", "proposition P will always be true throughout the future", "P will hold to be true until Q becomes true" or "P must be true unless". That is why additional linear inequalities or the introduction of additional binary variables to the traditional MLD model is necessary to enforce the constraints associated with the time-varying sequential decision policies.

Linear temporal logic (LTL) is a popular formalism for the specification and verification of concurrent and reactive systems [91], and it is an extension of classical propositional logic which extends classical operators such as "NOT", "AND", "OR", "IMPLICATION" with "EVENTUALLY", "ALWAYS", "UNTIL" AND "UNLESS". Most approaches that use LTL adopt a discrete model of time, where a run of a system produces a sequence of observation.

The other most widely known extension of propositional logic is metric temporal logic (MTL) in which the modalities of LTL are augmented with timing constraints [92]. It extends all the temporal operators with real intervals.

The main reason to consider the use of temporal logic in the future is that it can address the ordering of the event, which indicates its capability to handle more complex sequential decision policies in behavioral health. For example, the augmentation rule that the increase of physical activity active learning can occur only one assessment cycle after healthy eating active learning reaches its full augmentation, can be easily expressed with "UNTIL" operator in temporal logic. Therefore, the formulation of LTL or MTL associated with the dosage sequence in behavioral intervention, and its integration into the traditional MLD system represent a promising approach and an interesting research direction for complex sequential decision policies in behavioral interventions.

6.2.5 Adaptive Intervention for Infant Birth Weight

In Section 2.8, we expanded our work to discuss how the intervention can not only manage GWG for the mother, but also alter the obesogenic fetus environment to regulate infant birth weight. Based on the adaptive GWG intervention model, an intergenerational fetal energy balance model was included to examine the effects of creating a healthy maternal-fetus eating and physical activity environment on infant birth weight. In this exploratory simulation work, the result is generated and obtained based on the energy balance model and artificial parameters. Therefore, just like the GWG intervention, an observational trial is necessary to fully validate this model and observe its true usefulness. This fetal birth weight model, together with the GWG intervention model can enable controller design which achieves the automated dosages using Hybrid Model Predictive Control algorithm, with the ultimate goal as to test the effectiveness of a real-life implementation of our intervention on both GWG and infant birth weight (i.e., short term effects). Further, the fetal birth weight model could be expanded to examine the long-term sustainable effects of individually tailored adaptive interventions on the eating and physical activity environments of mothers and their offspring. Specifically, future extensions of the model might include the impact of changes in percent breastfeeding and use of controlling feeding practices on post-partum weight retention and child weight [7].

6.2.6 Metabolic Model for Gestational Diabetes

As mentioned in earlier chapter, excessive GWG is a strong predictor of the development of obesity and diabetes for both childbearing women and their offspring. Gestational diabetes (or gestational diabetes mellitus, GDM) is a condition in which women without previously diagnosed diabetes exhibit high blood glucose levels during pregnancy (especially during their third trimester). It has long been known that women with a history of GDM are at increased risk of developing type 2 diabetes mellitus (type 2 DM) later in life,

and this was originally the purpose of identifying GDM.

As with diabetes mellitus in pregnancy in general, babies born to mothers with untreated gestational diabetes are typically at increased risk of problems such as being large for gestational age (LGA), low blood sugar, and jaundice [93, 94]. If untreated, it can also cause seizures. Gestational diabetes is a treatable condition and women who have adequate control of glucose levels can effectively decrease these risks. The food plan is often the first recommended target for strategic management of GDM. Generally, the treatment of gestational diabetes includes regular monitoring of blood sugar levels and eating a carefully controlled diet prescribed by a health care professional. It also includes regular exercise appropriate to pregnancy as prescribed.

Therefore, the treatment of GDM is very close to the behavioral interventions to prevent GWG; both of them rely on healthy eating habits and proper physical activity. If it is possible to establish a metabolic model for gestational diabetes, the dynamical systems model framework can also play a significant role in helping manage and treat the gestational diabetes during women's pregnancy.

BIBLIOGRAPHY

[1] Y. Dong, D. E. Rivera, D. S. Downs, J. S. Savage, D. M. Thomas, and L. M. Collins. Hybrid model predictive control for optimizing gestational weight gain behavioral interventions. In *Proceedings of the 2013 American Control Conference*, pages 1970 – 1975, Washington, D.C, USA, June 17 - June 19 2013.

[2] N. F. Butte, K. J. Ellis,W.W.Wong, J. M. Hopkinson, and E. O. Smith. Composition of gestational weight gain impacts maternal fat retention and infant birth weight. *Am J Obst Gynecol*, 189(5):1423–1432, 2003.

[3] N. F. Butte, W. W. Wong, M. S. Treuth, K. J. Ellis, and E. O. Smith. Energy requirements during pregnancy based on total energy expenditure and energy deposition. *Am J Clin Nutr*, 79(5):1078–1087, 2004.

[4] D. M. Thomas, J. E. Navarro-Barrientos, D. E. Rivera, S. B. Heymsfield, C. Bredlau,L. M. Redman, C. K. Martin, S. A. Lederman, L. M. Collins, and N. F. Butte. A dynamic energy balance model predicting gestational weight gain. *Am J Clin Nutr*, 95:115–122, 2012.

[5] Institute of Medicine National Research Council. *Weight gain during pregnancy: reexamining the guidelines.* The National Academies Press, Washington, DC, 2009.

[6] D. S. Downs and J. S. Savage. Decision rules for an adaptive GWG intervention. *Personal communication*, 2012.

[7] J. S. Savage, D. S. Downs, Y. Dong, and D. E. Rivera. Control systems engineering for optimizing a prenatal weight gain intervention to regulate infant birth weight. *American Journal of Public Health*, 104(7):1247–1254, July 2014.

[8] E.B. Hekler, M. P. Buman, N. Poothakandiyl, D. E. Rivera, J. M. Dzierzewski, A. Aiken-Morgan, C. S. McCrae, B. L. Robers, M. Marsiski, and P. R. Giacobbi. Exploring behavioral markers of long-term physical activity maintenance: A case study of system identification modeling within a behavioral intervention. *Health Education and Behavior*, 40(IS):51S – 62S, 2013.

[9] C. S. Carver and M. F. Scheier. *On the Self-Regulation of Behavior*. New York, 1998.

[10] Y. Dong, D. E. Rivera, D. M. Thomas, J. E. Navarro-Barrientos, D. S. Downs, J. S. Savage, and L. M. Collins. A dynamical systems model for improving gestational weight gain behavioral interventions. In *Proceedings of the 2012 American Control Conference*, pages 4059 – 4064, Montreal, Quebec, Canada, June 27 - June 29 2012.

[11] K. A. Bollen. *Structural Equations with Latent Variables*. John Wiley & Sons, Inc, 1989.

[12] C. Brosilow and B. Joseph. *Techniques of model-based control*. Prentice Hall PTR, Upper Saddle River, New Jersey, 2002.

[13] E. R. Camacho and C. Bordons. *Model predictive control in the process industry*. Springer, London, 1999.

[14] J. H. Lee, M. C. Gelormino, and M. Morari. Model predictive control of multi-rate sampled-data systems: a state space approach. *Int. J. Control*, 55(1):153–191, 1992.

[15] D. E. Rivera, M. D. Pew, and L. M. Collins. Using engineering control principles to inform the design of adaptive interventions: A conceptual introduction. *Drug and Alcohol Dependence*, 88S:S31–S40, 2007.

[16] P.Wellstead, E. Bullinger, D. Kalamatianos, O. Mason, and M. Verwoerd. The role of control and system theory in systems biology. *Annual Reviews in Control*, 32(1):33–47, 2008.

[17] A. C. Ahn, M. Tewari an C. Poon, and R. S. Phillips. The clinical applications of a systems approach. *PLoS Med*, 3(7):e209, 2006.

[18] R. Vanerwater and D. E. Davison. A dynamic control approach to studying the effectiveness of rewards in inducing behavior and attitude change. In *Proceedings of the IEEE International Conference on Control and Automation*, pages 1062 – 1067, Christchurch, New Zealand, December 9 - December 11 2009.

[19] R. Vanderwater and D. E. Davison. Using rewards to change a person's behavior: a double-integrator output-feedback dynamic control approach. In *Proceedings of the 2011 American Control Conference*, pages 4046–4052, Montreal, Quebec, Canada, June 29 - July 1 2012.

[20] D. E. Davison, R. Vanerwater, and K. Zhou. A control-theory reward-based approach to behavior modification in the presence of social-norm pressure and conformity pressure. In *Proceedings of the 2011 American Control Conference*, pages 1861–1866, San Francisco, June 27-June 29 2011.

[21] J. D. Schwartz, W. Wang, and D. E. Rivera. Optimal tuning of process control-based decision policies for inventory management in supply chains. *Automatica*, 42:1311–1320, 2006.

[22] W. Wang and D. E. Rivera. Mode predictive control for tactical decision-making in semiconductor manufacturing supply chain management. *IEEE Trans. Control Systems Tech.*, 16(5):841–855, 2008.

[23] N. N. Nandola and D. E. Rivera. An improved formulation of hybrid model predictive control with application to production-inventory systems. *IEEE Trans. Control Systems Tech.*, 21(1):121–135, 2013.

[24] R. Neck. Control theory and economic policy: Balance and perspectives. *Annual Reviews in Control*, 33(1):79–88, 2009.

[25] L. M. Collins, S. A. Murphy, and K. L. Bierman. A conceptual framework for adaptive preventive interventions. *Prevention Science*, 5(3):185–196, 2004.

[26] A. Zafra-Cabeza, D. E. Rivera, L. M. Collins, M. A. Ridao, and E. F. Camacho. A risk-based model predictive control approach to adaptive interventions in behavioral health. *IEEE Trans. Control Systems Tech.*, 21(4):891–901, 2011.

[27] S. Kumar, W. Nilsen, M. Pavel, and M. Srivastava. Mobile health: revolutionizing healthcare through transdisciplinary research. *Computer*, 46(1):28–35, 2013.

[28] S. A. Murphy, D. W. Oslin, A. J. Rush, J. Zhu, and MCATS. Methodological challenges in constructing effective treatment sequences for chronic psychiatric disorders. *Neuropsychopharmacology*, 32(2):257–262, 2007.

[29] Y. Dong, S. Deshpande, D. E. Rivera, D. S. Downs, and J. S. Savage. Hybrid model predictive control for sequential decision policies in adaptive behavioral interventions. In *Proceedings of the 2014 American Control Conference*, pages 4198–4203, Portland, Oregon, USA, June 4 - June 6 2014.

[30] S. Deshpande, N. Nandola, D.E. Rivera, and J. Younger. A control engineering approach for designing an optimized treatment plan for fibromyalgia. In *Proceedings of the 2011 American Control Conference*, pages 4798 – 4803, San Francisco, CA, June 29 - July 1 2011.

[31] K. P. Timms, D. E. Rivera, M. E. Piper, and L. M. Collins. A hybrid model predictive control strategy for optimizing a smoking cessation intervention. In *Proceedings of the 2014 American Control Conference*, pages 1800 – 1805, Portland, Oregon, USA, June 4 - June 6 2014.

[32] F. S. Collins. The future of personalized medicine. *NIH Meline Plus*, 5:2–3, 2010.

[33] H. Lei, I. Nahum-Shani, K. Lynch, D. Oslin, and S. A. Murphy. Using sequential, multiple assignment, ranomized trial (smart) designs to build individualized

[34] treatment sequences. Technical report, The Methodology Center, Penn State Univ, 2004.

[35] A. Beyerlein, B. Schiessl, N. Lack, and R. von Kries. Optimal GWG ranges for the avoidance of adverse birth weight outcomes: a novel approach. *Am J Clin Nutr*, 90:1552–1558, 2009.

[36] P. Moreira, C. Padez, I. Mourao-Carvalhal, and V. Rosado. Maternal weight gain during pregnancy and overweight in portugeses children. *Int J Obes*, 31:608–614, 2007.

[37] Centers for Disease Control. 2011 pregnancy nutrition surveillance nation summary of trends in maternal health indicators. 2011.

[38] American College of Obstetricians and Gynecologists. Committee option no. 549: weight gain during pregnancy. *Obstet Gynecol*, 121(1):210–212, January 2013.

[39] J. M. Wojcicki and M. B. Heyman. Let´s move - chilhood obesity prevention from pregnancy and infancy onward. *N Engl J Med*, 362(16):1457–14599, 2010.

[40] S. Y. Chu, W. M. Callaghan, C. L. Bish, and D. DAngelo. Gestational weight gain by body mass index among us women delivering live births, 20042005: Fueling future obesity. *American Journal of Obstetrics & Gynecology*, 200(3):207.e1–7, 2009.

[41] S. M. Asbee, T. R. Jenkins, J. R. Butler, J. White, M. Elliot, and A. Rutledge. Preventing excessive weight gain during pregnancy through dietary and lifestyle counseling: a randomized controlled trial. *Obstet Gynecol*, 113(2):305–312, 2009.

[42] C. M. Olson, M. S. Strawderman, and R. G. Reed. Efficacy of an intervention to prevent excessive gestational weight gain. *Am J Obst Gynecol*, 191:530–536, 2004.

[43] A. Bemporad and M. Morari. Control of systems integrating logic, dynamics and constraints. *Automatica*, 35(3):407–427, 1999.

[44] J. E. Navarro-Barrientos, D. E., and L. M. Collins. A dynamical model for describing behavioral interventions for weight loss and body composition change. *Mathematical and Computer Modeling of Dynamical Systems*, 17(2):183–203, 2011.

[45] L. de Jonge, J. P. Delany, T Nguyen, J. Howard, E. C. Hadley, L. M. Rdeman, and E. Ravussin. Validation study of energy expenditure and intake during calorie restriction using doubly labeled water and changes in body composition. *Am J Clin Nutr*, 85:73–79, 2007.

[46] IOM/NAS. *Dietary reference intakes for energy, carbohydrate, fiber, fat, fatty acids, cholesterol, protein, and amino acids*. Institute of Medicine, Washington, DC, 2005.

[47] I. Ajzen. *Attitudes, personality, and behavior*. Open University Press, Milton Keynes, England, 1988.

[48] I. Ajzen and T. J. Madden. Prediction of goal-directed behavior: attitudes, intentions,and perceived behavioral control. *Journal of Experimental Social Psychology*, 22:453–474, 1986.

[49] M. Fishbein and I. Ajzen. *Predicting and changing behavior: The reasoned action apprach.* Psychology Press, New York, 2010.

[50] I. Ajzen and M. Fishbein. *Understanding attitudes and predicting social behavior.* Prentice Hall, Englewood Cliffs, NJ, 1980.

[51] M. Fishbein and I. Ajzen. *Belief, attitude, intention and behavior: An introduction to theory and research.* Addison-Wesley, Reading, MA, 1975.

[52] A. Bandura. Social cognitive theory of self-regulation. *Organizational behavior and human decision processes*, 50:248–287, 1991.

[53] R. F. Baumeister, T. F. Heatherton, and D. M Tice. *Losing control: How and why people fail at self-regulation.* Academic Press, San Diego, CA, 1994.

[54] R. F. Baumeister. *The nature and structure of the self: An overview.* Psychology Press, Philadelphia, PA, 1999.

[55] K. D. Vohs and R. F. Baumeister. *Understanding self-regulation: An introduction.* New York:Guilford, 2004.

[56] R. F. Baumeister. *The cultural animal: human nature, meaning, and social life.* Oxford University Press, New York, 2005.

[57] N. Cantor. From thought to behavior: “having” and “doing” in the study of personality and cognition. *American Psychologist*, 45:735–750, 1990.

[58] J. Kuhl. A functional-design approach to motivation and self-regulation: The dynamics of personality systems interactions. *Handbook of Self-regulation*, pages 111–169, 2000.

[59] M. Zeidner, M. Boekaerts, and P. R. Pintrich. Self-regulation: Directions and challenges for future research. *Handbook of Self-regulation*, pages 750–768, 2000.

[60] C. Abraham, P. Norman, and M. Conner. Towards a psychology of health-related behavior change. *Understanding and changing health behavior: From health beliefs to self-regulation*, pages 343–369, 2000.

[61] C. Abraham and P. Sheeran. Understanding and changing health behavior: From health beliefs to self-regulation. *Understanding and changing health behavior: From health beliefs to self-regulation*, pages 3–24, 2000.

[62] I. Streuling, A. Beyerlein, and R. von Kries. Can gestational weight gain be modified by increasing physical activity and diet counseling? a meta-analysis of intervention trials. *American Journal of Clinical Nutrition*, 92(4):678–187, 2010.

[63] D. S. Downs, J. MDiNallo, and E. Rauff. Design of Active MOMS: Physical activity intervention for pregnant women. *Maternal and Child Health Journal*, in preparation, 2011.

[64] B. A. Polley, R. R. Wing, and C. J. Sims. Randomized controlled trial to prevent excessive weight gain in pregnant women. *Int J Obes Relat Metab Disord*, 26:1494–1502, 2002.

[65] T. Shirazian, S. Monteith, F. Friedman, and A. Rebarber. Lifestyle modification program decreases pregnancy weight gain in obese women. *Am J Perinatol*, 27:411–414, 2010.

[66] I. M. Claesson, G. Sydsjo, and J. Brynhildsen J. Weight gain restriction for obese pregnant women: a case-control intervention study. *BJOG*, 115:44–50, 2008.

[67] S. Phelan, M. G. Phipps, B. Abrams, F. Darroch, A. Schaffner, and R. R. Wing. Randomized trial of a behavioral intervention to prevent excessive gestational weight gain: the Fit for Delivery study. *American Journal of Clinical Nutrition*, 93(4):772–779, 2011.

[68] G. Bray, E. Gregg, S. Haffner, XF. Pi-Sunyer, L.E. WagenKnecht, M. Walkup, and R. Wing. Baseline characteristics of the randomized cohort from the look AHEAD (Action for Health in Diabetes) study. *Diabetes and Vascular Disease Research*, 2006.

[69] D. S. Downs, M. Feinberg, M. H. Hillemeier, C. S. Weisman, G. A. Chase, C. H. Chuang, R R. Parrott, and L. A. Francis. Design of the Central Pennsylvania Womens Health Study (CePAWHS) strong healthy women intervention: Improving preconceptional health. *Maternal and Child Health Journal*, 2009.

[70] D. S. Downs, J.M. DiNallo, E. L. Rauff, J. S. Ulbrecht, L. L. Birch, and I. M. Paul. Pregnant womens exercise motivation and behavior: Preliminary findings from a randomized physical activity intervention. *Journal of Sport & Exercise Psychology*, 2010.

[71] D. S. Downs. Determinants and outcomes of physical activity in pregnancy: Findings from Active MOMS, a randomized physical activity intervention for pregnant women. *Annals of Behavioral Medicine*, 2011.

[72] J. A. Martin, B. E. Hamilton, S. J. Ventura, M. J. Osterman an E. C. Wilson, and T. J. Mathews. Birth: Final data from 2010. *National Vital Statistics Reports*, 61(1), 2012. U.S. Department of Health and Human Services. Centers for Disease Control and Prevention.

[73] J. F. Chapp D. M. Thomas and S. Shernce. A foetal energy balance equation based on maternal exercise and diet. *Journal of the Royal Society interface*, 5(21):449–455, 2008.

[74] R. F. Baumeister and K. D. Vohs. Self-regulation, ego depletion, and motivation. *Social and personality Psychology Compass*, 1(1):115–128, 2007.

[75] M. H. Appley. Motivation, equilibration, and stress. in r.a. dienstbier (ed.). *Perspectives on Motivation. Nebraska Symposium on Motivation*, 38(1):1–67, 1990.

[76] G. A. Miller, E. Galanter, and K. H. Pribram. *Plans and the structure of behavior*. Holt, New York, 1960.

[77] C. E. Garcia and M. Morari. Internal model control - 1. a unifying review and some new results. *Ind. Eng. Chem. Process Des. Dev.*, 21:308–323, 1982.

[78] G. C. Newton, L. A. Gould, and J. F. Kaiser. *Analytic design of feedback controls*. John Wiley & Sons, New York, 1957.

[79] C. E. Garcia and M. Morari. Internal model control - 3. multivariable control law computation and tuning guidelines. *Ind. Eng. Chem. Process Des. Dev.*, 24:484–494, 1985.

[80] D. E. Rivera, M. Morari, and S. Skogestad. Internal model control - 4. pid controller design. *Ind. Eng. Chem. Process Des. Dev.*, 25:252–265, 1986.

[81] M. Morari. Design of resilient processing plants - iii: A general framework for the assessment of dynamic resilience. *Chem. Eng. Sci.*, 38:1881–1891, 1983.

[82] M. Morari. Robust stability of systems with integral control. *IEEE Trans. Autom. Control*, AC-30:574–577, 1985.

[83] M. Morari and E. Zafiriou. *Robust process control.* Prentice-Hall, Englewood Cliffs, New Jersey, 1989.

[84] P. J. Antsaklis. Special issue on hybrid systems: Theory and applications. In *Proceedings of the IEEE*, volume 88, 2000.

[85] M. S. Branicky, V. S. Borkar, and S. K. Mitter. A unified framework for hybrid control: Model and optimal control theory. *IEEE Trans. Automatic Control*, 43(1):31–45, 1998.

[86] S. Hedlund and A. Rantzer. Optimal control of hybrid systems. In *Proceedings of the 38th IEEE Conference on Decision and Control*, pages 3972 – 3976, Phoenix, Arizona, USA, Dec 7 - Dec 10 1999.

[87] A. Bemporad, G. Ferrari-trecate, D. Mignone, M. Morari, and F. D. Torrisi. Model predictive control - ideas for the next generation. In *European Control Conference*, 1999.

[88] J. H. Lee and Z. H. Yu. Tuning of model predictive controllers for robust performance. *Comput. Chem. Eng.*, 18(1):15–37, 1994.

[89] R. Cagienard, P. Grieder, E.C. Kerrigan, and M. Morari. Move blocking strategies in receding horizon control. In *Proceedings of the 43rd IEEE Conference on Decision and Control (CDC)*, volume 2, pages 2023–2028, dec. 2004.

[90] D. J. Leith andW. E. Leithead. Survey of gain-scheduling analysis and design. *International Journal of Control*, 73(11):1001–1025, 2000.

[91] A. K. Tangirala, D. Li, R. Patwardhan, S. L. Shah, and T. Chen. Issues in multirate process control. In *Proceedings of the 1999 American Control Conference*, pages 2771–2775, San Diego, CA, USA, June 2 - June 4 1999.

[92] A. Pnueli. The temporal logic of programs. In *Proceedings of FOCS. IEEE Computer Society Press*, 1977.

[93] R. koymans. Specifying real-time properties with metric ttemporal logic. *Real-time Systems*, 2(4):255–299, 1990.

[94] H. M. Ehrenberg, B. M. Mercer, and P. M. Catalano. The influence of obesity and diabetes on the prevalence of macrosomia. *Am J Obstet Gynecol*, 191:964–968, 2004.

[95] T. J. Rosenberg, S. Garbers, H. Lipkind, and M. A. Chiasson. Maternal obesity and diabetes as risk factors for adverse pregnancy outcomes: differences among 4 racial/ethnic groups. *Am J Public Health*, 95:1545–1551, 2005.